Functional Specialization & Parallel Processing within Retinotopic Subdivisions of Lateral Occipital Cortex

Edward Harry Silson

Submitted for the degree of PhD

University of York

Psychology

September 2013

Abstract

This thesis aimed to probe the functional specializations present within several retinotopic divisions of human lateral occipital cortex (LO). The divisions of interest were LO1 and LO2, two neighbouring visual field maps that are found within object-selective LO; the posterior portion of a larger area referred to as the lateral occipital complex (LOC), and V5/MT, the well-known visual complex that is highly selective to visual motion. In order to seek out the causal roles played by these divisions in human visual perception, I used transcranial magnetic stimulation to temporarily disrupt neural processing within these areas, while observers performed visual tasks. The visual tasks I employed examined both spatial vision, through orientation and shape discriminations, and motion processing, through speed discrimination.

The data revealed a number of double dissociations. A double dissociation was present between LO1 and V5/MT in the perceptions of orientation and speed. A similar pattern of results was present during orientation and speed discrimination of the same moving stimuli, although this effect was markedly weaker. Additionally, a double dissociation was present between LO1 and LO2 in the perceptions of static orientation and shape, respectively. These double dissociations suggest that LO1, LO2 and V5/MT exhibit functional specializations for orientation, shape and speed, respectively and moreover, perform these specialized roles largely independently of one another.

It is unsurprising that I found evidence for parallel processing of motion and aspects of spatial processing because: (1) V5/MT has been shown to be a cluster of multiple visual field maps with a common foveal representation – a feature that has led to the idea that the maps within clusters perform related aspects of processing, but are independent of the processing undertaken in adjacent visual field map clusters like LO; (2) neuropsychological evidence, from studies of akinetopsia and visual form agnosia, points to a double dissociation in processing of motion and form and (3) there is evidence of parallel processing pathways from early visual areas and even subcortical structures to V5/MT.

The parallel processing of orientation and shape in LO1 and LO2 is a novel and more surprising finding for the following reasons: (1) These visual field maps are adjacent maps

within a single cluster and therefore, might be expected to perform a series of related and dependent roles and (2) shape, as defined here by curvature, could be seen as a property that is dependent on orientation processing. These findings therefore, point to an architecture whereby the extrastriate visual maps in LO sample visual information from antecedent visual areas in parallel, to extract higher order spatial statistics. Mutual retinotopic information and parallel processing not only reduces replicated information across maps but also, provides a common mechanism for communication between maps which exhibit different specializations.

Importantly, the well-known category-selectivity of extrastriate regions, like LO, may simply emerge from patterns of unique and low-level visual computations, which encode category specific image statistics, performed by the individual visual field maps that subdivide these areas.

Table of Contents

Chapter 5   131

Is Orientation Processing of Moving Stimuli Reliant Upon LO1?

List of Figures

List of Tables

Acknowledgements

There are many people without whom the completion of this thesis would not have been possible. First and foremost, I want to take this opportunity to thank my supervisor Professor Antony Morland. Throughout the three years he has been a constant source of encouragement, determination and direction. The lessons he has taught me about Science (and life) will not be forgotten trivially. I thank also my unofficial second supervisor Professor Declan McKeefry, who played the *'good-cop'* role to Tony's *'bad-cop'* with aplomb. The guidance, patience and above all confidence you both have shown in me have made the three years not only possible, but also incredibly rewarding and enjoyable – I cannot thank you both enough. To Professors Beth Jefferies and Tim Andrews I thank you for the constructive discussions of my work during our TAP meetings and the confidence that you both have had in me. I thank Professor Alex Wade for technical support and constructive discussion of the data reported in this thesis. The technical support provided to me from all members of staff at YNiC but in particular Andre Gouws and Dr Mark Hymers require a special mention. Any successes originating from this thesis could not have been achieved without your contributions – Thank you. I have felt very much at home at YNiC and that is mostly attributable to the efforts of Dr Rebecca Millman and Claire Fox.

My family and friends have always been a source of great support and so it is to them that I am also truly grateful. It is necessary for me to personally thank several of my fellow PhD colleagues with whom I have shared my ideas, troubles and successes. In particular I thank '*The Soft Lad'* and Mladen Sormaz for many informative and constructive discussions of the work carried out throughout the thesis. I also thank Vanesssa Huke for being a permanent source of comfort, constructive criticism and companionship.

Declaration

This thesis contains original work carried out by myself under the supervision of Prof. Antony B. Morland.

Data reported in **Chapter 3** were presented at the Applied Vision Association conference (2011), University of York, York, as;

Silson, E.H., McKeefry, D.J., & Morland, A.B. LO1 plays a causal role in orientation discrimination.

Data reported in **Chapter 6** were accepted for publication as;

Silson, E.H., Rodgers, J., Gouws, A., Hymers, M., McKeefry, D.J., & Morland, A.B. (2013). Specialized and independent processing of orientation and shape in visual field maps LO1 and LO2, *Nature Neuroscience* doi:10.1038/nn.3327.

and presented at the Society for Neuroscience conference (2012), New Orleans, USA, as;

Silson, E.H., Rodgers, J., Gouws, A., Hymers, M., McKeefry, D.J., & Morland, A.B. Double dissociation within the retinotopic subdivission of the lateral occipital cortex.

Chapter 1

Introduction

1.1: Overview

The precise neural mechanisms, by which humans identify complex visual forms, remains poorly understood. One reason for this may reflect the fact that little is known about the functional properties of individual visual field maps (Zeki, 1990), of which there are many throughout visual cortex (Wandell, Dumoulin & Brewer, 2007). These visual field maps can be thought of as discrete computational units, each one of which containing the potential to contribute uniquely to visual perception (Zeki, 1990). Investigating the functional properties of individual visual field maps is considered, by some, to be a fundamentally important endeavour. Indeed as Wandell and colleagues comment: *"Characterizing the responses within specific visual field maps is an essential task in understanding the cortical organization of visual function"* (Wandell et al., 2007, *p369*, **56**). The identification of retinotopic subdivisions LO1 and LO2 within the object-selective Lateral Occipital Cortex (LO) (Larsson & Heeger, 2006) provides a unique and timely opportunity to study the nature of neural computations within these retinotopic subdivisions at a relatively unachieved spatial scale. Throughout the thesis I aim to probe the causal nature of computations performed within LO1 and LO2, plus other sites, using the combination of functional magnetic resonance imaging (fMRI) visual field mapping techniques (Engel, Rumelhart, Wandell, Lee, Glover, Chichilnisky & Shadlen, 1994; Sereno, Dale, Reppas, Kwong, Belliveau, Brady, Rosen & Tootell, 1995; DeYoe, Carman, Bandettini, Glickman, Weiser, Cox, Miller & Neitz, 1996) and transcranial magnetic stimulation (TMS) (Cowey, 2005).

The principle aims of this chapter are to: (1) provide a description of the arrangement of the visual field on the retina, the major projections from the retina to the cortex, including achromatic and chromatic channels and how the visual field is reconstructed within cortex, using early visual cortex (V1-V3) as an example; (2) outline two fundamental organisational principles of human visual cortex – functional specialization and parallel (and serial) processing; (3) highlight two commonly adopted, but largely separate,

ways of dividing visual cortex – category-selectivity or retinotopic organisation; (4) outline how these two methods converge on the question of what role individual visual field maps play in visual perception and how the thesis will attempt to answer this question with respect to LO1 and LO2 and finally; describe the theoretical and analytical framework adopted throughout the thesis.

1.2:   Visual Processing from the Retina to Visual Cortex

LO1 and LO2 are by definition, maps of the visual field (Larsson & Heeger, 2006). It is necessary therefore, to consider how the visual field is represented on the retina and how that representation projects to visual cortex. A schematic of the visual field representation on the retinas is provided in Figure 1.1. The retina can be divided into four sections – nasal, temporal, upper and lower. Convention dictates that these sections are referred to according to their representation of the visual field. Thus, the nasal retina represents the temporal field of view, with the temporal retina representing the nasal field of view (Lavidor & Walsh, 2004). Due to the eyes' optics the nasal retina of the left eye and the temporal retina of the right eye represent the left visual field (left hemifield); whereas the right nasal retina and the left temporal retina represent the right visual field (right hemifield) (Zeki, 1993). Similarly, the lower retinal section represents the upper visual field and the upper retinal section represents the lower visual field. Each hemifield can then in turn be subdivided into upper and lower quadrants. The retina is further divided into foveal and peripheral sections, with foveal vision covering the first 3-5° of visual angle, with peripheral vision representing eccentricities greater than 5° (Zeki, 1993). Consideration of these retinal sections is important as the representation of the retina varies across different visual field maps throughout visual cortex (Zeki, 1993).
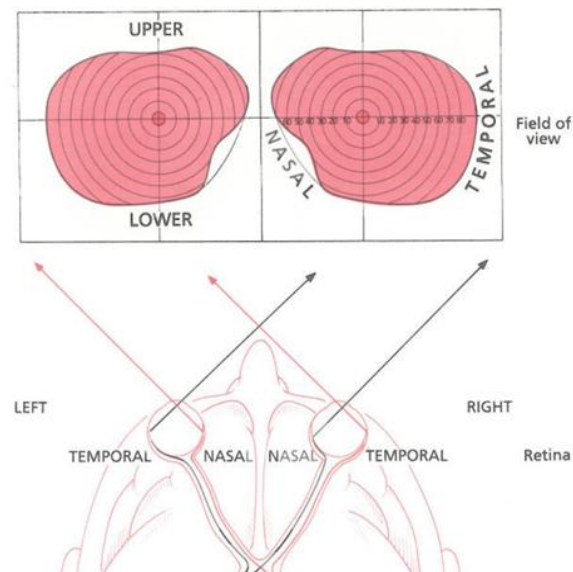
Figure 1.1: *Representation of the visual field on the retinas. The right and left visual fields are displayed, with the upper/lower and nasal/temporal sections labelled **(top).** The nasal retina of the left eye and the temporal retina of the right eye represent the left visual field. Likewise the nasal retina of the right eye and the temporal retina of the left eye represent the right visual field. Adapted from Figure 3.1, Zeki, 1993.*

As light enters the eye, it is represented on the photoreceptor layer of the retina (made up of three cones types and rods). Signals from these photoreceptors pass via bipolar cells to ganglion cells. The retinal ganglion cells transmit visual information from the retina to visual cortex via three independent channels. The L + M or luminance channel, effectively adds together the outputs from L and M cones in order to compute the intensity of a stimulus. In the L - M colour opponent channel, the outputs from the L and M cones are subtracted from one another in order to compute the red-green element of a stimulus. In the S – (L + M) channel, the output from the L and M cones are summed and subtracted from the S cone output in order to compute the amount of blue-yellow within a stimulus (Gegnenfurtner, 2003). The major projections from the retina to visual cortex are schematised in Figure 1.2. The axons of retinal ganglion cells form the *optic nerve*, the only projection from retina-to central nervous system. The optic nerve consists of many fibres, which cross over at the *optic chiasm* in a very specific manner (Zeki, 1993). Fibres that originate in the nasal retina project to the contralateral hemisphere, whereas fibres that originate in the temporal retina project to the ispilateral hemisphere (Zeki, 1993). Beyond

the *optic chiasm* the visual pathway is re-labelled as the *optic tract*, which projects to the lateral geniculate nucleus (LGN), a sub-cortical structure within the thalamus (Solomon & Lennie, 2007). The LGN is a complex, six-layered structure, which acts as a relay station for visual processing. Two features of the LGN are noteworthy. First, the highly specific nature of projections from the eye to the LGN is important, the signals from the two eyes are segregated such that projections from the ipsilateral eye project to layers 2, 3 and 5, whilst projections from the contralateral eye terminate in layers 1, 4 and 6 (Zeki, 1993). Second, this highly organised structure is coupled with a point-point mapping from the retina, so that adjacent points on the retina project to adjacent points in each layer of the LGN (Zeki, 1993). The LGN layers are further stacked upon one another maintaining the adherence to retinotopic organisation. The vast majority of LGN axons project directly to primary visual cortex (V1), specifically layer 4 of V1. The precise location of termination within layer 4 depends on the origin of axons in the LGN. The majority of Parvocellular cells (P-cells) project to layer 4Cβ, with Magnocellular cells (M-cells) projecting to layer 4Cα and finally Koniocellular cells (K- cells) projecting to layer 4A and lower level 3 (Livingstone & Hubel, 1988; Zeki, 1993; Solomon & Lennie, 2007). Several important differences have been documented between Magnocellular and Parvocellular cells. Most notably, single-unit recordings in non-human primates reveal that the majority of Parvocelluar cells are highly sensitive to wavelength as opposed to Magnocellular cells, which exhibit a striking insensitivity to wavelength (Livingston & Hubel, 1988). Magnocelluar cells have also been reported to contain larger receptive field centres than Parvocellular cells across eccentricities. Further, Magnocellular cells have been shown to respond faster and more transiently than their Parvocellular counterparts, making Magnocellular cells critical to motion perception (Livingstone & Hubel, 1988).
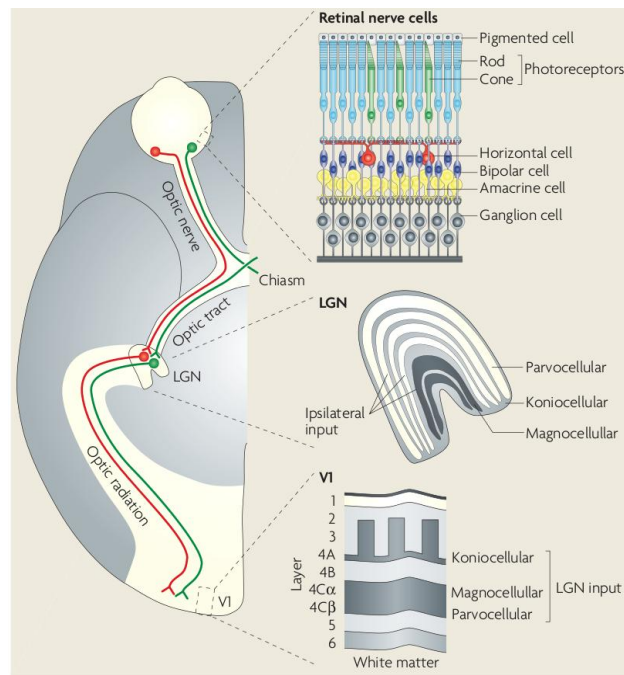
Figure 1.2: *Schematic representation of the major projections from the retina to the cortex. A ventral view of the right hemisphere is shown. As light enters the eye it is imaged on the retina. The axons of ganglion cells form the optic nerve which projects primarily to the LGN. Axons from the nasal retina **(green line)** project to the contralateral LGN, whereas those from the temporal retina **(red line)** project to the ipsilateral LGN. Within the LGN, the signals from the nasal and temporal retinas are aligned in all six layers, maintaining retinotopic organisation. Projections from the LGN terminate predominantly in layer 4 of V1, with the precise site of termination depending on whether the LGN projections are Parvocellular **(layer 4Cβ)**, Magnocellular **(layer 4Cα)**, or Koniocellular **(layer 4A and lower level 3)**. Adapted from Box 1, Solomon & Lennie, (2007).*

1.2.1:   Human Colour Vision

Humans have the capacity to distinguish between lights based on their wavelength content alone – colour vision. In order to achieve this, the human visual system makes use of different signals that originate from the three different types of cone photoreceptor in the retina. The three different cone photoreceptors have peak sensitivities to three different wavelengths, depicted in Figure 1.3. S-cones have a peak sensitivity to short wavelengths of light (~430nm), M-cones peak sensitivity is to medium wavelengths (~530nm) and finally L-cones exhibit a peak to long wavelengths (~560nm) of light. The absolute peak sensitivities of these cones vary across individuals. Despite these peak sensitivities, the tuning curves of these cones are broad enough such that each will respond to light across a wide range of wavelengths of the visible spectrum (Livingston & Hubel.

1988). Once a photon of light has been absorbed by a cone, the identity of the wavelength is lost. The result is that no single photoreceptor can distinguish between changes in the wavelength of light from changes in the intensity of that light – the principle of univariance (Rushton, 1972). Colour vision therefore, relies on the comparison of signals from different photoreceptors with different spectral sensitivities. The existence of three different cone types thus, makes human colour vision 'trichromatic' (Solomon & Lennie, 2007).
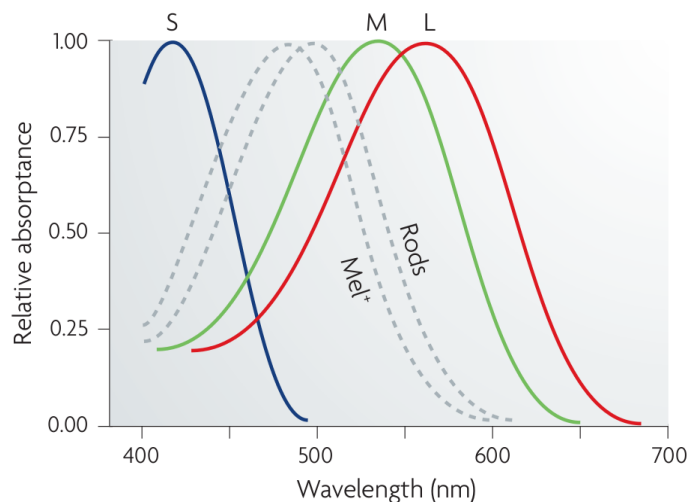
Figure 1.3: *Spectral sensitivity of cones in the human retina. The spectral sensitivities of S-cones (blue line), M-cones (green line) and L-cones (red-line) are shown. For comparison, the spectral sensitivities of rods and photosensitive ganglion cells, which express melanopsin (Mel+), are shown. The broad tuning of cones is evident. A large proportion of the visible spectrum would elicit a signal in either all or at least two of the cones. Adapted from Figure 1, Solomon & Lennie, (2007).*

1.2.2: Representation of Visual Field in Cortex

Much of visual cortex is organised retinotopically (Wandell et al., 2007). That is, adjacent points on the retina project to adjacent points in cortex, creating a point-point mapping of visual space in cortical space. In both humans and non-human primates, the first three visual areas follow a very similar configuration; three complete hemifield maps of the contralateral visual field near the calcarine sulcus in the occipital lobe (Dougherty, Koch, Brewer, Fischer, Modersitzki & Wandell, 2003). To demonstrate this more explicitly, consider the visual field representations in V1-V3, depicted in Figure 1.4. V1 represents a complete contralateral hemifield and runs parallel to the calcarine sulcus. The lower vertical meridian is represented on the superior bank of the calcarine, the polar angle representation continues towards the horizontal meridian (represented in the fundus of the calcarine), with the upper vertical meridian represented on the inferior bank of the calcarine. Two additional maps (V2 and V3) encircle V1 both dorsally and ventrally, and

contain quadrant maps, respectively. The combined dorsal/ventral divisions of V2 and V3 create two hemifield representations. The eccentricity representations in these three maps run in parallel, beginning at the large foveal representation (foveal confluence) near the occipital pole. Increasingly eccentric positions of visual space are represented at increasingly anterior positions along the calcarine sulcus (V1) and medial surface (V2, V3) of the occipital lobe. The polar angle and eccentricity representations in V1, V2 and V3 are directly orthogonal to one another (Wandell et al., 2007).
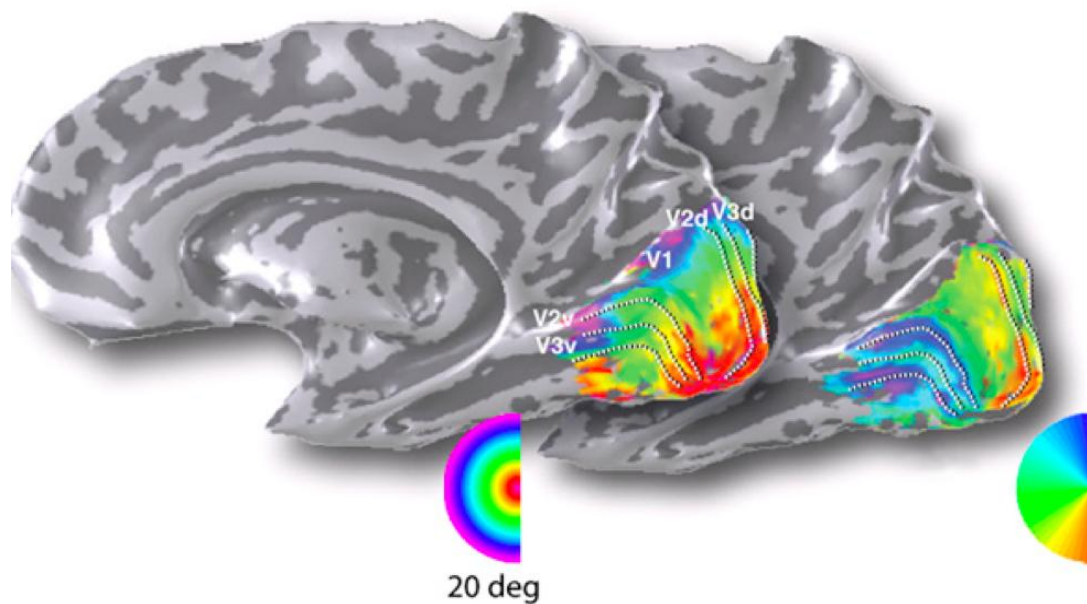
Figure 1.4: *Early visual field maps V1, V2 and V3 in the right hemisphere of a single subject. The representations of eccentricity **(left)** and polar angle **(right)** are overlaid in false colour (see hemifield colour wheel inset into each figure). The colour indicates the stimulus position that elicited the largest BOLD response. The polar angle data clearly show the split representations of V2 and V3. Moving ventrally from V1, the polar angle representation in V2v progresses from the upper vertical meridian **(blue)** towards the horizontal meridian **(green)**. The representation in V3v is the mirror-reverse, from the horizontal to the upper vertical meridian. Moving dorsally from V1, the polar angle representation in V2d progresses from the lower vertical meridian **(orange)** towards the horizontal meridian. The representation in V3d is the mirror-reverse of V2d. The eccentricity representations in all three maps follow a very similar pattern, extending anteriorly from the shared foveal representation **(red)** at the occipital pole. Figure adapted from Wandell et al., (2007).*

1.3:   Fundamental Principles of Human Visual Cortex

Two fundamental organisational principles of the human brain are functional specialization and parallelism (Zeki, 1990). The specific questions asked throughout this thesis were influenced heavily by consideration of these principles. The following sections provide an overview of the evidence for functional specialization in the human brain derived from neuropsychological, neuroimaging and neurostimulation studies and the evidence for parallelism within human cortex at a number of different spatial scales.

1.3.1:   Functional Specialization

Functional specialization is a fundamental organisational principle of the human brain (Zeki, 1990). The origins of functional specialization in human trace back to the post mortem observations made by Broca in 1861 (Broca, 1861), where he identified a region of the left frontal lobe that was damaged in a patient who had a profound inability to speak. Despite the origins of functional specialization residing in the frontal lobes, nowhere has functional specialization been more extensively researched, or demonstrated directly, than within visual cortex (Zeki, Watson, Lueck, Friston, Kennard & Frackowiak, 1991; Zeki, 1990). Human visual cortex contains areas that exhibit functional specializations for different visual properties, such as colour (Meadows, 1974; Lueck, Zeki, Friston, Deiber, Cope, Cunningham, Lammertsma. Kennard & Frackowiak, 1989; McKeefry & Zeki, 1997; Zeki, McKeefry, Bartels, & Frackowiak, 1998) and motion (Zihl, Voncramon & Mai, 1983; Zeki et al., 1991; Walsh, Ellison, Battelli & Cowey, 1998; McKeefry, Burton, Vakrou, Barrett, & Morland, 2008) as well as selective responses to stimulus categories including faces (Kanwisher, McDermott, & Chun, 1997; Grill-Spector, Kushnir, Edelman, Avidan, Itzchak & Malach, 1999;Andrews & Ewbank, 2004), places (Epstein & Kanwisher, 1998), bodies (Taylor, Wiggett, & Downing, 2007) and commonly encountered objects (Malach, Reppas, Benson, Kwong, Jiang, Kennedy, Ledden, Brady, Rosen & Tootell 1995; Kourtzi & Kanwisher, 2001; Grill-Spector, 2003). The selectivity exhibited by these areas has been demonstrated consistently across a number of investigative paradigms, including neuropsychological (Meadows, 1974; Zihl et al., 1983; Zeki, 1990; Goodale, Milner, Jakobson & Carey, 1991), neuroimaging (Malach et al., 1995; Kanwisher et al., 1997; McKeefry & Zeki, 1997; Epstein & Kanwisher, 1998; Taylor et al., 2007) and neurostimulation (Beckers & Homberg, 1992; Walsh et al., 1998; McKeefry

et al., 2008; Pitcher, Charles, Devlin, Walsh, & Duchaine, 2009; Pitcher, Duchaine, Walsh, Yovel, & Kanwisher, 2011) studies.

A schematic representation of the locations of these functionally specialized areas is provided in Figure 1.5, overlaid on the Montreal Neurological Institute (MNI) average brain. Inspection of Figure 1.5, not only reveals functionally specialized areas throughout dorsal and ventral regions of visual cortex, but also, the close proximity of these functionally specialized areas. The dorsal and lateral surface of visual cortex contains motion-selective V5/MT (Zihl et al., 1983; Zeki, 1990; Zeki et al., 1991), body-selective Extrastriate Body Area (EBA) (Taylor et al., 2007), object-selective LO (Malach et al., 1995) and the face-selective Occipital Face Area (OFA) (Silvanto, Schwarzkopf, Gilaie-Dotan & Rees, 2010). The ventral surface of visual cortex contains colour-selective V4 (Zeki, 1990; McKeefry & Zeki, 1997), place-selective Parahipocampal Place Area (PPA) (Epstein & Kanwisher, 1998) and the face-selective Fusiform Face Area (FFA) (Kanwisher et al., 1997).

A noteworthy feature regarding the evidence for functional specialization is that of spatial scale. For instance, many of the aforementioned specialized areas are large relative to the size of many visual field maps (Wandell et al., 2007). An important aspect of the thesis will be whether or not functional specializations can be observed at the smaller spatial scale of individual visual field maps.
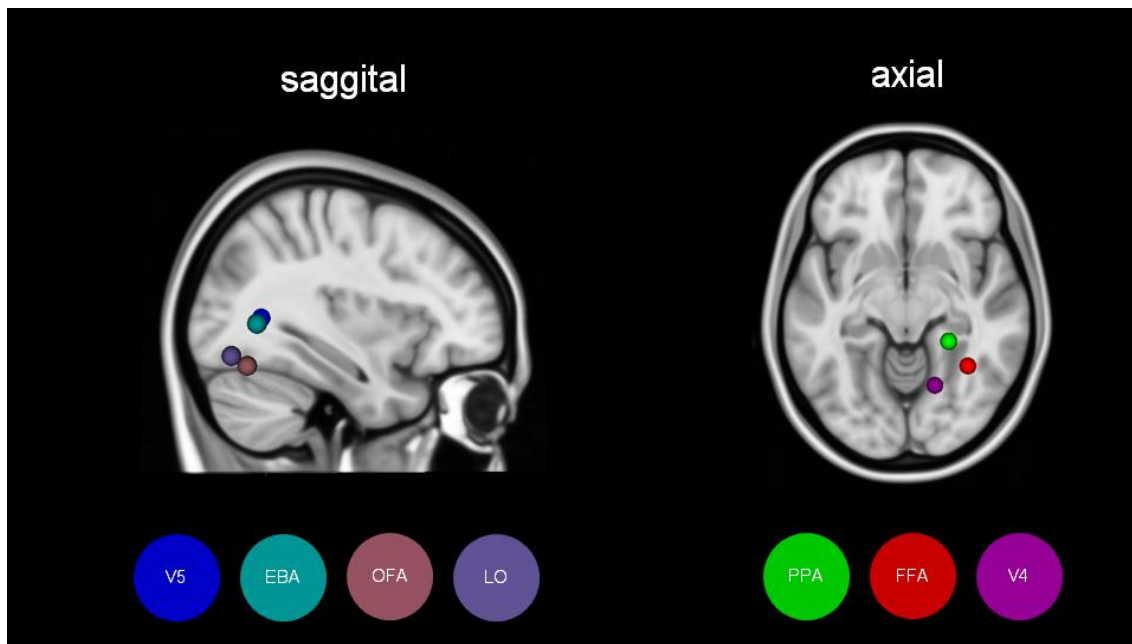
Figure 1.5: *Functionally specialized regions of human visual cortex. The locations of functionally specialized areas are depicted by 5mm spheres overlaid on saggital and axial slices of the MNI average brain. Images are displayed in neurological convention. Coordinates were taken, where possible, from the original papers defining these regions. A saggital view **(left)** depicts the location of four functionally specialized regions on the dorsal and lateral surface of the occipital lobe; motion-selective V5/MT **(blue),** body-selective EBA **(turquoise)**, object-selective LO **(purple)** and the face-selective OFA **(burgundy)**. An axial view **(right)** depicts the location of three functionally specialized areas on the ventral surface of visual cortex; colour-selective V4 **(fuchsia)**, place-selective PPA **(green)** and the face-selective FFA **(red)**. The coordinates for these areas were transformed from Talairach to MNI space for all areas except the OFA, which was already in MNI space.*

1.3.2:   Parallel Processing

The second fundamental organisational principle of human visual cortex is that of parallelism or functional independence (Zeki, 1990). Different spatial scales of parallelism, depicted in Figure 1.6, have been identified in human cortex through a variety of paradigms. First, at the largest spatial scale neuropsychological studies demonstrated parallel processing streams in dorsal (Perenin & Vighetto, 1988) and ventral (Goodale et al., 1991) cortex. These parallel processing streams, encode different visual features and mirror those originally found through selective ablation in non-human primates (Mishkin, Ungerleider, & Macko, 1983). Neuropsychological evidence regarding the perception of colour and motion also suggests that these visual attributes are processed independently within spatially segregated visual areas V4 and V5/MT, respectively (Zihl et al., 1983; Lueck et al., 1989).

Indeed deficits in colour processing (achromatopsia) are seldom associated with deficits in motion processing (akinetopsia) and vice-versa (Zeki, 1990). Second, within these processing streams, at a smaller spatial scale, neuropsychological (Goodale et al., 1991), neuroimaging (Malach et al., 1995; Kanwisher et al., 1997; Epstein & Kanwisher, 1998; Taylor et al., 2007) and neurostimulation (Pitcher et al., 2009) studies have identified specialized areas that encode specific stimulus categories such as faces, places, bodies and objects independently. An influential study by Pitcher et al., (2009) demonstrated the causal roles played by three such category-selective areas. Disruptions to face, body and object processing only occurred following stimulation of the OFA, EBA and LO regions, respectively. Third, the existence of visual field map clusters has been proposed as an organisational principle of human visual cortex (Wandell, Brewer & Dougherty, 2005; Brewer & Barton, 2011). These maps are suggested to form clusters around a central visual field representation. Whilst the maps within a cluster are suggested to perform similar visual computations, different clusters of maps are suggested to perform different visual computations independently of one another (Wandell et al., 2005).

It is unclear whether or not this functional independence extends to adjacent visual field maps within a cluster; however, pioneering work in non-human primates would suggest parallel processing of visual information exists at this spatial scale. Visual field maps V4d and V5/MT have been shown to not only exhibit specializations for colour and motion, respectively, but also, receive parallel projections from antecedent V2 (Shipp & Zeki, 1985; Zeki & Shipp, 1988; Zeki, 1990). An important factor for the thesis will be whether parallelism can be identified at the level of individual visual field maps in human cortex.
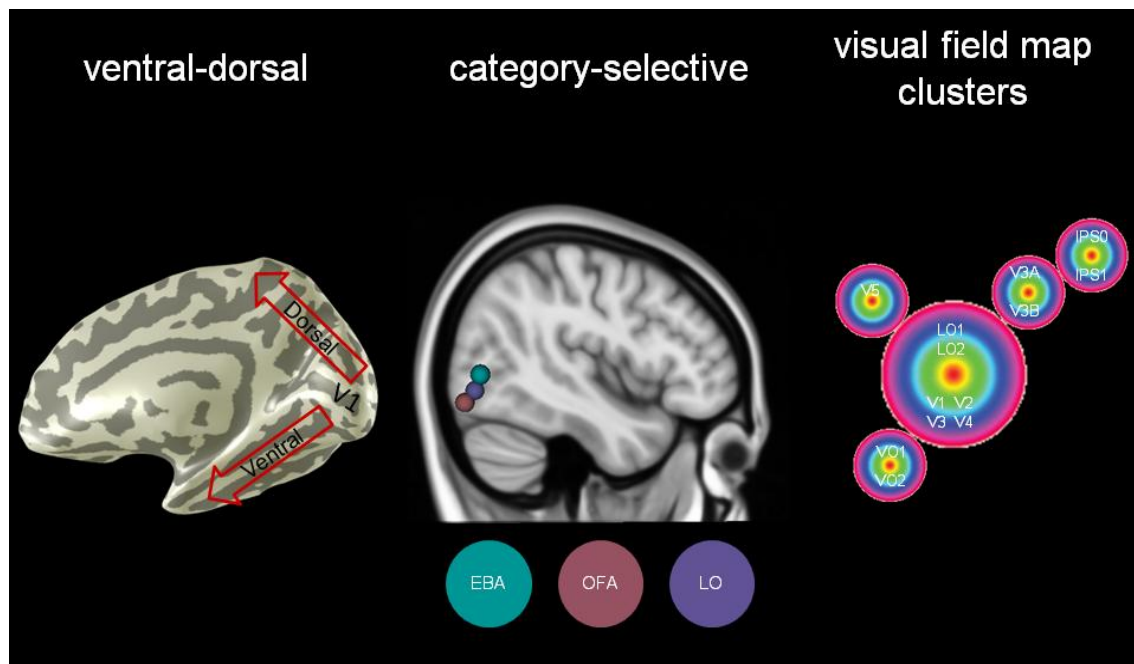
Figure 1.6: *Different spatial scales of parallelism in human visual cortex. At the largest spatial scale **(Left),** a medial view of the right hemisphere is shown. Two parallel processing streams are depicted **(red arrows)** flowing ventrally and dorsally from V1. Within those streams, at a smaller spatial scale **(Middle),** the locations of three functionally specialized areas, depicted by 5mm spheres, overlaid on the MNI brain. Pitcher et al., (2009) demonstrated through TMS the independent processing of preferred categories in these areas. At a smaller spatial scale **(Right)** schematic representation of visual field map clusters. Five clusters are depicted, each one of which is centred around a foveal representation. The maps within a cluster are suggested to perform similar functions but be largely independent from the functions of adjacent clusters.*

Although parallel processing appears a fundamental principle of the human brain, it is imperative to also acknowledge the presence and importance of serial connections between areas, which have been a persistent feature of various models of primate visual function (Felleman & Van Essen, 1991; Felleman & Mcclendon, 1991). The interconnections between visual field maps allow for both serial and parallel processing pathways (Shipp & Zeki, 1985; Zeki, 1990). As a consequence, a computation in one map may be performed, either independently of, or be reliant upon, computations performed in another map. Accordingly, an important aspect of the thesis will be to establish whether computations within individual visual field maps are performed in serial or parallel.

1.4:   Category-Selectivity *versus* Retinotopic Organisation

Many visual neuroscientists adopt one of two general approaches to understanding the neural underpinnings of human visual perception. The first and possibly most widely adopted approach identifies and subsequently divides visual cortex into areas that exhibit selective responses to different visual stimuli. These areas are often labelled 'category-selective' regions of cortex. The second approach divides visual cortex into discrete maps of the visual field.   These two alternative methods have created two largely bifurcated research strands that have developed in parallel with little overlap. The following sections outline, albeit briefly, some of the chief findings from both approaches before describing how they can be seen to converge on a simple yet important question.

1.4.1:   Category-Selectivity

The category-selective approach to dividing visual cortex has led to a number of important demonstrations, some of which were considered above, but expanded upon here. Early neuropsychological studies suggested that selective and localised damage to visual cortex could lead to selective disturbances in the perceptions of particular visual features such as colour (achromatopsia) and motion (akinetopsia), respectively (Verrey, 1988; Meadows, 1974; Zihl et al., 1983; Zeki, 1990). Further neuropsychological studies provided compelling evidence for category-selective deficits in face (termed prosopagnosia) and object (termed object-agnosia) perception following damage to fusiform and lateral occipital areas, respectively (Charcot, 1883; Meadows, 1974; Damasio, Damasio & Van Hoesen, 1982; Goodale et al., 1991). The advent of functional imaging techniques such as positron emission topography (PET) provided compelling and complimentary evidence to these neuropsychological findings. Indeed, PET led to the first direct demonstrations of functional specialization in human visual cortex, locating the colour centre in man on the ventral surface (Lueck et al., 1989) and motion-selective cortex on the lateral surface of the occipital lobe (Zeki et al., 1991). The inception of fMRI however, has arguably had the largest impact on the category-selective approach, leading directly to the demonstration of a number of different category-selective regions of visual cortex. The literature on each area is vast and therefore, for brevity, the original studies are prioritised here. One of the first reported category-selective regions was the lateral occipital complex (LOC) (Malach et al.,

13

1995). This region of cortex was shown to preferentially respond to objects and faces compared with scrambled versions of the same stimuli. The LOC is a large area of extrastriate cortex and covers both dorsal and ventral regions of the occipital lobe. Subsequent fMRI studies identified different hubs of selectivity within the LOC, with dorsal regions responding preferentially to objects (LO), and ventral regions responding more to faces, located around the posterior fusiform gyrus (pFS) (Grill-Spector et al., 1999). One of the most impactful findings of category-selectivity was that of the FFA, an area on the fusiform gyrus that responds preferentially to faces over other stimulus categories (Kanwisher et al., 1997). The identification of the FFA led to a large body of work exploring face-selectivity in human cortex (Haxby, Hoffman & Gobbini, 2000; Andrews & Ewbank, 2004; Andrews, 2005; Andrews, Davies-Thompson, Kingstone & Young, 2010). Very recently, fMRI has been used to identify two spatially distinct hubs of activity within the FFA, termed FFA-1 and FFA-2, respectively, although, it is yet to be discovered as to whether they are functionally separable (Weiner & Grill-Spector, 2012).

Following the discovery of the FFA, regions of cortex selective to places, bodies and even parts of bodies were identified. The PPA located on the ventral surface has been shown to respond preferentially to images of scenes than other stimulus categories (Epstein & Kanwisher, 1998). Additionally, the EBA was originally identified on the basis of preferential responses to bodies over other stimulus categories (Taylor et al., 2007). A further region has been suggested to exist, which exhibits spatially distinct activation to different body parts (Weiner & Grill-Spector, 2010). As mentioned above, several neurostimulation studies have confirmed the selectivity's within a number of these regions including V5/MT's specialization for motion (Walsh et al., 1998; Mckeefry et al., 2008), the object, face and body selectivity of the LO, OFA and EBA, respectively (Pitcher et al., 2009) and a very recent demonstration of the place selectively of an area referred to as the occipital place area (OPA) (Dilks, Julian, Paunov & Kanwisher, 2013).

1.4.2:   Retinotopic Organisation

Whilst the existence of category-selective divisions of visual cortex is well established, visual cortex can also be divided on the basis of maps of the visual field. Indeed, to date human cortex comprises more than twenty separate and discrete representations of the visual field across its surface (Wandell & Wade, 2003; Wandell et al., 2007; Wandell & Winawer, 2011). Such retinotopically organised maps extend, not only throughout visual cortex, both dorsally and ventrally from V1, but also, within temporal (Arcaro, Pinsk, Li, & Kastner, 2011) and frontal cortices (Kastner, DeSimone, Konen, Szczepanski, Weiner & Schneider, 2007; Silver & Kastner, 2009). The identification of visual field maps throughout visual cortex runs contrary to a long-standing belief (of some) that retinotopic organisation be restricted to the first four visual areas (V1-V4). Indeed, many of the category-selective areas mentioned above were originally labelled as non-retinotopic. Recently however, functionally selective areas of cortex, originally considered to either lack or have weak retinotopic organisation (Grill-Spector et al., 1999; Levy, Hasson, Avidan, Hendler, & Malach, 2001), have been subdivided into multiple visual field maps (Larsson & Heeger, 2006; Wandel et al., 2007).

Prior to the explicit demonstration of visual field maps within higher-level areas, the importance of location information within these areas was documented (Malach et al., 1995; Levy et al., 2001). One of the first signs of the importance of position information was the finding that face and place selective areas of cortex exhibited biases toward foveally and peripherally presented stimuli, respectively (Levy et al., 2001). Since then, a number of other studies have highlighted the importance of location information throughout visual cortex (Gardner, Merriam, Movshon & Heeger, 2008; Cichy, Chen, & Haynes, 2011; Cichy, Heinzle, & Haynes, 2012). The importance of location information during visual processing has been explored recently using fMRI multi-voxel pattern analysis (MVPA) techniques (Cichy et al., 2011; Cichy et al., 2012; Golomb & Kanwisher, 2012). One can think about location information in two different frames of reference. One is relative to the eye, and therefore the retina (retinotopic). The other is relative to the world around us (spatiotopic). A number of studies have investigated the relative contribution of, and extent to which, retinotopic and spatiotopic information is present throughout visual cortex (Gardner et al.,

2008; Golomb & Kanwisher, 2012). Across studies, the influence of retinotopic information consistently outweighed spatiotopic information (Gardner et al., 2008). Indeed, a ventral-dorsal segregation was suggested to exist within the retinotopic frame of reference (Cichy et al., 2012). Retinotopic information was found to vary systematically in its influence across the cortical surface, with dorsal-lateral areas showing more marked exploitation of this retinotopic information (Cichy et al., 2012). Despite this division however, all areas were found to be more reliant on retinotopic than spatiotopic information (Cichy et al., 2012). The results suggest even putative 'higher-order' visual areas encode visual information on a retinotopic basis (Gardner et al., 2008; Kravitz, Kriegeskorte, & Baker, 2010; Cichy et al., 2011; Cichy et al., 2012; Golomb & Kanwisher, 2012). The exsitence of retinotopic location information within these high-level areas runs contrary to a long-held belief that visual object representation becomes increasingly position invariant and abstract as one moves further along the visual heirachy. The importance and functional significance of retinotopic location information therefore, appears to be crucial when considering how we perceive complex stimuli.

To date, retinotopic, functionally selective regions of cortex have been identified in both dorsal and ventral streams. A schematic representation of the overlap between category-selective and retinotopic areas is given in Figure 1.7. Ventrally, the place-selective PPA has been shown to comprise two retinotopic maps (PHC1, PHC1) (Arcaro, McMains, Singer & Kastner, 2009). Likewise, adjacent to colour-selective V4, two more visual field maps have been identified (VO1, VO2) (Brewer, Liu, Wade, & Wandell, 2005). Dorsally, motion-selective V5/MT contains two visual field map divisions (TO1, TO2) (Amano, Wandell & Dumoulin, 2009), and finally, the object-selective LO comprises two more retinotopic areas, (LO1, LO2) (Larsson & Heeger, 2006). In each case, two adjacent visual field maps were identified within the encompassing functionally selective area; both maps containing a complete hemifield representation of the contralateral visual field. Additionally, the face-selective OFA is considered, by some (Brewer & Barton, 2011), to be comprised of multiple visual field maps (LO3-6), although this is yet to be accepted formally. The existence of these retinotopic subdivisions suggest that perhaps the category selectivity observed in these areas emerges from computations performed by their respective retinotopic components.
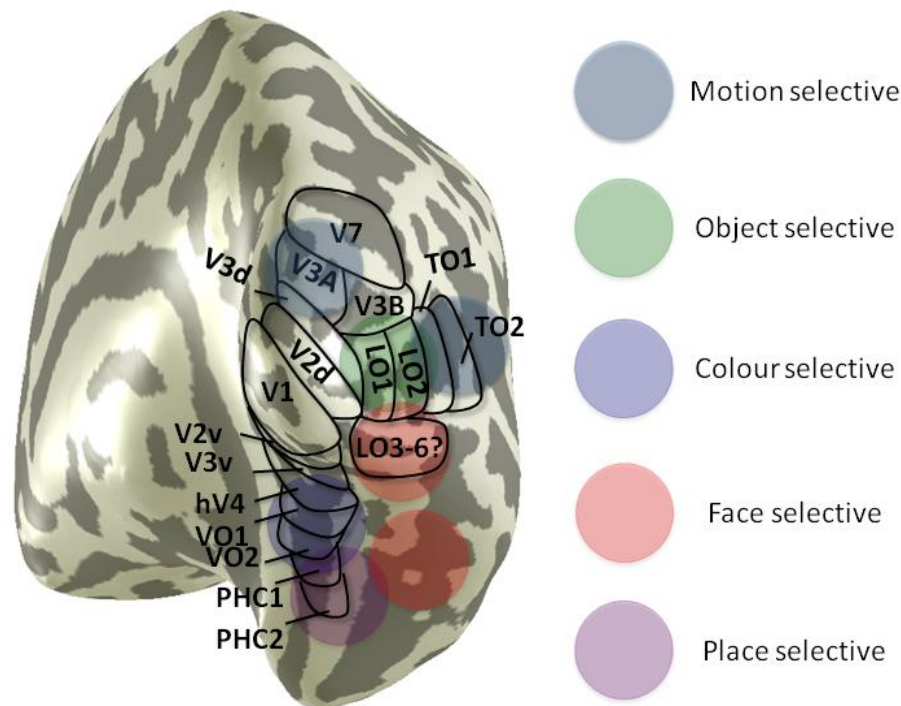
Figure 1.7: *Schematic representation of the overlap between category-selective regions and known visual field maps in human cortex. A partially inflated surface reconstruction of the right-hemisphere of a single subject is shown. The hemisphere is viewed from behind, gyri are light grey, sulci are dark grey. The approximate locations of several category-selective regions are overlaid in colour (see key inset). Also overlaid are the approximate locations of known visual field maps. In many cases, category-selective regions can be seen to encompass multiple visual field maps. It is clear that retinotopic information is present throughout visual cortex and not restricted to early visual areas V1-V4.*

Computationally, these retinotopic subdivisions have the potential to perform unique sets of visual analyses and therefore, contribute uniquely to visual perception (Zeki, 1990). In macaque, neighboring visual field maps V4d and V5/MT, exhibit dissociable specializations for colour and motion, respectively (Shipp & Zeki, 1988; Zeki, 1978). Indeed, it is unlikely that adjacent visual field maps in human sub-serve exact visual functions; if such functional replications were evident, the second, third or nth map within a cluster would effectively be redundant. A more plausible explanation for the existence of multiple visual field maps (within a cluster) is that they allow numerous visual computations to be performed at every point of the visual field. The more independent representations of the visual field, the more visual computations can be performed within functionally selective regions. Mutual retinotopic information could provide a common mechanism for communication between regions of cortex with different selectivities (Kravitz, Saleem,

Baker, Ungerleider & Mishkin, 2013). The seemingly on-going discovery of retinotopic maps within higher-level areas also suggests that retinotopic organisation may be a general principle of human visual cortex (Kravitz et al., 2013). The mere presence of visual field maps within functionally selective areas, previously considered as non-retinotopic, warrants the investigation of their functional properties (Wandell et al., 2007). Taken together, these two largely separate research strands can now be seen to converge on the important question of what role (if any) individual visual field maps play in human visual perception, when those maps subdivide larger functionally selective cortical areas?

1.5: Retinotopic Organisation in LO, LO1 & LO2

A pertinent example which highlights the importance of asking the above question is the consideration of visual field maps LO1 and LO2 and their relationship with object-selective cortex. In order to do so, the identification of LO1 and LO2 needs to be placed in the context of the history of retinotopic organisation in LO. Until relatively recently, many researchers considered the expanse of cortex between V3d and V5/MT as non-retinotopic. Indeed, fMRI studies indicated that this region corresponded to the object-selective LO (Malach et al., 1995; Grill-Spector et al., 1998, 1999; Kourtzi & Kanwisher 2001; Hasson et al., 2003).

Larsson and Heeger (2006) reported the first clear indication of retinotopic organisation within LO, depicted in Figure 1.8. They identified two adjacent visual field maps between dorsal V3d and V5/MT, termed LO1 and LO2, respectively. Both maps contained a complete hemifield representation of the contralateral visual field. Unlike previous reports (Levy et al., 2001), Larsson and Heeger highlighted an orderly representation of both eccentricity and polar angle within these maps. The representation of polar angle in LO1 extended anteriorly from the boundary with V3d approximately half way towards V5/MT, progressing gradually from the lower vertical meridian toward the upper vertical meridian. The anterior boundary of LO1 was defined by a representation of the upper vertical meridian. Within LO2, the representation of polar angle was the mirror-reverse of LO1, showing a gradual progression from the shared representation of the upper vertical meridian towards the lower vertical meridian, which defined the anterior boundary of LO2. Larsson and Heeger (2006) found the foveal representations in LO1 and LO2 to be

coextensive with V1, V2 and V3d with the periphery being represented anterioraly and dorsally. In approximately half of the hemispheres tested, the eccentricity map in LO2 showed a distinctive and unusual pattern, in that the representation of eccentricity made a sharp shift from fovea to periphery. To date, a formal analysis of the extent of orthognaility in LO2 has not been conducted.
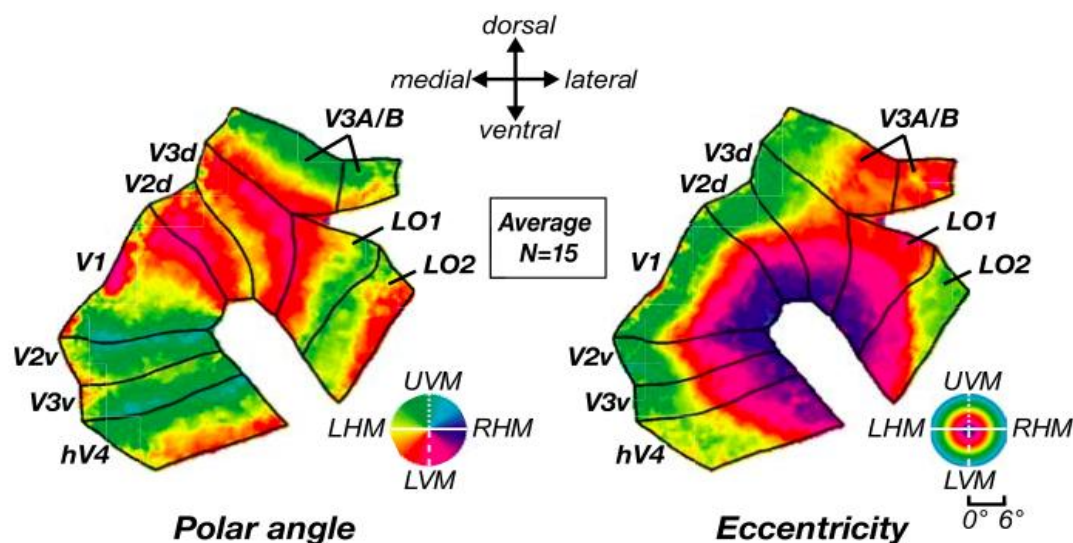
Figure 1.8. *Average visual field maps LO1 and LO2 on flattened schematics of the right hemisphere.* **Left:** *LO1 and LO2 can be seen to contain a hemifield representation of the left visual field, respectively. The polar angle representation in LO1 begins at the shared boundary with V3d at the representation of the lower vertical meridian and extends gradually through the horizontal meridian towards the upper vertical meridian. The polar angle representation in LO2 is the mirror-reverse of LO1, extending from the upper vertical meridian through the horizontal to the upper vertical meridian.* **Right:** *The eccentricity representation in LO1 and LO2 were found to be confluent with those of V1, V2 and V3. Figure Adapted from Larsson & Heeger, (2006).*

The existence of LO1 and LO2, within object-selective LO, suggests that these maps may perform unique computations and therefore, exhibit unique functional properties. Indeed, Larsson and Heeger proposed a segregation of function between LO1 and LO2, with LO1 extracting orientation information and LO2 encoding shape information. Importantly for this thesis however, the functional properties of LO1 and LO2 have thus far, been investigated exclusively using fMRI paradigms (Larsson & Heeger, 2006; Larsson, Landy &

Heeger, 2006; Sayres & Grill-Spector, 2008). Functional MRI provides a correlational measurement that is unable to determine the exact causal role that a specific area plays in perception. Neurostimulation techniques such as TMS have an important advantage in that TMS can induce temporary disruption to specific cortical areas and therefore, provide *causal* information regarding the functional properties of a given cortical area. The anatomical location of LO1 and LO2 make them superb and timely candidates for TMS (McKeefry, Gouws, Burton & Morland, 2009). The use of TMS will allow independent stimulation of these visual field maps and enable elucidation of the potentially unique and causal contributions made by these maps.

Whether one divides visual cortex on the basis of selectivity to stimulus features or visual field representations, both approaches nevertheless appear to converge on the simple, but important question of what roles (if any) do the multiple visual field maps that subdivide larger functionally selective areas play in human visual perception? Throughout the thesis this question will be addressed with respect to visual field maps LO1 and LO2. Through a series of TMS studies, this thesis aims to investigate whether functional specializations are observable at the level of adjacent visual field maps in human visual cortex and if present, whether these functional specializations are dependent or independent from one another (echoing that found in macaque). This thesis will attempt to answer these questions across two different spatial scales. The first, adopts a relatively conservative approach and considers whether specializations are observable between adjacent visual clusters, specifically between LO1 (part of the LO cluster) and V5/MT. The second, will explore whether specializations are present at the smaller scale of adjacent visual field maps within a cluster, specifically LO1 and LO2.

1.6:   Theoretical & Analytical Framework

The experiments conducted as part of this thesis were heavily influenced, both in design and interpretation, by two variants of a framework I term '*map specific*'. This framework is grounded in the concept that each discrete region of visual cortex underlies one or a number of specific visual functions (Zeki, 1990). Taken within this framework, our cortical areas of interest (LO1, LO2 and V5/MT) are hypothesised to perform unique sets of visual computations and therefore, exhibit functional specializations for different visual attributes. This framework has two components. The first, considers whether functional specializations operate within a strictly serial processing architecture. That is, whether the functional specializations of one area are dependent (to a degree) upon the computations performed within antecedent visual areas. The second component, considers whether these functional specializations operate largely independently of those performed by other areas including those directly antecedent. That is, whether these functional specializations exhibit parallelism.

In order to demonstrate these alternative components more explicitly, let us consider a scenario whereby there are two cortical targets of interest (A and B) and two visual tasks (1 and 2) – a classic 2 x 2 design. In this scenario let us consider that Site A is specialized for Task 1 and that Site B is specialized for Task 2. Let us also consider, for now, that these cortical targets are organised within a strictly serial processing architecture. The predicted effects of TMS within this serial framework are plotted in Figure 1.9. Accordingly, TMS of Site A should disrupt performance of Task 1, but TMS of Site B, should leave performance of Task 1 relatively preserved. The pattern however, is different when considering Task 2. If computations performed by Site B are reliant on those performed by Site A, as they must in a strictly serial processing architecture, then TMS of Site B should disrupt performance, but so should TMS of Site A. In this framework, the performance of Task 2 by Site B is dependent upon input from Site A and therefore, disrupting the processing in Site A, leads to reduced input into Site B, which in turn, disrupts performance.

Task 1   Task 2
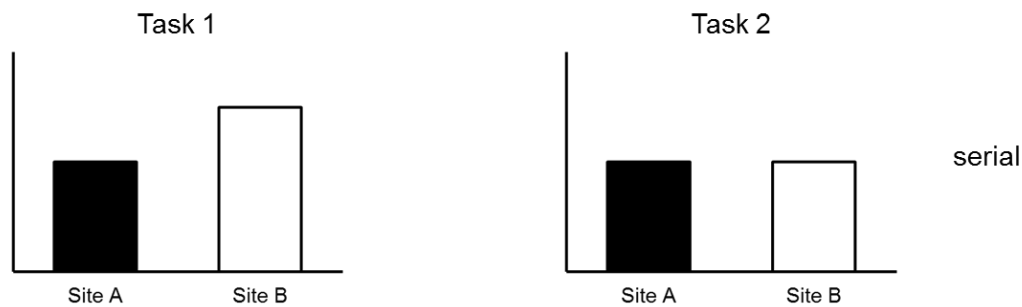
serial

Figure 1.9: *Schematic predictions of the effects of TMS for serial processing. In this scenario, Site A is specialized for Task 1, and Site B is specialized for Task 2. Sites A & B also operate within a strictly serial processing architecture. Accordingly, TMS of Site A disrupts performance on Task 1, but not Task 2, whereas TMS of both Sites A & B disrupt performance of Task 2.This framework assumes that computations performed by Site B are reliant on those performed by Site A.*

In contrast, let us now consider a scenario whereby Site A is specialized for Task 1 and Site B is specialized for Task 2, yet instead of being part of a strictly serial processing architecture, these specializations operate independently of one another, or in parallel. In this scenario, the pattern of results is crucially different. The predicted effects of TMS within this parallel framework are plotted in Figure 1.10. TMS of Site A, but not Site B should lead to selective disruption of Task 1 – same pattern as above for Task 1. In contrast TMS of Site B, but not Site A should disrupt Task 2 – a double dissociation.

Task 1   Task 2
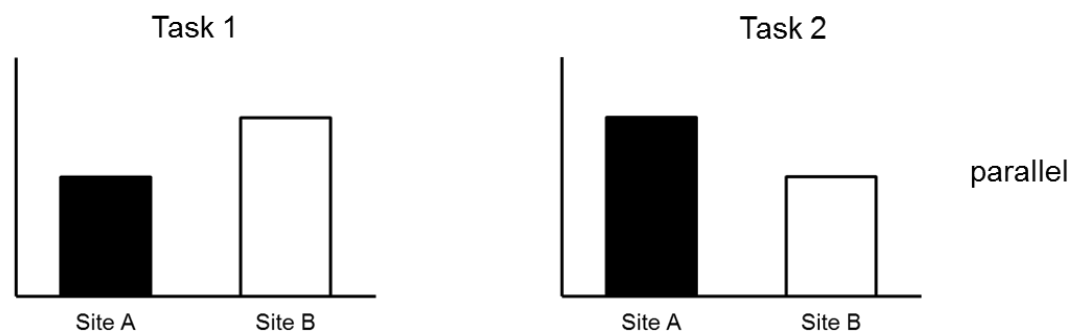
parallel

Figure 1.10: *Schematic predictions of the effects of TMS for parallel processing. In this scenario, Site A is specialized for Task 1, and Site B is specialized for Task 2. Sites A & B operate independently of one another. Accordingly, TMS of Site A disrupts performance on Task 1, but not Task 2, whereas TMS of Site B disrupts performance of Task 2, but not Task 1 – a double dissociation. .*

Consideration of both accounts however, raises the question as to whether either prediction truly allows *map specific* inferences to be made. In order to make inferences regarding both the task and location specificity of these effects there is a need to contextualise the effects of TMS at both sites A and B with the effects of TMS at a control site (CON). A *map specific* inference can only be made if (1) the effect of TMS at the target site is significantly different to the effect of TMS at both the non-target site and the CON, and (2) the effect of TMS of the non-target site is not significantly different from TMS of the CON.

The importance of contextualising the effects of TMS at both target sites with the effects of TMS at the CON is demonstrated in Figure 1.11. If we consider Task 1 alone, the predicted effects across Sites A and B are the same, whether they operate in serial or parallel. It is only when these effects are placed in the context of the effects at the CON can we make *map specific* inferences (red circle and arrows Figure 1.11). In the *map specific* model, there is no difference between the effects of TMS of Site B (no target site in this case) or the CON, making the effect specific to Site A. In contrast, in the location dependent effect, there is an effect at the CON and indeed that effect is larger than the effect at Site A. In this case, one would conclude that the performance of Task 1 is not specific to processing at Site A.

An additional consideration is whether there is a general effect of TMS. That is, whether the delivery of TMS to visual cortex, irrespective of the location of delivery, leads to disturbances in performance during visual tasks. It is important therefore, to also contextualise the effects of TMS with a no TMS baseline. If the effects are truly map specific then there should be no significant difference between the effects of TMS of the non-target site and both the CON and the no TMS baseline. All four TMS studies reported in Chapters 4-7 therefore, include CON and a no TMS baseline conditions.
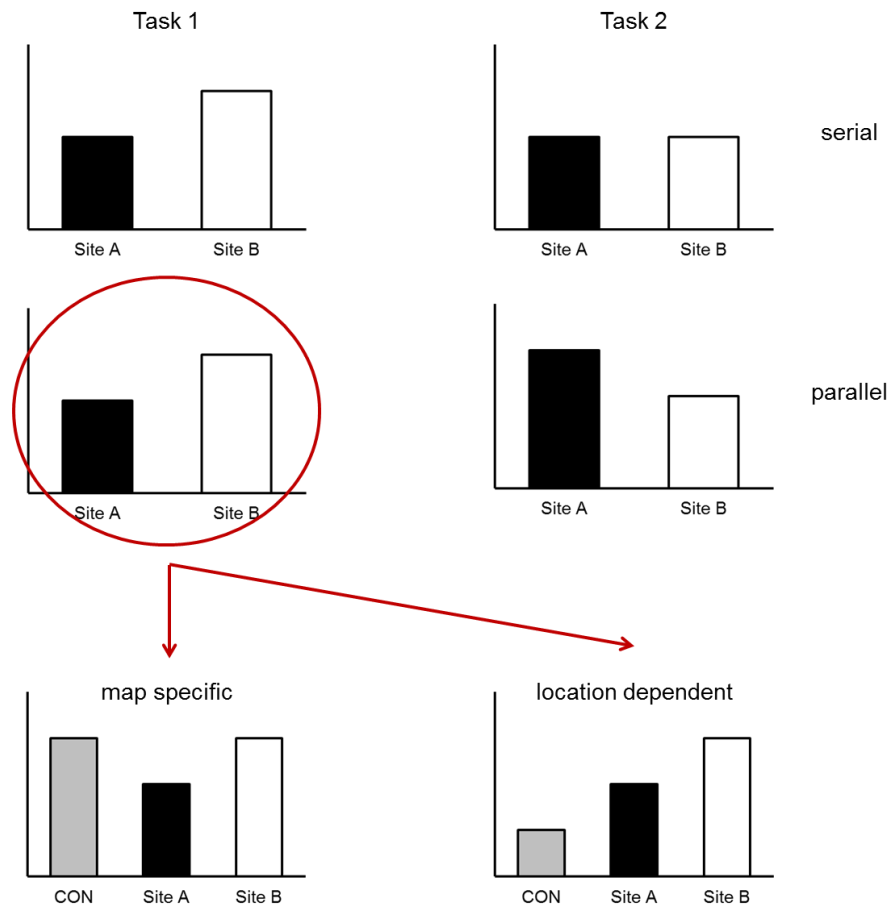
Figure 1.11: *Theoretical framework schematics for map specific processing. The predicted effects of TMS in both the serial and parallel frameworks are reproduced. When considering Task 1 alone, there is no difference in the predicted effects of TMS between the serial and parallel frameworks **(red circle)**. Only when we place the effects of TMS of Sites A & B in the context of TMS of the CON, can we make map specific inferences. The effects of TMS can only be interpreted as map specific (1) if there are significant differences between the effect of TMS at the target Site **(Site A in this case)** and the effects of TMS at both the non-target Site **(Site B in this case)** and the CON and (2) there is no significant difference between the effects of TMS at the non-target site and the CON. If however, this pattern is not observed, a more parsimonious explanation for the differential effects of TMS of Sites A & B may be that performance of Task 1 operates along a location dependent mechanism. In other words, performance of Task 1 involved multiple areas and is therefore, not specific to a single visual field map.*

Within each experimental chapter, the hypotheses were influenced heavily by the two components of the framework described above. Additionally, these components served to guide the analysis and subsequent interpretation of the results. The specific predictions are discussed in detail in each experimental chapter. Therefore, I provide a brief analytical overview here. In each experimental chapter, two visual tasks were employed. It was hypothesised that the two tasks would be underpinned by different regions. For this to be

the case, an interaction between Task and Site should therefore, be evident. The initial analysis step was to establish the significance of the Task by Site interaction using two-way repeated measures analysis of variance (ANOVA) tests. In order to make *map specific* inferences it will be essential to initially establish a significant Task by Site interaction. In the event that a significant Task by Site interaction is not found, the interpretation would be that the two tasks are not underpinned by different regions. If a significant Task by Site interaction is present, the effect of site across the two tasks needs to be considered separately. Within each task, it will be important to demonstrate a significant effect of Site (including no TMS baseline). A significant effect of Site however, cannot by itself differentiate between the two alternative frameworks; additional between Site comparisons are needed for that. If a significant effect of Site is not present, the interpretation must be that none of the cortical targets underpin performance of the task specifically.

1.7: General Aims & Objectives

I aim to use the relatively novel combination of fMRI visual field mapping and TMS to independently probe the functional specializations present within subdivisions of lateral occipital cortex, including LO1 and LO2 directly. This approach will allow, for the first time, the causal nature of computations performed within these maps to be determined. In order to do this TMS will be employed to examine the effects of stimulation across visual discriminations of three relatively low-level visual attributes. Specifically, I aim to examine the effects of lateral occipital cortex stimulation on discriminations of orientation, motion and shape.

Chapter 2

Methodology & Visual Stimuli

2.1: Overview

The initial aim of this chapter is to provide an overview of the major methodological considerations and approaches undertaken throughout the thesis. These include the use of visual psychophysics, the major factors involved in TMS and probing the properties of visual field maps using fMRI. Additionally this chapter aims to outline the rationale for employing retinotopically-guided TMS and describe the three-stage process adhered too for all TMS studies.

2.2: Measuring Behaviour with Visual Psychophysics

Throughout the thesis, we hoped to explore the functional roles played by subdivisions of lateral occipital cortex in the processing of three different visual attributes; orientation, motion and shape. In order to maximise the potential of TMS to elucidate the roles played by our cortical targets, precise measurements of behaviour were needed. Precise measurements of behaviour can be achieved through psychophysical techniques. The following section provides an overview of the method of constant stimuli; the psychophysical method employed here.

During the method of constant stimuli, the percentage of observations as a function of stimulus intensity is determined (Gescheider, 1997). A series of stimulus intensities or levels are chosen. This fixed set of stimulus intensities are presented multiple, but equal, times in a randomised fashion. After each stimulus presentation the observer reports whether or not the stimulus was detected (*establishing the absolute threshold*) or whether the stimulus was stronger or weaker than a fixed reference stimulus (*establishing the difference threshold*). In our psychophysical experiments we derived difference thresholds. Subjects were required to judge whether the test stimulus was of a greater or weaker magnitude than the reference. In such a discrimination experiment, we can calculate the *point of subjective equality (PSE),* which represents the value of the test stimulus that over a large number of trials was on average perceived subjectively as equal to the reference

(Gescheider, 1997). Often the *PSE* is not exactly equal to the reference value, with the difference between the two given as the constant error (Gescheider, 1997). Once each stimulus has been presented an equal number of times, the proportion of greater and weaker responses is calculated for each stimulus level. If there were fixed thresholds for detection, the psychometric function would show a sharp transition from perceived to not perceived. Psychometric functions, if acquired with appropriate stimulus intensities, seldom show this sharp transition. The resulting function is typically a sigmoid (s shape) curve. Often the cumulative Gaussian distribution is used to model the function. The method of constant stimuli is commonly adopted over other psychophysical paradigms, such as adaptive staircases, when subjects are naive or lack sufficient experience with psychophysics. The pool of subjects in the current body of work included both experienced psychophysical observers and entirely naive subjects and therefore, the method of constant stimuli was selected.

2.3:   Visual Stimuli

In order to explore the processing of orientation, motion and shape, our stimuli must be suitably selected and controlled precisely.   Throughout the thesis we employed sinusoidal gratings (either presented static or drifting) and radial frequency patterns, in order to probe orientation, motion and shape perception. The following sections describe some of the findings that have arisen through their use.

2.3.1:   Sinusoidal Gratings

The motion and orientation studies reported in Chapters 4-6 made use of luminance modulated sinusoidal gratings. These simple, yet important stimuli allow one to examine orientation and motion discrimination with a high level of accuracy. In both cases, one need only change a single stimulus feature at a time; either orientation or speed. These stimuli ensure a high level of experimenter control, which is important when measuring behaviour. Sinusoidal gratings, like the ones employed here, have been used repeatedly to demonstrate orientation and motion selectivity across different species and investigative paradigms. In terms of orientation discrimination, these stimuli have been used to provide a neural basis for the oblique effect (Taylor, 1963), by demonstrating significantly greater

proportions of neurons in cat V1 tuned to the cardinal axes than to oblique orientations (Li, Peterson & Freeman, 2003). Grating stimuli have also been used to demonstrate orientation, size and spatial frequency selectivity within human visual cortex (Blakemore & Campbell, 1969). In addition, the dependency of orientation discrimination on spatial frequency (Burr & Wijesundra, 1991), and the maintenance of the oblique effect across a large range of spatial frequencies (1-35 cpd) (Campbell & Kulikowski, 1966), were demonstrated through the use of luminance modulated sinusoidal gratings. A final point on the use of grating stimuli for orientation discrimination is that they have been used successfully to assess achromatic as well as chromatic orientation processing (Webster & DeValois & Switkes, 1990) - a feature that is important for the studies reported in Chapter 7.

Sinusoidal gratings have also been employed successfully to study a number of aspects of motion perception. Early work in non-human primates demonstrated direction selective neurons in both cat and macaque visual cortices (Adelson & Movshon, 1980). In human, these stimuli have been used to demonstrate that speed discrimination is contrast dependent (Thompson, Stone & Stone, 1992). Indeed, when two gratings drifting at the same speed are presented simultaneously, the lower-contrast grating appears slower across a wide range of contrasts (0.25-50%) (Thompson et al., 1992). More recent studies using imaging techniques have demonstrated direction (Singh, Smith & Greenlee, 2000) and motion selectivity in human V5/MT and V3A (McKeefry et al., 2008) and moreover, these stimuli have also been used in neurostimulation studies of human speed perception (McKeefry et al., 2008).

Taken together, the findings from previous studies of orientation and motion discrimination serve to highlight the value and importance of sinusoidal gratings. The choice of stimulus selection was heavily influenced by those studies mentioned above (and many more).

2.3.2:   Radial Frequency Patterns

Stimuli selected to probe shape processing were radial frequency (RF) patterns (Wilkinson, Wilson & Habak, 1998), created by deforming the radius of a circle via a sine wave, depicted in Figure 2.1. The solid black line in the top-left of Figure 2.1, (adapted from

Bell, Badcock, Wilson & Wilkinson, 2007) shows how sinusoidal modulation of a circle creates smooth deviations from circularity, with the frequency of complete cycles within 360° defining the number of deformations and the amplitude of the sine wave (radius°) defining the magnitude of those deformations. The top right of Figure 2.1, illustrates a RF3 pattern; there are three complete cycles and therefore, three smooth deviations from circularity. The bottom panel of Figure 2.1 illustrates three examples of RF3 patterns with different amplitudes. These three stimuli can be seen to vary from smooth to spiky (Left-right).
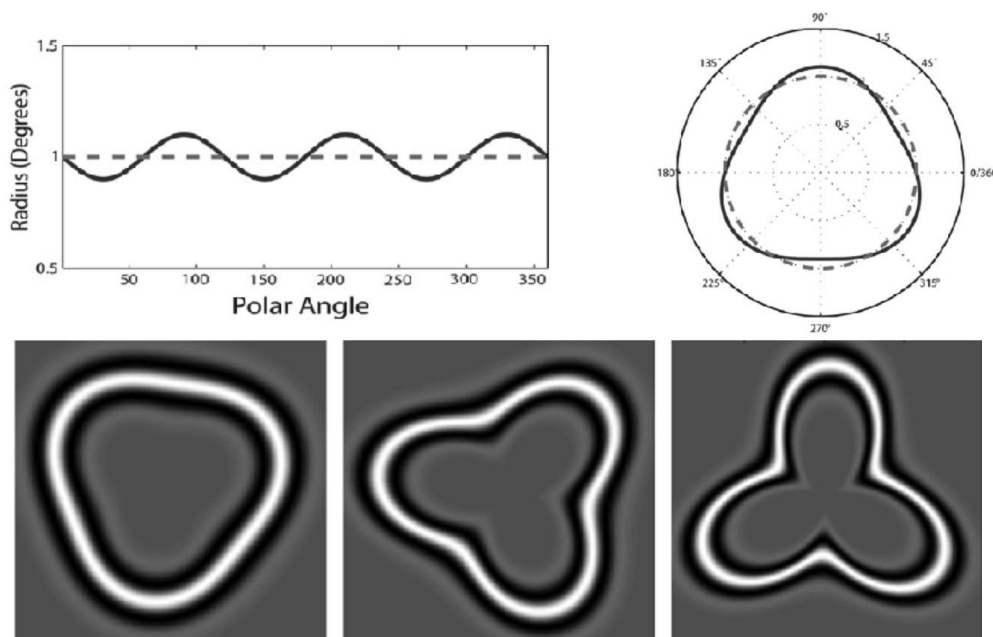
Figure 2.1: *Schematics and examples of radial frequency patterns. Deforming a circle with a sine wave creates smooth deviations from circularity (**solid black line**), defined by the frequency and amplitude of the sine wave (**top panel**). Examples of radial frequency patterns (**bottom panel**). The RF patterns have the same frequency (3), differing only in the amplitude of the sine wave. Modification of the amplitude of the sine wave (from small to large) creates shapes that vary on a smooth (**bottom panel: left**) to spiky (**bottom panel: right**) axis. The phases (orientation) of the radial frequency patterns have been randomised.*

RF patterns have been used previously to investigate various aspects of intermediate vision including contour integration (Wilkinson et al., 1998), local and global shape processing (Bell et al., 2007) and even the processing of biological shapes (Wilson, Loffler & Wilkinson, 2002; Wilson & Wilkinson, 2002). Wilkinson and colleagues (Wilkinson et al., 1998) measured subject's detection thresholds for several radial deformations of circular

contours. They found that even with 167ms presentation, subjects were able to identify radial frequencies of six cycles and below with over 90% accuracy, sensitivity peaked with radial frequencies of 3. Subject's ability to detect these radial deformations was said to be in the hyper-acuity (Westheimer, 1975) range. More recently RF patterns have been presented during fMRI experiments to demonstrate different spatial scales of shape similarity in lateral and ventral portions of the LOC (Drucker & Aguirre, 2009). The authors used RF patterns to demonstrate a coarse coding of shape within lateral LOC, and a fine-scale coding of shape within ventral LOC. The coarse shape coding in lateral LOC regions is suggested to allow the representations of features to be combined with orientation and/or retinotopic information (Edelman & Intrator, 2000) to capture shape information (Drucker & Aguirre, 2009). The use of RF patterns to study shape processing was influenced by previous work. Importantly, the shapes of the RF patterns could be modified with the same level of control as the sinusoidal gratings employed in our discriminations of orientation and motion. That is, through modification of the amplitude only, we could create different shapes.

Taken together these stimuli allowed us to probe the functional specializations present in lateral occipital cortex to orientation, motion and shape with equal levels of stimulus control.

2.4:   Disrupting Behaviour with Transcranial Magnetic Stimulation

Having measured behaviour psychophysically, we hoped to elucidate the regions of lateral occipital cortex causally involved in mediating such behaviours by inducing selective disruptions to normal neural processes, through the use of TMS. The following sections outline some of the major factors involved in TMS stimulation.

Notwithstanding the importance, nor impact that fMRI, has had on our understanding of human cognitive function, fMRI is limited by a major factor – causality. This technique cannot demonstrate that a particular cortical region is necessary for the performance of a particular cognitive function (Price & Fiston, 2002). In contrast, TMS allows causal inferences to made, via its ability to induce localised disruption to specific cortical areas and thus create 'virtual lesions' (Pascual-Leone, Walsh & Rothwell, 2000; Walsh & Cowey, 2000; Cowey & Walsh, 2000; Huang, Edwards, Rounis, Bhatia & Rothwell, 2005;

Cowey, 2005). TMS therefore, provides a means by which to study causal brain-behaviour relationships in the healthy individual which, prior to the inception of TMS was only possible through neuropsychological studies, the results of which can be troublesome to interpret. Deficits following head trauma, are typically catastrophic and diffuse in nature, making definitive interpretations as to which region underpins which task difficult. TMS avoids several interpretation issues associated with the results of patient studies, such as, individual differences in pre-trauma abilities. The great advantage of TMS however, lies in its ability to be delivered with a high degree of both spatial and temporal precision.

2.4.1:   Different Forms of TMS

TMS can be delivered in a number of ways. In its most basic form single TMS pulses are administered at a constant rate (typically 1Hz). Pulse trains can also be delivered repetitively (rTMS) in a series of pulse trains. A third method for TMS stimulation is referred to as 'theta burst', which involves the delivery of short burst, high frequency (50-100Hz) pulse trains (Huang et al., 2005).

2.4.2:   How Does TMS work?

TMS operates via the principle that when a rapidly alternating electrical current is passed through a metal coil (stimulating coil) a magnetic field is induced that flows orthogonally to the orientation of the coil (Walsh & Cowey, 2000; Cowey & Walsh, 2000; Cowey 2005). When the stimulating coil is placed upon the scalp, the magnetic field penetrates through the skull and induces an electrical current within the underlying cerebral cortex (Hallett, 2002; 2007). The induced electrical current runs perpendicular to the magnetic field, and in turn, temporarily alters normal neuronal functioning. The action of TMS is schematised in Figure 2.2.
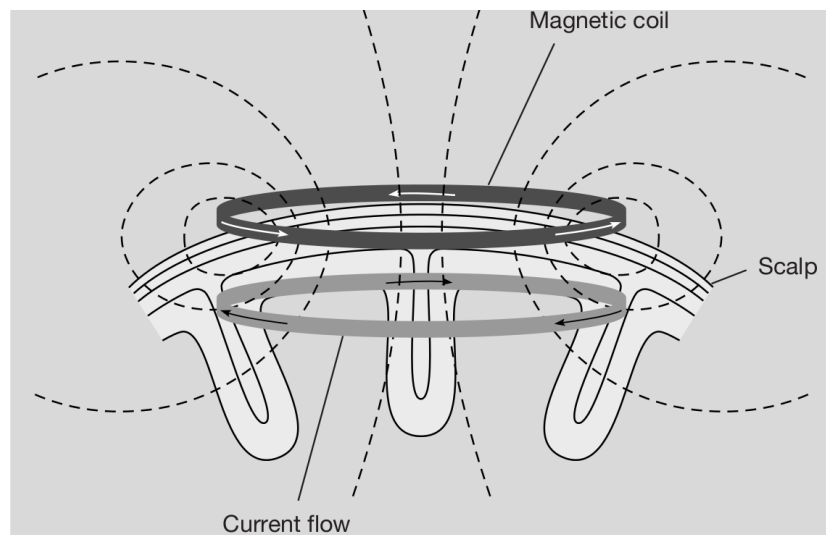
Figure 2.2: *Schematic representation of the action of TMS. The flux lines **(dashed lines running vertically)** of the magnetic field can be seen to flow perpendicular to the plane of the magnetic coil **(dark grey ring)**. The magnetic field penetrates the scalp and induces an electrical current flow perpendicular to the magnetic flux lines **(light grey ring)**. Adapted from Box 1 Hallett (2002).*

The exact mechanisms by which TMS exerts its effects, however, are not fully understood, presumably owing to reports of both facilitatory and inhibitory effects of TMS on various aspects of cognitive functioning (Hallett, 2007). Whether TMS produces excitatory or inhibitory neuronal effects appears to depend on a multitude of factors including the timing, strength and temporal make-up of the TMS pulses (Hallett, 2007).

Allen and colleagues (Allen, Pasley, Duong & Freeman, 2007) provided a direct neurophysiological demonstration of the effects of TMS in cat visual cortex. TMS of cat visual cortex during visual stimulus presentation led to a transient increase in the firing rate of neurons not typically responsive (under no TMS conditions) to the visual stimulus. The observed increase in background spontaneous activity was also accompanied by simultaneous inhibition in the firing rate of neurons actively responsive to the stimulus. The inhibitory effects of TMS were found to be temporally robust, suppressing visually evoked activity for up to 10 minutes post TMS stimulation. Allen and colleagues further demonstrated a coupling between the induced neuronal changes and changes in oxygenation and blood flow to the stimulated cortical area (Allen et al., 2007).

In human studies, TMS is typically employed to demonstrate causal roles between cortical areas and the performance or perception of particular stimulus attributes (McKeefry et al., 2008) or categories (Pitcher et al., 2009). In these instances, TMS is often described as disrupting normal cognitive functioning through the introduction of random neural firing or 'neural noise'. Several suggestions have been proposed to account for the induced reduction in signal to noise ratio, citing either a loss in the stimulus driven signal strength (Harris, Clifford & Miniussi, 2008) or an increase in spontaneous background neuronal noise (Ruzzoli, Marzi & Miniussi, 2010). Harris and colleagues (2008) had subjects make orientation judgements of simple orientated gratings whilst manipulating the background noise in the image. The interaction between the effect of V1 stimulation and background noise was interpreted as TMS reducing the relevant signal strength, rather than increasing the background neuronal noise in the system (Harris et al., 2008). In contrast, Ruzzoli and colleagues (2010) investigated the effects of single pulse TMS of V5/MT on the shape of psychometric functions for a motion-direction discrimination task. The task had two elements, dots that moved coherently in one direction and randomly moving dots. The effect of V5/MT stimulation was to reduce the slope of the psychometric function, which was interpreted as reflecting an increase in random neural noise plus a decrease in system sensitivity (Ruzzoli et al., 2010). Additionally, the relative degree to which TMS facilitates or suppresses cognitive function appears to depend on the activation state of the neurons prior to TMS delivery (Silvanto, Muggleton, Cowey & Walsh, 2007). Under neuronal adaptation (repeated exposure to the same stimulus decreases the firing rate of the encoding neurons over time) the delivery of TMS increases the firing of the adapted neural populations, whilst suppressing the activity of neural populations unaffected by the adaptor stimulus. In the case of adaptation, TMS is suggested to exert its effects on the least active neurons (Silvanto et al., 2007). Relatively recently, it was suggested that TMS investigators should strive to move away from the 'virtual lesion' conceptualisation of TMS and rather, interpret the effects of TMS with respect to models of psychological processing, with a special emphasis on signal detection theory (Miniussi, Ruzzoli & Walsh, 2010). In this framework, one can explain facilitatory and inhibitory effects of TMS within the same model, rather than interpreting inhibitory effects as virtual lesions and facilitatory effects as paradoxical (Miniussi et al., 2010).

2.4.3:   The Spatial Resolution of TMS

An exact measure of the spatial resolution of TMS (in mm or cm) cannot be given as the induced effects depend on a plethora of factors; initial activity of neurons in the stimulated region of interest (Silvanto et al., 2007) stimulation intensity (McKeefry et al., 2008) stimulation frequency (Huang et al., 2005) and the behavioural metric used to evaluate the effect of TMS, to name but a few. Estimates of the spatial resolution of TMS can however, be made and are aided by knowledge of cortical organisation. For instance, in visual cortex, Kammer (1999) demonstrated that phosphenes (perceived dots of light, in this case induced by stimulating parts of V1) can be elicited with a spatial resolution of 1-2 degrees of visual angle, which corresponded to approximately 10-20mm of cortex, mapped functionally (Kammer, 1999). Coil Displacement as small as 1cm along the scalps surface can shift the perceived retinal location of phosphenes (Walsh & Cowey, 2000; Cowey, 2005). Recently, TMS induced dissociations have been reported between stimulation sites separated by approximately 7.8mm (Pitcher et al., 2009); although of note, these measurements were derived from transformation between individual's native space and MNI space, which could therefore, lead to distortions. A commonly accepted estimate of the spatial resolution of TMS appears to be in the range of 1cm (Walsh & Rushworth, 1999; Cowey, 2005).

2.4.4:   Localising the Site of TMS stimulation

The limiting step in any TMS endeavour is the precision with which the TMS coil can be positioned so that the induced neural disruption is centred on the cortical target of interest. TMS investigators routinely employ a number of localisation methods, which differ in their accuracy and reliability. In order to maximise the potential of TMS to probe the functional properties of specific brain areas, it is fundamentally important to have detailed information regarding how and where specific visual areas are mapped across the cortical surface of individuals. Of paramount importance therefore, is to establish a spatial framework within which, areas are identified and localised in each individual. The use of retinotopic mapping techniques, which allows for detailed and precise delineation of visual areas, provides such a framework.

Although it is commonly hypothesised that the basic organisation of the visual cortex is maintained across individuals, subtle variation in the size, position and orientation of visual field maps illustrates the necessity of identifying these maps in individuals. For example, visual field map sizes can vary by a factor of two between different subjects (Stensaas, Eddington & Dobelle, 1974; Andrews, Halpern & Purves, 1997; Dougherty et al., 2003; Duncan and Boynton, 2003). The variations in location are not trivially solved using anatomical landmarks on an individual's scalp or cortex. Indeed, McKeefry et al., (2009) highlighted how this individual variation can be particularly problematic for visual TMS studies, where placement of the coil on the subjects scalp has often been performed with limited knowledge of the underlying cortical organisation of the individual being stimulated. A relatively common method in TMS studies is to localise particular cortical stimulation sites based on the external anatomy of the skull, measuring particular distances from a fixed location, such as the inion (Ellison & Cowey, 2006). As such, these methods do not account for the identified variation in visual area location across subjects.

Sack and colleagues (Sack, Kadosh, Schuhmann, Moerel, Walsh & Goebel, 2009) systematically compared the accuracy of four commonly employed methods of TMS coil localisation. The authors compared the accuracy with which each of the four methods could localise the inter-parietal sulcus (IPS) and measured the induced TMS effects on a subsequent mental arithmetic task. The effects of TMS of the IPS were compared using the following four methods (1) Individual fMRI-guided TMS neuronavigation, (2) individual MRI-guided TMS neuronavigation, (3) group functional Talairach coordinates and (4) 10-20 EEG position (P4). A systematic difference in the efficacy of the TMS effect was observed between the four approaches. The individual fMRI-guided TMS neuronavigation yeilded the strongest behavioural effect, with the P4 stimulation yielding the weakest. Power analyses indicated that the number of necessary participants needed to achieve a significant effect of TMS increased systematically across localisation methods. For instance, although five participants were sufficient to reveal a significant behavioural effect during fMRI-guided localisation, this number increased to 9 for the MRI anatomical localisation method, to 13 in the case of group averaged Talairach coordinates and to 47 when TMS was localized using the P4 method.

2.5:   The Use of fMRI

Probing the functional properties of specific visual field maps in human is not a novel endeavour. Indeed, throughout the literature many experiments that have done so using a variety of neuroscience tools, including PET (Lueck et al., 1989; Zeki, 1990) and fMRI (McKeefry & Zeki, 1997; Wandell et al., 2005; Brewer et al., 2005; Larsson and Heeger 2006; Wandell et al., 2007). Despite these endeavours however, a vanishingly small number of studies have employed TMS to probe the functional properties of individual visual field maps (McKeefry et al., 2009), presumably due to their small size and close proximity (adjacent visual field maps abut one another). One novel contribution made by this thesis lies in the successful use of retinotopic mapping to guide the TMS coil so that LO1 and LO2 may be stimulated independently. The following section provides a brief description of the fMRI methodology, how it has been employed in the study of visual field maps, including LO1 and LO2 and finally why, and under what circumstances TMS may provide a more fruitful and informative tool.

2.5.1:   Probing Visual Field Maps with fMRI

Functional MRI provides an indirect, correlational measurement of neuronal activity, through measuring hemodynamic responses over time. Critical to fMRI is the assumption that an active region of the brain requires an increase in energy in the form of glucose and oxygen (Logothetis 2008). An increase in neural firing in turn increases cells' metabolic demands and consequently, increases the demand for replenishment. The energy required for cell firing is transported throughout the body in the form of haemoglobin. Oxy and deoxy-haemoglobin have magnetic properties that are detectible at different strengths with fMRI. Changes in the concentration of oxy:deoxy haemoglobin within a region of the brain therefore, provides an indirect measure of neural activity. An active brain region will contain a higher concentration of deoxy-haemoglobin relative to non-active regions of cortex. The change in oxygenation concentration is referred to as the Blood Oxygenation Level Dependant (BOLD) response; fMRI measures changes in BOLD over time (Logothetis, 2008).

The great advantage of fMRI, over other neuroimaging techniques such as EEG and MEG, lies in its spatial resolution (Logothetis, 2008). Despite this ability however, fMRI is

limited in terms of temporal resolution, by the time-delay between neuronal activity and the replenishment of oxygen to active cells. Neural activity, in the form of action potentials, occurs rapidly (a few ms) following the onset of a stimulus, whereas the replenishment of oxygen is of the order of several seconds, with a peak occurring ~6sec post stimulus onset, referred to as the hemodynamic response function (HRF). The HRF is highly reliable, forming a canonical tool for many software packages (SPM, FSL) which employs the HRF to convolve fMRI time-series data. Despite the poor temporal resolution the BOLD response does however, correlate with action potentials (Logothetis, Pauls, Augath, Trinath, & Oeltermann, 2001).

A plethora of studies have successfully employed fMRI to elucidate the responsive nature of many different visual field maps across both dorsal (Larsson & Heeger, 2006; Amano et al., 2009) and ventral (McKeefry & Zeki, 1997; Wandell et al., 2005; Brewer et al., 2005; Arcaro et al., 2009; Winawer et al., 2010) surfaces of the occipital lobe. Notwithstanding the importance, nor impact of such findings, they are nonetheless constrained by the major limitation inherent in the BOLD signal – causality. As a result, fMRI cannot demonstrate definitively that neural activity within a spatially specific area of cortex is essential for, or causally related to, a particular characteristic of perception or cognition. In direct contrast, TMS has the ability to induce spatially specific disruption to normal cortical activity, providing a unique opportunity to identify causal links between brain and behavior in neurologically healthy human subjects. The application of TMS provides a means to examine the specific computations performed by individual human visual field maps. Indeed, the assessment of causality in brain-behaviour relationships is thought by some (Silvanto & Pascual-Leone, 2012), to require brain stimulation.

In the case of LO1 and LO2, previous work has exclusively employed fMRI (Larsson & Heeger, 2006; Larsson et al., 2006; Sayres & Grill-Spector, 2008; Amano et al., 2009). Utilising TMS offers the potential to demonstrate, for the first time, causal links between neural activity within LO1 and LO2 and particular features of visual perception. LO1 and LO2 are superb candidates for TMS stimulation (McKeefry et al., 2009). LO1 and LO2 are superficial sources, located on the dorsal and lateral surface of the brain, making them 'ripe' for TMS stimulation (McKeefry et al., 2009). The main point here is that where appropriate, TMS may provide a more valuable tool than fMRI to probe causal relationships. There are of

course, scenarios where the use of TMS is redundant. For instance, there are a number of visual field maps that have been identified on the medial and ventral surfaces of the brain (McKeefry & Zeki, 1997; Wandell et al., 2005; Arcaro et al., 2009). These visual field maps make it unlikely, if not it impossible to stimulate precisely with TMS. In these circumstances, the use of fMRI is clearly favorable; however, when the opportunity presents, TMS may provide a more informative neuroscience tool.

2.5.2:   Advantages of Retinotopically-Guided TMS

The results of Sack et al (2009) indicate that fMRI-guided TMS is the most accurate method to localise the site of TMS stimulation. Often the site of TMS localisation is selected on the basis of the peak responding voxel in functional localiser scans (Pitcher et al., 2009). Although these localisers can account for individual variation in anatomical location, they are inappropriate for identifying areas of cortex with poorly defined functional properties, such as LO1 and LO2. In these cases, retinotopic mapping allows the localisation of smaller and more specific regions of visual cortex, compared to regions defined using functional localisers, such as LO. Indeed, these functionally selective areas are often large and encompass multiple visual field maps (Larsson & Heeger, 2006; Wandell et al., 2007; Amano et al., 2009; Arcaro et al., 2009). Combining retinotopic mapping with TMS allows investigators to probe the contributions of single cortical areas to the performance of particular tasks in a precise and accurately targeted manner. The marrying of the two techniques provides visual neuroscientists with the platform to investigate the properties of human visual cortex at a relatively new spatial scale.

The current body of work diverges from previous studies of LO1 and LO2 in that it employs the use of fMRI visual field mapping in order to localise LO1 and LO2 so that they may be targeted with TMS. Such a paradigm has been implemented successfully in the study of visual areas, V5/MT and V3A (McKeery et al., 2008). The use of visual field mapping is essential given the individual variation in size, location and orientation of LO1 and LO2 reported previously (Larsson & Heeger, 2006). Importantly, the use of TMS in this regard allows for causal inferences to be made and is a necessary step (Silvanto & Pascual-Leone, 2012) in order to elucidate the functional specializations exhibited by LO1 and LO2 – which are currently unknown.

2.6:   Our Paradigm – Three Stage Experimental Approach

An important feature of the current body of work is that the experimental protocol for all psychophysical and TMS studies remained constant. That is, the basic spatial and temporal organisations of the psychophysical and TMS experiments were identical across studies, as were the TMS stimulation parameters and simulating coils. Each TMS study adhered to a strict three-stage process of: (1) Identification of cortical targets, either through fMRI visual field mapping techniques (in the case of LO1 and LO2) or anatomical landmarks (in the case of V5/MT); (2) measuring discrimination thresholds for each individual subject on a variety of visual tasks using the method of constant stimuli and (3) delivery of TMS pulses to our cortical targets (LO1, LO2 & V5/MT) in individual subjects whilst those subjects perform visual tasks at threshold. This adherence to the same methodological processes allows the results from the different experiments to be compared directly. The following sections describe in full the three stage process implemented in each TMS experiment.

2.6.1:   Stage 1 – Identification of Cortical Targets

The initial stage of each study relied upon identifying LO1 and LO2 in individual subjects. A full description of fMRI visual field mapping techniques, and how they were implemented is provided in Chapter 3, along with detailed descriptions and analyses of the retinotopic features defining LO1 and LO2. Briefly, LO1 and LO2 are adjacent mirror-image representations of the contralateral visual field on the lateral surface of the occipital lobe (Larsson & Heeger, 2006). The visual field mapping experiments conducted throughout the thesis allowed LO1 and LO2 to be identified in at least one hemisphere in each subject. Overall LO1 and LO2 were identifiable in ~90 % of hemispheres tested, an identification rate slightly higher than that reported previously (Larsson & Heeger, 2006).

Definitions of V5/MT were made anatomically following published guidelines (Dumoulin, Bittar, Kabani, Baker, Le Goualher, Pike & Evans, 2000). The V5/MT target site was located in the ascending limb of the inferior temporal sulcus (ALITS) in all subjects. Given the reliability in anatomical location of V5/MT relative to common gyral and sulcal patterns, an anatomical method of identification is justified (Dumoulin et al., 2000).

Additionally, functional confirmations of these anatomical targets were possible in a subset of subjects (n = 4). In these subjects the anatomically defined V5/MT target was not only located within the ALITS, but also, the region of cortex maximally responsive to the presentation of moving over static gratings during fMRI acquisition. Subjects S1, S6, S7 & S12, participated in a standard motion selective localiser (see Appendix for full fMRI protocol). Subjects viewed two luminance modulated sinusoidal gratings, presented in a circular aperture (diameter 4°) at 50% contrast. Stimuli were centred at 10° eccentricity along the horizontal meridian into both the left and right visual fields. A standard block design (12 sec on/12 secs off) was employed. Subjects fixated a central black dot (diameter 0.3°). Within a motion block, the stimuli drifted at 8°/sec. The direction of drift (left-right/right-left) reversed every 3 secs. Static and motion blocks were alternated. The results of the motion localiser are plotted in Figure 2.3, for subjects S1, S6, S7 and S12. The left column of Figure 2.3, depicts motion selective regions of cortex on saggital and axial slices of the right hemisphere. The crosshairs are centred on the anatomically defined V5/MT target sites. The middle column of Figure 2.3, depicts the BOLD responses derived from the contrast motion > static on right hemisphere surface reconstructions. In all subjects, the anatomically defined target sites (blue circles) can be seen to not only fall within the ALITS, but also within the region of cortex maximally active during motion blocks. The right column of Figure 2.3, depicts the average time-course from the functional V5/MT ROI. Given the correspondence between the anatomical and functional definitions of V5/MT illustrated in this subset of subjects, I am confident therefore, that the cortical region stimulated with TMS was indeed the V5/MT complex in all subjects.
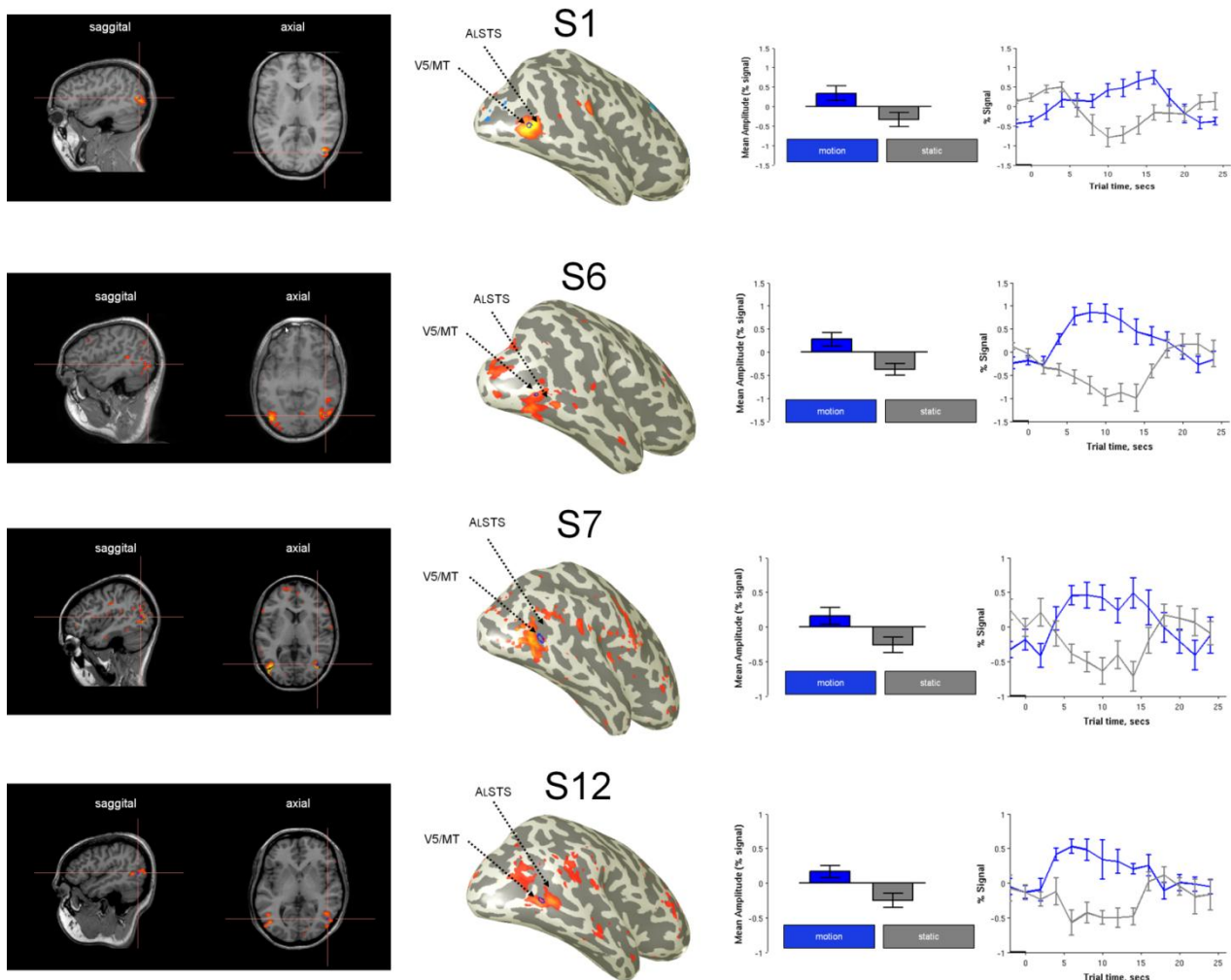
Figure 2.3: *Correspondence between anatomical and functional definitions of V5/MT. The anatomical and functional definitions of V5/MT are compared for subjects S1, S6, S7 & S12. **Left column:** motion selective regions of cortex are depicted on saggital and axial slices of the right hemisphere of all subjects. The crosshairs are centred on the anatomically defined V5/MT targets for TMS. Images are depicted in neurological convention. **Middle column:** motion selective regions of cortex are depicted on partially inflated surface reconstructions of the right hemisphere. In all subjects the anatomically defined V5/MT TMS targets are depicted by the blue circle and can be seen to (1) fall within the ALITS and (2) fall within functional definitions of V5/MT. **Right column:** mean time-series plots, plus mean signal amplitudes from the functionally defined V5/MT ROIs. In all subjects, activity within V5/MT can be seen to be modulated (positively) by the onset of moving stimuli. Taken together, these data show a good correspondence between our anatomical and functional definitions of V5/MT.*

2.6.2:   Stage 2 – Visual Psychophysics & the Method of Constant Stimuli

The second phase of each study was to establish individual discrimination thresholds using visual psychophysics employing the method of constant stimuli. Stimuli employed in all psychophysical and TMS studies reported in this thesis were generated using MATLAB (Mathworks, USA) and displayed on a Mitsubishi Diamond Pro 2070[SB] display with a refresh rate of 60 Hz, controlled by a VISAGE graphics card (Cambridge Research Systems [TM]). Prior to the acquisition of psychophysical data, the monitor was calibrated and Gamma correction procedures were undertaken. The luminance output of most monitors is not proportional to the voltage of the applied signal, but to some power of this voltage. The voltage/luminance can even vary across screens of the same make and model. Gamma correction was performed using the VISAGE in order to accurately reproduce stimulus contrast and/or absolute luminance values. The VISAGE outputs a sequence of voltage levels for each active colour-gun in a target area of the screen. The inverse voltage-luminance curves are calculated to correct the non-linearities. The values from the Gamma correction are provided in Table 2.1.

Table 2.1: *Results of Gamma correction. The values of the Gamma corrected colour-guns are given in CIE space along with the min and max luminance measurements for each colour-gun*

Gamma Correction				
Phosphor Coordinates CIE			Luminance cd/m^2	
	x	y	Min	Max
R	0.6100	0.3460	0.0000	14.9900
G	0.2800	0.5940	0.0000	51.7100
B	0.1420	0.0700	0.0000	9.7500

Psychophysical tasks for all TMS studies initially comprised seven linearly spaced stimulus intensity levels (including a reference) that spanned a range of values either side of the reference. Orientation discrimination psychometric functions from two representative subjects are shown in Figure 2.4. During orientation discrimination seven orientations were selected that spanned a range of orientations more vertical and more horizontal than 45° –

the reference. Subjects were required to judge whether the test grating was more vertical or horizontal relative to the reference. The proportion of vertical responses for each orientation was then calculated. In both examples, the functions are well described by sigmoid curves.
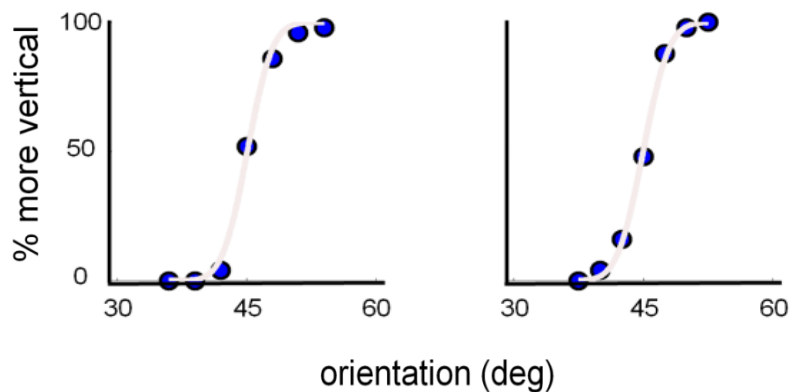
Figure 2.4 *Example psychometric functions. Orientation discrimination psychometric functions are plotted for two representative subjects. Orientation is plotted on the x axis, with the proportion of more vertical responses plotted on the y axis. Seven orientations (**blue circles**) were presented that spanned a range of orientations more vertical and more horizontal than the reference (**45deg).** In both examples, the psychometric function (**pale curve)** is well described by a sigmoid curve.*

Throughout the thesis, a single psychophysical protocol was adopted. The spatial and temporal organisation was identical across studies. The studies themselves differing only in the specific stimuli presented. As a result a single description of the psychophysical protocol is provided here, with details of the specific stimuli used in each study provided within each TMS experimental chapter.   The basic spatial and temporal organisation of a single psychophysical trial is plotted in Figure 2.5. In all subjects tested, visual stimuli were centred at 10° eccentricity along the horizontal meridian into the visual field contralateral to the hemisphere in which LO1 and LO2 were most readily identifiable (hemisphere stimulated during subsequent TMS experiments). That is, for subjects in whom LO1 and LO2 were identified in the right hemisphere, visual stimuli were presented into the left visual field and vice-versa. Stimuli were viewed monocularly with the subject's self-reported dominant eye from a fixed distance of 57cm. The placement of the stimuli ensured that they were presented into the visual field contralateral to TMS stimulation. Subjects fixated a central black dot (diameter 0.3°), which remained throughout the studies. A blank screen was

presented first (500ms), followed by a fixed reference stimulus (200ms), an inter-stimulus interval (1200ms) and finally a test stimulus (200ms). Subjects were required to judge whether the test stimulus was of a greater or weaker intensity than the reference, by pressing the appropriate key on a keyboard.
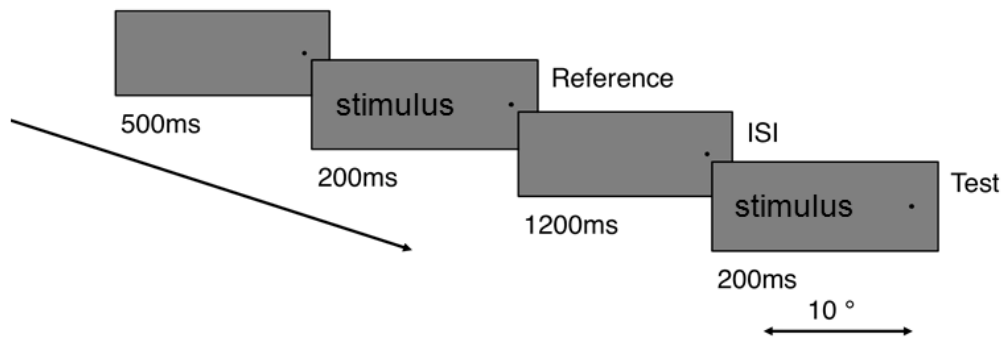
Figure 2.5: *Spatial and temporal organisation of a single psychophysical trial. Throughout all psychophysical studies, stimuli were centred at 10° eccentricity into the visual field contralateral to the hemisphere in which LO1 and LO2 were most readily identifiable – the left visual field In this case. Subjects viewed a central fixation dot (diameter 0.3°) for 500ms. A reference stimulus was then presented for 200ms, followed by a 1200ms ISI and then the test stimulus for 200ms. Subjects were required to judge whether the test stimulus was of a greater or weaker intensity than the reference, by pressing the appropriate key on a keyboard. Subject's responses were recorded after the presentation of the test stimulus.*

To capture individual psychometric functions, seven test stimuli were presented (including one that matched the reference). Selected stimuli spanned a range of values both greater and weaker in intensity than the reference. The seven stimulus levels were linearly spaced from one another. The spacing (step size) of the test stimuli were chosen for each subject on the basis of performance on a single 70 trial pilot run. Pilot runs were not included when calculating psychometric functions. Each subject completed five experimental runs, each run comprising 70 trials (10 trials per stimulus intensity level). Test stimuli were presented in a randomised order. A cumulative Gaussian was fitted to the average data of all runs from each subject to model the psychometric function. Initially thresholds (75% correct) were established for stimuli of a greater and weaker intensity than the reference. In some subjects the best fitting psychometric function may not pass through 50% correct identification when the reference and test stimuli were equal, the *PSE*. This in turn may lead to asymmetric psychometric functions which will result in asymmetric thresholds. In this case, one threshold may be closer to the reference than the other,

illustrated in Figure 2.6. In order to account for this, we defined stimuli that were equidistant from the reference stimulus, but also, approximated threshold (75% correct). Initially, we calculated the 75% correct values for stimuli greater and weaker than the reference. The range between the two 75% correct values was calculated and added to the following equation: TMS stimuli = reference ± range/2
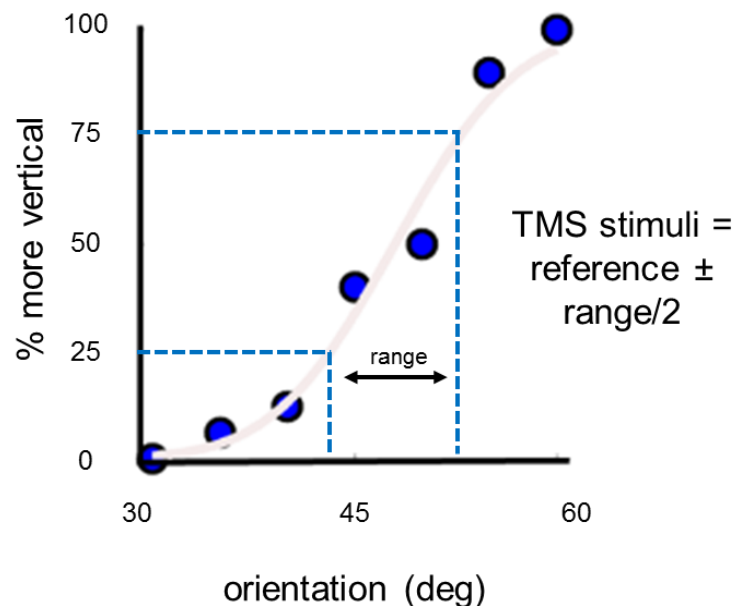
Figure 2.6: *Procedure for defining thresholds to be presented during TMS sessions. An orientation discrimination psychometric function for a single subject is shown. In this case, the function does not pass through 50 % identification when both reference and test stimuli were equal (45°), resulting in an asymmetric function. Initially, the 75% correct more vertical and the 75% correct more horizontal orientations were defined **(dashed blue lines)**. From these it is clear that these thresholds are asymmetrical – one is much closer to the reference than the other. To account for this, the range **(black double-arrow)** between these orientations was calculated and divided in half. TMS stimuli were created by the following equation: TMS stimuli = reference ± range/2. This created two stimuli that were equidistant from the reference.*

2.6.3:   Stage 3 – TMS Protocol

The spatial and temporal organisation of the TMS and psychophysical protocols differed in only one important aspect. During the application of TMS to cortical targets and baseline (no TMS), only the two threshold stimuli (described above) were presented as test stimuli during each TMS task. That is, during TMS sessions, subjects were required to discriminate between the reference stimulus and two test stimuli only (per task). Each TMS session comprised 100 trials (50 per threshold stimulus). The spatial and temporal organisation of a single TMS trial is depicted in Figure 2.7. Subjects viewed an initial blank screen (500ms) followed by the reference stimulus (200ms), an ISI (1200ms) and finally one of the two test stimuli (200ms) selected at random. TMS pulses were delivered concurrently with the presentation of the test stimuli (depicted by the red lightning bolt).
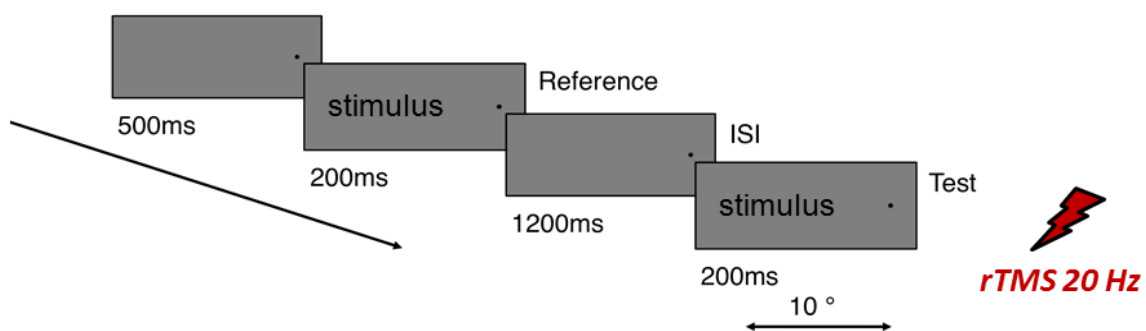
Figure 2.7: *Spatial and temporal organisation of a single TMS trial. Throughout all TMS sessions (and baseline), stimuli were centred at 10° eccentricity into the visual field contralateral to the hemisphere in which LO1 and LO2 were most readily identifiable – the left visual field In this case. Subjects viewed a central fixation dot (diameter 0.3°) for 500ms. A reference stimulus was then presented for 200ms, followed by a 1200ms ISI and then one of two test stimuli for 200ms. 4 biphasic TMS pulses, at 70% of the maximum stimulator output (2.6 Tesla) were delivered concurrently with the presentation of the test stimuli – depicted by the red lightning bolt.*

TMS sessions (task and condition) were counterbalanced across subjects within each study. During TMS sessions a train of 4 biphasic (equal relative amplitude) TMS pulses, separated by 50ms (20Hz) at 70% of the maximum stimulator output (2.6 Tesla) were applied to the subject's scalp using a figure-of-eight coil (50mm external diameter of each ring) connected to a Magstim Rapid2 ™ stimulator (Magstim, Wales). Selecting a fixed stimulation intensity is consistent with a number of recent TMS studies (McKeefry et al., 2008; Pitcher et al., 2009).

A practical consideration when conducting TMS studies is coil temperature, which increases during the delivery of TMS pulse trains. The Magstim ™ system monitors the temperature of the coil and ceases the delivery of pulses when coil temperature reaches a predetermined level. Pilot testing of the adopted TMS protocol indicated a total of 64 pulse trains could be delivered through a single 50mm coil before overheating occurred. Subsequent TMS sessions were therefore, split into two 50 trial (50 pulse trains) sessions. In order to minimise the delay between the first and second halves of each TMS session, two 50mm coils were utilised. The order of use was kept consistent throughout all TMS studies.

The TMS set up is depicted in Figure 2.8. Subjects were seated in a purpose built chair with chin rest and forehead support. The coil, which could be tracked in real-time with respect to the subjects head, was secured mechanically and placed directly above each cortical target with the handle orientated parallel with the floor. The use of a chin and forehead support, coupled with mechanical clamping of the coil dramatically reduced not only subject movement, but also, movement of the coil during stimulation (caused by vibrations) and operator error caused through manual handling of the coil.
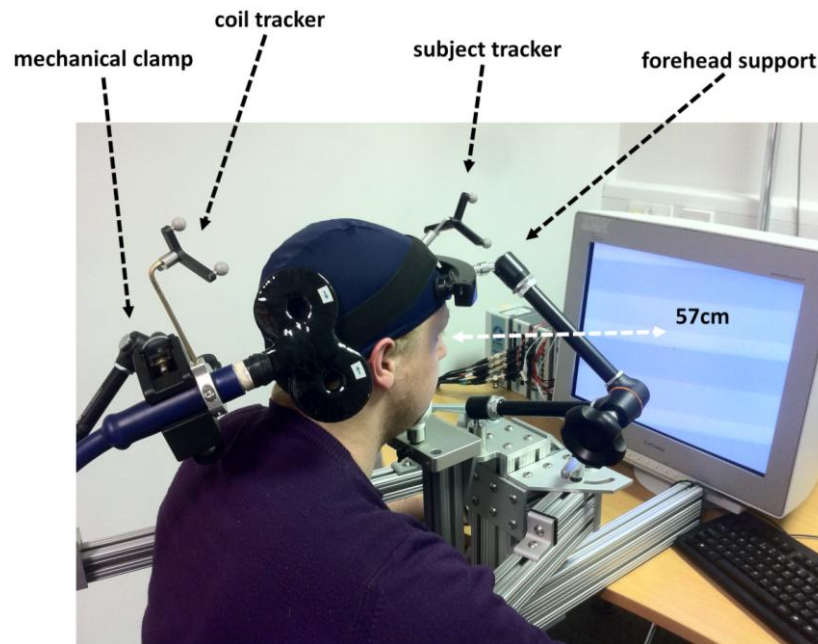
Figure 2.8: *TMS set up. A single subject can be seen seated in the purpose-built chair with chin and forehead support. Subjects viewed stimuli from a fixed distance of 57cm. The position of both subject **(subject tracker)** and stimulating coil **(coil tracker)** is monitored and tracked in real-time. The stimulating coil is secured in position via a mechanical clamp, which can be manoeuvred along the length of either arm of the chair. The set up greatly reduces localisation errors that are inherent when holding the stimulating coil by hand, and movement errors induced in both the subject and stimulating coil following the delivery of TMS pulses.*

The position of the coil could be monitored and tracked in real time with respect to the subject's head. The real-time navigation system built into Brainsight 2.1[TM] (Rogue Research, Canada) provides a measure of the precision of TMS targeting, depicted in Figure 2.9. During TMS sessions, a schematic representation of the figure-of-eight coil is presented on the screen, with crosshairs at the centre of the coil representing the coordinates of the selected cortical target. Assuming that coil calibration and subject registration procedures were implemented successfully, as the tracked coil moves across the subject's scalp, the location of the coil's calibration point (hot-spot) is updated with reference to the selected cortical target. As the coil moves close to the target (within ~ 20mm) a red-dot appears on the coil schematic. The coil can be manoeuvred into position, such that the red-dot falls on the crosshairs. The displacement error (mm) between the intended site of stimulation and actual site of stimulation is displayed and can be recorded with each pulse train. The error

represents the distance from the target to the closest point along the line projecting from the coils calibration point into the head along the coils trajectory.
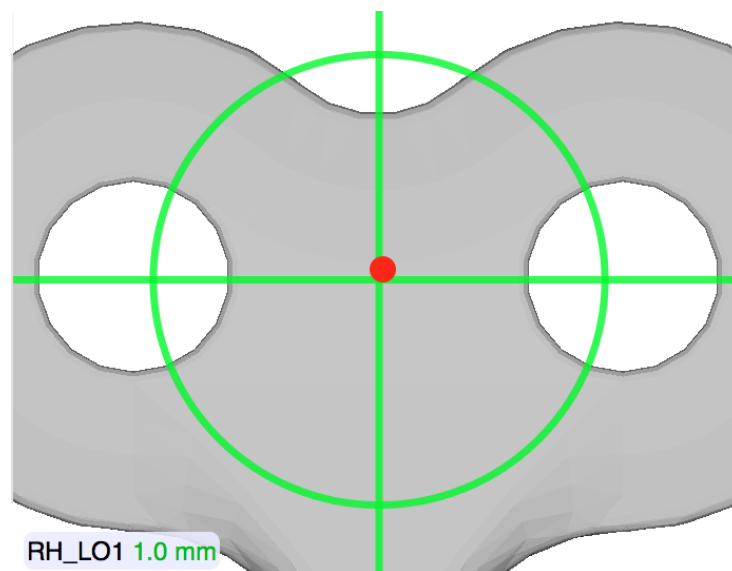
Figure 2.9: *Real-time tracking of the stimulating coil during TMS sessions. Taken from an active TMS session, a schematic representation of the figure of eight coil is shown with the crosshairs representing, in this case, the LO1 centroid in the right hemisphere of a single subject* ***(RH_LO1)****. The red-dot provides an estimate of the accuracy with which the calibration point (hot-spot) of the coil is directly in-line with the target. The green value (1.0 mm)* ***(bottom left)*** *provides an estimate of the error between the intended site of stimulation and the actual site of stimulation. Displacement error (mm) was recorded with each pulse train.*

The adopted TMS protocol allowed a number of important measurements to be recorded with each pulse train: (1) the displacement (mm) between the intended site and actual site of TMS delivery (described above); (2) the Euclidean distance (mm) from the calibration point (hot-spot) of the coil to the cortical target and (3) the orientation of the coil relative to the vector joining the calibration point (hot-spot) of the coil and the TMS target. Post TMS stimulation, the accuracy of TMS delivery can be reviewed. One can scroll through each TMS pulse train and observe the projected focal point of the TMS pulse. Figure 2.10 depicts the projected site of a single pulse train through three cortical targets (CON, LO1 & LO2) in the right hemisphere of a single subject. In each case, the projected site of the TMS pulse can be seen to pass through the cortical target of interest.
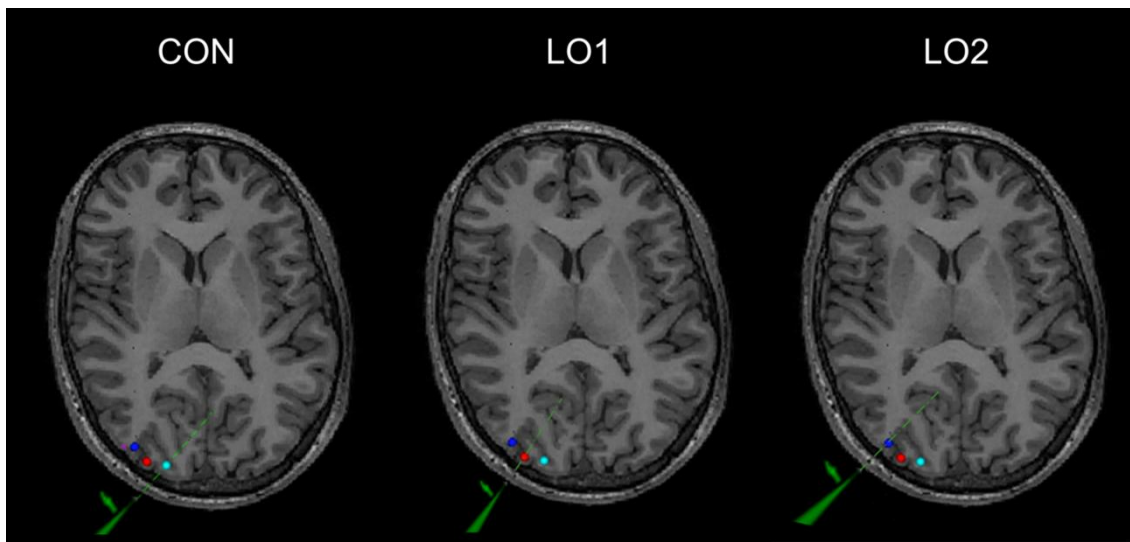
Figure 2.10: *Estimates of the most focal site of TMS delivery. The precision of TMS delivery is shown for three stimulation sites **(CON-cyan, LO1-red, LO2-blue)** within the right hemisphere of a single subject. Images are shown in radiological convention. In each image, the dashed green line represents the estimated focal point of TMS delivery. In each image the dashed green line can be seen to pass directly through the intended target. The shortest distance from the target to the green dashed line provides the displacement error illustrated in Figure 2.6. Additionally, measurements of the Euclidean distance (mm) between the coil and target, and the orientation (degrees) of the coil and target were recorded with each pulse train.*

TMS pulses were always delivered concurrently with the presentation of the TMS stimuli. The selection of this temporal configuration was influenced heavily by previously published work that employed TMS in this manner to successfully identify the causal roles played by different cortical areas (McKeefry et al., 2008; Pitcher et al., 2009). McKeefry et al., (2008) employed visual field mapping and TMS to probe the roles played by cortical areas V3A and V5/MT in motion perception. The study demonstrated causal links between activity in V3A and V5/MT and the accurate perception of motion. The study explored further the temporal characteristics of these effects, by varying the temporal delivery of TMS. TMS pulses were delivered at 11 different stimulus onset asynchronies within a single trial. The researchers measured the variation in the speed of a test grating needed to match an 8°/sec reference grating. The results indicated that the variation in speed of the test grating was maximised (faster speed was required) when TMS pulses were delivered concurrently with the presentation of the test stimulus at both V5/MT and V3A cortical sites. In addition, a recent study employed TMS to probe the causal nature of processing in

three category-selective areas of cortex (Pitcher et al., 2009). TMS pulses were delivered to the EBA, OFA and LO, whilst subjects performed body, face and object discriminations, respectively. The authors reported a triple-dissociation. Deficits in body, face and object perception were only evident following TMS of EBA, OFA and LO. TMS pulses were also administered concurrently with the presentation of the stimulus, albeit for a longer duration (500ms). Very recently, this paradigm has been employed to establish a causal link between neural activity within the Transverse Occipital Sulcus (TOS) and the discrimination of visual scenes (Dilks et al., 2013). The decision to administer TMS pulses concurrent with the presentation of the test stimulus was selected on the basis of these findings.

2.7:   Measuring the Precision of TMS Delivery

Several methodological advancements have improved the TMS paradigm. Most notably, the ability to monitor and track, in real time, the location of the stimulating coil with respect to the subject's head, has dramatically increased researchers ability to stimulate reliably their respective cortical areas of interest. Precise stimulation of cortical targets is important especially when targets are in close proximity to one another. Imprecise TMS stimulation can occur for a number of reasons. Movement of the coil (with respect to the target of stimulation) is inevitable because: (1) the action of the coil firing induces vibrations throughout the coil itself; (2) many subject's display an involuntary 'jerky' reaction to the administration of the TMS pulses, which can be substantially more pronounced if the target sites are located in close proximity to facial nerves and (3) the TMS coil itself is frequently held in place by the experimenter's hand, which is highly likely to move throughout the course of the TMS session. Even during 'theta burst' stimulation sessions, which are often short in duration, movement of the hand and therefore, the coil is likely if not inevitable. Throughout the current body of work a number of measurements were acquired with each pulse train in an attempt to overcome the potential shortcomings of imprecision.

2.7.1:   Mechanical Clamping

The current body of work employed the use of a mechanical clamp to secure the TMS coil in the desired position. The combination of the mechanical clamp, custom-built chair, chin and forehead supports ensured that during TMS stimulation, subjects were comfortable and stable. These measures dramatically reduced the absolute amount of movement inherent in TMS experiments.

2.7.2:   Measuring the Coil Displacement

One advantage of the TMS Brainsight 2.1^{TM} system (Rouge Solutions, Canada) is the ability to measure the displacement between the intended site of stimulation and the actual site of stimulation. The error (mm) is the closet distance from the target to the predicted focal point of the TMS pulse. Measurements of this displacement (mm) were acquired with each pulse train. This displacement measure was used to filter the TMS data. In any TMS session, trials for which the coil-displacement was large (> 2.5 mm) were removed prior to data analysis. This stringent criterion provides evidence for the precision of stimulation and allows one to be confident that TMS was delivered to the cortical targets independently.

2.7.3. Measuring the Coil-Target Distance

Along with the ability to measure coil displacement, the distance (Euclidean distance mm) between the calibration point and the target in cortex was recorded with each pulse train. It is important to show that the distance between the coil and target does not vary across tasks in a way that could explain any differential task effects observed in individual subjects. Crucially, the cortical targets of interest cannot change their location across tasks, and thus, the distance from the stimulating coil to those cortical targets should be equal. Differences in the coil-target distances between sites is likely, if not inevitable, given that cortical targets vary with respect to gyral and sulcal pattern, yet nevertheless the distance separating the coil to a single target should not differ across tasks. Errors in this distance measurement could arise from imprecise calibration of the TMS coil, and/or imprecise registration of the subject's location within the Brainsight ^{TM} systems field of view. If the coil-target distance does not differ significantly for a target across tasks, then one can be

confident that any behavioral changes observed are a reflection of the cortical targets and tasks examined, and not, differences in the precision of TMS delivery.

2.7.4:   *Measuring the Coil-Target Orientation*

The third measurement taken to control for spatial and geometric issues of TMS stimulation was the difference between the coil orientation and the vector joining the calibration point of the coil and the TMS target; accurate targeting corresponding to 90° on this measure. The importance of recording this measurement is that it provides a mechanism by which to evaluate the precision of TMS delivery. Any significant differences in the coil-target orientation across tasks for one site, or across sites within a task must be due to operator error. In this regard, it provides a means by which to exclude operator error as an alternative explanation for any behavioral deficits observed. For instance, if an effect was observed at LO1 for condition A and across subjects the mean coil orientated was 90°, yet for stimulation of LO1 during condition B the mean coil orientation was 60°, the difference in coil-target orientation and therefore, the precision of stimulation could provide an alternative account for any observed effects. On the other hand, if the coil orientation for a particular site does not vary (significantly) across task, or across sites for a single task, a functional dissociation is a far more parsimonious explanation of the data.

Chapter 3

Visual Field Mapping & Retinotopic Features of LO1 & LO2

3.1:   Overview

The main aims of this chapter are to outline the major hypotheses tested and results that relate to various features of visual field maps LO1 and LO2. The chapter begins with a brief history of retinotopic organisation within lateral occipital cortex, before outlining a number of hypotheses regarding the retinotopic, spatial and object-selective features of LO1 and LO2. A review of fMRI visual field mapping is also provided along with the specific fMRI protocol employed in all retinotopic mapping experiments.

3.2:   Retinotopic Organisation of Lateral Occipital Cortex

Until recently, the retinotopic organisation of human lateral occipital cortex remained relatively unknown and uncharacterised. A handful of studies reported a discontinuity in the eccentricity representation within this area of cortex, but argued that the representations of polar angle were insufficient to indicate a clear retinotopic organisation (Levy et al., 2001; Tootell et al., 1995; Tyler et al., 2005). Indeed, this area was labelled as 'non-retinotopic' by many researchers (Malach et al., 1995; Grill-Spector et al., 1999; Kourtzi & Kanwisher, 2001), and several fMRI studies demonstrated object selective responses in LO (Malach et al., 1995; Grill-Spector et al., 1999; Kourtzi & Kanwisher, 2001; Hasson, Harel, Levy, & Malach, 2003). Tootell & Hadjikhani (2001) reported measuring incomplete eccentricity and angular representations in LO, but nevertheless suggested that this region contained an eccentricity bias in which adjacent regions responded preferentially to central and peripheral stimuli, referring to this region of cortex as LOc/Lop, meaning lateral occipital central and lateral occipital peripheral, subdivisions (Tootell & Hadjikhani, 2001).

In contrast, Wandell and colleagues (Wandell et al., 2005) reported clear, yet inconsistent measurements of both polar angle and eccentricity in this area of cortex and suggested that with further advancements in visual field mapping techniques and stimulus protocols, clear maps would eventually become evident. Just one year later, the first

54

indication of a clear retinotopic organisation within LO was reported (Larsson & Heeger, 2006). Two adjacent visual field maps (LO1 & LO2) between dorsal V3d and V5/MT were identified, with both maps containing a complete representation of the contralateral visual field. Unlike previous reports (Levy et al., 2001; Tootell & Hadjikhani, 2001), Larsson and Heeger highlighted an orderly representation of both polar angle and eccentricity within LO1 and LO2, respectively. LO1 and LO2 were suggested to be two new and potentially unique human visual areas, lacking direct macaque homologues.

3.3:   Hypotheses & Aims

The specific empirical questions asked throughout the thesis were heavily dependent upon precise mapping of LO1 and LO2 in individual subjects. Given this dependency, a number of hypotheses regarding the retinotopic, spatial and object-selective features of LO1 and LO2 were tested here. First, we tested whether LO1 and LO2 could be reliably identified using fMRI visual field mapping techniques. Second, we tested whether the visual field representations within LO1 and LO2 were consistent with previous work, with respect to the visual dimensions of polar angle and eccentricity (Larsson & Heeger, 2006). Third, we tested whether our LO1 and LO2 definitions were commensurate in size and location with original definitions. Finally we tested whether our LO1 and LO2 targets exhibited object-selective responses consistent with functional definitions of the lateral occipital cortex (Malach et al., 1995).

3.4:   **Visual Field Mapping using fMRI - The Travelling Wave Method**

In order to probe the functional properties of LO1 and LO2 they must first be identified using fMRI visual field mapping techniques. The following section describes the travelling wave method for fMRI visual field mapping (Engel et al., 1994; Sereno et al., 1995; DeYoe et al., 1996). The travelling wave method measures the visual field position, which elicits the largest response (maximum BOLD signal) at each location within the brain. In this method a fixating observer is presented with high contrast (typically 100%) flickering checkerboard stimuli, which progress gradually through the visual field. Stimuli comprising a wedge and a series of concentric rings are most commonly employed allowing the representations of polar angle and eccentricity to be derived, respectively.

The expanding ring stimulus is designed to measure retinotopic organisation with respect to visual eccentricity. As one moves from posterior to anterior in early visual cortex (V1-V3) the representation of the visual field shifts from foveal to peripheral. The ring stimulus elicits sustained neural activity at each location in the brain that modulates at the stimulus frequency (*cycles per scan*). As the stimulus progresses from the centre of the visual field (foveal representation) to more eccentric (peripheral representation) locations, the activity within neurons containing peripheral receptive fields is delayed with respect to activity within neurons containing foveal receptive fields; creating a travelling wave of neural activity along the posterior-anterior axis. Due to the periodic nature of the neural activity, the delay in activation can be measured by the *phase* of the neural activity. Analysing the phase of the maximum signal at each voxel provides an estimate of the location of the stimulus in the visual field, with respect to visual eccentricity.

The rotating wedge stimulus is designed to measure retinotopic organisation with respect to polar angle. As the wedge rotates about the fixation point, activity at locations within the brain containing neurons with receptive fields further along the direction of rotation will be delayed with respect to areas containing neurons with receptive fields closer to the starting position of the stimulus. Again, because the neural activity modulates periodically, this delay can be measured by the *phase* of the neural activity. The stimulus creates a travelling wave of neural activity, which progresses between both the vertical and horizontal meridian representations. The phase informs as to the position of stimulus in

the visual field that elicited the largest signal at each voxel, with respect to polar angle. Combined, the measurements derived from the ring and wedge stimuli define the most effective visual field position for each voxel in polar coordinates (eccentricity, angle).

The key concept in the travelling wave method is to measure, within each voxel, the *harmonic function* (best fitting sin wave) that best correlates with the acquired fMRI time series (Engel, et al., 1994; Sereno et al., 1995; DeYoe et al., 1996). The amplitude of the best fitting harmonic relative to other harmonics provides a measure of the reliability of the signal; this ratio measures the signal *coherence*, which is used to threshold retinotopic data. Within each voxel, the *phase* of the best fitting harmonic informs as to the position within the visual field that most effectively stimulated that voxel. The travelling wave method has successfully identified approximately twenty separate visual field maps throughout human cortex, including those found in regions of the brain traditionally thought of as non-retinotopic (Wandell et al., 2007).

3.4.1:   The Travelling Wave in Action

The following section provides an example of the travelling wave method. This example is derived from visual field mapping scans of a representative subject acquired as part of the current body of work. Examples of the ring and wedge stimuli employed in visual field mapping experiments can be seen in Figure 3.1A. The centre of Figure 3.1 A, depicts a medial view of a surface reconstruction of the grey-white matter boundary of the right hemisphere of a single subject. The black dashed box focuses on the calcarine sulcus. V1 is located parallel to the calcarine sulcus and is outlined by the black line. An enlarged representation of V1 is shown in Figure 3.1B, with the calcarine sulcus (CaS) clearly labelled. The retinotopic organisation within V1 can be seen with respect to polar angle (Figure 3.1C) and eccentricity (Figure 3.1D).

Figure 3.1E, demonstrates the travelling wave in action. The travelling wave demonstration is taken from eccentricity scan data. At the onset of each eccentricity run, a ring subtending the first 3° of visual angle was presented at the centre of the screen (fixation point). Throughout the scan, rings at greater eccentricities replaced the preceding ring periodically. Eight different rings positions (eccentricities) were presented. When the ring reached its outer extent of 15°, a ring at the centre replaced it. Eight stimulus

repetitions (cycles) are shown, depicted by the eight peaks in amplitude as a function of time (secs). Within a single cycle, the time (*phase)* of the peak modulation in each voxel progresses smoothly across the cortical surface (*distance).*   In this example, distance measures the cortex along V1, in a posterior-anterior direction, indicated by the dashed line in Figure 3.1D. The time delay (*phase*) defines the most effective stimulus eccentricity along that line As the ring stimulus progresses gradually through the visual field, so activity along the cortical surface of V1 progresses gradually along the eccentricity dimension: That is, as the rings progresses from foveal to peripheral positions, activity in V1 progresses from posterior to anterior locations. Inspection of Figure 3.1E highlights several peaks of amplitude at different distances along V1, within each of the eight stimulus repetitions. Within a single cycle, each peak in amplitude represents a different *phase* of activity along the cortical surface of V1 (*distance)*; corresponding to the different eccentricity bands depicted in Figure 3.1D.
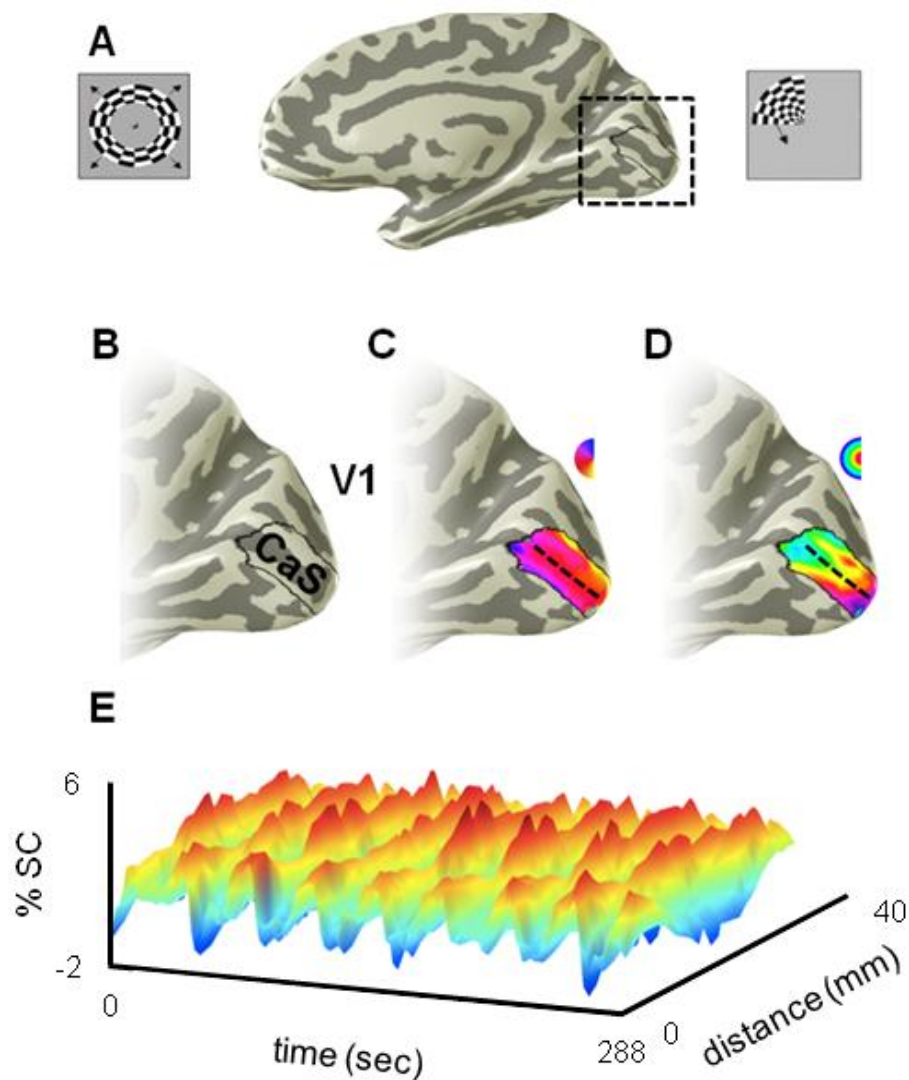
Figure 3.1: *Visual field mapping stimuli, visual field representation in V1 and the travelling wave. (A) Visual field mapping stimuli and right hemisphere surface reconstruction.* **Left:** *Example of a single frame of the eccentricity scans. A 100% contrast ring is presented; arrows indicate the direction of travel. In this case, the ring expands throughout the visual field.* **Middle:** *A medial surface reconstruction of the grey-white matter boundary of the right hemisphere of a single subject. The calcarine sulcus is outlined with solid black line. Dashed black box indicates the area of interest and is enlarged in B-D.* **Right:** *Example of a single frame from the polar angle scans. A 100 % contrast 90° wedge is presented; the arrow indicates the direction of travel. (B) Enlarged area of interest from A. The calcarine sulcus (CaS) is clearly defined, running along a posterior-anterior axis from the occipital pole on the medial surface. (C) Polar angle representation in V1. V1 contains a complete contralateral hemifield representation from the upper vertical meridian (blue) to the lower vertical meridian (yellow), see hemifield colour wheel inset. Dashed black line indicates the middle of the CaS, corresponding to the horizontal meridian representation. (D) Eccentricity representation in V1. Eccentricity can be seen to progress from foveal (purple) to peripheral (cyan) along a posterior-anterior axis, see hemifield colour wheel inset. Dashed black line indicates the middle of the CaS. (E) Travelling wave in action. Time-series data plotted along the dashed black line in D. Across time (x axis) eight peaks are depicted, one for each stimulus cycle. Within a single cycle, several peaks of activity (red) can be seen at different distances (z axis) along V1, corresponding to the different eccentricity bands present in D. As the ring progresses from central-peripheral visual field locations, activity in V1 travels from the foveal representation at the posterior end of the CaS (0mm on z axis) to more anterior portions of the CaS (40mm on z axis).*

3.5:   Visual Field Mapping Methods used in this Thesis

3.5.1:   Subjects

Throughout the thesis a total of 20 subjects (mean age = 26, range = 25, 7 male) participated in fMRI retinotopic mapping experiments. All subjects had normal or corrected to normal vision and gave informed consent in accordance with the Declaration of Helsinki. York Neuroimaging Centre (YNiC) Research Governance Committee approved the acquisition of fMRI retinotopic data.

3.5.2:   Structural & Functional MRI Imaging Parameters

Retintopic data were acquired using either an 8-channel phase-array head coil, or a 16-channel phase-array half-head coil (see section **3.5.3,** for analysis of coil comparison). All scanning took place on a GE 3-Tesla Sigma HD Excite scanner at YNiC (University of York). **Structural data 8 channel:** Multi-average, whole-head T1-weighted anatomical volumes were acquired for each subject (TR = 7.8ms, TE = 3ms, TI = 450ms, FOV = 290 x 290 x 176, matrix = 256 x 256 x 176, flipangle = 20°, 1.13 x 1.13 x 1.0mm^3). Imaging parameters provided good grey-white contrast allowing the segmentation of anatomical data into grey and white matter, and subsequent visualization in volume and inflated cortical views. **Functional data 8 channel:** Gradient recalled echo pulse sequences were used to measure T2* BOLD data (TR = 2000ms, TE = 30ms, FOV = 192cm, 64 x 64 matrix, 26 contiguous slices with 3mm slice thickness). **Functional data 16 channel:** Gradient recalled echo pulse sequences were used to measure T2* BOLD data (TR = 2000ms, TE = 30ms, FOV = 192cm, 128 x 128 matrix, 26 contiguous slices with 1.5mm slice thickness). Images were read out using an EPI sequence. Magnetisation was allowed to reach a steady state by discarding the first five volumes. On average 6 fMRI runs were acquired (3 x rings, 3 x wedges). The time courses were averaged across runs and used for visual field map identification.

3.5.3: Comparison of Coils

In August 2012 YNIC acquired a 16-channel phase array half-head coil. In order to test whether the new coil provided better signal-to-noise ratio than the existing 8-channel coil, analyses were conducted on the signal amplitude generated by both coils at two

different functional resolutions (3mm isotropic and 1.5mm isotropic). The analyses were conducted on one subject (EHS) and compared the average single cycle time series generated within a small region of interest (ROI) (diameter 4mm) from the centre of V1 in the right hemisphere, depicted in the left plot of Figure 3.2. Four retinotopic mapping sessions were undertaken (8 channel - $3mm^3$; 8 channel - $1.5mm^3$; 16 channel - $3mm^3$; 16 channel - $1.5mm^3$) on EHS. In each session four wedge runs were acquired and averaged together. Across each of the four sessions, the average time course of a single 36sec cycle was calculated. The single cycle data from each of the four sessions is plotted on the right of Figure 3.2.
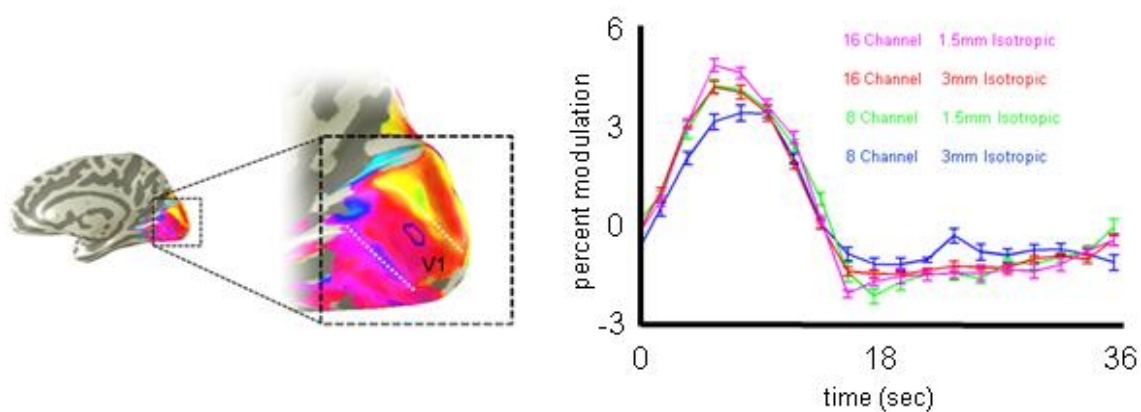
Figure 3.2: *Signal comparisons of the 8 & 16 channel coils at two functional resolutions.* **Left:** *V1 in the right hemisphere of subject EHS. A surface reconstruction of the medial surface of the right hemisphere is shown. The black dashed box highlights V1 and is enlarged. The white dashed lines delineate the full hemifield representation in V1, from the upper vertical meridian (purple/blue) to the lower vertical meridian (yellow/green). The ROI (blue ROI) has a diameter of 4mm and is centred in the middle of the calcarine sulcus at the representation of the horizontal meridian (red).* **Right:** *Single cycle comparisons for the 8 and 16 channel coils at 3mm and 1.5mm isotropic resolution. The average single cycle data are plotted from voxels within the ROI in the centre of V1. In all scans the wedge began in the top left of the visual field and rotated counter-clockwise. Accordingly, each single cycle can be seen to peak and return to baseline within the first half of the 36sec cycle. The 8 channel 3mm isotropic combination yielded the smallest signal change (blue line). There was no obvious difference in signal between the 8 channel at 1.5mm isotropic (green line) and the 16 channel at 3mm isotropic (red line). The 16 channel coil at 1.5mm isotropic (pink line) yielded the highest signal change.*

In all sessions, the wedge stimulus began in the upper left visual field and rotated counter- clockwise. Accordingly, activity within the ROI (right V1) occurs during the first half of the cycle. Inspection of Figure 3.2, reveals an increase in signal-to-noise when using the 16 channel head coil, but crucially, only when combining it with higher resolution acquisition (1.5mm isotropic). Using the 16 channel coil with standard voxel dimensions (3mm isotropic) yields a similar signal-to-noise ratio as using the 8 channel coil with higher resolution acquisition. Overall it appears, perhaps unsurprisingly, that using higher resolution fMRI acquisition yields better signal-to-noise ratios using either coil type. The continuing development of head-coils, coupled with increasingly higher resolution scans may reveal visual field maps that hitherto were not able to be resolved using standard fMRI visual field mapping protocols (Wandell et al., 2007).

3.5.4:   Retinotopic Mapping Visual Stimuli

Computer generated visual stimuli were rear projected (using a Dukane ImagePro 8942) onto an acrylic screen situated in the bore of the MRI scanner, behind the subject's head. Subject's viewed the stimuli via a mirror mounted on the head coil. Standard retinotopic mapping stimuli were employed: a rotating wedge to map polar angle, and an expanding annulus to map eccentricity. Stimuli were generated using MATLAB (Mathworks, USA) and controlled by MatVis (Neurometrics Institute, Oakland, CA). All stimuli were derived from a radial (radius 15°) checkerboard with 8 rings and 24 segments and were presented on a mean grey background. Contrast was 100 % and the reversal rate of the checks was 6 Hz. The wedge stimulus was a 90° wedge of the flickering checkerboard, rotating about the centre of the screen in 15° increments. The ring stimulus comprised 8 rings of the checkerboard, which increased in angular extent (to a maximum of 15°). As it moved to the limiting radius of the visual field a ring at the centre replaced it. Both the wedge and ring stimuli had a period of 36 seconds and were repeated for eight cycles in each run.

62

3.5.5: Retinotopic Data Analysis

Data were analysed using publicly available tools (http://white.stanford.edu/software/). Most analyses were performed in MATLAB using the mrVista toolbox. For anatomical data, individual hemispheres of acquired anatomical volumes were segmented into white and grey matter volumes using the Freesurfer4 "autorecon" script (http://surfer.nmr.mgh.harvard.edu) followed by manual topology checking using mrGray, part of the Stanford "VISTA" toolbox. Cortical surfaces (grey matter) of each subject were constructed and rendered in three dimensions from this segmentation for data visualisation using mrMesh, a visualization tool available in the "VISTA" toolbox. Functional volumes were motion corrected within and across runs using FSL's MCFLIRT. Images were also corrected for spatial inhomogeneity. The EPI volumes were initially aligned to individual high-resolution anatomical volumes manually and subsequently refined with automated procedures. This procedure allowed the parameters derived from the analysis of the functional data to be visualised on the inflated cortical surfaces.

3.6: Results

3.6.1: Delineation of Visual Field Maps

To identify visual field maps in individual subjects, the phase-encoded data were visualised and inspected for cortical representations of polar angle and eccentricity. Retinotopically organised cortical maps were identified in all tested hemispheres (n = 40). The main features of the maps, in particular, the reversals in the visual field representation at the vertical and horizontal meridians were consistent across subjects. In accordance with previous reports (Engel et al., 1994; Sereno et al., 1995; DeYoe et al., 1996; Larsson & Heeger, 2006; Wandell et al., 2007), retinotopic visual area boundaries were identified using the following criteria: (1) the response phases progressed smoothly across each visual area, consistent with a topographic organisation of the visual field representation on the cortical surface; (2) The polar angle components of the visual field maps displayed phase reversals. That is, the polar angle representations in neighbouring visual areas were mirror reversals of each other, with a phase reversal along their shared boundary and (3) the polar angle and

eccentricity components within each visual area were largely orthogonal to one another (Zeki, 2003).

The method for visual field identification was identical across subjects. In each subject, the response phases of the BOLD signal were overlaid initially in false colour onto partially inflated bilateral surface reconstructions. The hierarchical process of visual field map identification is illustrated in Figures 3.3 & 3.4, for the right hemisphere of a single subject; although importantly, the procedure was identical for visual field maps identified in the left hemisphere.
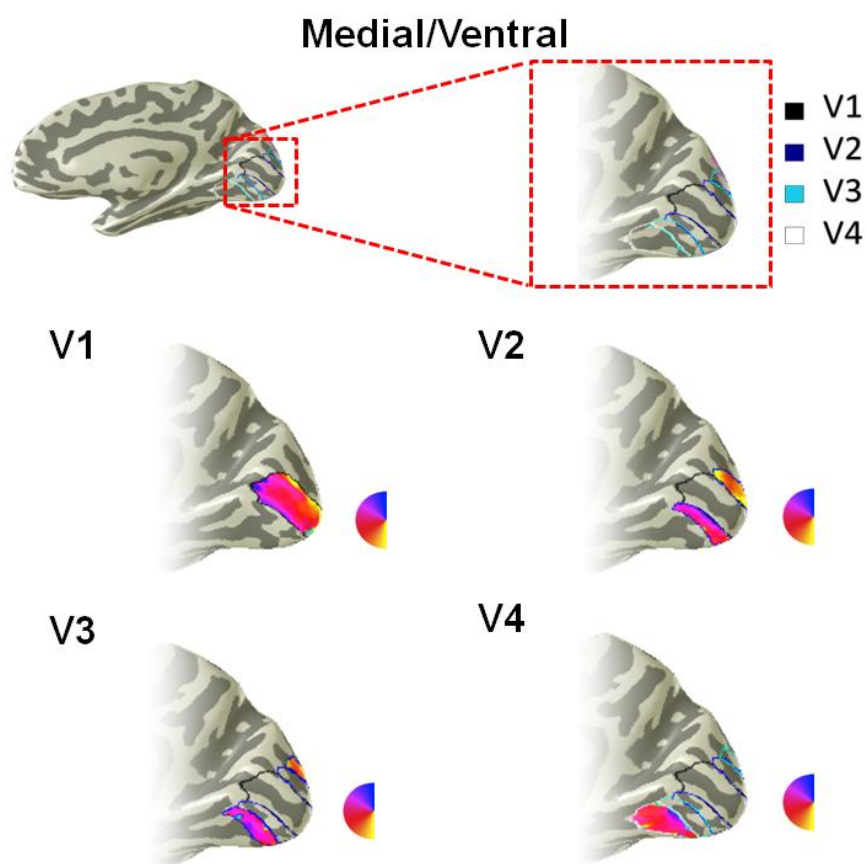
Figure 3.3: *Hierarchical stages of visual field map identification on the medial surface. At each stage of visual field map identification (successive visual field map), the response phase of the BOLD signal to the rotating wedge stimulus in that visual field map is overlaid in false colour onto a partially inflated surface reconstruction of the right hemisphere of a representative subject (gyri are light grey, sulci are dark grey). All data are thresholded at coherence of 0.25.* **Top row:** *A medial view of the right hemisphere of a single subject is shown. The red dashed box focuses on the occipital cortex and is enlarged to the right. Schematised depictions of the locations of visual field maps on the medial/ventral surface of visual cortex are shown:* **key:** *V1 (black), V2 (blue), V3 (cyan), V4 (white).* **Second row:** *depicts the visual field representation with respect to polar angle within V1 (left) and V2 both dorsally and ventrally (right).* **Third row:** *depicts the visual field representation with respect to polar angle within V3 both dorsally and ventrally (left) and V4 (right) on the ventral surface.*
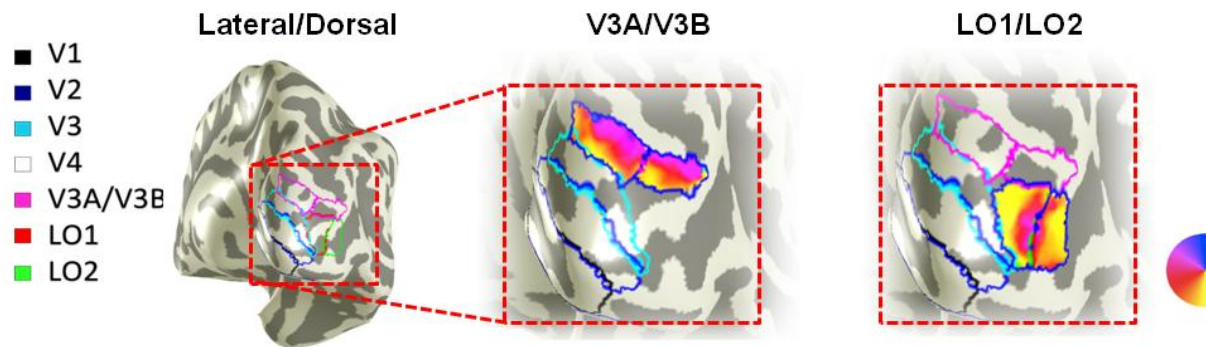
Figure 3.4: *Hierarchical stages of visual field map identification on the lateral surface. At each stage of visual field identification (successive visual field map), the response phase of the BOLD signal to the rotating wedge stimulus in that visual field map is overlaid in false colour onto a partially inflated surface reconstruction of the right hemisphere of a representative subject (gyri are light grey, sulci are dark grey). All data are thresholded at coherence of 0.25.* **Left:** *A posterior view of the right hemisphere is shown, with the dashed red box focusing on the posterior and lateral portions of the occipital lobe, which are enlarges to the right. Schematised depictions of the locations of visual field maps on the lateral/dorsal surface of human visual cortex:* **key:** *V1 (black), V2 (blue), V3 (cyan), V4 (white), V3A/V3B (magenta), LO1 (red) and LO2 (green).* **Middle:** *Depicts the visual field representation with respect to polar angle within V3A/V3B on the dorsal surface.* **Right:** *Depicts the visual field representation with respect to polar angle within and LO1/LO2 on the lateral surface.*

At the outset, visual field identification began with defining the lower vertical meridian (LVM) and upper vertical meridian (UVM) boundaries of V1. In all subjects, the representation of the UVM was found to fall along the inferior bank of the CaS with the representation of the LVM falling along on the superior bank of the CaS. The horizontal meridian was represented therefore, within the fundus of the CaS (Figure 3.3). Following the identification of V1, the visual field boundaries defining V2 and V3 (Figure 3.3) were identified. Moving dorsally, the visual field representation within V2d begins at the shared boundary with V1 at the representation of the lower vertical meridian and extends to the horizontal meridian. The representation within V3d begins at the horizontal meridian and extends back to the lower vertical meridian. Moving ventrally from V1, the visual field representation within V2v, begins at the shared boundary with V1 at the representation of the upper vertical meridian and extends to the horizontal meridian. V3v begins at this point and displays a representation from the horizontal meridian back to the upper vertical meridian. Following the delineation of early visual cortex (V1-V3), the representation within V4 on the ventral surface was defined as a hemifield map, beginning at the upper vertical

meridian boundary with V3v. Dorsally, the visual field representations within V3A and V3B were next (Figure 3.4). V3A abutted the dorsal boundary of V3d at the lower vertical meridian, both V3A and V3B containing hemifield representations. Finally, LO1 and LO2 were defined (see below for retinotopic delineation).

The identification of the visual field maps antecedent in the visual hierarchy to LO1 and LO2 is a crucially important step. As touched upon above, the borders of adjacent visual field maps share a visual field representation, with the reversal in that representation defining the boundary between the two maps. It is important therefore, to show consistent visual field representations in visual field maps antecedent to LO1 and LO2, because, if for instance, V3d and V3A/V3B were not clearly identifiable, then subsequently, LO1 (and in turn LO2) could not be indentified reliably.

3.6.2:   Delineation of Visual Field Maps LO1 & LO2

In all subjects tested, LO1 and LO2 were defined as two adjacent mirror-image representations of the contralateral visual field, located within the expanse of cortex between V3d and V5/MT (Larsson & Heeger, 2006; Wandell et al., 2007 Amano et al., 2009; Wandell & Winawer, 2011). It was originally reported (Larsson & Heeger, 2006) that the combination of V3d, V3A/V3B and LO1 created a chain of lower vertical meridian representations that together closely followed the contours of a 'Y'. Indeed, in almost all subjects it was reported that approximately half way along the lower vertical meridian boundary of V3d, the representation bifurcated into two branches; one extending dorsally and posteriorly along V3d and a second that extended anteriorly away from V3d (Larsson & Heeger, 2006). In accordance with previous reports, the posterior boundary of LO1 was defined at the shared boundary with V3d, at the representation of the LVM. The dorsal (superior) boundary of LO1 was defined as the LVM boundary with V3A/V3B. The convergence of the LVM representations in V3d, V3A/V3B and LO1, created a 'Y' configuration (Figure 3.5).
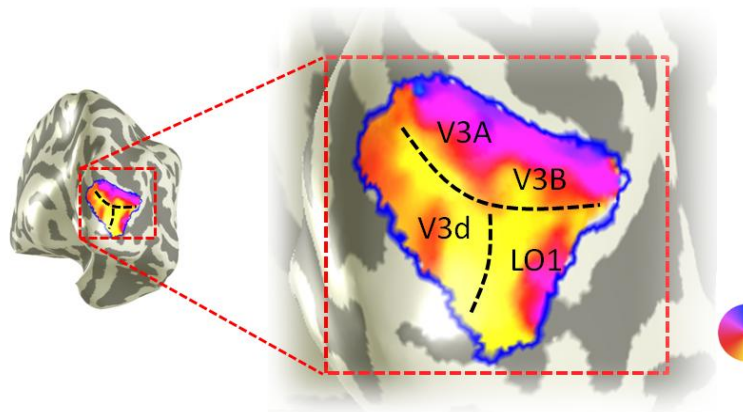
Figure 3.5: *Configuration defining the posterior and superior boundaries of LO1. A posterior view of the right hemisphere of a sinhle subject is shown **(left)**.The red dashed box outlines the area of interest and is enlarged **(right)**. The response phases of the BOLD signal in areas V3d, V3A/V3B and LO1 (outlined in blue) are overlaid in false colour. The convergence of the lower vertical meridian representations (yellow) in V3d, V3A/V3B and LO1 can be seen to form a 'Y' configuration (black dashed lines). The polar angle representation in LO1 begins at the junction of the 'Y' and progresses anteriorly from the lower vertical meridian (yellow), towards the upper vertical meridian (blue).*

The representation of polar angle in LO1 begins at the junction of the 'Y' and extends anteriorly and laterally from this junction, displaying a gradual progression from the LVM, through the horizontal to the UVM.The anterior boundary of LO1 is defined by a representation of the UVM and abuts the posterior boundary of LO2. LO2 is the mirror-reverse of LO1, and also contains an orderly representation of polar angle, extending from the UVM (at its shared boundary with LO1) towards the LVM (Figure 3.6).
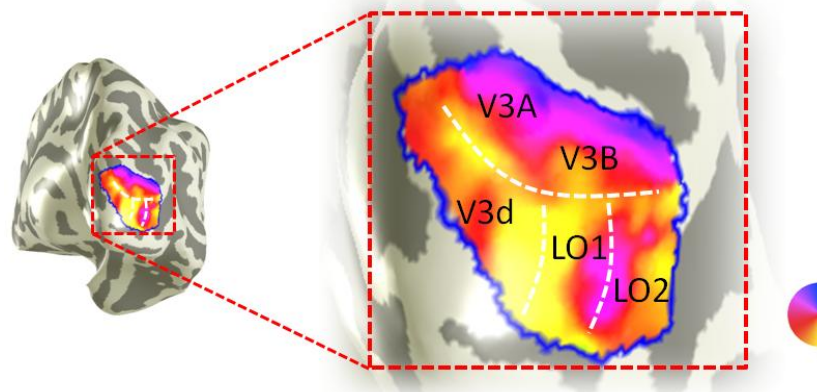
Figure 3.6: *Polar angle representations in LO1 and LO2. A posterior view of the right hemisphere of a sinhle subject is shown **(left)**.The red dashed box outlines the area of interest and is enlarged **(right)**. The response phases of the BOLD signal in areas V3d, V3A/V3B, LO1 & LO2 (outlined in blue) are overlaid in false colour. LO1 begins at the 'Y' junction created as the lower vertical meridian representations in V3d and V3A/V3B converge. LO1 displays a complete contralateral hemifield representation of polar angle, extending from the shared boundary with V3d at the LVM (yellow) towards the UVM (blue). LO2 also displays a complete contralateral hemifield representation of polar angle, progressing gradually from the shared representation with LO1 at UVM towards the LVM.*

3.6.3:   Representation of Eccentricity in LO1 & LO2

Larsson and Heeger found the foveal representations in LO1 and LO2 to be coextensive with V1, V2d and V3d with the periphery being represented anteriorly and dorsally (Larsson & Heeger, 2006). In the original description, it was reported that in approximately half of the hemisphere tested the eccentricity representation in LO2 showed an unusual pattern. That is, eccentricity representations made a sharp shift from foveal to peripheral (Larsson & Heeger, 2006). Unlike earlier visual areas, where the representations of polar angle and eccentricity are directly orthogonal, in LO1 and LO2, there were not. It was reported that isoeccentricity contours ran at an acute angle to isoangle contours, resulting in visual field representations that were noticeably skewed in both maps, but particularly in LO2, in some subjects.

Throughout the thesis, similar patterns were observed in the eccentricity representations within LO1 and LO2, with examples of both orthogonal (unskewed) and nearer parallel (skewed) representations shown in Figures 3.7A and 3.7B. Figure 3.7A, depicts the representation of eccentricity across V3d, LO1 and LO2 in a single subject. In this subject the eccentricity representations within these areas run along a ventral-dorsal axis, directly orthogonal to the polar angle representation, which ran along a posterior-anterior axis (black arrows Figure 3.7A). In all three visual field maps, the polar angle and eccentricity representations are directly orthogonal to one another, consistent with early visual cortex (V1-V3). In addition, the foveal representation within LO1 and LO2 can be seen as confluent with the representation in V3d. Figure 3.7B depicts eccentricity across V3d, LO1 and LO2 in a different subject. In this subject the eccentricity representation within V3d and LO1 run along a ventral-dorsal axis, directly orthogonal to the polar angle representation, which ran along a posterior-anterior axis. In contrast however, the eccentricity representation in LO2 appears to not only make a sharp shift from foveal to peripheral, but, also appears to run close to parallel with the polar angle representation (black arrows Figure 3.7B).

68
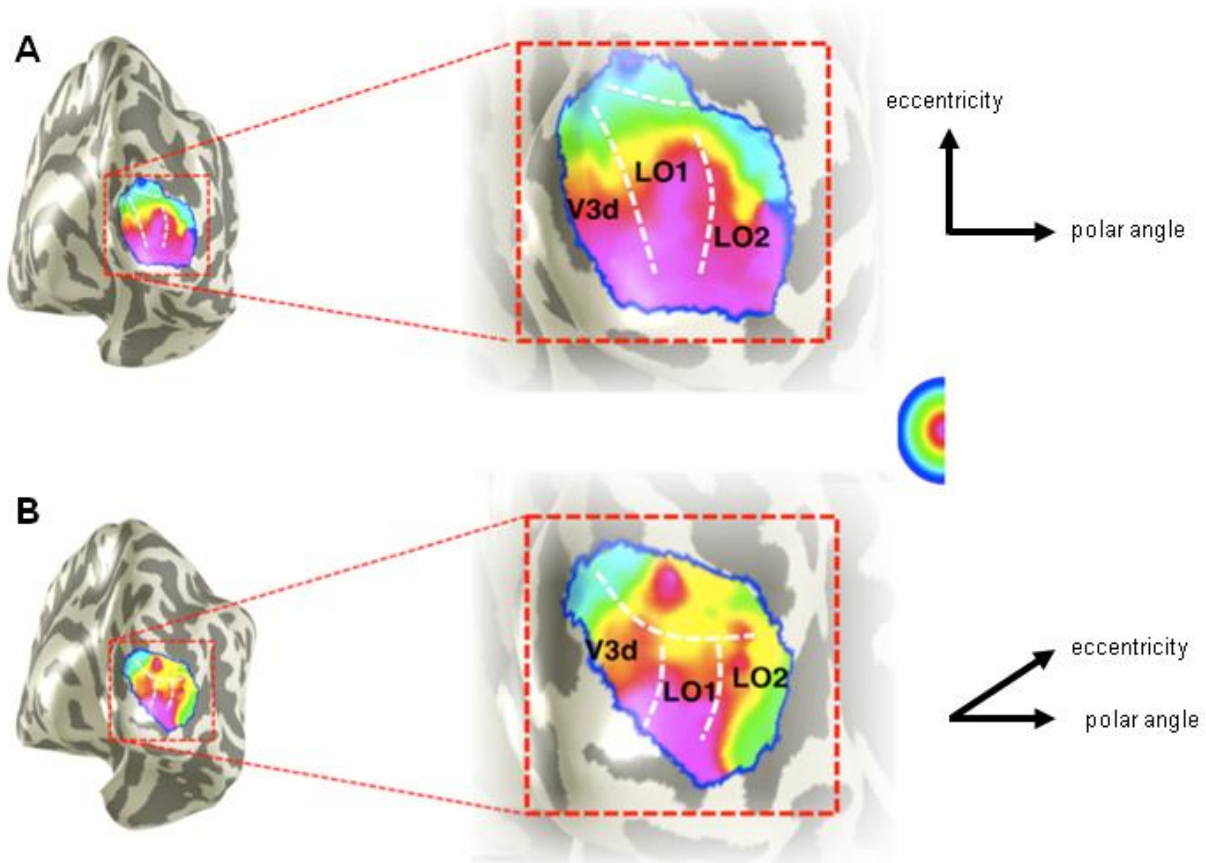
Figure 3.7: *Representation of visual field eccentricity in LO1 and LO2. **(A)** A surface reconstruction of the right hemisphere of a single subject in shown **(left)**. The area of interest incorporating V3d, LO1 and LO2 (outlined in blue) is shown (dashed-red box) and is enlarged **(right)**. Visual field eccentricity within the area of interest is overlaid in false-colour. The eccentricity representation in LO1 and LO2 progresses from foveal-peripheral along an inferior-superior axis, directly orthogonal to the representation of polar angle in this subject, which, progressed along a posterior-anterior axis – depicted by the black arrows. **(B)** A surface reconstruction of the right hemisphere of a second subject in shown **(left)**. The area of interest incorporating LO1 and LO2 is down (dashed-red box) and is enlarged **(right)**. Visual field eccentricity within the area of interest is overlaid in false-colour. The eccentricity representation in this subject is dramatically different from the example above it. Here the eccentricity representation in LO1 runs along the inferior-superior axis and is orthogonal to polar angle. The eccentricity representation in LO2 is however, skewed. The representation appears to progress along a largely posterior-anterior axis and thereby parallel with the representation of polar angle found across LO1 and LO2 in this subject – depicted by the black arrows.*

3.6.4:   Visual Field Map Gallery

The initial step in each experiment of the thesis was to identify LO1 and LO2 in each subject. The reliability with which LO1 and LO2 were identified varied across subjects, a feature consistent with a number of previous reports on LO1 and LO2 (Larsson & Heeger, 2006; Sayres & Grill-Spector, 2008; Amano et al., 2009). Nevertheless, LO1 and LO2 were identifiable in at least one hemisphere in each subject. In each case, the identification of LO1 and LO2 adhered to the guidelines set out by others (Sereno et al., 1995; DeYoe et al., 1996; Engel et al., 1997; Larsson & Heeger, 2006; Wandell et al., 2007). The following sections illustrate the retinotopic maps (with respect to polar angle) acquired from each subject (Figure 3.8). Medial and lateral views of partially inflated surface reconstructions of the left (shown on the left) and right (shown on the right) hemispheres are presented such that visual field maps are visible on both the medial and lateral surfaces of visual cortex. Where possible visual field maps V1, V2d, V2v, V3d, V3v, V4, V3A, V3B, V7, LO1 & LO2 were identified. For each subject, the phase encoded data were statistically thresholded at a coherence level equivalent to significance at the $P = < 0.05$ level, according to the number of samples acquired (Bandenttini, Jesmanowicz, Wong & Hyde, 1993).

In each subject, the response elicited by the rotating wedge stimulus is overlaid in false-colour. The colour represents the location (*phase*) of the wedge in the visual field that elicited the maximum activity at that location within cortex (see colour wheel inset at the top). Due to the dominent contralteral representations within visual cortex, the left hemisphere maps are represented by the right side of the colour wheel, whilst the right hemisphere maps are represented by the left side of the colour wheel. In both hemispheres, the lower vertical meridian is represented by yellow, with the upper vertical meridian represented by blue (white dashed lines). The horizontal meridians in the left and right hemispheres are represented by cyan and red, respectively (solid white lines).
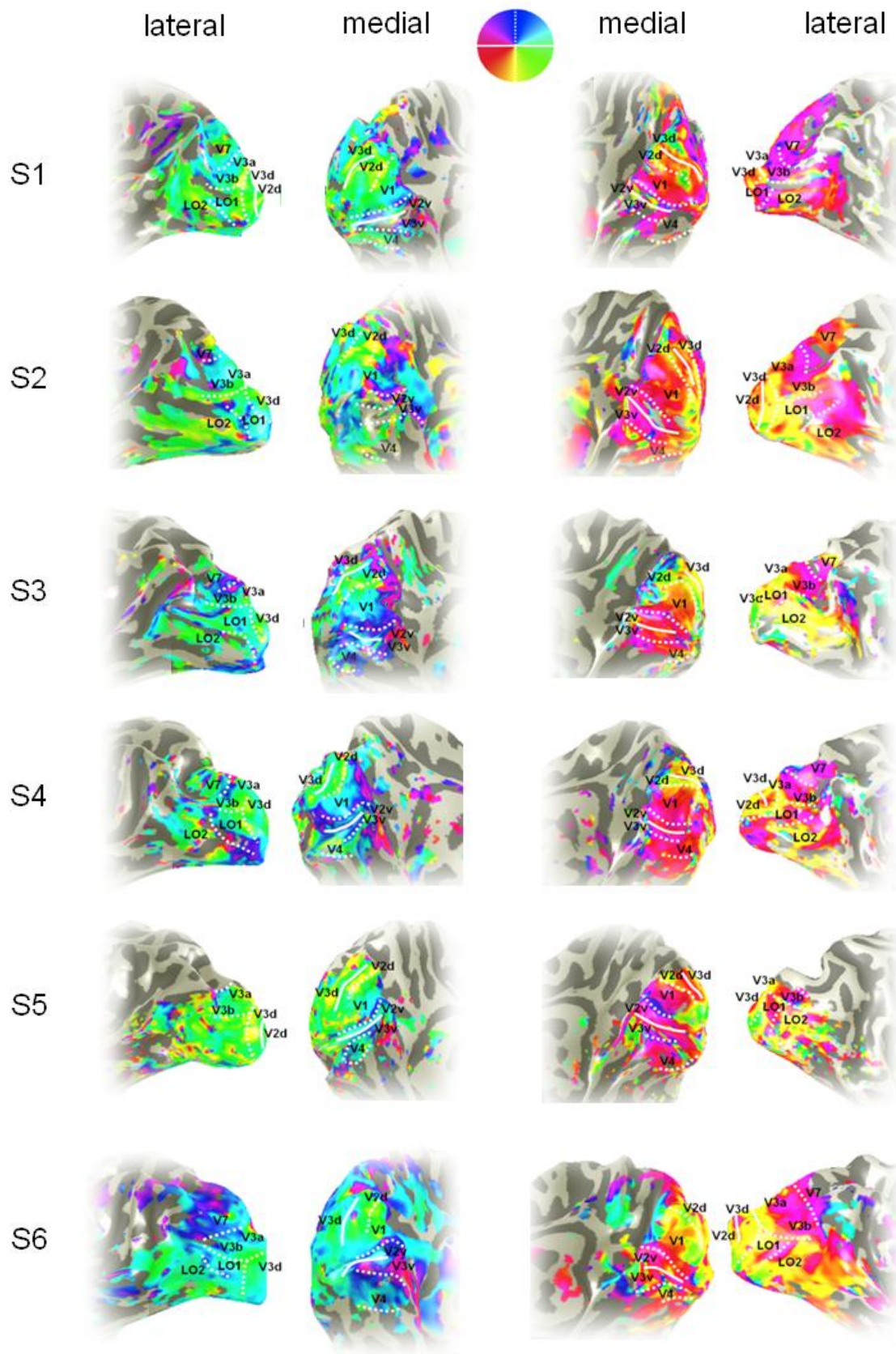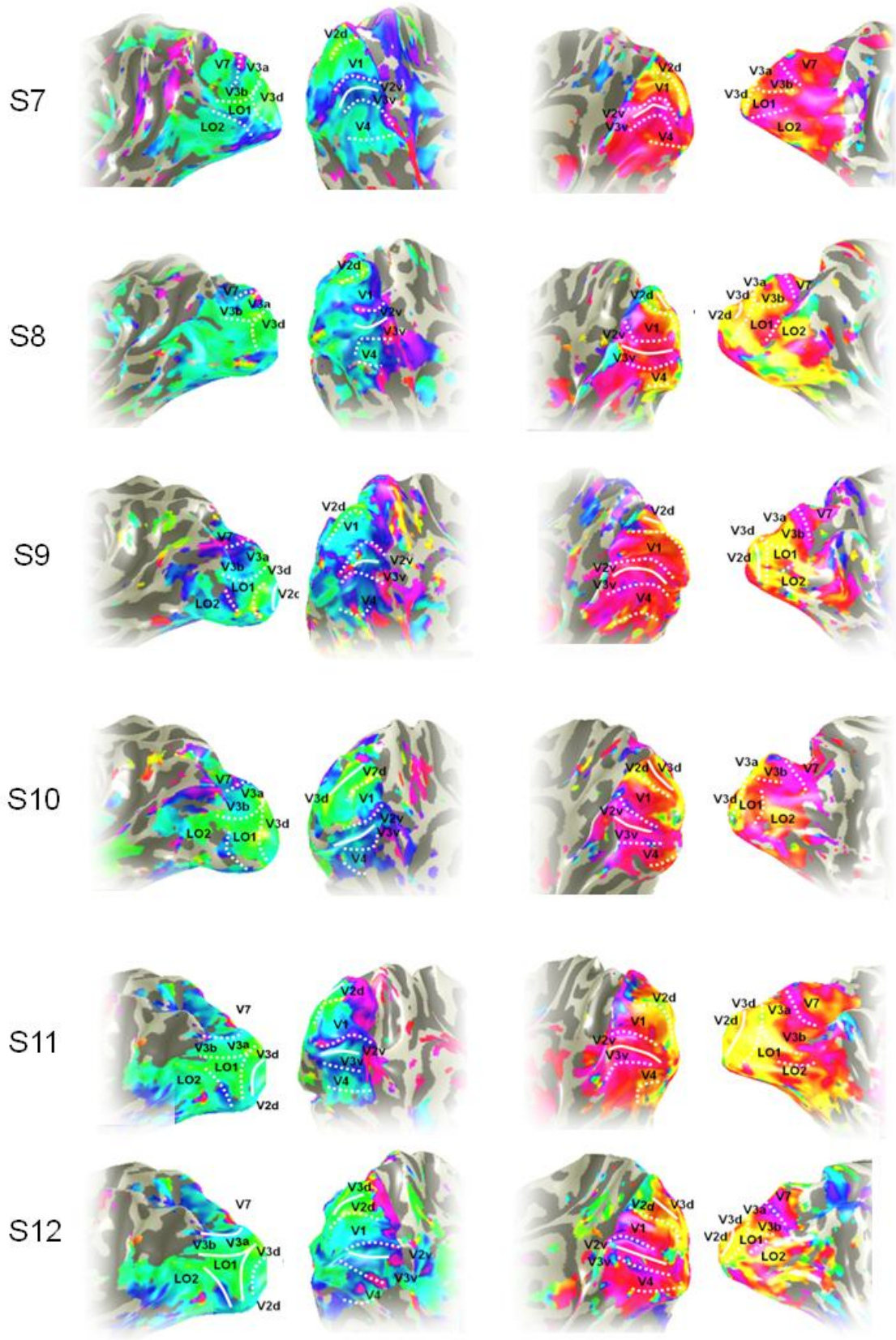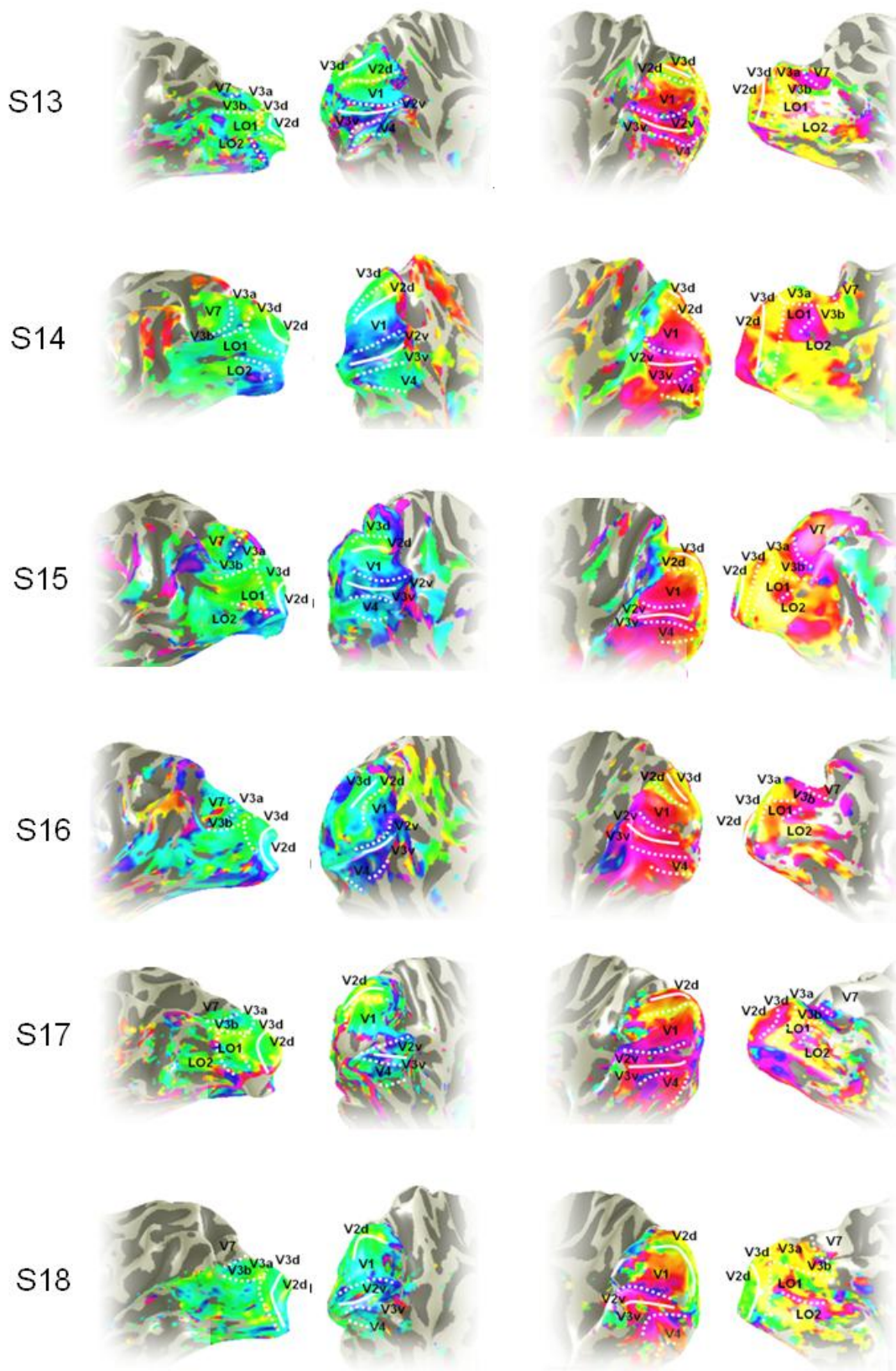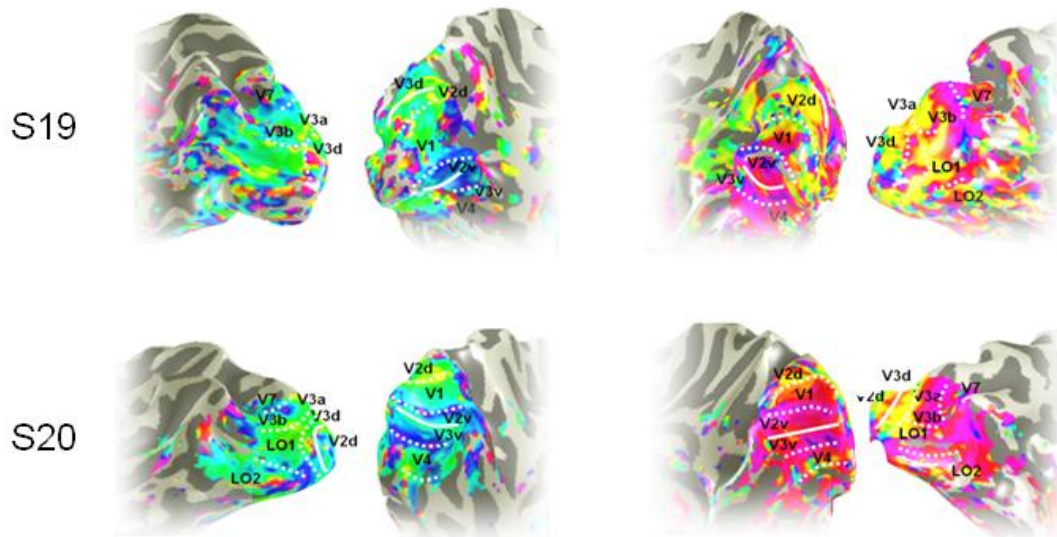
Figure 3.8: *Visual field maps in the right and left hemispheres of all subjects tested. Lateral and medial views of the occipital lobe of both hemispheres are shown for all subjects. Images have been restricted to the occipital lobe for clarity. LO1 and LO2 can appear as two adjacent mirror-image representations of the contralateral visual field in the majority of hemispheres.*

The retinotopic mapping experiments conducted throughout the thesis allowed the visual field representations within LO1 and LO2 to be identified reliably in at least one hemisphere in all subjects. In each subject, the hemisphere in which LO1 and LO2 were more readily identifiable was chosen as the stimulated hemisphere. In many subjects LO1 and LO2 were identifiable in both hemispheres, yet the representations were more easily delineable in the right than the left hemispheres.

3.6.5: Visual Field Coverage & Surface Based Averaging

In addition to the visual field map gallery presented above, we computed group average visual field coverage plots for several retinotopic areas (V1, V2d, V2v, V3d, V3v, V4, LO1 & LO2) in order to compare them to previous literature (Larsson & Heeger, 2006; Wandell et al., 2007). To compute these plots we assessed the phase (*delay*) of the BOLD responses across all subjects to the ring and wedge stimuli presented during fMRI visual field mapping. Initially, we divided the visual field into 16 equal sectors of polar angle and then subsequently divided those sectors into different eccentricity bands. Three eccentricity bands were selected, representing foveal portions of the visual field (central 3°), parafoveal portions of the visual field (3-8°) and peripheral portions of the visual field (8-15°), respectively. Taken together, these patches form a dartboard-like pattern. A grey-scale depicts the proportion of voxels within each ROI that represents a patch of visual field (Figure 3.9). For some participants (n = 4) the cortical visual field maps were identified in the left, rather than the right hemisphere. These data have been flipped to present a group average with respect to the right hemisphere (left visual field).

In the top row of Figure 3.9, the average visual field coverage for V1, V2d, V2v, V3d, & V3v are plotted. Inset to the right of each plot is a schematic representation of the visual field coverage within these visual areas reported previously (Larsson & Heeger, 2006; Wandell, et al., 2007; Amano et al., 2009; Wandell & Winawer, 2011). The data are unthresholded. The visual field coverage in these maps are largely consistent with previous studies, demonstrating close to a full hemifield representation within V1, lower quadrant representations within V2d and V3d, with upper quadrant representations present within V2v and V3v. The coverage in V1 is largely symmetrical about the horizontal meridian (green dashed line), whereas the coverage in the other maps are largely asymmetrical about the horizontal meridian. The bottom row of Figure 3.9, depicts the visual field coverage within V4, LO1 and LO2. Each plot contains a complete, or close to complete hemifield representations of the contralateral visual field, evidenced by the largely symmetrical pattern about the horizontal meridian. There is clear evidence of coverage in both the upper and lower quadrants of the visual field, a pattern consistent with previous findings (Larsson & Heeger, 2006; Wandell., et al 2007; Amano et al., 2009; Wandell & Winawer, 2011). The

marginal coverage in the opposite visual fields (right visual field) within V4, LO1 and LO2 is likely due to noise as these data were unthresholded. One feature of the LO1 and LO2 plots is noteworthy. The sector with the highest proportion of voxels in LO1 can be seen within the inner eccentricity ring (foveal vision), whereas in LO2, the highest proportion of voxels is found within the outer eccentricity ring (peripheral vision). It was originally reported that the eccentricity representation within LO1 was more heavily dominanted by foveal representation, whereas LO2 showed a sharp shift from foveal to more eccentric visual field locations in many subjects. The visual field coverage in these maps is consistent with that interpretation (Larsson & Heeger, 2006).
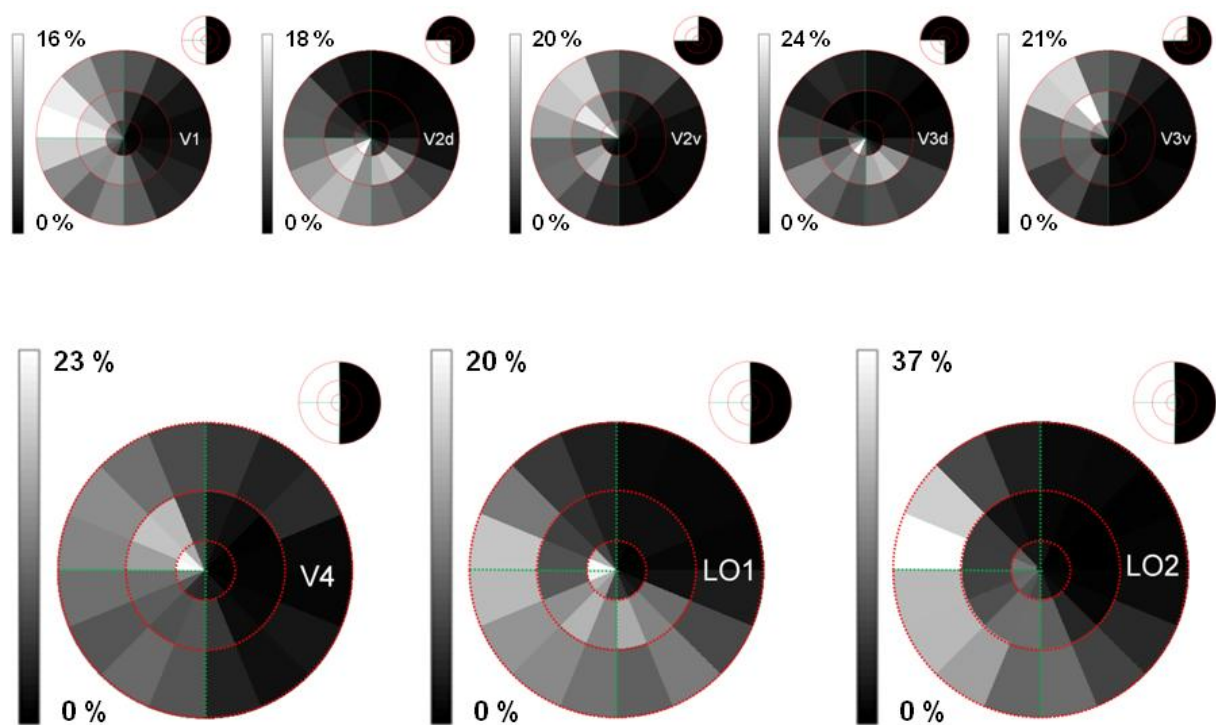
Figure 3.9: *Average visual field coverage plots. The average visual field coverage is plotted for visual field maps V1, V2d, V2v, V3d, V3v, V4, LO1 and LO2. Inset to the right of each plot is a schematic representation of the visual field coverage from previous studies, with white representing the expected area of coverage. In both the schematics and plots the vertical and horizontal meridians are represented by the dashed green lines, with the red dashed rings demarking foveal (inner ring) parafoveal (middle ring) and peripheral (outer ring) eccentricities, respectively. **Top row:** V1 displays a full hemifield representation, whereas V2d and V3d display a more weighted representation of the lower quadrant, with V2v and V3v displaying a more weighted representation of the upper quadrant. **Bottom row:** V4, LO1 and LO2 display full hemifield representations, with representations largely symmetrical about the horizontal meridian. The pattern of visual field coverage across all tested maps is entirely consistent with previous reports.*

In addition to the average visual field coverage plots, we also conducted a surface based averaging procedure in order to establish whether LO1 and LO2 adhered to common gyral and sulcal patterns. In their original paper, Larsson and Heeger identified a number of features regarding the location of LO1 and LO2 relative to common gyral and sulcal patterns. First, LO1 and LO2 were localised to the fundus of the lateral (middle) occipital sulcus (LOS), with LO2 anterior of LO1. Secondly, it was reported that in many subjects, either or both visual field maps extended over the inferior and/or superior boundaries of the sulcus onto the lateral occipital gyrus (LOG). Thirdly, in a handful of subjects where a lunate sulcus could be identified, the authors report that LO1 was more often than not located within this sulcus. Finally, it was observed that in a few hemispheres the dorsal parts of LO1 extended into the transverse occipital sulcus, and in a small number of hemispheres, both LO1 and LO2 extended onto the inferior occipital gyrus (IOG).

Surfaced based averaging was performed using the Freesurfer image analysis suite, which is documented and freely available for download (http://surfer.nmr.mgh.harvard.edu/). Anatomical volumes were initially segmented into grey and white matter. Once complete, each surface volume was inflated and registered to a spherical atlas which utilised individual cortical folding patterns to match the cortical geometry across subjects with the cortical geometry template taken from a single subject (EHS) (Fischl, Sereno & Dale, 1999a). This is an iterative procedure which aligns each subject's cortical geometry with the target geometry (EHS in this case). Once aligned to the target template, the representations of polar angle and eccentricity were averaged together and projected onto the template geometry. The results of the averaging procedure are depicted in Figure 3.10, with respect to both polar angle and eccentricity across medial and lateral views of both hemispheres,
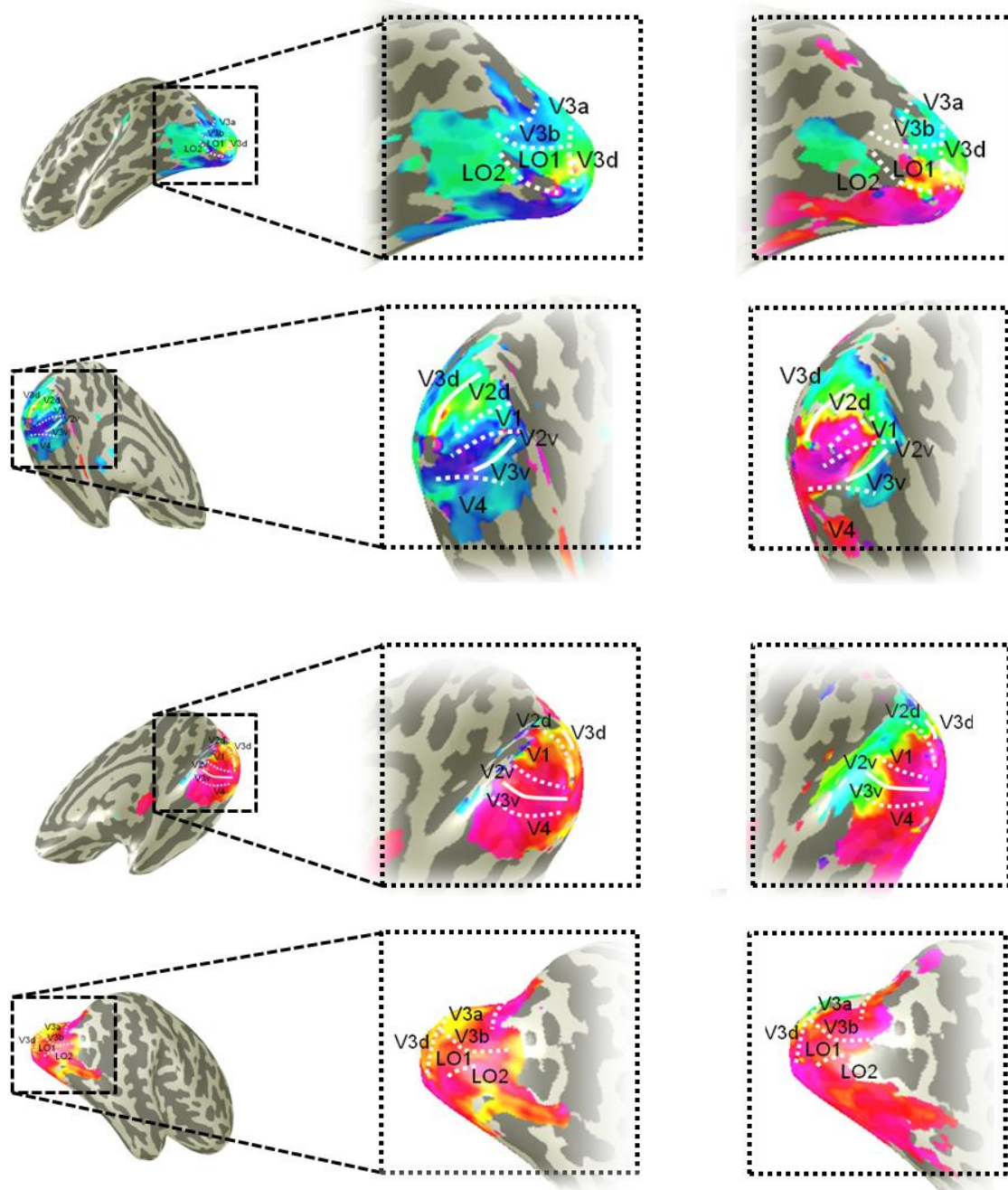
Figure 3.10: *Polar angle and eccentricity representations derived from surface-based averaging of all subjects.* **Left column:** *Medial and lateral views depict partially inflated surface reconstructions of the left* **(top two rows)** *and right* **(bottom two rows)** *hemispheres of EHS are show.* **Middle column:** *The average representations of polar angle are overlaid. Visual field map boundaries are defined by the vertical (dashed white lines) and horizontal (solid white lines) respectively.* **Right column:** *The average representations of eccentricity are overlaid, the visual field map boundaries defined by the reversals in polar angle are overlain onto the same anatomy.*

From Figure 3.10, one can see that visual field maps are delineable in both the left and right hemispheres. The location and visual field representations within these areas are largely consistent with those defined in individual subjects. It is quite remarkable that the structure of LO1 and LO2 is largely maintained throughout this procedure. Although the visual field representation at the boundary with LO1 and LO2 is not quite at the upper vertical meridian, this can be attributed to the averaging process. Nevertheless, the fact that two adjacent mirror-image representations can be found anterior of V3d highlights that LO1 and LO2 show a reasonable correspondence to common gyral and sulcal patterns. Figure 3.11 depicts close up views of the retinotopic organisation within the LO complex of the right hemisphere of a single subject and the group average. In both cases, the visual field representations within LO1 and LO2 are clearly evident. Additional visual field maps LO3-6 (Brewer & Barton, 2011) are also evident in both the single subject and group average. These additional maps also exhibit largely hemifield representations of the contralateral visual field. In both cases, reversals in the visual field representations define the boundaries between each of the six LO maps.
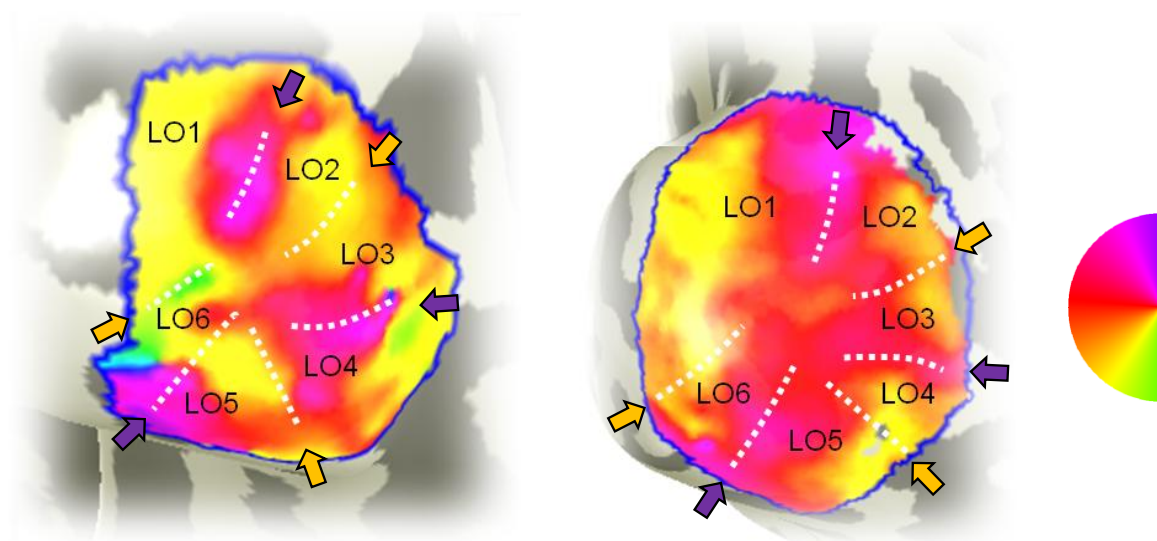
Figure 3.11: *Enlarged images of visual field maps within the LO cluster. Enlarged images of the LO cluster in the right hemisphere are shown from a single subject **(left)** and the group average **(right)**. In both cases, the hemifield representations within LO1 and LO2 are clearly delineable, with LO1 beginning at the lower vertical meridian boundary (yellow) and extending towards the upper vertical meridian (purple/blue). LO2 is the mirror-reverse of LO1. Additional visual field maps LO3-6 are also delineable in both cases. All six LO maps contain complete hemifield representations of the contralateral visual field.*

3.6.6:   Size & Location of LO1 & LO2

The average volume (mm^3) of visual field maps V1, V2, V3, V4, LO1 and LO2 and the percentage of V1 volume within LO1 and LO2 are plotted in Figure 3.12. A number of features are noteworthy. First, LO1 and LO2 were found to be very similar in size, a paired-t test (two-tailed) revealed no significant difference in volume between LO1 and LO2 (t $_{(19)}$ = 1.153, *p* = 0.377). Second, LO1 and LO2 were found to be considerably larger than those first identified by others (Larsson & Heeger, 2006), with the volume in LO1 being ~37% of V1, and LO2 having a volume of ~41% of V1. In their original report, the sizes of LO1 and LO2 were reported to be ~30% of V1 (Larsson & Heeger, 2006). The ring and wedge stimuli employed during visual field mapping had an angular extent of 15°, considerably larger than employed previously. The additional visual field stimulation likely underpins the larger estimates of size relative to previous reports (Larsson & Heeger, 2006).
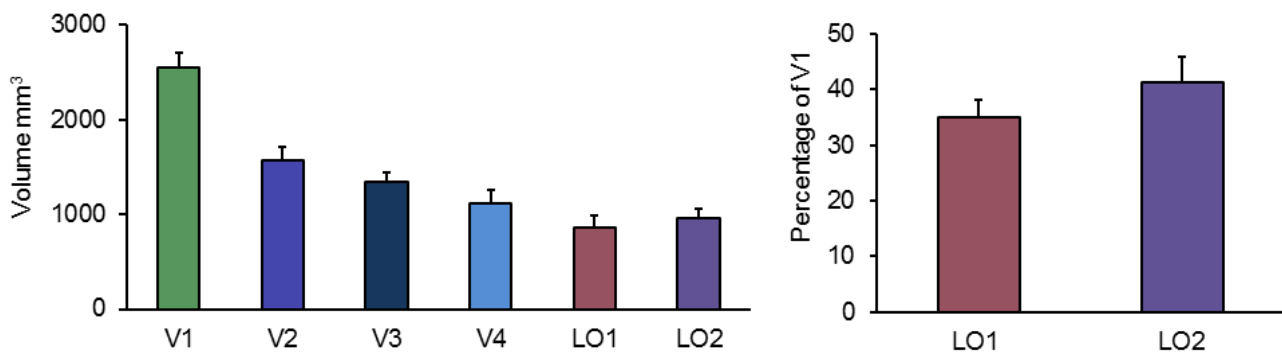
Figure 3.12: *Visual field map size.* **Left:** *The average volume mm^3 of visual field maps V1, V2, V3, V4, LO1 and LO2 is shown.* **Right:** *The percentage of V1 volume in LO1 and LO2. Error bars represent s.e.m.*

As described in Chapter 2, in order to target LO1 and LO2 for TMS, the centroids or centre of mass coordinates were calculated for each subject. The centroids for LO1 and LO2 were transformed into Talairach space (Table 3.1), for comparison with previously published work (Larsson & Heeger, 2006). Inspection of Table 3.1, demonstrates that the mean centroid locations of LO1 and LO2 (in both hemispheres) were within the range previously published (Larsson & Heeger, 2006). However, with closer inspection, systematic increases within the *Z* coordinate can be seen. The wedge used in the current polar angle mapping experiments had an angular extent of 15°, rather than the 6° wedge used previously (Larsson & Heeger, 2006). The eccentricity representations in LO1 and LO2 extend along the

Z dimension, on an inferior to superior axis, and therefore the larger stimuli likely account for the observed increase in the *Z* dimension.

Table 3.1. *Average centroid locations of LO1 and LO2 (Talairach coordinates), including those from Larsson & Heeger (2006).*

		Talairach coordinates						
		LO1				LO2		
		x	y	z		x	y	z
Current Thesis	Right	28	− 87	9		34	− 80	9
	Range	28, 35	− 93, − 80	-7, 11		26, 42	− 87, − 72	-2, 19
	Left	− 29	− 92	7		− 37	− 83	7
	Range	− 38, − 22	96, − 87	4, 13		− 46, −31	− 87, − 76	3, 11
			Averages					
Larsson & Heeger	Right	32	− 89	2.6		38	− 82	0.6
	Range	24, 38	− 98, − 81	− 8, 13		32, 46	− 89, − 72	− 13, 12
	Left	− 31	− 90	1.4		− 38	− 83	− 0.1
	Range	− 37, − 26	− 101, − 82	− 12, 11		− 43, − 31	− 92, − 67	− 13, − 11

In order to test this, new LO1 and LO2 ROIs (and therefore centroids) were defined for each subject, restricted to a maximum eccentricity of 6°, as follows. First, the *phase* representing the foveal confluence (at the occipital pole) was calculated. Second, the *phase* window was restricted from this start-point to a phase reflecting 6° eccentricity. Third, in those subjects in whom LO1 and LO2 were found to extend beyond this 6° eccentricity cut-off, new (6°) LO1 and LO2 ROIs were defined, and the centroids of those maps were calculated and transformed into Talairach space for comparison (Table 3.2). Restricting LO1 and LO2 to 6° eccentricity resulted in mean centroid locations that were more inferior (lower *Z* dimension) and closer to the LO1 and LO2 centroids originally reported (Larsson and Heeger, 2006).

81

Table 3.2: *Centroid locations of LO1 and LO2 restricted to 6° eccentricity (Talairach coordinates), including those from Larsson & Heeger.*

		Talairach coordinates						
		LO1				LO2		
		x	y	z		x	y	z
Current Thesis	Right	24	−82	5		35	−81	5
	Range	19, 28	−92, −70	−7, 20		26, 43	−88, −70	−4, 21
	Left	−28	−89	1		−32	−80	−1
	Range	−37, −23	−94, −70	−6, 2		−40, −22	−90, −70	−6, 7
		Averages						
Larsson & Heeger	Right	32	−89	2.6		38	−82	0.6
	Range	24, 38	−98, −81	−8, 13		32, 46	−89, −72	−13, 12
	Left	−31	−90	1.4		−38	−83	−0.1
	Range	−37, −26	−101, −82	−12, 11		−43, −31	−92, −67	−13, −11

Across subjects there was a large degree of individual variation in the centroid locations of LO1 and LO2. This feature is consistent with previous reports (Larsson & Heeger, 2006) and serves to highlight the necessity of identifying these visual field map targets on an individual basis and not relying on measuring fixed distances across the scalp as used previously (Ellison & Cowey, 2006). The extent of the variation is captured in Figure 3.13. Centroid locations of LO1 and LO2 have been transformed into MNI space and overlaid onto wire representations of the MNI brain, courtesy of the DV3D software (Gouws, Woods, Millman, Morland, & Green, 2009).
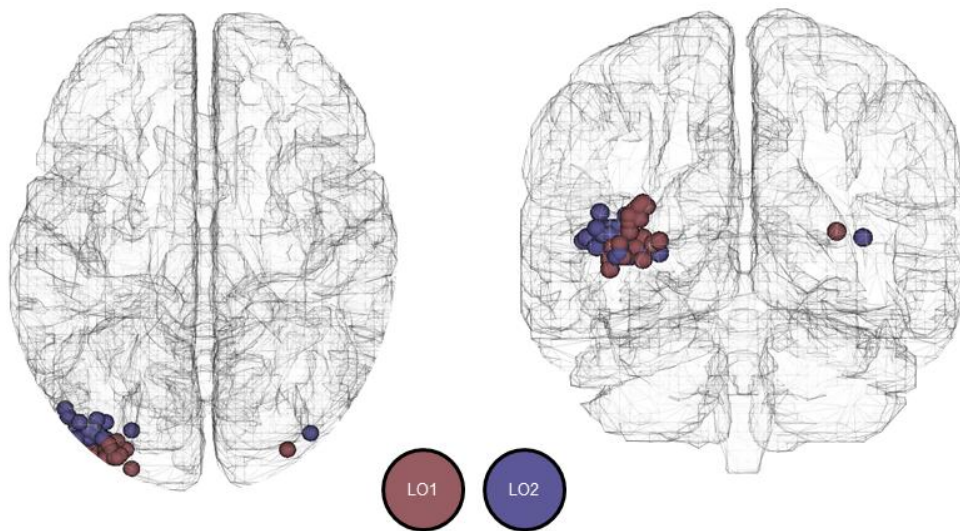
Figure 3.13: *Individual variation in LO1 and LO2 centroid location. The centroids (3mm³ spheres) of LO1 **(burgundy)** and LO2 **(purple)** have been transformed into MNI space and overlaid onto wire representations of the MNI brain. The individual variation in LO1 and LO2 centroid location is evident in the left hemisphere of the axial **(left)** and coronal **(right)** images. For comparison the right hemisphere of both images illustrates the average LO1 and LO2 centroid locations.*

Additionally, the transformed LO1 and LO2 centroids were plotted in 3D space for comparison with the location of the inion (a bony protrusion at the back of the head), which is often used as a landmark for TMS localisation (Ellison & Cowey, 2006; 2009). The left plot in Figure 3.14 depicts the transformed LO1 (red) and LO2 (blue) centroids for all 20 subjects. The inion (green circle, green arrow) is also plotted to provide a reference point. Even after normalisation to an average coordinate space the centroids of LO1 and LO2 show marked individual variation. The left plot of Figure 3.14 serves to underscore the necessity to map the location of LO1 and LO2 in individuals. Previous methods of TMS localisation such as measuring a fixed distance from the inion would be an inappropriate method for localising these regions. The right plot in Figure 3.14, depicts the average LO1 and LO2 centroids with the inion plotted, again as a reference.
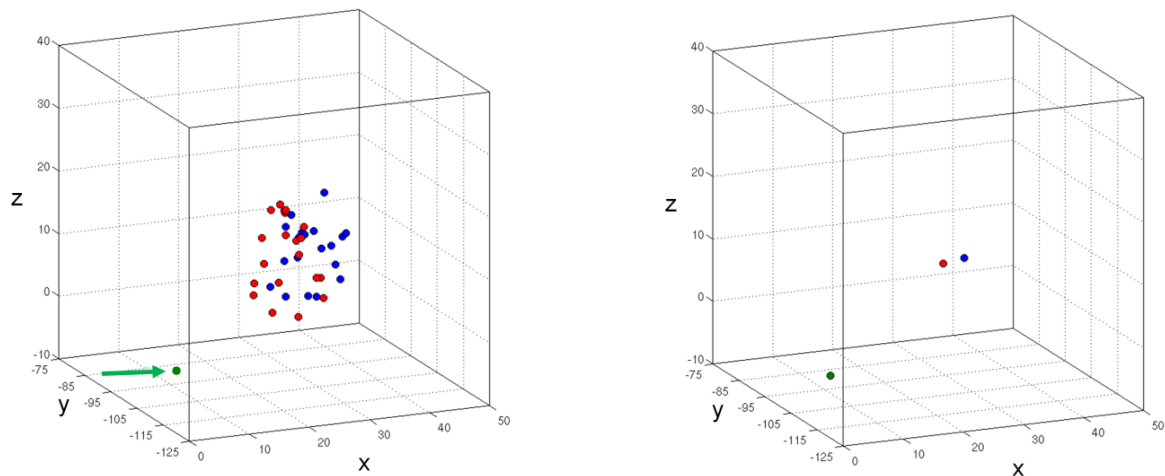
Figure 3.14: *LO1 and LO2 centroids in MNI space. LO1 **(red)** and LO2 **(blue)** centroids in MNI space for each individual subject **(left)** with the inion **(green dot, green arrow)** as a reference. The marked individual variation in LO1 and LO2 location is evident by the desertion of centroid locations. Mean LO1 and LO2 centroids in MNI space, relative to the inion **(right)**.*

Additionally, and for comparison with previous work, the transformed LO1 and LO2 centroids were compared to the peak MNI coordinate of object-selective responses reported by Pitcher et al., (2009), depicted in Figure 3.15. Inspection of Figure 3.15 reveals that the peak LO voxel falls on the outer range of LO1 and LO2 centroids. Of note the centroids, along with the peak voxel are simply that, one voxel coordinates. The overlap therefore, between the definitions of object-selective LO and LO1 and LO2 likely extend beyond this. The right plot of Figure 3.15 depicts the mean MNI centroids for LO1 and LO2 along with the peak LO voxel from Pitcher et al., (2009) and the mean centroids for LO1 (light red circle, light red arrow) and LO2 (cyan circle, cyan arrow) from Larsson & Heeger (2006). Of note, these coordinates were transformed from Talairach to MNI. In comparison with Larsson and Heeger (2006), the current LO1 and LO2 centroids can be seen to be slightly more anterior and superior.
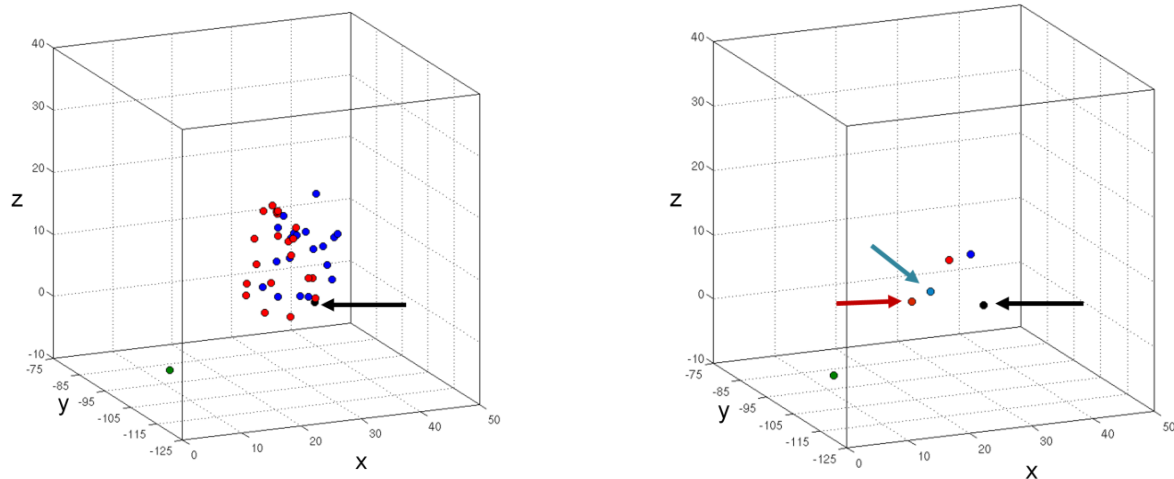
Figure 3.15: *LO1 and LO2 centroids relative to previously published work.* **Left:** *LO1* **(red)** *and LO2* **(blue)** *centroids in MNI space for each individual subject with the inion* **(green)** *as a reference are compared to the peak LO voxel from Pitcher et al., (2009)* **(clack circle, black arrow).** **Right:** *Mean LO1 and LO2 centroids in MNI space, relative to the inion, the peak voxel from Pitcher et al. (2009) and the mean centroids for LO1* **(light red circle, light red arrow)** *and LO2* **(cyan circle, cyan arrow)** *from Larsson & Heeger (2006).*

3.6.7:   Are LO1 & LO2 Part of Object-Selective Cortex?

The extent to which LO1 and LO2 are considered part of object selective cortex has been a recent source of debate (Larsson & Heeger, 2006; Sayres & Grill-Spector, 2008). In this section, I briefly review the previous work demonstrating object-selective responses in LO1 and LO2, before describing the object-selective analyses undertaken as part of the thesis on a subset of subjects (n = 5).

The lateral occipital complex (LOC) is a large area of extrastriate cortex, extending across both dorsal and ventral surfaces of visual cortex; defined operationally as the cortical area on the lateral and ventral surfaces of the occipital lobe that exhibit larger BOLD responses to images of common objects and faces, compared with scrambled images of the same stimuli (Malach et al., 1995; Grill-Spector et al., 1999; Kourtzi & Kanwisher, 2001). Anatomically, LOC has been divided into a more dorsal and posterior region, referred to as the lateral occipital cortex (LO), and a more ventral and anterior region, located in the posterior aspect of the fusiform gyrus (pFs). A number of studies report a functional division within the LOC, with responses to faces clustering in and around the pFs (Malach et al., 1995) (in close proximity to the FFA), and neural activity related to the perception of objects

centred around LO (Kourtzi & Kanwisher, 2001). The object-selective nature of LO has been demonstrated consistently across a number of paradigms including neuropsychological (Goodale et al., 1991), neuroimaging (Kourtzi & Kanwisher, 2001; Sayres & Grill-Spector, 2008; Amano et al., 2009) and neurostimulation studies (Pitcher et al., 2009).

Importantly, LO1 and LO2 have been shown to exhibit the same selectivity to objects as the larger area that encompasses them, LO (Larsson & Heeger, 2006). Subjects were shown alternate sequences of greyscale images of faces and commonly encountered objects. These blocks were alternated with blocks (12sec) of scrambled versions of the same stimuli. Objects and faces were shown in alternating (12sec) sequences, allowing the segmentation of the LOC into face and object preferring regions, respectively. A large proportion of visual cortex, including LO1 and LO2 showed a larger response to intact over scrambled images of objects and faces. Object-selective responses evoked in LO1 and LO2 were highly significant. The magnitude of responses to intact objects and face stimuli differed markedly across visual areas, and was larger in LO2 than any other retinotopically defined visual area, including LO1. Given the common division of the LOC into anterior face-selective (pFus/pOTS) and posterior object-selective (LO) regions, a separate analysis of the responses evoked in LO1 and LO2 by images of faces and common objects, respectively, was undertaken. LO1 and LO2 were found to respond significantly more strongly to images of intact objects over images of faces. These combined results confirm LO1 and LO2 as part of the LOC with object-selective responses consistent with the posterior object-selective portion, LO, a finding more recently replicated (Amano et al., 2009). LO1 and LO2 therefore, represent the retinotopic subdivisions of LO, although the extent to which LO is restricted to these retinotopic boundaries is a source of debate (Larsson & Heeger, 2006; Sayres & Grill-Spector, 2008).

In a subset of subjects (n = 5) the overlap with object selective cortex and object-selectivity within LO1 and LO2 were assessed. Subjects participated in a standard LOC localiser (see appendix for full fMRI protocol). Subjects were presented with alternating blocks (9sec) of objects, faces and scrambled versions of these images. Each block contained ten images presented in a randomised order (700ms) with a short ISI (200ms). In an attempt to maintain attention, subjects were required to detect a red dot on a subset of images by pressing a response button. All images were centred at fixation and subtended 6 x 8° of

visual angle. Images were overlaid onto a mid-grey background. The aims of this analysis were twofold. First, to demonstrate that responses in LO1 and LO2 exhibit greater responses to the presentation of objects over the presentation of faces. This finding would be consistent with previous work and serve to strengthen the view that the object-selective responses exhbibited in LO1 and LO2 are consistent with the object-selective LO (Larsson & Heeger, 2006). Second, to assess whether a dissociation is present in the object selectivity observed in LO1 and LO2. The spatial overlap between functional definitions of object-selective LO (objects > scrambled objects) and the retinotopic boundaries of LO1 and LO2 in a single subject is plotted in Figure 3.16.
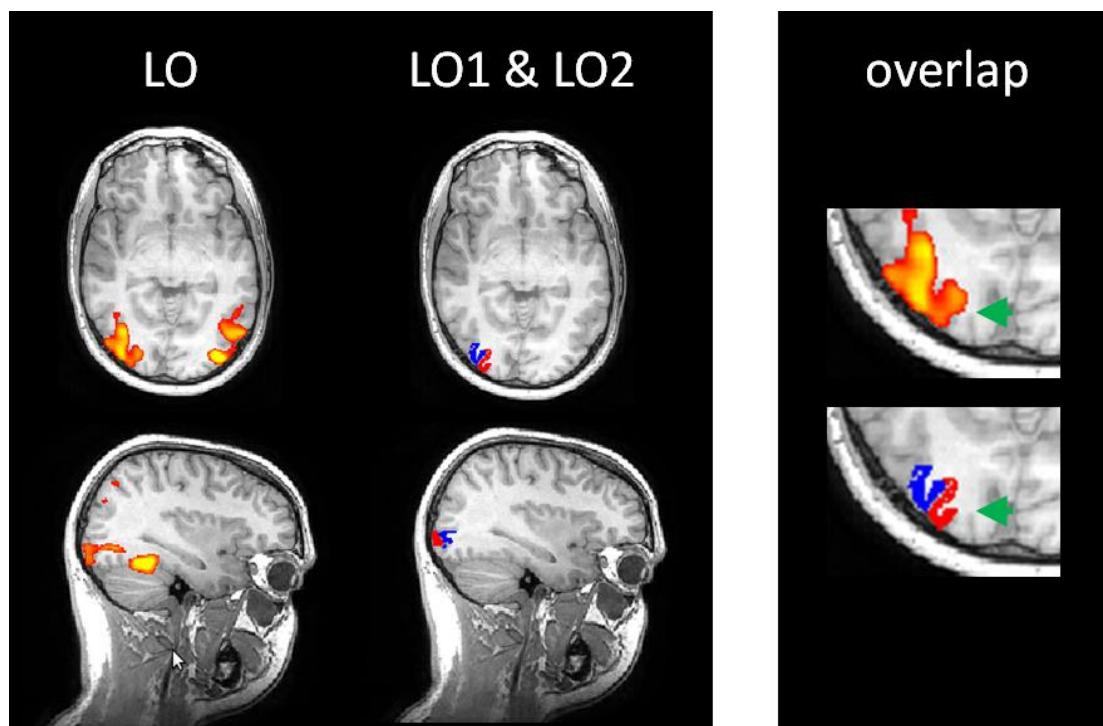
Figure 3.16: *Overlap between object-selective cortex and LO1 and LO2 in a single subject. All images are in radiological convention. LO is shown* ***(left column)*** *on axial* ***(top)*** *and saggital* ***(bottom)*** *slices by contrasting the BOLD responses elicited by the presentation of objects over scrambled objects. LO1* ***(red)*** *and LO2* ***(blue)*** *are shown* ***(middle column)*** *on axial and saggital slices in the right hemisphere. The overlap between LO and LO1 and LO2 is shown* ***(right column)****. Axial slices have been enlarged to focus on the occipital lobe of the right hemisphere. Object selective responses* ***(top)*** *and LO1 and LO2* ***(bottom)*** *can be seen to show a close anatomical correspondence. The green arrow highlights the same sulcus in both images.*

LO1 and LO2 were intially defined on inflated surface reconstructions, but were later transformed back into the individuals native anatomical space. LO1 and LO2 can be seen to be adjacent visual field maps on posterior and lateral surface of the occipital lobe (middle column Figure 3.16). In the same subject, LO was defined by contrasting the responses elicited by the presentation of objects over scrambled objects, using FSL. In order to demonstrate the overlap between these independant definitons of LO, the data were overlaid onto the same anatomical volume (right column Figure 3.16). In accordance with previous reports (Larsson & Heeger, 2006), the functional definition of LO encompasses both LO1 and LO2. The functional definition of LO however, is not restricted to the retinotopic boundaires of LO1 and LO2, a feature that is consistent with previous reports (Sayres & Grill-Spector, 2008).

The mean percentage signal change across all subjects for each condition is shown in Figure 3.17. The responses to objects were larger in LO1 and LO2 than the responses to either faces or scrambled objects. These findings are consistent with previous reports and add to the evidence suggesting that LO1 and LO2 are the retinotopic subdivisions of LO. In order to assess the object selective nature of responses in LO1 and LO2, a series of paired t-tests (one-tailed) were conducted comparing the responses in LO1 and LO2 across object, face and scrambled conditions. The object-selective responses in LO1 were not significantly different to the responses to either faces ($t_{(4)} = 2.003$, $p = 0.051$) or scrambled objects ($t_{(4)} = 1.352$, $p = 0.117$). The comparison with faces however did approach significance. The object-selective responses in LO2 were not significantly greater than the responses to faces ($t_{(4)} = 1.327$, $p = 0.121$), but were significantly greater compared to scrambled objects ($t_{(4)} = 2.641$, $p = 0.023$). The differences in object responsiveness between LO1 and LO2 were also not significantly different ($t_{(4)} = -0.179$, $p = 0.887$).
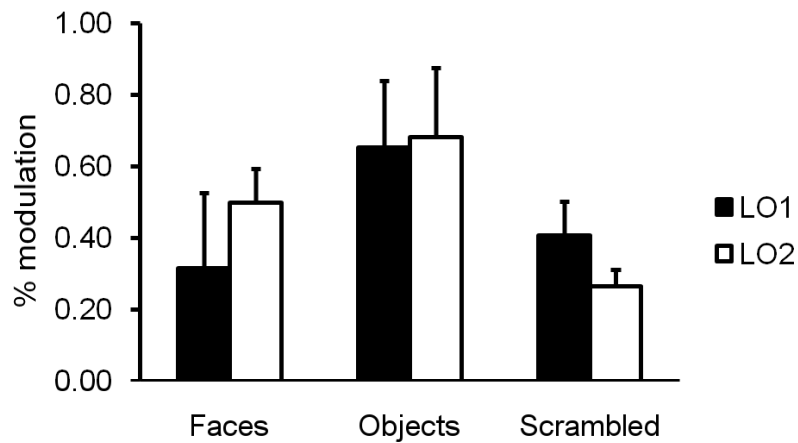
Figure 3.17: *Group averaged percent signal change across LO1 and LO2 to objects, faces and scrambled objects. The BOLD signals elicited across LO1 and LO2 were larger following the presentation of objects than either faces or scrambled objects. Error bars represent s.e.m.*

In addition to the analyses reported above, all subjects were put through a high-level group analysis. Statistical analysis of the fMRI data was performed using FEAT (http://www.fmrib.ox.ac.uk/fsl). The initial 9sec of data from each scan were removed to minimise the effects of magnetic saturation. Motion correction was followed by spatial smoothing (Gaussian, FWHM 6 mm). The group averaged data along with the mean LO1 and LO2 centroids are shown in Figure 3.18, overlaid onto the MNI brain. Data were cluster thresholded at Z = 2.3. In order to compare the location of LO1 and LO2 with respect to the LOC, the mean LO1 and LO2 centroids were transformed into MNI space and overlaid onto the same MNI brain. The centroids appear as 5mm spheres.
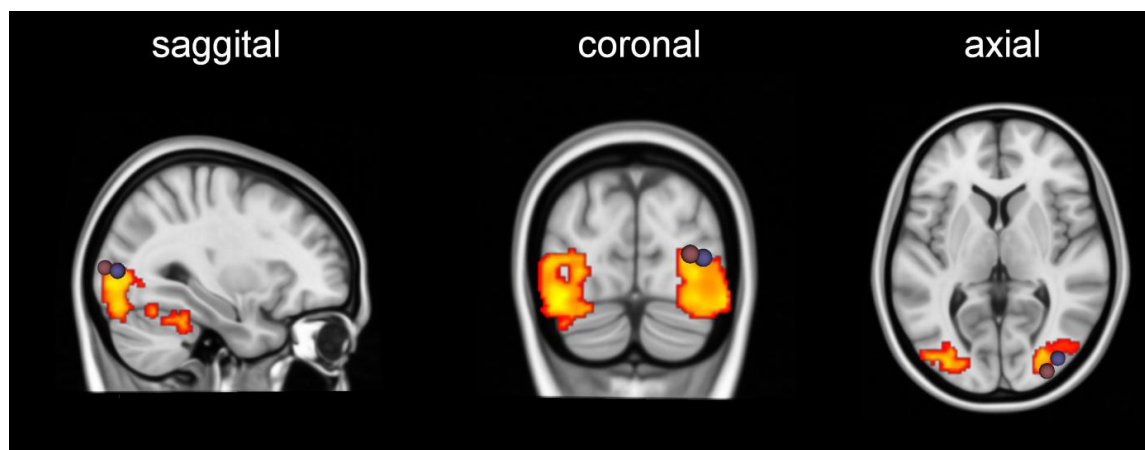
Figure 3.18: *Overlap between object selective cortex and visual field maps LO1 and LO2 in MNI space. Images are displayed in neurological convention. The group BOLD response to images of objects > scrambled objects is shown on saggital **(left)**, coronal **(middle)** and axial **(right)** slices of the MNI (0.5mm) brain. 5mm spheres centred on the mean centroids for LO1 **(burgundy)** and LO2 **(purple)** are also shown on the same slices. There is a good correspondence between the locations of LO1 and LO2 and functional definitions of LO. Of note, LO1 and LO2 extend beyond the areas depicted by these 5mm spheres.*

The current analyses revealed a number of features of LO1 and LO2, consistent with previous reports. First, LO1 and LO2 were found to exhibit object-selective responses consistent with typical functional definitions of LO (Malach et al., 1995; Grill-Spector et al., 1999). The BOLD responses in LO1 and LO2 were greater to the presentation of objects, than to either faces or scrambled objects. This is consistent with the original definitions of the posterior portion of the LOC, the object selective LO. Second, despite the object-selective responses in LO1 and LO2, the functional definition of LO were found not to be restricted to the retinotopic boundaries of LO1 and LO2. That is, statistically significant activation to objects was observed outside of LO1 and LO2, suggesting that either LO extends beyond retinotopic cortex or that LO may be comprised of more visual field maps than LO1 and LO2. The latter explanation is consistent with recent reports of four additional visual field maps (LO3-6) ventral of LO1 and LO2 (Brewer & Barton, 2011).

3.7:   Discussion

This chapter aimed to outline the retinotopic mapping protocol employed throughout the thesis and test several hypotheses which relate to the retinotopic, spatial and object-selective properties of visual field maps LO1 and LO2. The results reported in this chapter reveal a number of important features of LO1 and LO2, which are discussed in turn below.

First, the results reported here demonstrate that retinotopic definitions of LO1 and LO2 were reliably made in at least one hemisphere in all subjects tested. Indeed, LO1 and LO2 were delineable in ~90% of hemispheres tested, an identification rate slightly higher than that previously reported (Larsson & Heeger, 2006). The visual field representations within LO1 and LO2 were also largely consistent with previous definitions (Larsson & Heeger, 2006). The representation of polar angle in LO1 began at the lower vertical meridian junction ('Y') with V3d, V3A /V3B and continued anteriorly and laterally towards the upper vertical meridian. LO2 was found to be the mirror-reverse of LO1, displaying polar angle representations from the upper vertical towards the lower vertical meridian. These visual field representations were found to be consistent not only across individual subjects, but also, when group average visual field coverage and surface based analysis techniques were employed.

Second, the sizes and anatomical locations of LO1 and LO2 were found to be commensurate with the original definitions of these visual areas (Larsson & Heeger, 2006). The precise location of our LO1 and LO2 centroids varied across subjects, even following normalisation to an average coordinate space - a feature previously reported. Despite this variation LO1 and LO2 nevertheless show some adherence to common gyral and sulcal patterns, evidenced through the surface based averaging results.

Third, LO1 and LO2 were found to exhibit object-selective responses. The BOLD responses in LO1 and LO2 were greater following the presentation of objects compared to either faces or scrambled objects – a feature consistent with previous work (Larsson & Heeger, 2006), and the original definitions of object-selective LO (Malach et al., 1995).

Finally, the retinotopic organisation and visual field coverage observed in our LO1 and LO2 definitions were entirely consistent with the delineation of lateral occipital cortex proposed by Larsson and Heeger (2006). The largely complete hemifield representations observed within LO1 and LO2 runs contrary to a recent suggestion which purports the existence of a dorsal component to human V4 (V4d) (Hansen, Kay & Gallant, 2007). This alternative organisation is illustrated in Figure 3.19 and is compared with the retinotopic delineation of LO as proposed by Larsson and Heeger. Hansen and colleagues argue that V4d is homologous to the dorsal component of V4 found in macaque visual cortex. The argument for human V4d originated from studies, which reported that V4 contained only a lower quadrant representation, rather than the complete hemifield representation originally reported (McKeefry & Zeki, 1997). In addition, human V4d is purported to contain a lower quadrant representation anterior of V3d (Hansen et al., 2007). The alternative account, argues that part of the LO1 map should be combined with V4 to complete the hemifield representation. V4d is also suggested to directly abut LO1, but importantly, without displaying a phase reversal at this boundary (Hansen et al., 2007).
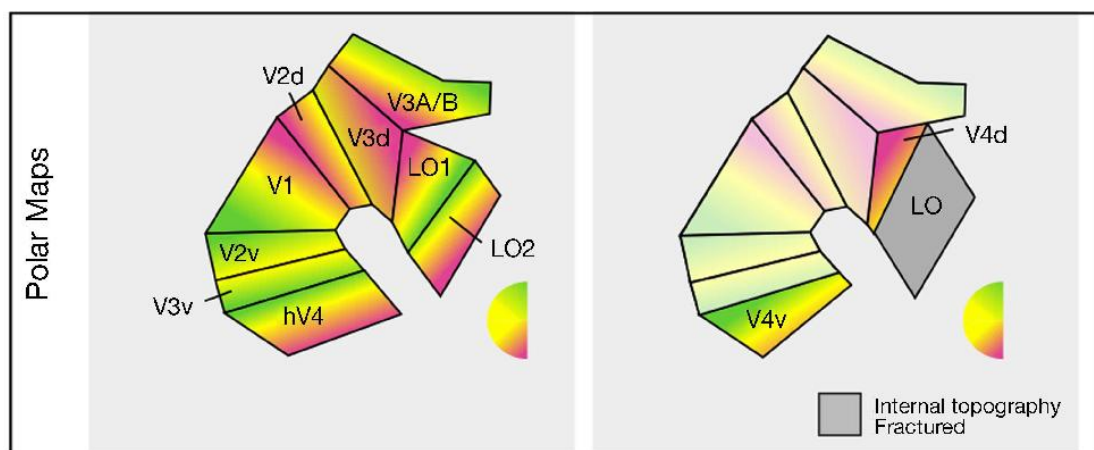
Figure 3.19: *Two alternative models for the existence of human hV4. The model proposed by Larsson and Heeger is shown to the **left**. In this model both hV4 and LO1 contain full hemifield representations. The model proposed by Hansen and colleagues is shown to the **right**. This model proposes that hV4 contains an upper quadrant representation only, with the lower quadrant being represented by a region of cortex anterior of V3d, which would constitute half of the LO1 map. Adapted from Goddard et al., (2011).*

The V4d proposal faces two major challenges. First, a number of independent laboratories have not only demonstrated a complete hemifield map in V4 (McKeefry & Zeki, 1997; Wandell et al., 2007; Goddard et al., 2011), which reduces the likelihood of there being a dorsal component of V4, but also, a complete hemifield representation anterior of V3d, LO1 (Larsson & Heeger, 2006; Wandell et al., 2007; Amano et al., 2009; Goddard et al., 2011). Second, if one accepted the model, then the spared portion of LO1 (upper quadrant) would be stand-alone, with no identified ventral counterpart, this would constitute an 'improbable area' (Zeki, 2003). Third, the proposal is reliant on V4d abutting LO1, but crucially, without a reversal in the visual field representation at this boundary. This scenario represents a divergence from the accepted method of visual field map identification, with reversals in the phase being the gold standard for retinotopically defining boundaries between visual areas. In contrast to Hansen et al., (2007) but consistent with previous reports (McKeefry & Zeki, 1997; Larsson & Heeger, 2006), our visual field mapping experiments reveal that (1) V4 is a single visual field map on the ventral surface of the brain that contains a complete hemifield representation and (2) anterior of V3d lies a complete hemifield representation LO1, rather than the lower quadrant that the alternative proposal relies upon. The visual field representations observed in V4 and LO1 are entirely consistent with previous reports and argues against LO1 being the dorsal component of V4.

The visual field representations of our LO1 and LO2 definitions also run in contrast to the visual field representations observed at the commensurate level of the macaque visual cortex, depicted in Figure 3.20. In macaque, visual field maps V4d and V4t (V4 transitional) occupy the expanse of cortex between V3d and V5/MT (Orban, Van Essen, & Vanduffel, 2004; Larsson & Heeger, 2006). Both V4d and V4t are reported to contain a lower quadrant representation of the visual field only. In contrast, the visual field coverage we observe in LO1 and LO2 is consistent with previous reports (Larsson & Heeger, 2006; Gardner et al., 2008; Goddard et al., 2011), demonstarting complete hemifield represetnations in these regions, arguing against a direct homology between LO1 and LO2 and macaque V4d and V4t. LO1 and LO2 could therefore, represent two uniquely human visual field maps.
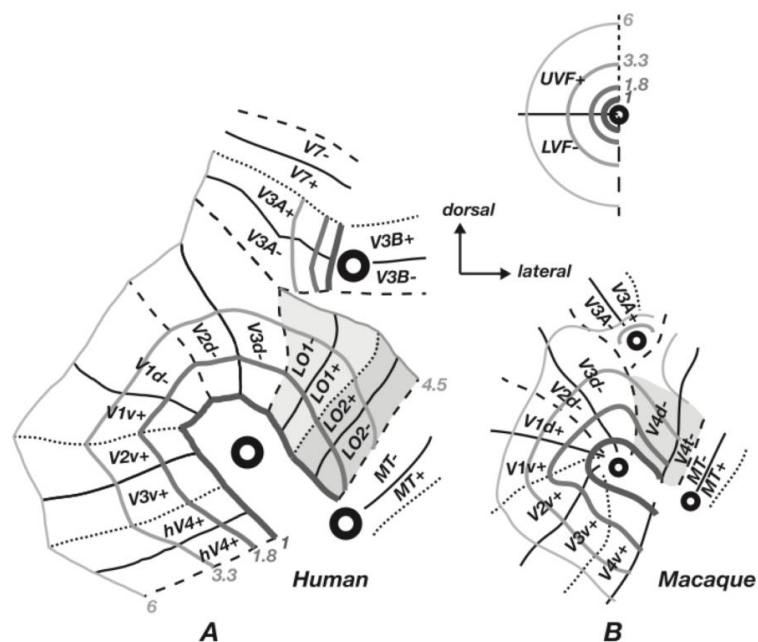
Figure 3.20: *Flattened schematics of visual field maps in the right hemisphere of human and macaque visual cortex. In early visual cortex, V1, V2 and V3, there is clear homology between the two species. However, beyond V3d, the homology is less straightforward. In the macaque, V4d and V4t (shaded) represent the lower quadrant, respectively. In contrast, LO1 and LO2 (shaded) in the human, contain a hemifield representation, respectively. LO1 and LO2 appear therefore, to be two uniquely human visual areas. Figure adapted from Larsson & Heeger (2006).*

3.8:   Conclusion

This chapter has described and demonstrated the travelling wave method for fMRI visual field mapping adopted throughout the thesis. In addition, the retinotopic features, sizes and locations of LO1 and LO2 were assessed and found to be consistent not only with the original LO1 and LO2 report (Larsson & Heeger, 2006), but also, a number of more recent studies (Wandell et al., 2007; Amano et al., 2009; Goddard et al., 2011). LO1 and LO2 were also shown to exhibit object-selective responses, consistent with previous definitions of LO (Malach et al., 1995). The data presented in this chapter are consistent with the retinotopic organisation of lateral occipital cortex proposed by Larsson and Heeger (2006) and not the more recent model proposed by others. Finally, the retinotopic mapping experiments allowed LO1 and LO2 to be clearly defined in at least one hemisphere in all subjects tested. This was the crucial and initial step in all of the experiments conducted throughout the thesis.

Chapter 4

Motion & Orientation Processing in Lateral Occipital Cortex – A Pilot Study

4.1:   Overview

The aim of this study was to investigate whether applying TMS to three relatively closely separated cortical targets could induce selective disturbances to performance on two visual tasks. The cortical targets for stimulation were LO1, LO2 and V5/MT. Given the previous literature in both macaque and human detailing V5/MT's causal role in motion perception, a motion discrimination task was selected. Specifically, the motion task was designed to replicate a previously published finding regarding the effect of V5/MT stimulation on speed discrimination (Mckeefry et al., 2008). The second task was orientation discrimination – a visual task which may crucially depend on computations performed by LO1. The causal role played by LO2 in these visual tasks remains unknown, but we include this site in order to determine whether or not it plays a role in either task. If LO2 is causally involved in a visual task that is independent of both LO1 and V5/MT and moreover, contributes little to motion or orientation discrimination then TMS of LO2 should have no effect on discrimination relative to our No TMS baseline condition.

4.2:   The Processing Characteristics of V5/MT, LO1 & LO2

This study aimed to reveal specializations for motion and orientation processing in cortical areas V5/MT and LO1, respectively. In order to place the current study in the appropriate empirical context, the following sections outline the evidence for motion and orientation processing in several cortical visual areas. Evidence is taken from both macaque and human studies across a number of investigative paradigms.

4.2.1:   Motion Processing in Primate Visual Cortex

In both macaque and human cortex, the study of visual motion has revealed a number of areas specialized for motion perception. The following section reviews the role of V5/MT (the major contributor in this network) in motion processing, beginning with single

unit studies in macaque and culminating in the application of TMS to V5/MT in human. Macaque visual cortex contains multiple visual areas, each one of which may be responsible for the analysis of one or more visual features (Zeki, 1990). Among these visual areas the evidence in favour of functional specialization is particularly strong for the middle temporal (MT/V5) area. Originally identified as an extrastriate area of cortex receiving direct input from V1, V5/MT was shown to contain a high proportion of directionally tuned neurons (Zeki, 1978). A subsequent wealth of physiological and behavioural studies confirmed the critical role that V5/MT plays in the perception of motion. In addition to directionally tuned neurons, V5/MT has been shown to contain neurons that are tuned to different speeds (Maunsell & Newsome, 1987). Indeed the directional tuning of V5/MT neurons has been shown to be similar across speeds (Rodman & Albright, 1987). The specialization of V5/MT neurons was also shown to be somewhat independent of V1 input. Selective ablation and inactivation (via targetted cooling) of V1 in macaque cortex did not alter the visual responsiveness of the majority of tested V5/MT neurons and left recpetive field size and topographic represenation relatively unaltered (Rodman & Gross, 1989). In contrast, selective ablation of V5/MT directly led to increased thresholds for motion discrimination of dynamic random dot displays (Newsome & Pare, 1988). More recently, recordings from macaque V5/MT have demonstrated that the speed encoding of V5/MT neruons are relatively form invarient (Priebe, Cassanello, & Lisberger, 2003). Using single square-wave gratings, the preferred speed of ~75 % of neurons were found to be dependent to an extent on spatial frequency, whilst ~25 % maintained speed tuning despite changes in spatial frequecny. When two gratings were superimposed onto one another, neurons prefered speed became less dependent on spatial frequency, suggesting that V5/MT neurons contain form-invariant speed tuning. Neuronal activity within macaque V5/MT has also been shown to correlate with speed perception judgements, whilst microstimulation of V5/MT actively altered speed judgements (Lui & Newsome, 2003; 2005).

In human, the existence of and role played by V5/MT has been demonstarted repeatedly across neuropsychological and neuroimaging studies. In 1983, Zihl and colleagues reported the case of Patient L.M, who suffered bilateral damage to the lateral temporo-occipital cortex (Zihl et al., 1983). Across a large battery of neuropsychological tests, L.M exhibited selective disturbances of visual motion despite relatively normal visual

functions including acuity, visual field topography and colour vision, among others (Zihl et al., 1983). Patient L.M was the first case of a pure motion deficit, refered to as visual akinatopsia (Zeki 1991). Later studies using PET and fMRI have not only confirmed the selectivity of V5/MT to the perception of visual motion (Zeki et al., 1991; Huk, Dougherty, & Heeger, 2002; Orban, Fize, Peuskens, Denys, Neilssen, Sunaert, Todd & Vanduffel 2003; Tootell, Tsao, & Vanduffel, 2003), but also, revealed the topographical representations within and surrounding this area (Huk, Dougherty, & Heeger, 2002; Amano et al, 2009; Kolster, Peeters & Orban, 2010). Very recently, V5/MT was shown to contain two retinotopic subdivisions termed TO1 and TO2, respectively. Both visual field maps contain complete contralateral hemifield representations (Amano et al., 2009).

A number of TMS studies have also been undertaken in order to probe the functioning of V5/MT. TMS has a distinct advantage over neuroimaging techniques as it can provide causal, rather than correlational information regarding cortical function. TMS has been employed therefore, to provide evidence in normal individuals that compliments the neuropsychological evidence reported in patients with seletive lesions. Early TMS studies of V5/MT showed selective disturbances to the accurate discrimination of direction (Beckers & Homberg, 1992; Beckers & Zeki, 1995). An investigation into the role of V5/MT on visual attention of motion confirmed the critical role played by V5/MT during six visual search tasks. TMS of V5/MT caused a disproportianate disruption to visual search tasks when motion, but not form, was the attended visual cue (Walsh et al., 1998). An additional TMS experiment, which is repeated here to form one part of the current study, investigated the role of V5/MT (plus other sites) in the perception of speed (McKeefry et al., 2008). Given that V5/MT is the cortical target common to both the previous and current studies, I focus on V5/MT alone. TMS was applied to V5/MT to transiently disrupt the processing in this area whilst subjects performed delayed speed discrimination psychophysical experiments. The reference grating had a fixed speed of 8°/sec, while test gratings moved at one of seven predetermined speeds, specified to span a range of speeds both quicker and slower than the reference. A two-interval forced choice paradigm was employed, with subjects required to report which one of the two gratings appeared to move faster. Three experimental blocks (10 trials per test speed) were completed to derive psychometric functions, allowing the effect of TMS on the *PSE* and discrimination threshold to be determined relative to a no

TMS baseline. The delivery of TMS to V5/MT produced two main effects: (1) There was a right-ward shift in the psychometric functions, indicating that as a result of TMS stimulation the test gratings were perceived as slower than the reference and (2) a significant reduction in the slope of the psychometric function, indicating an elevation in speed discrimination thresholds. Importantly, the effect of TMS of V5/MT exhibited task and location specificity. TMS of V5/MT did not alter performance on a spatial frequency discrimination task and furthermore, displacement of the coil ~2cm away from the V5/MT target removed the disruptive effect of TMS on performance. The demonstration that TMS of V5/MT exhibits location and task specificity are important control measurements, which add compelling evidence to the large body of work supporting the specialized role of primate V5/MT's in motion processing.

Along with V5/MT, a second cortical area, V3A, has been shown to be selective to motion through neuroimaging (Smith, Greenlee, Singh, Kraemer, & Hennig, 1998; Tootell et al., 2003) and neurostimulation studies (Mckeefry et al., 2008). Intriguingly, LO1 and LO2 are located between the V3A and V5/MT motion selective areas (Figure 4.1) (Larsson & Heeger, 2006). The posterior and dorsal boundary of LO1 abuts the ventral boundary of V3A. Likewise the lateral boundary of LO2 lies either in close proximity with the posterior boundary of V5/MT, or in some cases abuts it directly (Larsson & Heeger, 2006). The fact that LO1 and LO2 are located in between two cortical areas specialized for motion perception raises the question as to whether or not computations performed by LO1 and LO2 are also causally involved in motion perception.

The motion selective nature of computations in LO1 and LO2 has been previously investigated using fMRI (Larsson & Heeger, 2006). Subjects were presented with alternating blocks of moving and stationary dot patterns. The authors report the identification of three cortical areas that were selectively responsive to moving over stationary patterns (V1, V3A, and V5/MT). The average responses across subjects to moving dot patterns in LO1 and LO2 were, however, not significantly different from the responses to stationary dot patterns (two-tailed t-test, df = 6, p = 0.62 and p = 0.06, for LO1 and LO2, respectively), suggesting that neither LO1 nor LO2 contain neurons that exhibit motion selectivity. Although of note, the response in LO2 approach significance (p = 0.06). Causal inferences however, cannot be made as a result of fMRI contrasts. In order to establish the role (if any) that LO1 and LO2

play in human motion perception there is a need to probe the functioning of these maps at a causal level through the application of TMS and furthermore, compare the effects to those found following TMS of V5/MT.
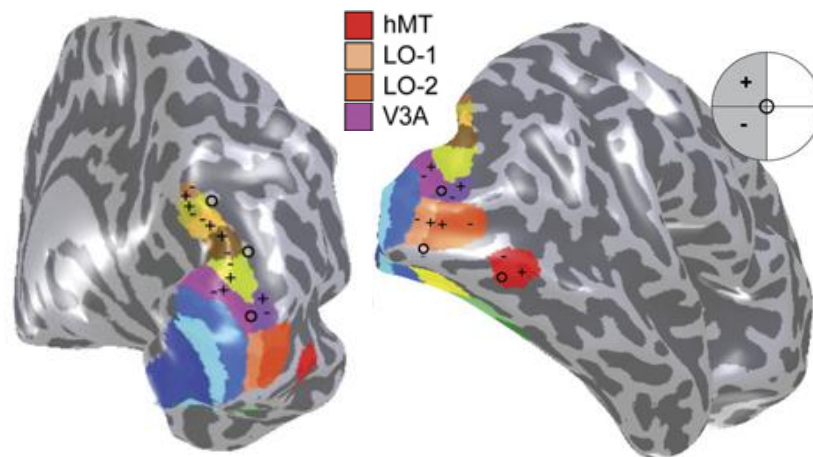
Figure 4.1: *Visual field maps in the right hemisphere. Visual field maps are shown on posterior **(Left)** and lateral **(Right)** views of surface reconstructions of the right hemisphere of a single subject. V3A (purple) abuts the posterior and dorsal boundary of LO1 (peach), with V5/MT (hMT) (red) located slightly anterior of the posterior boundary of LO2 (orange). Adapted from Figure 2, Wandell et al., 2007).*

4.2.2:   Orientation Processing in Striate & Extrastriate Cortex

Early electrophysiological studies in non-human primates provided the first demonstrations of orientation selectivity in primary visual cortex. Pioneering single-unit studies of cells within cat V1 demonstrated that the most effective stimulus for V1 neurons was not a single spot of light, as previously thought, but rather, long narrow rectangles of light, referred to as 'slits' (Hubel & Wiesel, 1963). Hubel & Wiesel observed that a given V1 cell would respond vigorously when an appropriate stimulus was shone on or moved across the receptive field, provided that the stimulus was of a particular orientation. The orientation selectivity of V1 neurons were shown to be structured in a columnar organisation. Later studies confirmed the columnar organisation of orientation selective neurons in macaque V1 (Hubel, Wiesel & Stryker, 1978). These neurons, like those in the cat were found to respond selectively to specifically orientated straight-line segments, rather than single spots of light placed within their receptive fields. Human fMRI experiments have

largely confirmed the existence of orientation-tuned neurons in V1 (Furmanski & Engel 2000). Indeed, the authors report fMRI data demonstrating the 'oblique effect', the finding that human orientation discrimination is more sensitive at the vertical and horizontal meridians, relative to oblique angles (Cambell & Kulikowski, 1966).

Orientation selectivity has also been explored beyond striate cortex. Indeed, previous fMRI work identified a possible segregation of function between LO1 and LO2 in terms of their selectivity to stimulus orientation (Larsson et al., 2006). LO1, but not LO2, was found to show robust and significant orientation selective MR adaptation (Larsson et al., 2006). Subjects were required to count the frequency with which an 'X' was present in an array of rapidly changing letters at fixation. During a single trial, a high-contrast adapting grating was presented parafoveally for 4sec. The adapting gratings were orientated either vertically or horizontally. One second after cessation of the adapting grating, a probe grating was presented. Probe gratings were either presented at orientations parallel or orthogonal to the adapting stimulus.

An area with orientation selectivity should exhibit a greater response to the probe oriented orthogonal to the adapting grating than parallel to it. This greater response to orthogonal than parallel probes is referred to as a release from adaptation. LO1 exhibited a significant release from adaptation as did many other retinotopic visual areas, depicted in Figure 4.2. Interestingly however, LO2 exhibited no significant release from adaptation. The results indicated that a large number of extrastriate cortical areas exhibited orientation selective adaptation to the luminance modulated grating stimuli. The adaptation in extrastriate regions could occur for at least two reasons. First, the extrastriate regions exhibiting the adaption effect may contain neurons that explicitly compute orientation and adapt to orientation. Second, the extrastriate areas may simply inherit orientation adaptation which is set by neurons in a lower level visual area (likely V1) to which the extrastriate areas are connected. The authors (Larsson et al., 2006) adopted the second explanation for these data and suggested that the majority of extrastriate adaptation to luminance-modulated orientation was attributable to feed-forward propagation from V1 (Larsson et al., 2006).
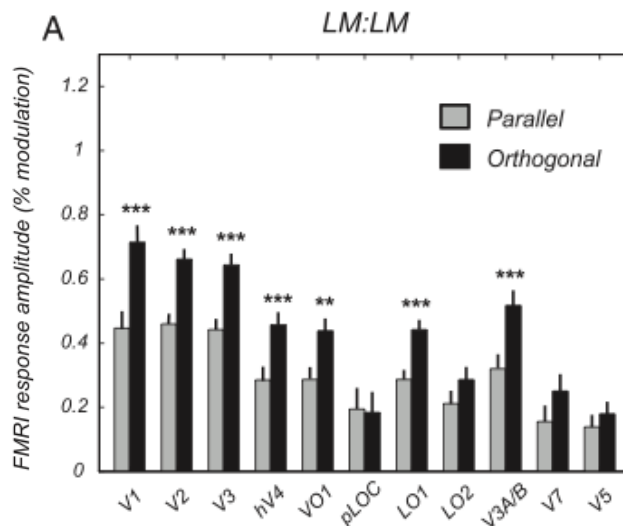
Figure 4.2: *Orientation-selective fMRI adaptation in human visual cortex. The response to an orthogonally orientated grating can be seen to exhibit a significant release from adaptation in a number of visual field maps. Importantly, the significant release from adaptation observed in LO1, is not reflected in LO2. Adapted from Figure 10 (Larsson et al., 2006).*

The result suggested a segregation of function between LO1 and LO2, with LO1 exhibiting highly significant orientation selective neural responses, a result not evident in LO2 (Larsson et al., 2006). The orientation selective activation observed in LO1 extended to all stimulus dimensions tested; luminance, contrast and orientation (Larsson et al., 2006). Interestingly, and in addition to LO2, V5/MT also showed a lack of selectivity to stimulus orientation.

Despite the strong evidence for orientation processing in LO1, but not LO2, the analysis suffers from the limitation inherent in the fMRI signal, that of causality. Although signals in LO1 displayed significant adaptation to orientation, that signal in of itself cannot establish whether the neural processing within LO1 is causally related to the processing of orientation, or simply a correlated hemodynamic response. In order to address this issue, TMS was employed in the current study to elucidate the causal role played by LO1 in processing orientation. Specifically, this study aimed to establish whether neural activity within LO1 processes orientation information directly. To be consistent with the motion experiment we also investigated the roles of LO2 and V5/MT in the processing of orientation.

4.3:   Theoretical Considerations

As outlined in the ***theoretical & analytical framework*** section of Chapter 1 ***(1.6)***, the design and interpretation of studies conducted throughout the thesis were heavily influenced by consideration of two components of a framework I term '*map specific',* which proposes that each visual area exhibits functional specialization for the processing of particular visual features. Within this framework these functional specializations could be expressed either in a strictly serial and dependent processing architecture or alternatively independent of the computations performed by other areas, in other words in parallel.

In regard to the current study, there is considerable evidence in both macaque and human that V5/MT exhibits parallel processing capabilities. In macaque, V4d and V5/MT abut one another on the lateral aspect of the occipital lobe. These visual areas have been shown to be functionally specialized for visual attributes of colour and motion, respectively (Zeki et al., 1978; Zeki, 1990). These areas also receive parallel projections from antecedent V2 (Shipp & Zeki, 1988), providing a plausible anatomical mechanism underlying these functionally parallel processes. In human, one of the first celebrated demonstrations of parallelism and functional specialization came with the observation that, V4 and V5/MT exhibited specializations for colour and motion processing, respectively. Indeed, damage to V5/MT, is seldom associated with deficits in colour processing and vice-versa – damage to V4 is seldom associated with deficits in motion processing (Zeki, 1990). Direct projections from subcortical structures such as the LGN to V5/MT have been identified in macaque cortex (Sincich, Park, Wohlgemuth & Horton, 2004). These direct projections bypass several stages of the visual hierarchy and therefore offer a plausible explanation for parallel processing. Intriguingly, LO1 and LO2 are in a commensurate location within the visual hierarchy in human as V4d and V5/MT are in the macaque, making the existence of parallel anatomical connections and functional specializations at least plausible.

It is only following the demonstration of task and location specificity that a genuine claim of functional specialization can be made. These considerations echo those employed by McKeefry et al., (2008). The need for a control site is therefore, paramount. In the current experiment a control site (CON) was selected posterior of LO1 and therefore, closer in proximity to V1. The reason underpinning the location of the CON was that it provided a

sensible means by which to test whether any effect observed at LO1 during orientation discrimination is attributable to LO1's closer proximity to V1 than our other target sites. Of note, LO1's orientation selective adaptation was originally explained in terms of selective inheritance due to V1 proximity (Larsson et al., 2006). Although consideration of the effects of TMS at the CON, LO1 and V5/MT alone fits the requirements of the framework, we include LO2 as a target site, despite having no strong directional hypotheses regarding LO2's role in either task. An absence of effect of TMS of LO2 for either task however, would be profoundly important for: (1) interpretation of functional specialization in the event that TMS of V5/MT and LO1 selectively disrupt motion and orientation, respectively; (2) the precision of TMS and (3) the nature of computations performed by LO2.

4.4:   Aims & Predictions

The studies described in this chapter aimed to examine functional specialization in two closely separated cortical areas for two visual tasks. Given the clear evidence for parallel processing at the level of V5/MT reported above, we focus here on the predicted effects of TMS on our tasks based upon '*map specific*' and '*parallel*' processing only. It should be noted that these predictions are reliant upon the following three assumptions: (1) that the spread of TMS will be focal enough to allow stimulation of the intended target site without the effects spreading markedly into adjacent sites; (2) LO1 and V5/MT's specializations and parallel processing capabilities exist and (3) that LO2 does not play a causal role in either motion or orientation processing.

The map specific and parallel predictions are plotted in Figure 4.3. If V5/MT is specialized for motion processing and that processing is independent of other areas then TMS of this site and no other should disrupt motion discrimination (Left plot Figure 4.3). As explained above, this prediction brings with it a number of assumptions demonstrated by the bi-directional red arrows above the LO2 site. The bi-directional red arrow demonstrates that the exact role played by LO2 in motion processing is currently unknown. If LO1 is specialized for orientation processing independently of other visual areas then TMS of LO1 alone should disrupt orientation processing (Right plot Figure 4.3). Again, the bi-directional red arrow depicts the uncertain effect that TMS of LO2 will have on orientation discrimination. Taken together the two plots predict a double dissociation. That is, V5/MT

and LO1 will exhibit functional specializations for motion and orientation processing, respectively, and moreover, that these functional specializations will operate in parallel.
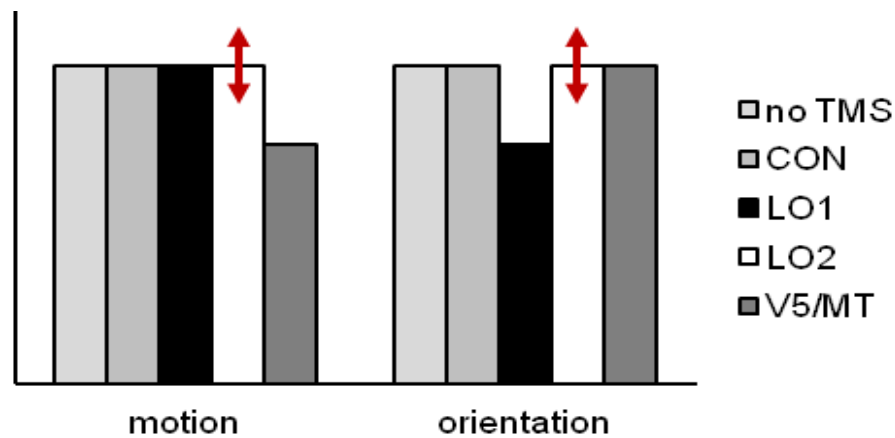
Figure 4.3: *Schematic predictions of the effects of TMS on motion and orientation discrimination. For motion discrimination, TMS of V5/MT should disrupt processing relative to all other conditions. For orientation discrimination, TMS of LO1 should disrupt processing relative to all other conditions – a double dissociation. The bi-directional red arrows above LO2 in both tasks, represents the unknown effect that TMS of this site may have.*

4.5:   Methods

4.5.1:   Subjects

Six subjects (mean age = 32, range = 23, 3 male) participated in the study. All subjects had normal or corrected to normal vision and gave informed consent in accordance with the declaration of Helsinki. York Neuroimaging Centre (YNiC) Research Governance Committee approved the study.

4.5.2:   Visual Field Mapping

All subjects completed retinotopic mapping sessions using standard fMRI visual field mapping techniques, as outlined in Chapter 3. Data analysis, segmentation and delineation of visual areas were also completed in accordance with previously published work (Baseler et al., 2011) and the steps described in Chapter 3.

4.5.3:   Identification of Visual Field Maps LO1 & LO2

LO1 and LO2 were identified in at least one hemisphere in all six subjects in accordance with previous reports (Larsson & Heeger, 2006). LO1 extended anteriorly and laterally from the boundary of V3d, progressing gradually from the lower vertical meridian toward the upper vertical meridian. LO2 neighboured and was the mirror-reverse of LO1, displaying a gradual progression from the upper vertical meridian toward the lower vertical meridian.

4.5.4:   Identification of V5/MT

V5/MT was identified anatomically in each subject, in accordance with published methods (Dumoulin et al, 2000). V5/MT was located within the ascending limb of the inferior temporal sulcus (ALITS). In accordance with previously published data the posterior boundary of V5/MT was either in close proximity to, or directly abutted the anterior boundary of LO2 (Larsson & Heeger, 2006). Newly identified visual field maps TO1 and TO2 (Amano et al., 2009), which lie within the V5/MT area, were present in some, but not all, subjects, so were not used to localise V5/MT.

4.5.5:   Defining the Control Site

Anatomically, LO1 is closer in proximity to V1 than either LO2 or V5/MT. The closer proximity, coupled with the clear evidence for orientation selectivity of neurons within cat (Hubel & Wiesel, 1963), macaque (Hubel, Wiesel & Stryker, 1978) and human V1 (Furmanski & Engel, 2000), it was desirable to control for V1 proximity by selecting a control TMS site even closer to V1 than LO1. For orientation discrimination, if dissociations were evident between LO1 and LO2, and/or between LO1 and V5/MT then the inclusion of a control site closer to V1 would provide a means by which to assess whether or not this dissociation was due to LO1's proximity to V1. If V1 proximity explained these dissociations, one would predict the greatest disruption to orientation discrimination the closer the target to V1. That is, the effects of TMS on orientation discrimination should be maximised at the point of closest V1 proximity. Of note, this interpretation cannot hold if no effect is observed at the control site (compared to no TMS baseline). In an attempt to define an unbiased control site (in terms of retinotopic organisation), the control site was specified on a geometric basis only by calculating the Euclidean distance between the LO1 and LO2 centroids in each

subject and subsequently moving that distance from the LO1 centroid towards the midline and therefore, V1.

4.5.6:   Psychophysical Stimuli & Procedures

Stimuli for the behavioural and TMS experiments were generated using MATLAB (Mathworks, USA) and displayed on a Mitsubishi Diamond Pro 2070[SB] display with a refresh rate of 60 Hz, controlled by a VISAGE graphics card (Cambridge Research Systems [TM]). Grating stimuli were luminance modulated sinusoidal gratings (50% contrast) presented in a circular aperture (diameter 4°) with a spatial frequency of 2 cpd. All stimuli had a mean luminance of 31 cd.m^{-2} and were presented on a uniform grey background of the same luminance.

The visual tasks employed were motion (speed) and orientation discrimination of sinusoidal gratings. The parameters for psychophysical and TMS experiments followed the protocols outlined in the **Psychophysical & TMS Protocol** sections of Chapter 2. Prior to TMS stimulation each subject completed motion and orientation discrimination psychophysical experiments using the method of constant stimuli described in full in Chapter 2. The spatial configuration of the gratings and temporal trial structure for the motion and orientation experiments were identical (see schematic Figure 4.4). The motion discrimination task was based heavily on the work by McKeefry et al., (2008). That is, the reference grating drifted at a constant speed (8°/sec) and test stimuli were randomly selected from seven predetermined speeds that spanned a range of speeds both slower and faster than the reference. In an attempt to make the orientation task as similar as possible, the reference orientation was fixed (45°), and thus, test stimuli were selected from seven predetermined orientations that spanned a range of orientations both more vertical and more horizontal than the reference. The stimuli for the orientation task were static. For both tasks the phase of the reference and test gratings were randomised within each trial to prevent either task being solved via local luminance cues. In addition, for the motion task the direction of drift (left-right/right-left) was randomised between trials to avoid any directional adaptation. Individual psychometric functions for orientation and motion discrimination were plotted from the average for each subject (average of 350 trials – 50

presentations per stimulus level), in order to determine the individual thresholds (75% correct) to be tested on during subsequent TMS sessions.

In some subjects, the best fitting psychometric function may not pass through 50% correct identification when the reference and test stimuli were identical – the *PSE*. This may result in an asymmetrical function, which in turn will lead to asymmetric thresholds relative to the reference. In order to create symmetrical thresholds with respect to the reference stimulus, we calculated the 75% correct values for speeds both faster and slower than the reference and orientations more vertical and more horizontal than the reference. The range between these values was then calculated and divided in half. Stimuli used in TMS sessions were created using the following equation: TMS Stimuli = reference ± range/2. If for example, during orientation psychophysics the 75% correct more vertical orientation were 51° and the 75% correct more horizontal orientation were 38°. The range (13°) would be halved (6.5°) and then added too and taken away from the reference (45°). This results in a more vertical (38.5°) and a more horizontal (51.5°) test grating, both of which are equidistant from the reference.
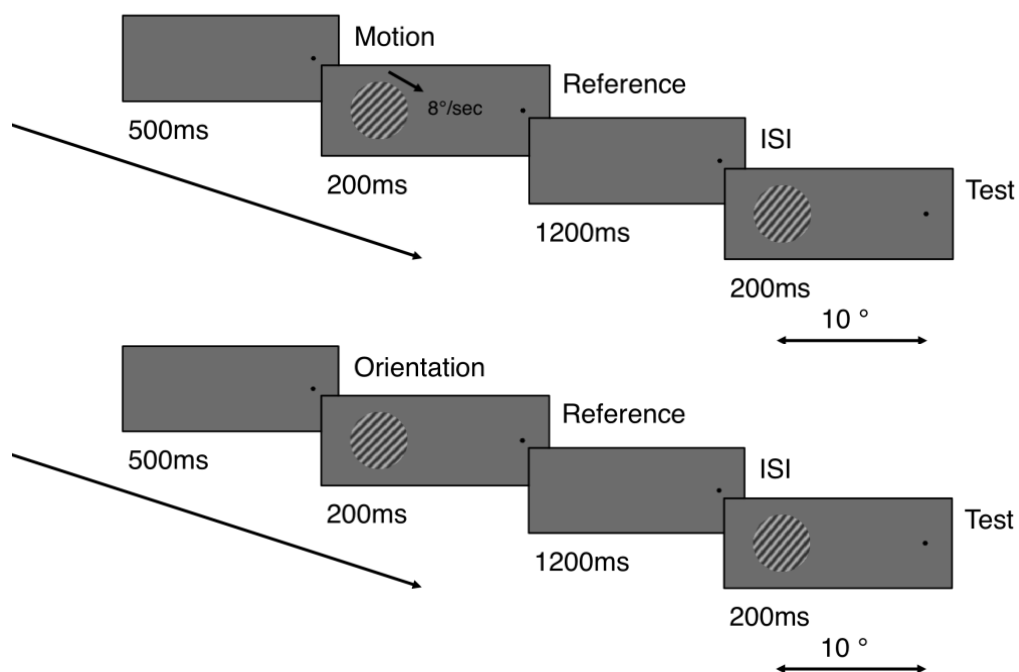
Figure 4.4: *Trial structure schematics for motion **(top)** and orientation **(bottom)** psychophysical tasks. During motion discrimination the reference grating drifted at a fixed speed of 8°/sec. During orientation discrimination the orientation of the reference grating was fixed at 45°. Test stimuli for both tasks were randomly selected from a pre-determined list of seven speeds (motion task) and orientations (orientation task) that spanned a range of values either side of the reference stimuli.*

4.5.7:   TMS Protocol

A train of 4 biphasic (equal relative amplitude) TMS pulses, separated by 50ms (20Hz) at 70% of the maximum stimulator output (2.6 Tesla) were applied to the subject's scalp using a figure-of-eight coil (50mm external diameter of each ring) connected to a Magstim Rapid2 ^{TM} stimulator (Magstim, Wales). Subjects were seated in a purpose built chair with chin rest and forehead support. The coil was secured mechanically and placed directly above each cortical target (CON, LO1, LO2 and V5/MT) with the handle orientated parallel with the floor. The position of the coil was monitored and tracked in real time with respect to the subjects head, allowing several measurements to be recorded with each pulse train. Each subject underwent 10 counterbalanced sessions (2 tasks x [4 TMS sites + 1 No TMS baseline]).

During TMS sessions (and no TMS baseline) only the two stimuli defined using the method described above were randomly presented in a trial structure identical to that used to establish thresholds. Each TMS session comprised 100 trials (50 per threshold stimulus). TMS pulses were delivered concurrently with the presentation of the test stimulus (Figure 4.5). This temporal configuration was identical to that used in previous studies of motion perception (McKeefry et al., 2008) where induced functional deficits were maximised when TMS pulses were delivered coincident with stimulus onset.
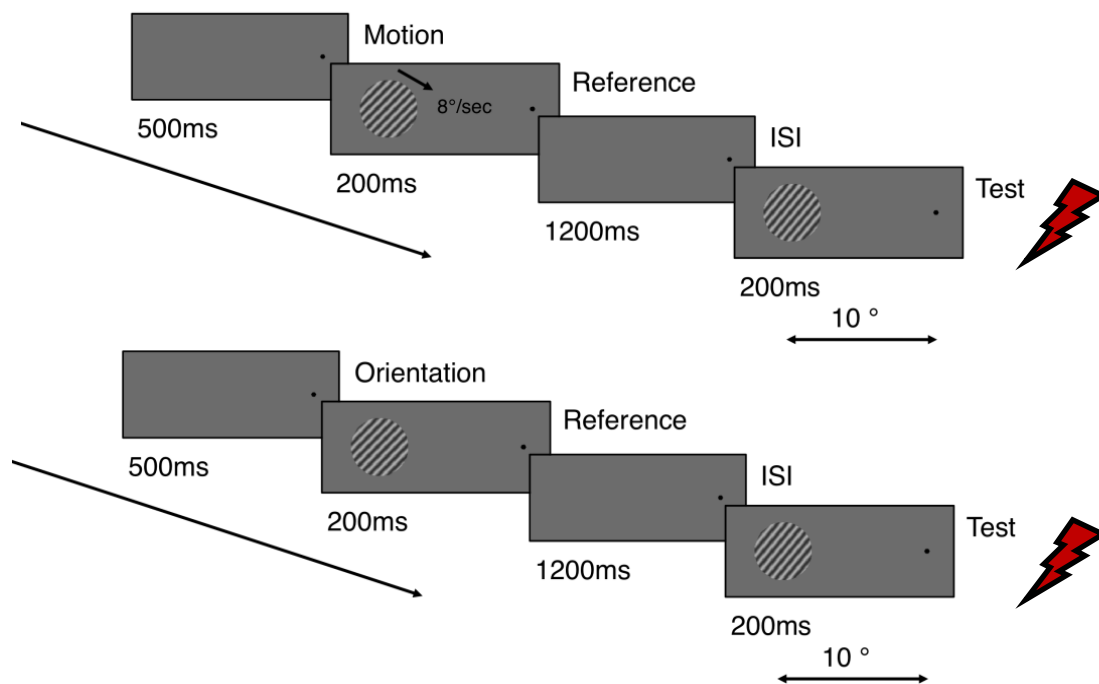
Figure 4.5: *Trial structure schematics for motion (top) and orientation (bottom) TMS tasks. During TMS sessions for both tasks (and no TMS baseline) only the two threshold stimuli were presented as test stimuli in a randomised order. TMS pulses were delivered coincident with the presentation of the threshold stimuli symbolised by the red lightning bolt.*

4.5.8:   Data & Statistical Analysis

Before data analysis some trials (~3%) were removed on the basis of two criteria: trials for which coil displacement was large (>2.5 mm) and trials for which reaction time was greater than 2,000 ms after the cessation of the presentation of the test stimulus. Statistics were calculated using the SPSS software package (IBM [TM]). A series of two-way repeated-measures ANOVAs were employed initially to examine the effects of discrimination (% correct) and reaction times (secondary measure), along with two potentially confounding variables (coil-target distance and coil-target orientation), which relate to spatial relationships between the TMS coils and the cortical targets. These measurements provide a means to assess the amount of variance in the data that can be explained by imprecision in the delivery of TMS pulses, caused by operator error or head movement. In the case of a significant interaction, subsequent one-way repeated-measures ANOVAs were calculated for each task considered separately, followed by paired *t*-tests. For each ANOVA, whether or

not the ANOVA adhered to the assumption of sphericity was established initially using Mauchly's test. When the assumption of sphericity is violated, two approaches to correcting the degrees of freedom are typically adopted to allow appropriate interpretation of the *F* value that resulted from the ANOVA. The Greenhouse-Geisser correction to the degrees of freedom is routinely used when the estimate of sphericity is less than 0.75, but when the estimate of sphericity exceeded this value, the more liberal Huynh-Feldt correction is considered more appropriate.

4.6:   Results

4.6.1:   Identification of Visual Field Maps LO1 & LO2

Visual field maps LO1 and LO2 were clearly identifiable in at least one hemisphere in all subjects (See **Visual Field Map Gallery** in Chapter 3 for full retinotopic breakdown of subjects S1-S6). Figure 4.6 illustrates visual field maps with respect to polar angle (including LO1 and LO2) on lateral views of both the left and right hemispheres of a representative subject (S6). In both hemispheres, LO1 extends anteriorly from the shared boundary with V3d, at the representation of the lower vertical meridian. LO1 displays a gradual progression from the lower vertical meridian towards the upper vertical meridian. LO2 is the mirror-reverse of LO1 and therefore, displays a gradual progression from the upper vertical meridian towards the lower vertical meridian. The retinotopic features of LO1 and LO2 are entirely consistent with previous definitions (Larsson & Heeger, 2006). Centroids of LO1 and LO2 were calculated in order to define TMS targets.
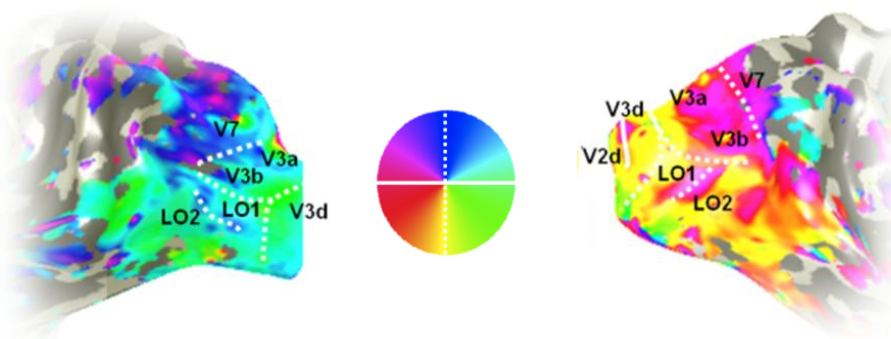
Figure 4.6: *Bilateral visual field maps in a single subject. Lateral views depict visual field maps in the left and right hemispheres of a representative subject (S6). The BOLD responses to the rotating wedge stimulus are overlaid in false colour (see colour wheel, centre) onto surface reconstructions of the grey-white matter boundary of the left and right hemispheres. The vertical meridian representations are shown by the dashed white lines, with the horizontal meridian representations shown by the solid white lines. In both hemispheres the visual field representations in LO1 and LO2 are clearly identifiable. LO1 begins at the shared boundary with V3d at the representation of the lower vertical meridian. LO1 extends anteriorly from the lower vertical meridian toward the upper vertical meridian. LO2 is the mirror-reverse of LO1 and displays a gradual progression from the upper vertical meridian back toward the lower vertical meridian. LO1 and LO2 were identified in at least one hemisphere in each subject.*

4.6.2: Identification of V5/MT

In all subjects, the V5/MT target site for TMS was located in the ascending limb of the inferior temporal sulcus (ALITS) in accordance with previous literature (Dumoulin et al., 2000). Figure 4.7, demonstrates the anatomical location of V5/MT in a representative subject (Left of Figure 4.7), along with an example of the close proximity of our cortical targets (Right of Figure 4.7). The Euclidean distances between cortical targets in each subject are given in Table 4.1. Distances were calculated within individual's native space and therefore, reflect the actual distances without normalisation to an average coordinate space.
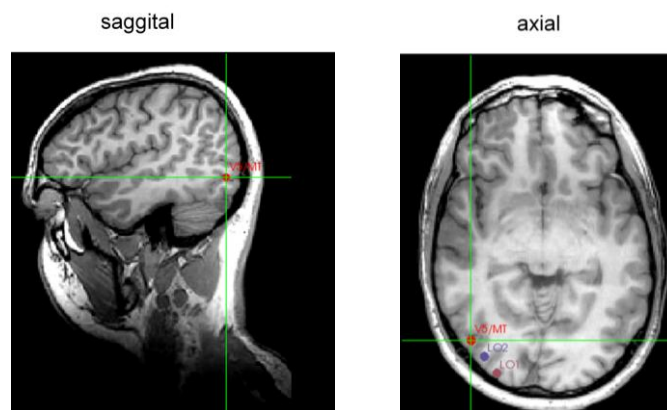
Figure 4.7: *Anatomical identification of V5/MT. Saggital and Axial slices depict the location of the V5/MT target in a typical subject. Images are displayed in radiological convention. The superior temporal sulcus (STS) and ascending limb of the Inferior temporal sulcus (AIITS) are illustrated with the dashed white arrows. The V5/MT target, depicted at the centre of the green crosshairs can be seen to fall within the ALITS **(left)**. The V5/MT target is in close proximity to the LO1 and LO2 cortical targets identified through retinotopic mapping procedures **(right)**. The V5/MT target was either found to be close to or abutting the anterior boundary of LO2 in many subjects.*

Table 4.1: *Euclidean distances (mm) between LO1, LO2 and V5/MT in all subjects. The average distances demonstrate the two spatial scales of investigation: LO1 – V5/MT between clusters and, LO1-LO2, within cluster.*

Subject	Euclidean distance (mm) between targets		
	LO1-LO2	LO1-V5/MT	LO2-V5/MT
S1	10.7700	29.8998	16.1864
S2	9.0200	38.4448	24.3516
S3	10.2900	24.7386	20.3224
S4	13.7400	26.7208	16.0312
S5	6.0600	30.0167	12.6886
S6	11.8700	24.8596	12.0830
Average	10.1960	29.1134	16.9439

4.6.3:   Motion & Orientation Psychophysics

Motion and orientation psychometric functions for subjects (S1-S6) are plotted in Figure 4.8. Inspection of Figure 4.8, demonstrates the high individual variation across subjects. Of particular note, the range of orientations required for S6 is substantially larger than the range of orientations needed for Subjects S1-S5. The x axis for S6 is rescaled to account for the greater range of orientations required by this subject. This individual variation underscores the necessity in defining individual discrimination thresholds. If arbitrary stimulus intensities were selected, then during TMS some subjects may exhibit floor effects, whilst others may exhibit ceiling effects.
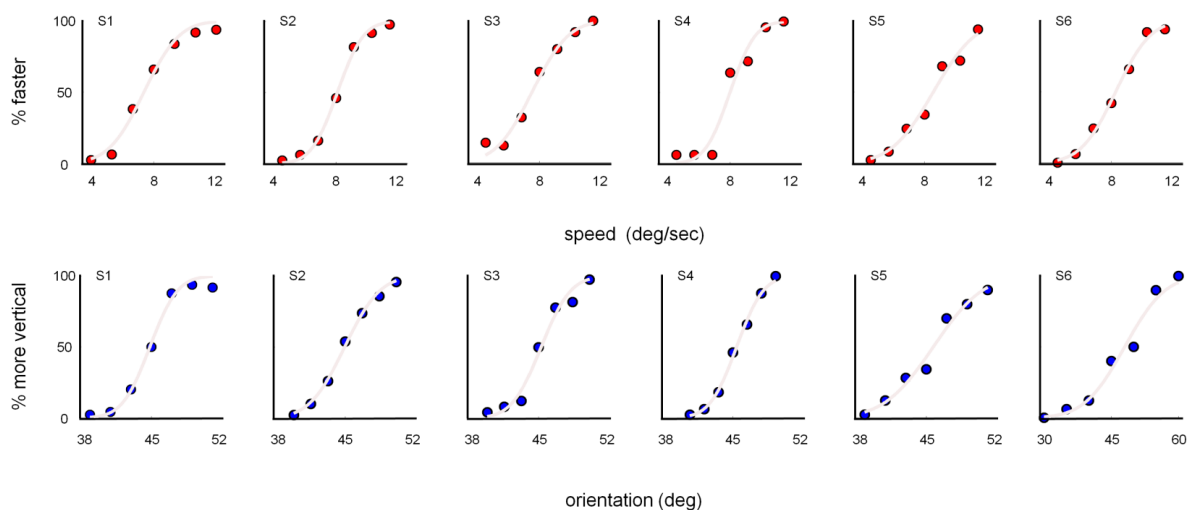
Figure 4.8: *Motion and orientation psychometric functions. Individual psychometric functions for the motion **(top)** and orientation **(bottom)** discrimination tasks for subjects S1-S6. The threshold stimuli to be used in subsequent TMS sessions were derived from these psychometric functions. For motion, the 75% correct faster and slower speeds were calculated. The range between these values was divided in half and added to and subtracted from the reference speed to create the two stimuli for TMS. For orientation, the 75% correct more vertical and more horizontal orientations were calculated. The range between these values was divided in half and added and subtracted from the reference orientation to create the stimuli for TMS.*

We defined, in each individual subject, two stimuli to be presented during each TMS task. These stimuli were equidistant from the reference stimulus. Table 4.2, contains the 75% correct thresholds for speeds faster and slower than the reference (motion) and orientations more vertical and more horizontal than the reference (orientation), for all subjects. Table 4.2, also includes the value added too and subtracted from the reference stimulus and the actual values presented during TMS for all subjects.

Table 4.2: *Threshold and TMS values derived from the motion and orientation psychometric functions for subjects S1-S6. For motion **(top)**, table includes the 75% correct values for speeds slower **(threshold S)** and faster **(threshold F)** than the reference, plus the value added too and taken away from the reference **(ref ±)** and the values used during TMS for the slower **(TMS S)** and faster **(TMS F)** test stimuli. For orientation **(bottom)**, table includes the 75% correct values for orientations more horizontal **(threshold H)** and more vertical **(threshold V)** than the reference, plus the value added too and taken away from the reference **(ref ±)** and the values used during TMS for the more horizontal **(TMS H)** and more vertical **(TMS V)** test stimuli.*

speed (degrees/sec)					
Subject	threshold S	threshold F	ref ±	TMS S	TMS F
S1	6.4075	8.5075	1.0500	6.9500	9.0500
S2	7.3100	8.5550	0.7725	7.2275	8.7725
S3	6.5150	8.6750	1.0800	6.9200	9.0800
S4	7.2650	8.7500	0.7425	7.2525	8.7425
S5	7.2500	9.7550	1.2525	6.7475	9.2525
S6	7.2200	9.2900	1.0350	6.9650	9.0350
orientation (degrees)					
Subject	threshold H	threshold V	ref ±	TMS H	TMS V
S1	43.4400	46.3200	1.4400	43.5600	46.4400
S2	43.1250	46.8000	1.8375	43.1625	48.8375
S3	43.7250	46.7750	1.5250	43.4750	46.5250
S4	44.2800	46.2600	0.9900	44.0100	45.9900
S5	43.1400	48.2700	2.5650	42.4350	47.5650
S6	43.2000	52.8000	4.8000	40.2000	49.8000

4.6.4: Effects of TMS on Motion & Orientation Discrimination

Group average performance (% correct) for all conditions are plotted for both tasks in Figure 4.9. Inspection of Figure 4.9, reveals a number of important and interesting patterns of results across conditions for both tasks. For motion discrimination, the data indicate that: (1) performance is maximally disrupted following TMS of V5/MT, relative to all other conditions; (2) performance is largely equivalent following TMS of the CON, LO1 and LO2 and (3) performance during the no TMS condition is surprisingly high, relative to the collective TMS conditions.   For orientation discrimination, the data indicate that: (1) the greatest disturbance to performance occurred following TMS of LO1, relative to all other conditions; (2) the effects of TMS were very similar following TMS of the CON, LO2 and V5/MT and (3) the no TMS condition displays slightly worse performance relative to TMS of the CON, LO2 and V5/MT. Comparing the overall pattern of deficits across tasks also indicates lower performance in the motion over orientation tasks for all conditions, suggestive of a general effect of task.
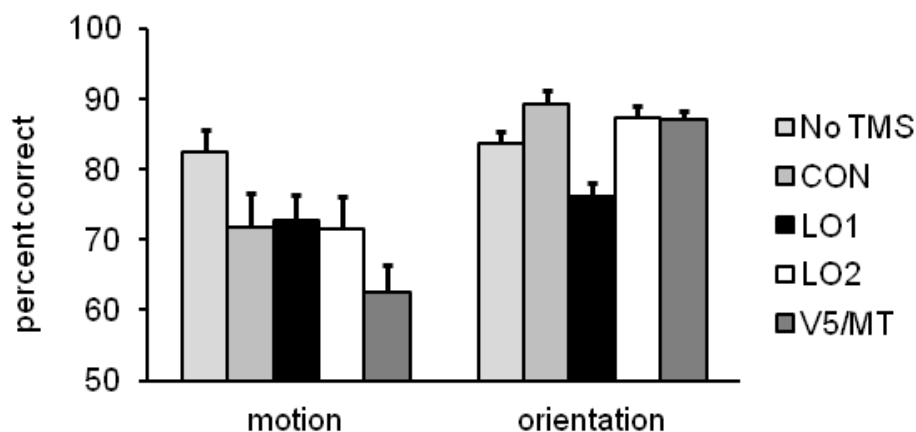
Figure 4.9: *Effects of TMS on motion and orientation discrimination performance. Group average performances are plotted for all conditions grouped by task. Prediction schematics for parallel processing are inset above each task. The pattern of deficits induced by TMS closely follows that predicted by map specific and parallel processing of motion and orientation, respectively. For motion discrimination, performance is maximally disrupted following TMS of V5/M. For orientation discrimination, performance is maximally disrupted following TMS of LO1. TMS effects at V5/MT and LO1 are specific to motion and orientation tasks, respectively. Error bars represent s.e.m.*

If V5/MT and LO1 are specialized for motion and orientation perception, respectively, an interaction between Task and Site should be evident. Accordingly, a 2 x 5 repeated measures ANOVA was conducted with conditions Task (motion & orientation) and Site (no TMS, CON, LO1, LO2 & V5/MT). The ANOVA revealed a significant Task x Site interaction ($F_{(4, 20)}$ = 11.936, p = < 0.0001). The main effect of Task ($F_{(1, 5)}$ = 23.186, p = 0.005) was significant, reflecting poorer performance during motion than orientation discrimination across conditions. The main effect of Site was also significant ($F_{(1, 20)}$ = 6.242, p = 0.002), presumably reflecting the lower performances during V5/MT and LO1 simulation across the motion and orientation tasks, respectively. There were no significant pairwise site comparisons (p = > 0.152, in all cases: Bonferroni corrected). Although the identification of a significant Task x Site interaction was essential to the analysis, additional analyses are required to determine whether or not the effects of TMS of V5/MT and LO1 exhibit both Task and Site specificity. Accordingly, one-way ANOVAs were conducted on each task considered separately, to elucidate whether task dependant effects were specific to V5/MT and LO1, respectively.

For motion discrimination, a one-way repeated measures ANOVA revealed a significant effect of Site ($F_{(4, 20)}$ = 8.429, p = < 0.0001). Due to our 'a priori' hypothesis the effect of TMS of V5/MT on performance was compared to all other conditions using paired t-tests (one-tailed). TMS of V5/MT caused a significant and selective disturbance to motion discrimination performance compared to all other conditions (V5/MT *versus* No TMS: $t_{(5)}$ = -4.587, p = 0.003; V5/MT *versus* CON: $t_{(5)}$ = -2.569, p = 0.025; V5/MT *versus* LO1: $t_{(5)}$ = -4.073, p = 0.005; V5/MT *versus* LO2: $t_{(5)}$ = -2.822, p = 0.0185). As mentioned above, performance on the no TMS condition was surprisingly high relative to all other TMS conditions. This could be indicative of a general effect of TMS, which is further pronounced following TMS of V5/MT. Indeed paired t-tests (two-tailed) indicate significant differences between the no TMS condition and TMS of LO1 and LO2, but not the CON (no TMS *versus* CON: $t_{(5)}$ = 2.122, p = 0.088; no TMS *versus* LO1: $t_{(5)}$ = 2.815, = 0.037; no TMS *versus* LO2: $t_{(5)}$ = 3.276, p = 0.022). Given the data one would be tempted to infer that TMS in general led to a significant reduction in performance relative to no TMS condition, which was further pronounced following TMS of V5/MT. It will be important however, to consider the reaction time data in order to examine whether a speed-accuracy trade off is present for this condition.

The lack of a significant effect following TMS of LO2 would be profoundly important for further work. Accordingly, paired t-tests (two-tailed) were conducted in order to elucidate whether TMS of LO2 disrupted performance relative to TMS of the CON, LO1 and the no TMS baseline. There was a significant difference between the effect of TMS of LO2 and the no TMS (reported above), but no significant difference between the effect of TMS of LO2 and either the CON or LO1 (LO2 *versus* CON: $t_{(5)}$ = -0.105, p = 0.921; LO2 *versus* LO1: $t_{(5)}$ = -0.630, p = 0.556).

For orientation discrimination, a one-way repeated measures ANOVA revealed a significant effect of Site ($F_{(4, 20)}$ = 9.995, p = < 0.0001). Due to our '*a priori*' hypothesis the effect of TMS of LO1 during orientation discrimination was compared to all other conditions using paired t-tests (one-tailed). TMS of LO1 induced significant disruption to orientation discrimination compared to all other conditions (LO1 *versus* No TMS: $t_{(5)}$ = -3.588, p = 0.008; LO1 *versus* CON: $t_{(5)}$ = -5.350, p = 0.0015; LO1 *versus* LO2: $t_{(5)}$ = -4.313, p = 0.004; LO1 *versus* V5/MT: $t_{(5)}$ = -3.659, p = 0.0075). We also assessed the effect of TMS of LO2 on orientation performance using paired t-tests (two-tailed). TMS of LO2 did not significantly alter performance relative to the no TMS condition or TMS of the CON or V5/MT (LO2 *versus* CON: $t_{(5)}$ = 1.008, p = 0.360; LO2 *versus* V5/MT: $t_{(5)}$ = 0.177, p = 0.867).

Taken together, the patterns of deficits induced by TMS closely follow that predicted by *map specific* and *parallel* processing of motion and orientation, respectively. TMS of V5/MT maximally disrupted motion, but not orientation performance, whereas TMS of LO1 maximally disrupted orientation, but not motion performance – a double dissociation.

4.6.5:   Is There a Perceived Slowing of Motion Following TMS of V5/MT?

In accordance with previous research, we analysed the extent to which TMS of V5/MT resulted in a perceived slowing of motion (McKeefry et al., 2008). In order to do this the percentages of slower responses across conditions was calculated. In each TMS condition there were 100 stimulus presentations, 50 presentations of the stimuli both faster and slower than the reference stimulus. If a response bias is not present, the percentage of faster responses minus 50 should therefore, not be significantly different from zero. If a positive value is observed this would be indicative of a bias towards the faster grating,

whereas if a negative value is observed, this would indicate a bias towards the slower moving grating. Group averaged response biases are plotted for all conditions in Figure 4.10.
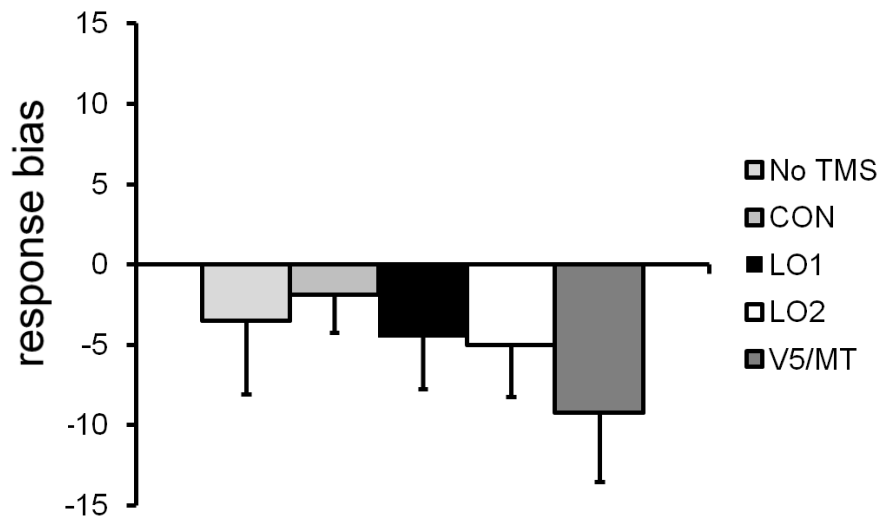
Figure 4.10: *Response biases during motion discrimination. The mean percentages of responses (either slower or faster) are plotted for all conditions. In all TMS conditions (as well as no TMS baseline), TMS caused a response bias towards the slower moving grating. These response biases were only significantly different from zero following TMS of V5/MT. Error bars represent s.e.m.*

Inspection of Figure 4.10, indicates that a perceived slowing was evident in all conditions, but was greatest during stimulation of V5/MT. One-tailed (V5/MT) and two-tailed (no TMS, CON, LO1 and LO2) t - tests were calculated, in order to evaluate whether these biases were significantly different from zero. The perceived slowing of motion was significantly different from zero following TMS of V5/MT only (no TMS: $t_{(5)}$ = -1.414 p = 0.217; CON: $t_{(5)}$ = -0.872 p = 0.423; LO1: $t_{(5)}$ = -0.330 p = 0.755; LO2: $t_{(5)}$ = -1.658, p = 0.152; V5/MT: $t_{(5)}$ = -2.360, p = 0.032). Across subjects there was a significant bias towards the slower moving grating following TMS of V5/MT. A result not found following TMS of any other site or during the no TMS baseline. The current result successfully replicates previous findings, demonstrating that TMS of V5/MT induces a perceptual slowing of motion (McKeefry et al., 2008).

4.6.6:   The Effect of TMS on Reaction Times

Discrimination performance (% correct) was used as the primary measure of the effects of TMS. Nevertheless, reaction times were recorded as they are often the primary measure in TMS studies and can add valuable information when interpreting the effect of TMS on behaviour. For instance, reaction time data can be used to determine the presence of a speed-accuracy trade off, which if present, would confound the interpretation of the discrimination performances reported above. If one assumes that TMS to a particular site increases task difficulty, one may also assume that reaction times should increase or remain unchanged. Quicker reaction times that are associated with poorer performance – a speed accuracy tradeoff - present a challenge to interpretations regarding functional specialization. This is particularly important here given the high level of performance observed for the no TMS condition during motion discrimination.

Group averaged reaction times for all conditions and tasks are plotted in Figure 4.11. Inspection of Figure 4.11, reveals a number of interesting patterns. For motion discrimination: (1) the slowest reaction time during TMS stimulation was observed during TMS of V5/MT. That is, the slowest reaction times during TMS stimulation were associated with the poorest performance, suggesting the lack of a speed-accuracy trade of for the V5/MT condition; (2) reaction times during TMS stimulation of the CON, LO1 and LO2 were very similar, echoing the discrimination data reported above and (3) reaction times during the no TMS condition were substantially slower than all other TMS conditions, including V5/MT. In this case, the slowest reaction times across all conditions were associated with the best performance – hinting at a speed-accuracy trade off. For orientation discrimination, there is little suggestion of a speed-accuracy trade off across conditions. Indeed, the condition in which reaction times are the slowest during LO1 is associated with the poorest performance – TMS of LO1.
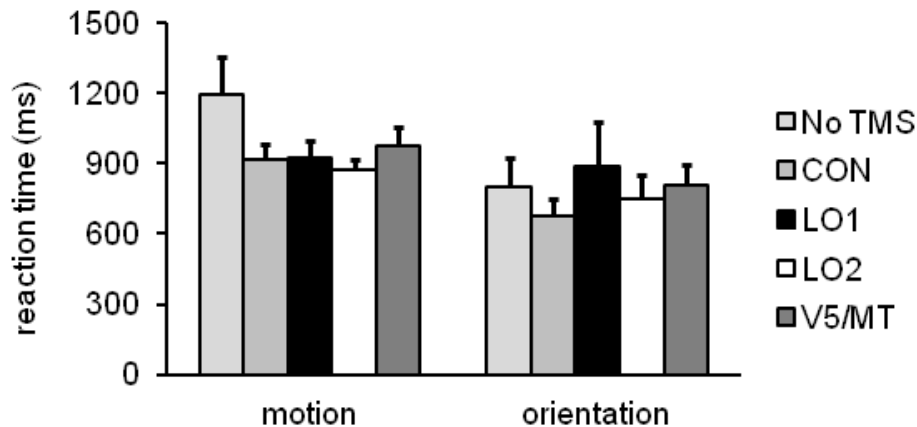
Figure 4.11: *Effect of TMS on reaction times during motion and orientation discrimination. For motion discrimination, there is no evidence of a speed-accuracy trade off during TMS conditions. Stimulation of V5/MT, which led to maximum disruption to performance, is associated with the slowest reaction times compared to other TMS sites. In contrast the increased performance during no TMS is associated with slower reaction times, suggesting the possibility of a speed-accuracy trade off for this condition. For orientation discrimination, there is no evidence that quicker reaction times led to the reduction in performance observed following TMS of LO1.This is in the predicted direction and is the opposite of a speed-accuracy trade off. Error bars represent s.e.m.*

To assess formally the effect of reaction times, a 2 x 5 repeated measures ANOVA was conducted with conditions Task (motion & orientation) and Site (no TMS, CON, LO1, LO2 & V5/MT). There was a significant effect of Task ($F_{(1, 5)} = 15.418$, $p = 0.011$), indicating slower reaction times during motion discrimination, but neither a significant effect of Site ($F_{(4, 20)} = 1.192$, $p = 0.345$) nor a significant Task by Site interaction ($F_{(4, 20)} = 2.772$, $p = 0.055$). Given that the Task x Site interaction approached significance and in order to echo the analysis of discrimination task specific one-way repeated measures ANOVAs were conducted, followed by *t*-tests to explore further these effects.

For motion discrimination, there was a significant effect of Site ($F_{(4, 20)} = 3.129$, $p = 0.038$). This effect is likely driven by the substantially slower reaction times during the no TMS baseline relative to all other conditions. The best performance was observed during the no TMS condition, relative to all other TMS sites. One interpretation of this is that there was a general effect of TMS to all sites, and further pronounced following TMS of V5/MT. In order to rule out speed-accuracy trade off as an explanation for the no TMS performance and therefore accept this interpretation, the reaction times during the no TMS condition

were compared to all TMS conditions using paired *t*-tests (one-tailed). Reaction times were significantly different for all condition except V5/MT (no TMS *versus* CON: $t_{(5)}$ = 2.103, *p* = 0.0445; no TMS *versus* LO1: $t_{(5)}$ = 2.061, *p* = 0.047; no TMS *versus* LO2: $t_{(5)}$ = 2.111, *p* = 0.044; no TMS *versus* V5/MT: $t_{(5)}$ = -1.630, *p* = 0.164). The increase in performance during no TMS is associated with significantly slower reaction times, making a speed-accuracy trade off the most parsimonious explanation for this result.

For orientation discrimination, the main effect of site was not significant ($F_{(4, 20)}$ = 0.677, *p* = 0.616). Given the lack of a significant effect of Site, further tests were not conducted. There is no evidence that the significant disruption to orientation discrimination induced following TMS of LO1 is due to speed-accuracy trade off. Indeed, reaction times during LO1 stimulation were longer than any other condition. Taken together, the analyses of reaction times strengthen the main interpretation of the effects of TMS on performance of our visual tasks. The selective disturbances to motion and orientation performance following TMS of V5/MT and LO1, respectively, were not due to quicker reaction times during these conditions.

4.6.7:   Analysis of Potentially Confounding Variables

Additional measurements were recorded with each TMS pulse train in an attempt to account for two potentially confounding variables that relate to the spatial relationships between the stimulating coil and the targets within cortex; coil-target distance and coil-target orientation. These measurements are included as they provide a means by which to rule out differences in the precision of TMS, caused by operator error, as an alternative account of the discrimination data reported above.

4.6.7.1:   Coil -Target Distance

The mean Euclidean distances (mm) separating the calibration point of the coil and the targets in cortex are plotted for all TMS targets and tasks in Figure 4.12.
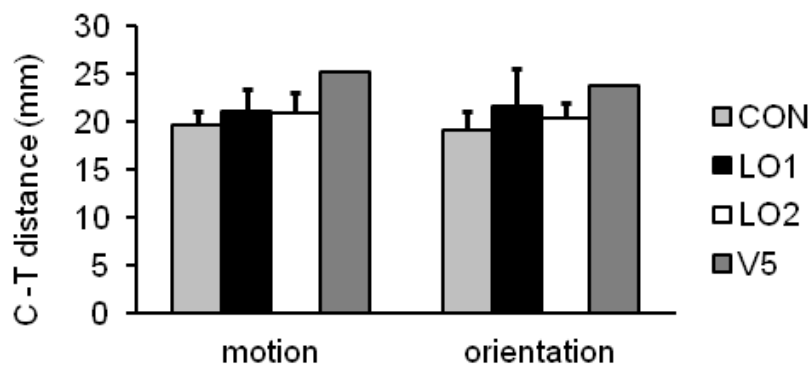
Figure 4.12: *Mean Euclidean distance between stimulating coil and cortical targets during motion and orientation discrimination. The results indicate that coil-target distance did not vary in a manner that explains the observed patterns of TMS on performance. There is no evidence that differences in the distance between the stimulating-coil and cortical targets led to the dissociable effects observed. Error bars represent the s.e.m.*

From figure 4.12, one can see that for both tasks the coil-target distances vary as a function of site – a feature that may reflect the method for defining these cortical targets. Variation in the coil-target distance could be underpinned by the location of the targets with respect to gyri and sulci. Recall that V5/MT was defined anatomically and located in the ascending limb of the inferior temporal sulcus, the depth of which may underlie the greater distances relative to other targets. The pattern across sites is largely equivalent for both tasks. This is important as the target locations within cortex are identical for both tasks, and

122

therefore, any variation between tasks must be caused by operator error. Potential sources of operator error include imprecise calibration and/or registration procedures. In order to assess whether the coil-target distances varied in such a way that could explain the discrimination data a 2 x 4 repeated measures ANOVA was conducted with conditions Task (motion & orientation) and Site (CON, LO1, LO2 & V5/MT). The Task x Site interaction violated sphericity (Mauchly's $W_{(5)}$ = 0.015, p = 0.01, estimate of non sphericity = 0.525) the degrees of freedom were therefore, corrected using Greenhouse-Geisser. There was a significant effect of Site ($F_{(2.082, 10.412)}$ = 4.457, p = 0.020, Greenhouse-Geisser corrected), but neither a significant effect of Task ($F_{(1, 5)}$ = 0.117, p = 0.747), nor a significant Task by Site interaction ($F_{(3, 15)}$ = 0.087, p = 0.966). The significant effect of site likely reflected the larger coil-target distance between V5/MT and all other sites across both tasks. There were no significant pairwise site comparisons (p = > 0.101, in all cases, Bonferonni corrected).

As with all variables, task specific one way ANOVAs were conducted. For motion discrimination, the main effect of Site violated sphericity (Macuhly's $W_{(5)}$ = 0.026, p = 0.022, estimate of non sphericity = 0.637) the degrees of freedom were therefore, corrected using Greenhouse-Geisser. The main effect of Site was not significant ($F_{(1.911, 9.554)}$ = 2.227, p = 0.162, Greenhouse-Geisser corrected). Given the non significant effect of site no further tests were conducted. For orientation discrimination, the main effect of Site was not significant ($F_{(3, 15)}$ = 1.124, p = 0.371). Given the non significant effect of site no further tests were conducted.

4.6.7.2:   Coil-Target Orientation

Coil orientation provides a measure of the difference between the coil orientation and the vector joining the calibration point of the coil and the TMS target, with accurate targeting corresponds to 90° on this measure. The group averaged coil-target orientations for all TMS sites and tasks are plotted in Figure 4.13.
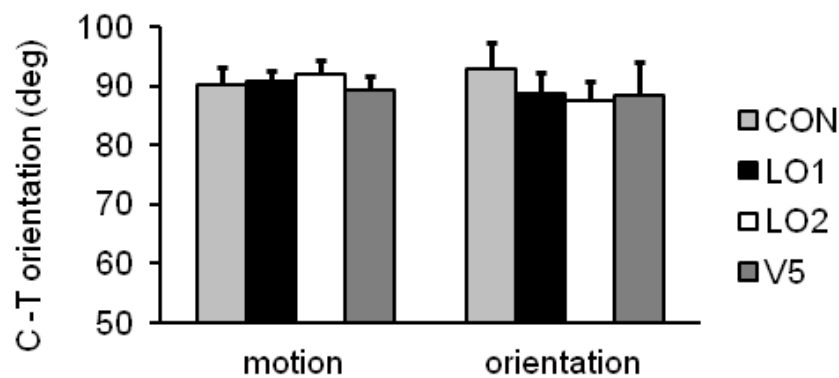
Figure 4.13: *Mean coil-target orientation during motion and orientation discrimination. The results indicate that changes in the orientation of the coil relative to the cortical targets did not vary in a manner that explains the observed patterns of performance. Indeed, the orientation across all conditions was very close to 90 degrees, indicating accurate targeting. Error bars represent s.e.m.*

Inspection of Figure 4.13, indicates that across all sites and conditions the coil-target orientations are largely grouped around 90°. Indeed, the mean coil-target orientations are largely similar across sites and tasks. The orientation of the stimulating coil relative to the scalp is important, even slight changes in coil position can alter the locus of effective stimulation (Cowey, 2005). In order to determine whether variations in the orientation of the coil relative to the target might explain the discrimination results, a 2 x 4 repeated–measures ANOVA with conditions Task (motion & orientation) and Site (CON, LO1, LO2 & V5/MT) was conducted. There were neither significant effects of Site ($F_{(3, 15)}$ = 0.504, p = 0.685), nor Task ($F_{(1, 5)}$ = 0.129 p = 0.734), nor a Task by Site interaction ($F_{(3, 15)}$ = 1.106, p = 0.378).

As with all variables, task specific one way ANOVAs were conducted. For motion discrimination, the main effect of Site was not significant ($F_{(3, 15)}$ = 0.633, p = 0.605). Given the non significant effect of site no further tests were conducted. For orientation discrimination, the main effect of Site was not significant ($F_{(3, 15)}$ = 0.804, p = 0.511). Given the non significant effect of site no further tests were conducted. There is no evidence that variations in the spatial relationships between the stimulating coil and the cortical targets varied in such a way that could explain the selective disturbances to performance on our visual tasks.

4.7:   Discussion

In this chapter TMS was delivered to three closely separated targets (LO1, LO2 & V5/MT) in order to assess its effects on performances of motion and orientation discrimination. TMS stimulation of V5/MT resulted in significant and selective disturbances to normal motion discrimination performance, relative to all other conditions. Interestingly, TMS of additional cortical sites disrupted motion discrimination relative to baseline, but to a lesser degree than TMS of V5/MT. Similarly, TMS stimulation of LO1 induced significant and selective disruption to normal orientation discrimination performance relative to all other conditions. The pattern of deficits induced by TMS could be interpreted as demonstrable of a double dissociation between motion and orientation processing. TMS of V5/MT disrupted motion maximally, but left orientation discrimination relatively preserved; whereas TMS of LO1 disrupted orientation maximally,and led to modest disruption of motion discrimination.. These selective disturbances were found to be immune to speed-accuracy tradeoffs and variations in the spatial relationship between the stimulating coil and the cortical targets.

4.7.1:   V5/MT Functionally Specialized for Motion Processing

The results from the motion experiment reveal a successful replication of previous work (McKeefry et al., 2008). TMS of V5/MT significantly deteriorated subject's ability to accurately discriminate speed, relative to all other conditions. The current TMS results, combined with others (Beckers & Homberg, 1992; Walsh et al., 1998; Mckeefry et al., 2008) confirm the critical role that V5/MT plays in the neural mechanisms that underpin motion perception.

The effect of TMS of V5/MT was found to exhibit both task and site specificity. Displacement of the coil away from V5/MT (targeting LO1, LO2 or the CON) did not alter discrimination performance. Additionally, TMS of V5/MT left orientation discrimination unaltered. In addition, the effect of TMS delivery to V5/MT also replicated a previously reported bias (Mckeefry et al., 2008). TMS of V5/MT resulted in an inflated number of slower over faster responses, compared to all other conditions, which likely led to the decreased performance values (% correct) observed. Although, it must be noted that TMS of

all other sites also resulted in a slower, but non-significant response biases. The significant bias towards the slower moving grating is consistent with previous studies applying TMS to V5/MT (McKeefry et al., 2008). The effect of TMS to human V5/MT likely causes a decrease in stimulus driven neural firing, the frequency of which has been suggested to underpin the perception of speed (Priebe et al., 2003).

The results of the motion discrimination experiment, also extend previous fMRI findings regarding the functional properties of LO1 and LO2 (Larsson & Heeger, 2006), by demonstrating that LO1 and LO2 are less causally involved in the perception of speed than V5/MT, despite lying directly adjacent to cortical areas specialized for motion perception (Larsson & Heeger, 2006). Larsson and Heeger (2006) measured the BOLD responses to moving and stationary dot patterns throughout visual cortex. Neither LO1, not LO2 responded strongly to motion, although the BOLD signal elicited in LO2 did approach statistical significance (p = 0.06). TMS of LO1 and LO2 during motion discrimination led to largely equivalent levels of performance across subjects. That is, although differences were observed relative to baseline, TMS of V5/MT disrupted speed discrimination further, a decrease in performance that was significantly different; a pattern consistent with the lack of selectivity observed through fMRI (Larsson & Heeger, 2006). Intriguingly, it appears that neural representations encoding motion largely by-pass LO1 and LO2 on its route from V1-V3A-V5/MT. Direct projections to V5/MT from both V1 and subcortical structures (Sincich et al., 2004) offer a plausible explanation for the reduced effect following TMS of LO1 and LO2, relative to TMS of V5/MT.

4.7.2:   LO1 Functionally Specialized for Orientation Processing

The results of the orientation discrimination experiment are novel. They demonstrate that human orientation discrimination can be selectively impaired when TMS is precisely targeted so as to disrupt the normal functioning within LO1. The fact that disruption to LO1 can generate impairments in orientation discrimination represents a significant finding. Hitherto V1 has been considered the main cortical locus for the neural mechanisms underpinning orientation perception (Hubel & Wiesel, 1963; Hubel, Wiesel & Stryker, 1978; Furmanski & Engel, 2000; Larsson et al., 2006). The results presented here demonstrate that behaviourally relevant information concerning orientation is encoded by

126

activity in LO1 and strongly suggests that information regarding orientation is available at this level of the visual hierarchy.

The current results are consistent with previous fMRI reports (Larsson et al., 2006), but extend them to show that LO1 plays an active and causal role in encoding orientation, even when defined by luminance modulation, rather than the more complex encoding of orientation by second order cues that might be thought to be processed by extrastriate areas. The lack of effect following TMS of LO2 and V5/MT on orientation discrimination is also consistent with previous fMRI findings demonstrating a lack of orientation selectivity within these areas (Larsson et al., 2006). The effect of TMS of LO1 exhibited both location and task specificity, moving the TMS coil away from LO1 (to sites either closer to V1 (CON) or further from V1 (LO2 and V5/MT) reduced the effects of TMS on orientation discrimination. Additionally, TMS of LO1 left motion discrimination unaltered. In their original assessment of orientation selective adaptation in LO1 (Larsson & Heeger, 2006), Larsson and Heeger accounted for the majority of orientation selective adaptation through feed-forward propagation from V1. The results of the current experiment run contrary to this and suggest that neurons in LO1 encode orientation information directly. TMS of the CON, which lay closer to V1 than all other target sites, did not disrupt orientation discrimination to the same degree as TMS of LO1. The significant difference between LO1 and CON demonstrates that the orientation specific nature of computations in LO1 is not due to TMS of LO1 spreading into representations of the target in V1.

4.7.3:   Double Dissociation & Parallel Processing

The current findings could be interpreted as supporting a double dissociation between two closely separated cortical areas (average separation between LO1 and V5/MT targets was ~30mm). The parallel nature of processing reported here is consistent with previous work in both macaque and human demonstrating parallel processing at the level of V5/MT. In both species, the processing of colour and motion has been shown to operate in parallel, with both visual features being computed in distinct and relatively distant visual areas (Lueck et al., 1989; Zeki, 1990; Zeki et al., 1991). The current demonstration that motion and orientation are predominantly processed in distinct visual areas echo's the parallelism observed previously. Notably, the parallel processing of motion and orientation

reported here is at a smaller spatial scale than the parallel processing of colour and motion in the human brain. In that regard, it is more similar to the parallel processing colour and motion in macaque, which occurs in neighbouring retinotopic maps (Zeki, 1990).

The parallel processing observed here is likely underpinned by parallel anatomical connections. For instance, direct anatomical connections from the LGN to V5/MT have been reported (Sincich et al., 2004), which bypass V1 and as a consequence bypass the major access point into the serial system. Additionally, direct V1-V5/MT projections have been reported (Beckers & Zeki, 1995), offering a plausible account for how motion signals can be processed in parallel to the orientation signals that could rely on connections from V1-LO1. In macaque, V4d and V5/MT receive parallel inputs from antecedent visual field map V2 (Zeki & Shipp, 1988). These visual areas are in a commensurate stage of the visual hierarchy of the macaque as LO1 (LO2) and V5/MT are in human. Although the homology between human and macaque is less clear at this level of the hierarchy (Tootell et al., 2003; Larsson & Heeger, 2006), the parallel anatomical connections may nevertheless remain.

The results would suggest that contrary to a strictly serial model of visual processing, information necessary for the encoding of motion and orientation are processed in parallel. The conclusion that TMS of V5/MT and LO1 reduces the activity of neurons in these areas is consistent with recent assertions that TMS operates via the suppression of neural signals that directly relate to the target stimulus (Harris et al, 2008). Physiological measurements from cat visual cortex (Allen et al., 2007) are consistent, with TMS suppressing activity, which leads to a decrease in signal to noise ratio in the cortical area under stimulation (Walsh & Cowey, 2000; Cowey, 2005). An alternative account argues that TMS exerts its effects by decreasing signal-to-noise via the increase in the background neural noise (Ruzzoli et al., 2010). The effects of TMS may ultimately lie with a combination of reduced firing of neurons encoding stimulus relevant features and an increase in spontaneous background activity, although the neuronal state of the underlying cortical area also plays an important role in mediating TMS effects (Silvanto et al., 2007).

4.7.4:   Implications for the Thesis

The results reported in this chapter make several important implications for the progression of the thesis. First, the results demonstrate that TMS can be used to elucidate functionally specialized roles of close proximity cortical targets with a sample size of six subjects. Of note however, both the motion and orientation discrimination experiments were heavily influenced by strong '*a priori*' hypotheses, based on the results from macaque single-unit as well as human neuropsychological, neuroimaging and neurostimulation studies. In future studies, where the effects are less predictable or currently unknown, a larger sample size is desirable. Future studies will therefore, include double the number of subjects.

Second, the results provide compelling evidence that, if targeted precisely, TMS can elucidate the functional properties of close proximity targets. The single dissociation observed between LO1 and LO2 in terms of orientation processing, at an average separation of ~10mm provides good evidence that TMS could be used to tease apart the functional properties of these two adjacent visual field maps. This separation is similar to that reported in previous TMS work probing category selective areas of visual cortex, where independent effects were reported at separations as small as 7.8mm (Pitcher et al., 2009). Of note, these distances were calculated following transformation from native anatomical to MNI space, which could distort the actual separations.

Third, the results raise an important question regarding the role played by LO2. The current results would suggest that LO2 is neither maximally selective for nor crucially involved in either motion or orientation discrimination. LO2's lack of selectivity to stimulus orientation (Larsson et al., 2006) and motion (Larsson & Heeger, 2006) has been demonstrated previously using fMRI. The current data extends these findings to demonstrate a lack of causality. The absence of an effect on orientation discrimination and the effect on motion discrimination has a number of important implications. The lack of effect provides some evidence as to the effective spread of TMS. If TMS exerted its effects over a large area, then TMS of LO2 should have disrupted both the orientation and motion tasks not just motion, as LO2 lay in-between the V5/MT and LO1 sites. The lack of consistent effects could be interpreted as confirming that TMS has sufficient spatial specificity to allow

stimulation of individual, but closely separated, cortical targets. The lack of effect, coupled with the specialized and parallel processing observed in areas both anterior (V5/MT) and posterior of (LO1) LO2, suggests that LO2 may underpin the processing of a visual feature that is independent of both motion and orientation and moreover, that this feature may be computed independently of LO1's computations – in parallel. It has been suggested that perhaps LO2 undertakes more complex spatial processes and encodes shape information (Larsson & Heeger, 2006), however, it remains to be seen what, if any, visual attributes LO2 is selective for.

Finally, the results reported here open up two avenues for further investigation, which form the basis of Chapters 5 and 6. The first avenue, explored in Chapter 5, is a logical and systematic extension of the current work and will investigate whether LO1 maintains orientation selectivity over V5/MT when stimuli move. The key conceptual advance here is whether orientation discrimination of moving stimuli is reliant on computations within LO1 – a feature currently unknown. The second avenue, explored in chapter 6, will explicitly test whether LO2 exhibits a specialization for shape processing, as suggested previously (Larsson & Heeger, 2006). This will be contrasted against a replication of the specialization for orientation in LO1, in an attempt to demonstrate functional specialization at the spatial scale of adjacent visual field maps within a cluster of human visual cortex.

4.8: Conclusion

TMS of V5/MT results in maximal disturbance to normal motion processing, confirming the functional specialization exhibited by this cortical area. Similarly, TMS of LO1, a potentially uniquely human visual area, results in selective disturbances to normal orientation processing – a new finding. The functional specializations exhibited by these closely separated targets appear to operate independently, possibly facilitated by parallel anatomical projections from antecedent visual areas. The ability of TMS to demonstrate functional specializations of areas within such close proximity of one another, provides promising evidence that TMS could be used to probe the functional properties of LO1 and LO2 independently – the ultimate aim of the thesis.

Chapter 5

Is Orientation Processing of Moving Stimuli Reliant Upon LO1?

5.1: Overview

This study aimed to investigate whether LO1 is specialized for the orientation perception of moving stimuli. Specifically, we ask here whether LO1 maintains its causal involvement in orientation discrimination of gratings, but this time when they move. We also include a second task – motion discrimination of oriented gratings in order to test whether V5/MT maintains its specializations for motion processing in the presence of orientation noise. It is possible that for moving gratings the direction of motion, a feature that could be computed by V5/MT might be the most useful cue for orientation. Demonstrating a causal role for LO1 during orientation perception of moving stimuli will provide further evidence for the functional specializations exhibited by LO1, and indicate the presence of cue-invariant representations. The main comparison of interest is between the effects of TMS of LO1 and V5/MT on performance of both tasks however, we include the CON, LO2 and no TMS conditions in order to echo the approach adopted in Chapter 4. The role played by LO2 in these tasks remains unclear. Importantly, if computations in LO2 are independent of those required for these tasks, TMS of LO2 should have no effect on discrimination relative to baseline (No TMS condition).

5.2: Introduction

The data reported in Chapter 4 revealed a number of important features regarding the processing of motion and orientation within subdivisions of lateral occipital cortex. First, the results of the motion experiment successfully replicated a previously reported effect (McKeefry et al., 2008) by demonstrating that TMS of V5/MT induced a selective disturbance to motion perception whilst simultaneously inducing a perceptual slowing of visual stimuli (McKeefry et al., 2008). The results, combined with previous TMS studies (Beckers & Homberg, 1992; Walsh et al., 1998; McKeefry et al., 2008) confirm the specialized role played by V5/MT in the perception of motion. Second, the results of the orientation experiment revealed, for the first time, a direct link between computations

performed within LO1 and the accurate discrimination of orientation. Third, the results from both tasks revealed a lack of selectivity within LO2 for either stimulus. TMS of LO2 neither disrupted motion nor orientation discrimination, suggesting that orientation and motion signals are not encoded in LO2. Finally, the results demonstrated a double dissociation between LO1 and V5/MT. Anatomically dissociable routes from antecedent visual areas may well underpin the functional dissociation observed between these nearby regions. Taken together, the results from Chapter 4 demonstrated specializationss for orientation and motion processing in isolation. There are times however, when there is a need to encode more than one visual feature at a time. Where is the information regarding orientation and motion combined? Do computations in LO1 causally underpin our orientation discrimination of moving stimuli? In order to address this, the current experiment investigated the effects of TMS on orientation discrimination of moving gratings and motion discrimination of oriented gratings.

5.2.1:   Motion & Orientation Processing in V5/MT, LO1 & LO2

This study aimed to investigate whether orientation discrimination of moving stimuli is reliant upon computations performed by LO1. We also include the converse condition – motion discrimination of oriented gratings as an appropriate foil for our orientation discrimination task. The following sections outline the evidence for motion and orientation processing in V5/MT, LO1 and LO2.

Evidence from both macaque and human studies highlights the important role that V5/MT plays in the perception of motion. In macaque, single-unit recordings have demonstrated the existence of directionally-tuned neurons within V5/MT (Zeki, 1969). In addition to directionally-tuned neurons, V5/MT contains a high proportion of neurons tuned to different speeds (Maunsell & Newsome, 1987; Rodmann & Albright, 1987), the tuning of which has been reported to be relatively form invariant (Priebe et al., 2003). Some V5/MT neurons also exhibit joint direction and orientation selectivity (Albright, 1984), with the peak orientation sensitivity of these neurons being typically, but not exclusively, perpendicular to that neurons preferred direction (Maunsell & Van Essen, 1983). The evidence from macaque V5/MT suggests that neurons are capable of processing motion information from a number of different cues. In human, evidence for V5/MT's role in

motion processing comes from multiple investigative paradigms, including neuropsychological (Zihl et al., 1983), neuroimaging (Zeki et al., 1991; Orban et al., 1995; Amano et al., 2009) and neurostimulation (Beckers & Homberg, 1992; Walsh et al., 1998; McKeefry et al., 2008) studies. The results of the motion component of Chapter 4 are entirely consistent with previous literature and highlight the specialization of V5/MT in the perception of motion. The processing of motion within LO1 and LO2 has also been investigated previously using fMRI. Larsson and Heeger (2006) report that neither visual field map exhibited preferential responses to moving dot patterns compared to static dot arrays, although a noteworthy feature is that the responses observed in LO2 approached, but did not reach significance (p = 0.06). Again, the data reported in Chapter 4 are consistent with a lack of motion sensitivity within these visual field maps.

Previously, orientation selective responses have been reported in cat (Hubel & Wiesel, 1963), macaque (Hubel, Wiesel & Stryker, 1978) and human V1 (Furmanski & Engel, 2000). The processing of orientation in extratriate cortical areas using fMRI adaptation demonstrated orientation selective responses in LO1, but not LO2 (or V5/MT) (Larsson & Heeger, 2006), a segregation of function confirmed by the results of the orientation discrimination experiment reported in Chapter 4. Importantly however, whether LO1 encodes orientation of moving stimuli is not well understood. Evidence from both macaque and human cortex highlights the presence of regions of cortex selective to the orientation of motion boundaries. Single-unit studies identified neurons selective to the orientation of moving boundaries not only in early visual cortex (V1-V3) (Marcar, Raiguel, Xiao & Orban, 1995), but also, several extrastriate areas (V4, V3A) (Mysore, Vogels, Raiguel & Orban, 2006), including macaque inferotemporal cortex (IT) (Sary, Vogels, Kovacs & Orban, 1995) which is commonly believed to be the macaque homologue of human LOC (Malach et al., 1995; Grill-Spector et al., 1998). In human, the Kinectic Occipitial (KO) area was found, using fMRI, to be more responsive to random-dot stimuli that contained motion-boundaries than to transparent motion control stimuli (Dupont et al., 1997). More recent studies suggest that KO is not a single entity, rather it extends across multiple retinotopic visual areas including V3, V3A/V3B, LO1 and LO2 (Zeki, Perry & Bartels, 2003; Larsson & Heeger, 2006). Larsson, Heeger and Landy (2010) investigated orientation-selectivity of motion-boundary responses in human visual cortex. They employed fMRI adaptation techniques to identify

regions of cortex selective for motion-boundary orientation. The study had two main aims; the first was to identify regions of human visual cortex that exhibited selectivity to orientation defined by motion-boundaries and measure the extent to which these regions were selective to motion-boundary orientation and second, determine whether the degree of orientation selectivity within each area was related to motion-boundary preference; defined as stronger responses to motion-boundary stimuli than to transparent motion control stimuli. In their paradigm, an adapting stimulus (either a vertically or horizontally orientated motion-boundary grating) was presented (4sec). Following a 1sec ISI, a probe grating was presented. Three probe gratings were employed: 1) motion-boundary gratings oriented parallel with the adaptor; 2) motion-boundary gratings oriented orthogonally to the adapter and 3) transparent motion control stimuli. Subjects were required to count the frequency with which an 'x' appeared in a rapidly changing array of letters presented at fixation.

The authors report eight retinotopically organised areas (V2, V3, V3A, V3B, V4, V7, LO1 & LO2) that exhibited significant orientation-selective adaptation. That is, the mean fMRI response following the presentation of a parallel probe was significantly weaker than that following an orthogonal probe. Within the areas mentioned above, differences in the response amplitudes between parallel and orthogonal probes were largest in V3A, V3B and LO1. These were found to be ~50% greater than the responses in V2, V3, V4, V7 and LO2. One interesting finding was that LO2 exhibited orientation-selectivity to motion boundaries, although the difference between motion-boundary and transparent motion exhibited by LO2 was not significant. The authors state therefore, that they cannot rule out the possibility that the orientation-selectivity observed in LO2 was due to variability in the measured response coupled with the effects of statistical thresholding, rather than reflective of a genuine difference in response properties within LO2.

Whether or not LO1 is causally involved in processing the orientation of moving stimuli remains unknown. We address this in the current study by measuring the effects of TMS of LO1 (plus other sites) on performance of orientation discrimination of moving stimuli. The converse condition is also included in order to assess whether V5/MT maintains its specializations for motion processing in the presence of orientation 'noise'. The exact role played by LO2 in these combined tasks is also unclear.

134

5.3:   Theoretical Considerations

There is considerable evidence, from macaque and human studies, suggesting parallel processing capabilities at the level of V5/MT (Zeki, 1990; Zeki et al., 1991). In macaque, V4d and V5/MT abut one other on the lateral surface and exhibit specializations for colour and motion processing, respectively. These specializations have also been directly related to parallel anatomical connections from antecedent cortical (Shipp & Zeki, 1988) and subcortical (Sincich et al., 2004) regions. In human, the parallel processing of colour and motion between V4 and V5/MT is maintained, although over a larger spatial scale (Lueck et al., 1989; Zeki et al., 1991; McKeefry & Zeki, 1997). The double dissociation reported in Chapter 4 is consistent with previous work, provided compelling evidence for parallel processing of motion and orientation within LO1 and V5/MT.

Consistent with the approach adopted in Chapter 4, a control site (CON) was defined in each subject that lay medial to LO1 by the distance separating our LO1 and LO2 centroids. As mentioned previously, the CON provides a mechanism to rule out V1 proximity as an alternative explanation for any differential effects observed following TMS of LO1 and our other target sites. If orientation discrimination is only disrupted following stimulation of LO1 and not the more medial control site (CON), a pattern reported in Chapter 4, then the effects of TMS spreading into V1 cannot explain the result. Given the results of Chapter 4, it was predicted that TMS of the CON would not disrupt orientation processing. We also include a no TMS baseline, in order to examine any general effects induced by TMS. Additionally we include LO2 as a fourth target site, despite predicting no effect of TMS of LO2 on performances of either task. An absence of effect following TMS of LO2 will provide valuable interpretative information regarding the potential specializations exhibited not only by LO1 and V5/MT, but also, LO2 itself.

5.4:   Aims & Predictions

The experiments reported here aimed to evaluate whether LO1's specialization for orientation extended to moving stimuli and whether V5/MT maintained its specialization for motion processing in the presence of additional orientation information. There is considerable evidence, from multiple species, for parallel processing at the level of V5/MT,

and even LO1. Given this, we focus here primarily on the predicted effects of TMS on our tasks based upon *map specific* and *parallel* processing, although two additional predictions, not built into the framework our nonetheless, noteworthy.

Initially, let us consider the two additional predictions. The first, suggests that performance of both tasks is largely V5/MT driven – Top left plot Figure 5.1. That is, due to the speed and directional tuning of V5/MT neurons, one could solve both the motion and orientation tasks by engaging V5/MT alone. The discriminations of speed required to complete the motion task, are predicted to be underpinned by V5/MT's speed selectivity. In the orientation task, it is possible that directionally tuned V5/MT neurons could underpin performance of this task; the orientation of the gratings will be orthogonal to the direction of drift. The second prediction suggests that the motion task is driven solely by the speed tuning of V5/MT neurons, but the orientation task is driven by computations performed by both LO1 and V5/MT – Top right plot Figure 5.1. The map specific and parallel prediction is plotted at the bottom of Figure 5.1. If LO1 is specialized for orientation processing of moving stimuli, then TMS applied here should disrupt performance alone. Likewise If V5/MT maintains its specializations for motion processing then TMS of V5/MT should disrupt performance – a double dissociation.
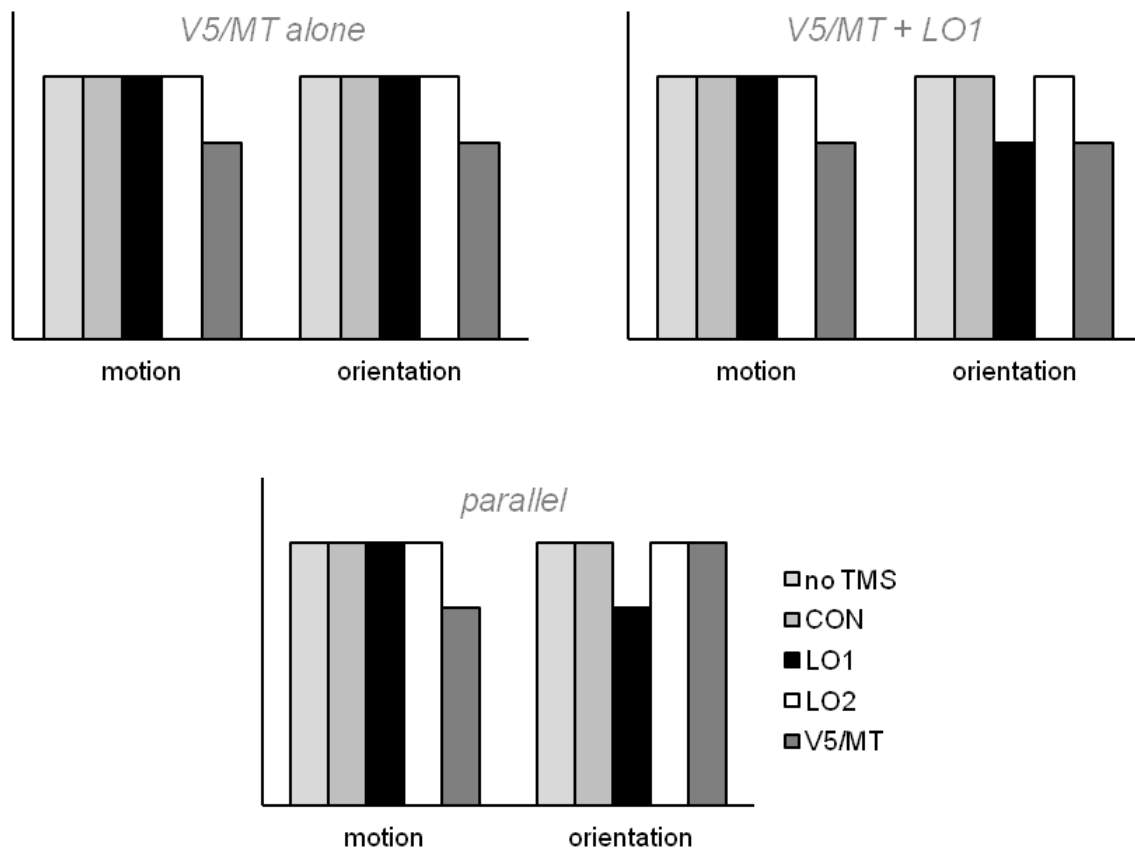
Figure 5.1: *Three alternative predications for the effects of TMS during performance of combined motion and orientation discrimination.* ***Top left:*** *predicted effects of TMS if both tasks are driven by computations within V5/MT. During both motion and orientation tasks, performances are only disrupted following TMS of V5/MT alone, due to V5/MT's speed and directionally tuned neurons.* ***Top right:*** *predicted effects of TMS if V5/MT and LO1 interact. During motion discrimination, performance is only disrupted following TMS of V5/MT; however during orientation discrimination performances are disrupted following TMS of LO1 and V5/MT.* ***Bottom:*** *predicted effects for map specific and parallel processing. Motion discrimination is only disrupted following TMS of V5/MT; likewise orientation discrimination is only disrupted following TMS of LO1 – a double dissociation.*

5.5:   Methods

5.5.1:   Subjects

This study included 12 subjects (mean age = 28, range = 24, 5 male). All subjects had normal or corrected to normal vision and gave informed consent in accordance with the Declaration of Helsinki. York Neuroimaging Centre (YNiC) Research Governance Committee approved the study.

5.5.2: Visual Field Mapping

All subjects participated in full fMRI retinotopic mapping experiments (~1 hour) employing standard visual field mapping techniques (Engel et al, 1994; Sereno et al., 1995; DeYoe et al., 1996). Data analysis, segmentation and identification of visual field maps followed the steps outlined in previous work (Baseler, et al., 2011) and Chapter 3.

5.5.3:   Identification of Visual Field Maps LO1 & LO2

LO1 and LO2 were identified in at least one hemisphere in all subjects. The visual field representations within LO1 and LO2 were consistent across subjects and with previous reports (Larsson & Heeger, 2006). Both maps displayed complete hemifield representations of the contralateral visual field and were located between V3d and V5/MT on the lateral surface of the occipital lobe.

5.5.4:   Identification of V5/MT

V5/MT was identified anatomically in each subject, in accordance with published guidelines (Dumoulin et al, 2000). V5/MT was located within the ALITS in all cases. The posterior boundary of V5/MT was either in close proximity to, or directly abutted the anterior boundary of LO2. In a subset of subjects (n = 4) visual field maps TO1 and TO2 were defined according to previous reports (Amano et al., 2009). Due to the inconsistency in identification of these maps, they were not used for V5/MT target identification.

5.5.5:   Psychophysical Stimuli & Procedures

Stimuli for the behavioural/TMS experiments were generated using MATLAB (Mathworks, USA) and displayed on a Mitsubishi Diamond Pro 2070^{SB} display with a refresh rate of 60 Hz, controlled by a VISAGE graphics card (Cambridge Research Systems ^{TM}). Grating stimuli were luminance modulated sinusoidal gratings (50% contrast) presented in a circular aperture (diameter 4°) and had a spatial frequency of 2 cpd. All stimuli had a mean luminance of 31 cd.m^{-2} and were presented on a uniform grey background of the same luminance.

The visual tasks employed were orientation discrimination of moving sinusoidal gratings and motion discrimination of oriented sinusoidal gratings. Prior to TMS stimulation each subject completed orientation and motion discrimination experiments using the method of constant stimuli described in full in Chapter 2. The spatial and temporal organisation of the orientation and motion experiments was identical (see schematic Figure 5.2). Individual psychometric functions for orientation and motion discrimination were plotted for each subject in order to determine the individual thresholds (75% correct) to be tested on during subsequent TMS sessions. The phases of the reference and test gratings were randomised within trials to prevent the orientation task from being solved via local luminance cues. During motion discrimination, the directions of drift (left-right/right-left) were randomised between trials to prevent any directional adaptation. Definitions of stimuli to be used in TMS sessions initially followed the procedure outlined in Chapter 2. That is, 75% correct thresholds were defined for speeds quicker and slower than the reference and orientations more vertical and horizontal than the reference. The range between these values was calculated, divided in half and added to the following equation: TMS stimuli = reference ± range/2. These stimuli were then combined to create four possible test stimuli: **TMS stimulus 1** = faster + more vertical; **TMS stimulus 2** = faster + more horizontal; **TMS stimulus 3** = slower + more vertical; **TMS stimulus 4** = slower + more horizontal.
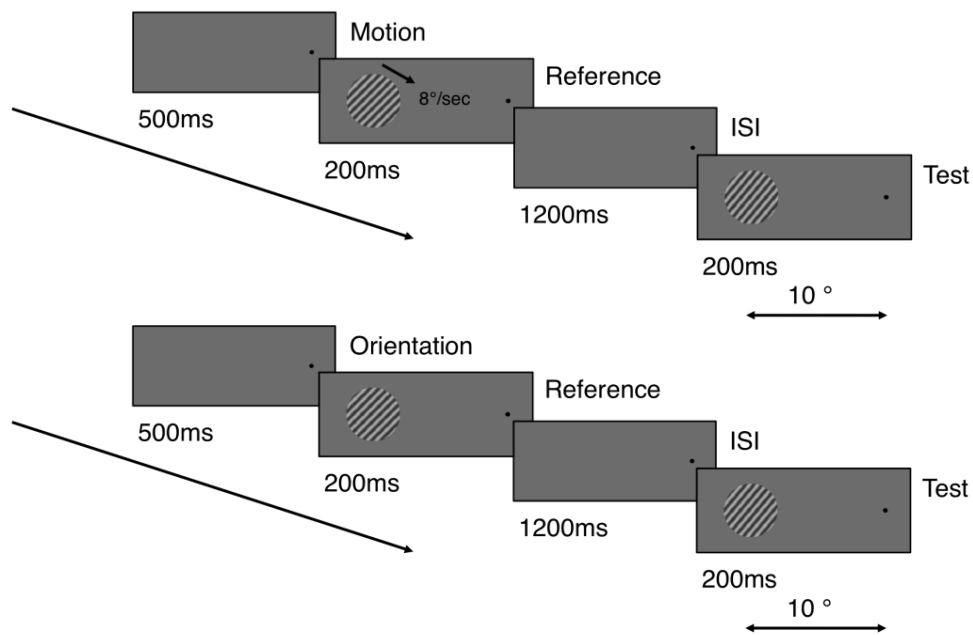
Figure 5.2: *Trial structure schematics for motion **(top)** and orientation **(bottom)** psychophysical tasks. During motion discrimination the test grating was at a fixed speed of 8°/sec. During orientation discrimination the reference grating was fixed at 45°. Test stimuli for both tasks were randomly selected from a pre-determined list of seven speeds (motion task) and orientations (orientation task) that spanned a range of values either side of the reference stimuli.*

5.5.6: TMS Protocol

A train of 4 biphasic (equal relative amplitude) TMS pulses, separated by 50ms (20Hz) at 70% of the maximum stimulator output (2.6 Tesla) were applied to the subject's scalp using a figure-of-eight coil (50 mm external diameter of each ring) connected to a Magstim Rapid2 ^{TM} stimulator (Magstim, Wales). Subjects were seated in a purpose built chair with chin rest and forehead support. The coil was secured mechanically and placed directly above each cortical target (CON, LO1, LO2 & V5/MT) with the handle orientated parallel with the floor. The position of the coil was monitored and tracked in real time allowing the displacement between the intended and actual site of TMS delivery to be recorded.

Each subject underwent 10 counterbalanced sessions (2 tasks x [4 TMS sites + 1 no TMS]). During subsequent TMS sessions (and no TMS baseline) only the stimuli defined

using the method above were presented in a trial structure identical to that used to establish thresholds. Each TMS session comprised 100 trials (25 per threshold stimulus). During motion discrimination, subjects were instructed to attend to the speed of the gratings, ignoring the orientation component. During orientation discrimination, subjects were instructed to attend to the orientation of the gratings only, ignoring the motion componentTMS pulses were delivered concurrently with the presentation of the test stimulus (Figure 5.3). This temporal configuration was identical to that used by Mckeefry et al., (2008), where induced functional deficits following TMS of V5/MT were maximised.
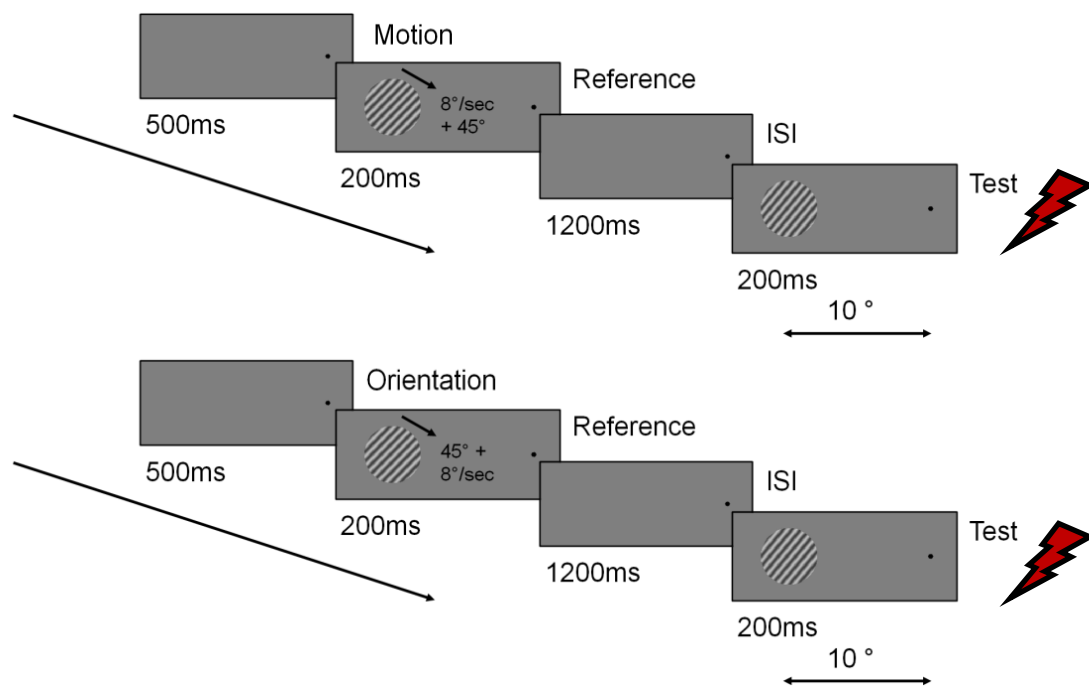
Figure 5.3: *Trial structure schematics for motion **(top)** and orientation **(bottom)** TMS tasks. During TMS sessions for both tasks (and no TMS baseline) only the two threshold stimuli were presented as test stimuli in a randomised order. TMS pulses were delivered coincident with the presentation of the threshold stimuli symbolised by the red lightning bolt.*

5.5.7:   Data & Statistical Analysis

Before data analysis some trials (~3%) were removed on the basis of two criteria: trials for which coil displacement was large (>2.5 mm) and trials for which reaction time was greater than 2,000 ms after the cessation of the presentation of the test stimulus. Statistics were calculated using the SPSS software package (IBM). A series of two-way repeated-measures ANOVAs were employed initially to examine the effects of discrimination (% correct) and reaction times (secondary measure), along with two potentially confounding variables (coil-target distance and coil-target orientation), which relate to spatial relationships between the TMS coils and the cortical targets. Statistically significant differences in these variables, caused by operator error, could confound the results. In the case of a significant interaction, subsequent one-way repeated-measures ANOVAs were calculated for each task considered separately. Given that our primary hypotheses related to the effects of TMS of LO1 and V5/MT we are justified in running planned comparisons in addition to the main ANOVAs to test the differences between these target sites with more sensitivity. For each ANOVA, whether or not the ANOVA adhered to the assumption of sphericity was established initially using Mauchly's test.

5.6:   Results

5.6.1:   Identification of Visual Field Maps LO1 & LO2

Definitions of LO1 and LO2 were made in at least on hemisphere in all subjects. The visual field representations within LO1 and LO2 were entirely consistent with previous work (Larsson & Heeger, 2006; Wandell et al., 2007), with both maps containing complete hemifield representations of the contralateral visual field. Figure 5.4, depicts visual field maps (including LO1 and LO2) on lateral views of both hemispheres of subject S7.
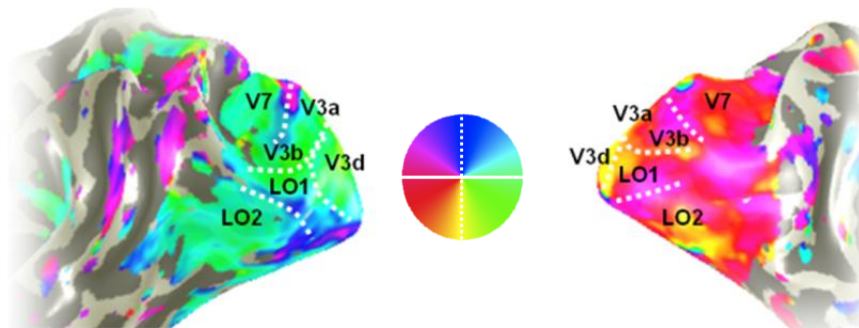
Figure 5.4: *Bilateral visual field maps in subject S7. Lateral views depict visual field maps in the left and right hemispheres of a representative subject (S7). The BOLD responses to the rotating wedge stimulus are overlaid in false colour (see colour wheel, centre) onto surface reconstructions of the grey-white matter boundary of the left and right hemispheres. The vertical meridian representations are shown by the dashed white lines, with the horizontal meridian representations shown by the solid white lines. In both hemispheres the visual field representations in LO1 and LO2 are clearly identifiable. LO1 begins at the shared boundary with V3d at the representation of the lower vertical meridian. LO1 extends anteriorly from the lower vertical meridian toward the upper vertical meridian. LO2 is the mirror-reverse of LO1 and displays a gradual progression from the upper vertical meridian back toward the lower vertical meridian.*

5.6.2:   Identification of V5/MT

The anatomical definition of V5/MT for a representative subject is depicted in Figure 5.5. Inspection of Figure 5.5, highlights the location of V5/MT (green circle) within the ALITS. The Euclidean distances (mm) between our cortical targets of interest (LO1, LO2 & V5/MT) in all subjects are displayed in Table 5.1. Distances were calculated within individual's native space and therefore, reflect the actual distances without normalisation to average coordinate spaces, which may distort these distance measurements.
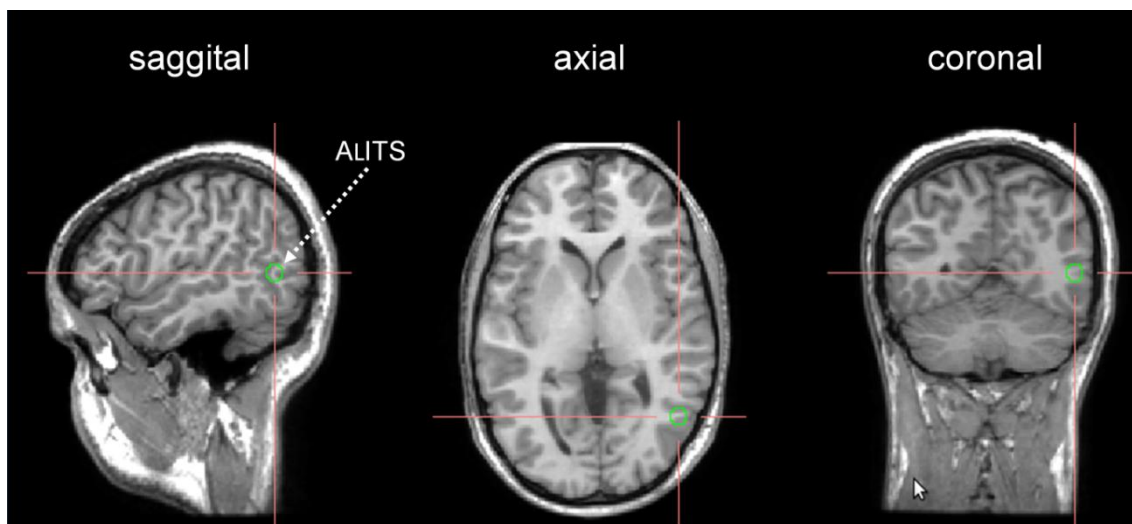
Figure 5.5: *Anatomical definition of V5/MT in a representative subject. Saggital, axial and coronal slices demonstrate the anatomical location of V5/MT in the right hemisphere of a single subject Images are displayed in neurological convention. The centre of the green disk is within the ascending limb of the inferior temporal sulcus (ALITS). Crosshairs centred in the middle of the green circle depict the V5/MT target site.*

Table 5.1: *Euclidean distances (mm) between LO1, LO2 and V5/MT in all subjects. The average distances demonstrate the two spatial scales of investigation: LO1 – V5/MT between clusters and, LO1-LO2, within cluster.*

	Euclidean distance (mm) between targets		
Subject	LO1-LO2	LO1-V5/MT	LO2-V5/MT
S1	10.7700	29.8998	16.1864
S2	9.0200	38.4448	24.3516
S3	10.2900	24.7386	20.3224
S4	13.7400	26.7208	16.0312
S5	6.0600	30.0167	12.6886
S6	11.8700	24.8596	12.0830
S7	14.8930	18.5472	4.3589
S8	11.2230	19.7990	12.3693
S9	10.4800	40.8167	31.0644
S10	10.8612	28.0000	15.6844
S11	12.6800	21.0000	14.2127
S12	14.7330	20.7123	14.4914
Average	11.3804	26.9630	16.1537

5.6.3: Motion & Orientation Psychophysics

In order to establish whether the motion and orientation discrimination tasks were behaviourally dissociable, two subjects (EHS and JR) completed orientation and motion psychophysical experiments both in isolation and when the two stimuli were combined. Identical stimulus intensities were used for each subjects across both types of psychophysical experiment (isolation and combined). Fitting of psychometric functions followed the method outlined in the ***psychophysical protocol*** section of Chapter 2. Briefly, both subjects completed 350 trials (50 per stimulus level) for each task, both in isolation and when combined. The average proportion of faster (motion) and more vertical (orientation) responses was calculated for each stimulus level and a cumulative Gaussian was used to plot each function. The psychometric functions for all conditions are plotted in Figure 5.6. For both subjects the isolated data are depicted by the red dots and pale lines, with the combined data depicted by the blue dots and darker lines.
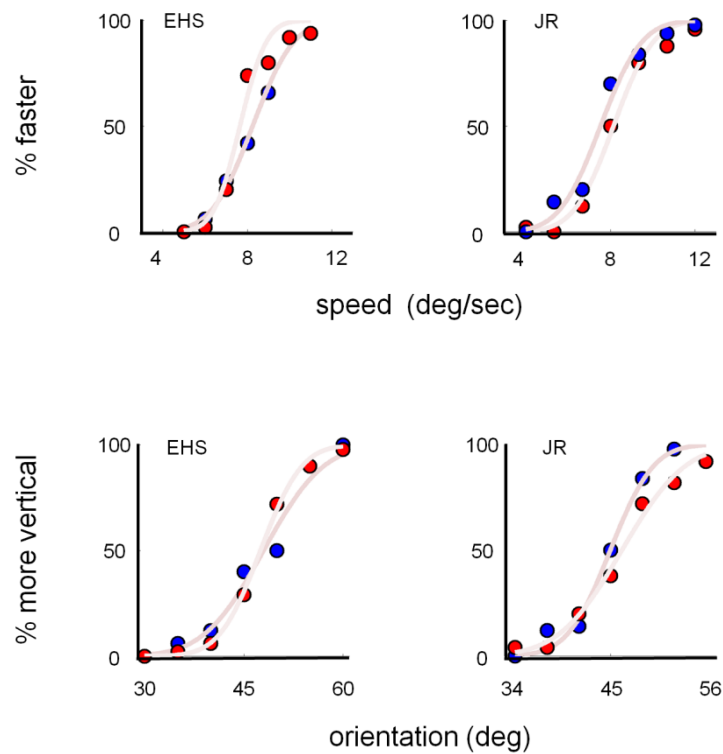
Figure 5.6: *Isolated and combined motion and orientation psychometric functions in two subjects. Psychometric functions for motion **(top row)** and orientation discrimination **(bottom row)** conducted in isolation **(red dots – pale lines)** or combined with a second stimulus dimension **(blue dots – darker lines)** for subjects EHS **(left column)** and JR **(Right column)**.*

Inspection of Figure 5.6, suggests performances differences between orientation and motion discrimination in isolation relative to the combined conditions. To test this, psychometric functions were randomly resampled 15 times using a bootstrap technique. Each psychometric function was created by averaging the responses to 350 stimulus presentations (50 x 7 stimulus levels). Initially, the 50 responses for each stimulus intensity were randomly selected and reordered. The first 25 choices were subsequently selected as a new sample. The *PSE* and just noticeable difference (*JND*) of the best fitting cumulative Gaussian of these samples were then computed using a least squared minimisation procedure. *JND* was computed as the standard deviation of the cumulative Gaussian, with smaller *JND* indicative of better discrimination. *PSE* provided a measure of shift of the curve, indicating bias in responses.

The results of the bootstrapping procedure are displayed in Table 5.2. The *PSE* and *JND* values derived from both the isolated and combined discrimination experiments for both EHS and JR are displayed.

Table 5.2: *Mean point of subjective equivalence (PSE) and just noticeable difference (JND) values derived from the isolated and combined motion and orientation psychophysical tasks for subjects EHS and JR.*

Subject	motion (deg/sec)		orientation (deg)	
	Isolation	Combined	Isolation	Combined
EHS				
PSE	8.1700	7.6300	47.8900	48.0100
JND	1.4800	0.9000	7.1300	5.6700
JR				
PSE	7.5500	8.1700	46.4000	45.0200
JND	1.2800	1.4900	4.8600	3.3200

The *PSE* and *JND* values derived from the isolated and combined psychophysical tasks were compared for EHS and JR using independent samples *t*-tests. For motion discrimination, the *PSE* of the isolated and combined psychophysics were significantly different for both participants but, interestingly, in opposite directions. The *PSE* was higher in the combined condition for JR ($t_{(28)}$ = -8.031, *p* = < 0.001), but lower for EHS ($t_{(28)}$ = 6.479, *p* = < 0.001). Participant JR showed no significant difference in *JND* between conditions ($t_{(28)}$ = -1.548, *p* = 0.067), whereas EHS showed significant difference in *JND*, which was smaller in the combined condition ($t_{(28)}$ = 7.541, *p* = < 0.001), indicative of better discrimination during combined presentation. For orientation discrimination, only participant JR showed significant differences in *PSE* ($t_{(28)}$ = 6.788, *p* = < 0.001, and JND, ($t_{(28)}$ =6.747, *p* = <0.001) between the isolated and combined conditions. EHS showed no significant difference in *PSE* ($t_{(28)}$ = -0.187, *p* = 0.853, or JND ($t_{(28)}$ =1.394, *p* = 0.087), between the isolated and combined conditions, suggesting that the combined presentation did not alter orientation discrimination ability relative to isolated presentation.

Taken together, motion and orientation discrimination appear to be dissociable behavioural tasks. Although significant differences in *JND* and *PSE* were found, these were not consistent across either subjects or tasks. In addition, the only significant differences found for *JND* were in the opposite direction predicted with better discrimination in the combined presentation, suggesting rather counter-intuitively, that combining motion and orientation signals together aided discrimination. On the basis of these inconsistent findings, it was decided that motion and orientation thresholds be derived from isolated presentations of both visual features. These thresholds were then combined to create the stimuli for TMS.

Table 5.3, contains the 75% correct thresholds for speeds faster and slower than the reference and orientations more vertical and more horizontal than the reference for all subjects. Table 5.2, also includes the value added to and subtracted from the reference stimulus and the actual values presented during TMS for all subjects. The two TMS stimuli for each task, were then combined together to define four TMS stimulus combinations: **TMS stimulus** 1 = faster + more vertical; **TMS stimulus 2** = faster + more horizontal; **TMS stimulus 3** = slower + more vertical; **TMS stimulus 4** = slower + more horizontal.

Table 5.3: *Threshold and TMS values derived from the motion and orientation psychometric functions for subjects S1-S12. For motion **(top)**, table includes the 75% correct values for speeds slower **(threshold S)** and faster **(threshold F)** than the reference, plus the value added too and taken away from the reference **(ref ±)** and the values used during TMS for the slower **(TMS S)** and faster **(TMS F)** test stimuli. For orientation **(bottom)**, table includes the 75% correct values for orientations more horizontal **(threshold H)** and more vertical **(threshold V)** than the reference, plus the value added too and taken away from the reference **(ref ±)** and the values used during TMS for the more horizontal **(TMS H)** and more vertical **(TMS V)** test stimuli.*

speed (degrees/sec)					
Subject	threshold S	threshold F	ref ±	TMS S	TMS F
S1	6.4075	8.5075	1.0500	6.9500	9.0500
S2	7.3100	8.5550	0.7725	7.2275	8.7725
S3	6.5150	8.6750	1.0800	6.9200	9.0800
S4	7.2650	8.7500	0.7425	7.2525	8.7425
S5	7.2500	9.7550	1.2525	6.7475	9.2525
S6	7.2200	9.2900	1.0350	6.9650	9.0350
S7	6.5000	8.5600	1.0250	6.9700	9.0300
S8	6.5450	9.0950	1.2750	6.7250	7.0700
S9	6.8000	8.6600	0.9300	7.0700	8.9300
S10	5.9000	9.4550	1.7775	6.2225	9.7775
S11	6.4850	9.7700	3.7200	6.3575	9.6425
S12	5.9000	9.6200	1.8600	6.1400	9.8600
orientation (degrees)					
Subject	threshold H	threshold V	ref ±	TMS H	TMS V
S1	43.4400	46.3200	1.4400	43.5600	46.4400
S2	43.1250	46.8000	1.8375	43.1625	48.8375
S3	43.7250	46.7750	1.5250	43.4750	46.5250
S4	44.2800	46.2600	0.9900	44.0100	45.9900
S5	43.1400	48.2700	2.5650	42.4350	47.5650
S6	43.2000	52.8000	4.8000	40.2000	49.8000
S7	43.1550	49.4100	3.1275	41.8725	48.1275
S8	43.9000	46.3250	1.2125	43.7875	46.2125
S9	43.5600	46.6650	1.5525	43.4475	46.5525
S10	44.1900	47.1900	1.5000	43.5000	46.5000
S11	43.3875	46.5750	1.5938	43.4062	46.5938
S12	42.8650	48.0450	2.5900	42.4100	47.5900

5.6.4:   Effects of TMS on Combined Motion & Orientation Discrimination

Group averaged performances (% correct) for all conditions and tasks are plotted in Figure 5.7. Inspection of Figure 5.7, reveals a number of interesting patterns of results for both motion and orientation tasks. For motion discrimination, the data indicate that: (1) performance was maximally disrupted following TMS of V5/MT, relative to all other conditions; (2) performances were largely similar following TMS of the CON, LO1 and LO2 and (3) performance during the no TMS condition was slightly improved, relative to the collective TMS conditions – a feature also observed in Chapter 4.   For orientation discrimination, the data indicate that: (1) TMS of LO1 induced maximum disturbance to performance, relative to all other conditions; (2) performances were very similar following TMS of the CON, LO2, V5/MT and the no TMS baseline, and (3) performance is best during V5/MT stimulation. Comparing the overall pattern of deficits across tasks also indicates slightly lower overall performances in the motion compared to orientation tasks for all conditions, a pattern also consistent with the data reported in Chapter 4. The slight overall drop in performance during motion task may suggest a potential main effect of task
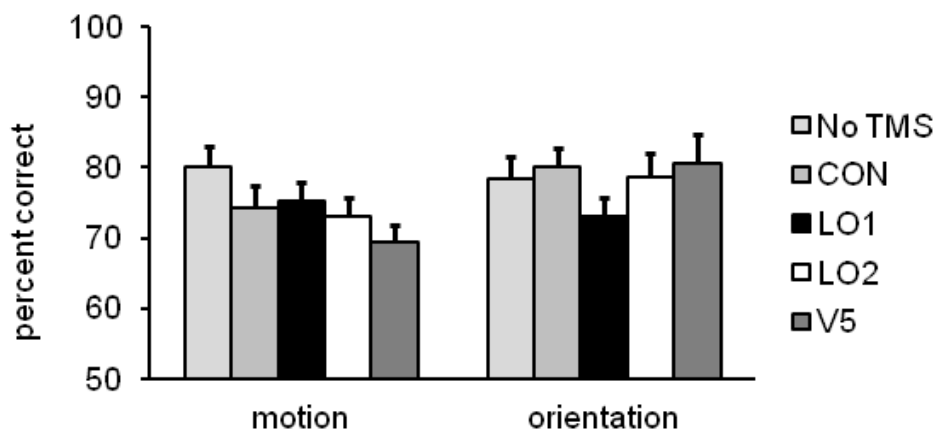
Figure 5.7: *Effect of TMS on combined motion and orientation TMS tasks. Mean discrimination performances (% correct) across all conditions for the combined motion and orientation TMS tasks. Motion discrimination was maximally disrupted following TMS of V5/MT, whereas orientation discrimination was maximally disrupted following TMS of LO1. Within each task, performances are largely equivalent across other conditions. Error bars represent s.e.m.*

Crucially, if orientation perception of moving stimuli is reliant upon computations performed by LO1, and V5/MT maintains its specializations for motion, even when combined with the presence of an additional irrelevant stimulus feature, an interaction between Task and Site should be evident. Accordingly, a 2 x 5 repeated-measures ANOVA was conducted with conditions Task (motion & orientation) and Site (no TMS, CON, LO1, LO2 & V5/MT). Sphericity was maintained across all main effects. The main effects of Task ($F_{(1, 11)}$ = 2.583, p = 0.136), and Site ($F_{(4, 44)}$ = 2.248, p = 0.079) were not significant. Despite the slightly lower performances, across conditions, during motion discrimination, performances across the two tasks were not significantly different, suggesting that both tasks were equivalently difficult. The ANOVA did however, reveal a significant Task x Site interaction ($F_{(4, 44)}$ = 3.415, p = 0.016). There were no significant pairwise site comparisons (p = > 0.214, in all cases: Bonferroni corrected). Although the identification of a significant Task x Site interaction was essential to the analysis, additional analyses were required to determine whether or not disruptions to performance were specific to TMS of LO1 and V5/MT. Accordingly, one-way repeated-measures ANOVAs were conducted on each task considered separately.

For motion discrimination, there was a significant effect of Site ($F_{(4, 44)}$ = 3.613, p = 0.012). It was hypothesised that V5/MT would exhibit specializations for motion perception despite the presence of orientation noise. In order to explore further the nature of the above effect, paired t-tests (one-tailed) were computed to compare the effects of TMS of V5/MT relative to all other conditions. TMS of V5/MT caused a significant and selective disturbance to motion discrimination despite the presence of different orientations, compared to all other conditions (V5/MT *versus* no TMS: $t_{(11)}$ = -3.699, p = 0.002; V5/MT *versus* CON: $t_{(11)}$ = -1.950, p = 0.0385; V5/MT *versus* LO1: $t_{(11)}$ = -1.995, p = 0.0355; V5/MT *versus* LO2: $t_{(11)}$ = -1.924, p = 0.0405). As noted above (and in Chapter 4), performance on the no TMS condition was slightly higher than all other TMS conditions. This could be indicative of a general effect of TMS, which in turn was more pronounced following TMS of V5/MT. In order to assess the validity of such an interpretation, paired t-tests (two-tailed) were conducted to compare performance during the no TMS with performances following TMS of the CON, LO1 and LO2. There were no significant differences between performance during the no TMS baseline and TMS of any site other than V5/MT (no TMS *versus* CON: $t_{(11)}$

= 1.781, p = 0.102; no TMS *versus* LO1: $t_{(11)}$ = 1.750, p = 0.108; no TMS *versus* LO2: $t_{(11)}$ = 1.890, p = 0.085). The data argue against a general effect of TMS on performance. Analysis of reaction times however, will be important in order to rule out speed-accuracy trade off as an explanation for the higher performance during no TMS.

For orientation discrimination, there was no significant effect of Site ($F_{(4, 44)}$ = 1.610, p = 0.189). Larger degrees of variance (evidenced by the large error bars relative to the motion tasks) could potentially account for the lack of a significant effect of Site. Indeed, from the data presented in Figure 5.7, one can clearly see that on average performance was maximally disrupted following TMS of LO1. Despite the lack of a significant effect of Site, paired *t*-tests (one-tailed) were nevertheless conducted to ascertain whether any site comparisons were significant. There were no significant differences between TMS of LO1 and either the no TMS condition (LO1 *versus* no TMS: $t_{(11)}$ = -1.138, p = 0.1395) or LO2 (LO1 *versus* LO2: $t_{(11)}$ = -1.549, p = 0.075), although the data approached significance for this condition. There were however, significant differences between TMS of LO1 and TMS of the CON (LO1 *versus* CON: $t_{(11)}$ = -1.924, p = 0.0405) and V5/MT (LO1 *versus* V5/MT: $t_{(11)}$ = -1.874, p = 0.044).

As mentioned above, our primary hypotheses related to whether computations in LO1 underpin the orientation perception of moving stimuli and whether the specializations for motion perception exhibited by V5/MT is maintained in the presence of stimuli that differ in orientation. It is therefore justified to refine our analysis to consider those two targets sites alone using planned contrasts. The interaction term between LO1 and V5/MT was significant ($F_{(1, 11)}$ = 15.087, p = 0.003). Subsequent paired *t*-tests (one-tailed) confirm a double dissociation between these two cortical regions; for motion TMS of V5/MT caused a significant disturbance to performance relative to TMS of LO1 ($t_{(11)}$ = -1.995, p = 0.035), whereas during orientation TMS of LO1 significantly deteriorated performance relative to TMS of V5/MT ($t_{(11)}$ = -1.874, p = 0.044).

5.6.5:   Effects of TMS on Reaction Times

Reaction times were recorded as a secondary measure of the effects of TMS. Reaction times are often the primary metric by which the effects of TMS are measured, in particular when the effects of TMS on discrimination are thought to be minimal. Group averaged reaction times across all conditions and tasks are plotted in Figure 5.8. Inspection of Figure 5.8, reveals a number of interesting pattern of results. Beginning with motion discrimination, the data indicate that the effects of TMS of V5/MT cannot be due to quicker reaction times relative to other conditions. Indeed, reaction times were very similar across all TMS conditions, this argues against speed-accuracy trade off as an explanation for the V5/MT effect. Interestingly, reaction times during the no TMS baseline were slower than any other condition. The slower reaction times may underpin the higher performance rates in the no TMS condition reported above – a pattern observed in Chapter 4. For orientation discrimination, reaction times were slowest during TMS of LO1, a pattern consistent with the effect of TMS of LO1. During LO1 stimulation, performance was maximally disrupted, and reaction times were slower, presumably due to increased task difficulty.
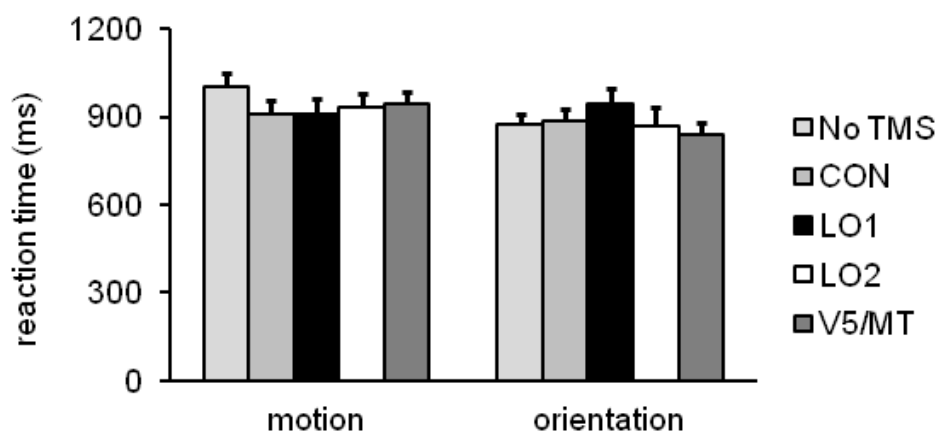
Figure 5.8: *Effect of TMS on reaction times during combined motion and orientation TMS tasks. Mean reaction time across sites and tasks. The results indicate that reaction times did not vary in a manner that explains the observed patterns of performance. For each task, the condition with the slowest reaction times was associated with the poorest performance, LO1 for orientation and V5/Mt for motion. This is in the predicted direction as is the opposite of a speed-accuracy trade off. Error bars represent s.e.m.*

To assess formally the effect of reaction times, a 2 x 5 repeated measures ANOVA was conducted with conditions Task (motion & orientation) and Site (no TMS, CON, LO1, LO2 & V5/MT). Mauchly's test of sphericity was only violated for the Task x Site interaction (Mauchly's $W_{(5)}$ = 0.121, p = 0.020, estimate of non-sphericity = 0.564), the degrees of freedom for the Task x Site interaction were therefore corrected using the Greenhouse-Geisser correction. The Task x Site interaction was not significant ($F_{(2.258, 24.837)}$ = 1.819, p = 0.180; Greenhouse-Geisser corrected). The main effect of Task was significant ($F_{(1, 11)}$ = 6.983, p = 0.023), whereas the main effect of Site was not significant ($F_{(4, 44)}$ = 1.507, p = 0.216). The main effect of task suggests that in general subjects took longer to respond during motion than orientation task.

Given the lack of a significant interaction, task specific ANOVAs were not conducted. As mentioned above, motion discrimination performance during no TMS was higher than all other conditions. This higher performance rate could have been caused by the slower reaction times during no TMS. In order to assess this statistically, reaction times during no TMS were compared to all other conditions using paired t-tests (two-tailed). There were no significant pairwise comparisons (no TMS *versus* CON: $t_{(11)}$ = -1.787, p = 0.101; no TMS *versus* LO1: $t_{(11)}$ = 0.482, p = 0.639; no TMS *versus* LO2: $t_{(11)}$ = 0.086, p = 0.933; no TMS *versus* V5/MT: $t_{(11)}$ = 0.424, p = 0.680). The higher performance rates during no TMS are not due to speed-accuracy trade-offs. There is no evidence that the effects of TMS of V5/MT and LO1 during combined motion and orientation discrimination are due to the presence of speed-accuracy trade-offs.

5.6.6:   *Analysis of Confounding Variables*

Additional measurements were recorded with each TMS pulse train to account for two potentially confounding variables that relate to the spatial relationship between the stimulating coil and the targets within cortex; coil-target distance and coil-target orientation. These measurements, which evaluate the precision of TMS delivery, are included as they provide a means by which to assess whether the discrimination data reported above were due to operator error.

5.6.6.1:   Coil - Target Distance

We assessed whether the distance from the calibration-point of the TMS coil (hot-spot of coil) to the TMS targets varied across tasks and conditions in a way that might explain the observed effects of TMS on motion and orientation discrimination, respectively. Group averaged coil-target distances (mm) for all TMS sites and tasks are plotted in Figure 5.9. From Figure 5.9, one can see that the coil-target distances across sites are very similar for both tasks.
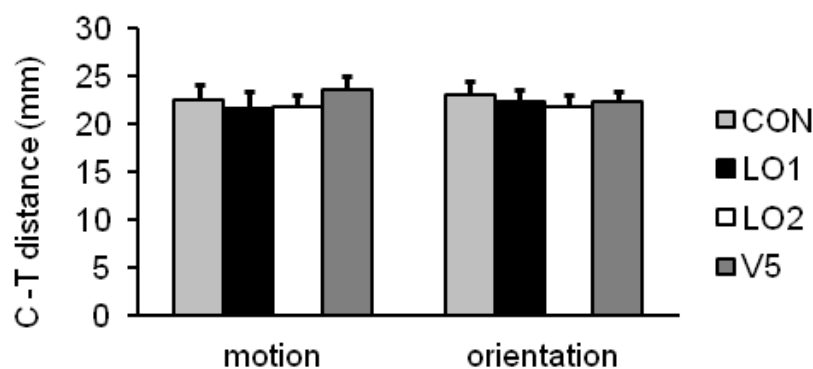
Figure 5.9: *Mean Euclidean distance between stimulating coil and cortical targets during combined motion and orientation discrimination Mean distance between stimulating coil and cortical targets. The results indicate that coil-target distance did not vary in a manner that explains the observed patterns of TMS on performance. There is no evidence that differences in the distance between the stimulating-coil and cortical targets led to the dissociable effects observed.Error bars represent the s.e.m.*

To assess the effect of coil-distance a 2 x 4 repeated-measures ANOVA was conducted with conditions Task (motion & orientation) and Site (CON, LO1, LO2, V5/MT). Sphericity was maintained across all main effects. There were neither significant effects of Task ($F_{(1, 11)}$ = 0.504, p = 0.611), nor Site ($F_{(2, 22)}$ = 0.028, p = 0.870), nor Task x Site interaction ($F_{(2, 22)}$ = 0.389, p = 0.682). Given the lack of significant main effects or a significant interaction further tests were not conducted. The result indicates that the effect of TMS on discrimination of motion and orientation cannot be explained by differences in the distance from the stimulating coil to the targets across tasks.

5.6.6.2:   Coil - Target Orientation

Coil orientation provides a measure of the difference between the coil orientation and the vector joining the 'hotspot' of the coil and the TMS target. Given the figure-of-eight coils used, the optimum coil-target orientation is 90° on this measure. Group averaged coil-target orientations for all TMS sites for both tasks are plotted in Figure 5.10. Inspection of Figure 5.10, demonstrates slight variations in the coil-target orientation across sites. For motion discrimination the coil-target orientation during CON stimulation is different from stimulation of LO1, LO2 or V5/MT, which are largely similar. For orientation discrimination less variation across sites is observed. Indeed, the coil-target orientations are largely equivalent across sites.
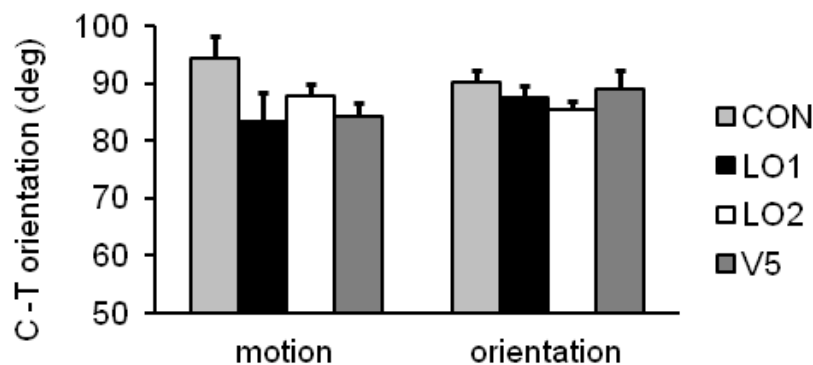
Figure 5.10: *Mean coil-target orientation during combined motion and orientation discrimination. For motion discrimination, the largest variation is evident between the CON and all other conditions. For orientation discrimination, the coil-target orientations were similar across tasks. Error bars represent s.e.m.*

To assess the effects of coil-target orientation a 2 x 4 repeated-measures ANOVA was conducted with conditions Task (motion & orientation) and Site (CON, LO1, LO2 & V5/MT). The Task by Site interaction was the only main effect to violate the assumption of sphericity (Mauchly's $W_{(2)}$ = 0.318, *p* = 0.003, estimate of non-sphericity = 0.594), therefore the degrees of freedom for the interaction were corrected using Greenhouse-Geisser. There was neither a significant effect of task ($F_{(1, 11)}$ = 2.391, *p* = 0.150), nor site ($F_{(2, 22)}$ = 0.178, *p* = 0.863), nor task by site interaction ($F_{(1.189, 13.076)}$ = 1.263, *p* = 0.291).   Given the lack of significant main effects or an interaction, subsequent one-way ANOVAs on each task were not conducted. There is no evidence that the angular displacement of the coil varied in a

way that could explain the main interaction or the double dissociation between LO1 and V5/MT reported above.

5.7: Discussion

In the current study TMS pulses were applied to cortical targets whilst subjects performed two visual tasks – orientation discrimination of drifting gratings and motion discrimination of oriented gratings. Our primary hypotheses concerned the effects of TMS of LO1 *versus* V5/MT, yet in a desire to be consistent with the practices in Chapter 4, we included the additional conditions of LO2, CON and no TMS. Overall the effects of TMS on discrimination performance produced a significant Task x Site interaction, with TMS of V5/MT maximally disrupting motion discrimination relative to all other conditions and TMS of LO1 inducing maximal disturbance to orientation discrimination relative to all other conditions. Indeed, planned contrast analysis between LO1 and V5/MT revealed a significant double dissociation between the effects of TMS on motion and orientation discrimination, respectively. The overarching pattern of deficits induced by TMS is consistent, to a degree, with the map specific and parallel predictions and also those reported in Chapter 4, although it is important to note however, that the effects observed here are markedly weaker than those reported in Chapter 4. Indeed, the one-way ANOVA for orientation was not significant, despite having double the number of subjects, and was only significant when planned contrasts were applied. The patterns of results are inconsistent with either the prediction that V5/MT underpins performance of both tasks or that of V5/MT and LO1 interact to perform the orientation task, whilst V5/MT alone underpins the motion task. These effects were immune to the presence of speed-accuracy trade-offs and to differences in the spatial relationships between the stimulating coil and the cortical targets, which could have arisen due to operator error.

5.7.1:   *LO1 Involved, but not Critical to Orientation Processing of Moving Stimuli*

The results of the orientation (plus motion) discrimination study indicate that the accurate perception of orientation of a moving stimulus is influenced (to a degree) by computations performed within LO1. The disturbance to performance following LO1 stimulation was significantly different relative to TMS of the CON and V5/MT. The effects were not significant relative to the no TMS baseline or following TMS LO2, although approached significance in the latter condition. Taken together, the current findings are consistent with the maximal disruption to static orientation processing following TMS of LO1 reported in Chapter 4, although much weaker in power. The results echo those reported in Chapter 4, by demonstrating that behaviourally relevant information regarding the orientation of moving stimuli is present at this level of the visual hierarchy. The data are also in-line with previous fMRI work investigating orientation selectivity of motion-boundaries in human visual cortex (Larsson et al., 2010). A number of extrastriate regions of cortex, including LO1 and LO2, were shown to exhibit orientation-selective releases from motion-boundary adaptation. Indeed, the release from adaptation within LO1 following the presentation of a probe grating orientated orthogonally to the adaptor was significant in 5/5 subjects tested and found to be ~50% greater than that observed in LO2. The orientation selective effect following TMS of LO1 was found not to be due to LO1's proximity to V1, as previously suggested (Larsson et al., 2006). The significant difference in discrimination following TMS of LO1 and the CON, echoes the pattern of results reported in Chapter 4. An important feature to note is that the effect of TMS of LO1 was markedly weaker here than that reported in Chapter 4, despite double the number of subjects. Indeed, the one-way ANOVA for orientation discrimination was not significant, making the additional planned contrasts less justified. Although orientation discrimination of moving gratings may depend on LO1, it appears less dependent on LO1 computations than for static orientation.

A noteworthy, but non-significant, feature of the discrimination data reported here is that during motion discrimination, TMS of LO1 resulted in the higher performance levels relative to all other TMS conditions. Although the differences in performances are small, they are nevertheless evident. Taken within the context of Walsh et al., (1998), one

158

interpretation of this effect is that TMS of LO1, reduced the demand placed on the system for the encoding of orientation and therefore, 'free-up' the capacity for encoding motion presumably, but not exclusively, by V5/MT.

One possibility for the reduced effect following TMS of LO1 and LO2 during motion discrimination may reflect the speed of our stimulus targets (8°/sec). An interesting possibility for future research would be to examine the effects of LO1 and LO2 stimulation during motion discrimination at a range of stimulus speeds.

5.7.2:   V5/MT Specialized for Motion Perception

In the first instance, TMS of V5/MT induced significant and selective disturbances to performance on our combined motion (plus orientation) discrimination task. The pattern of results is entirely consistent with the data reported in Chapter 4 during motion discrimination in isolation, where TMS of V5/MT maximally disrupted performance relative to all other conditions. The TMS data reported here are largely consistent with previous TMS studies probing the functional properties of V5/MT (Beckers & Homberg, 1992; Walsh et al., 1998; McKeefry et al., 2008). V5/MT neurons appear therefore to sufficiently sophisticated to extract the motion component of a stimulus, even in the presence of an additional visual feature. In this instance the presence of orientation information would be unlikely to aid in the discriminations of speed required by our subjects. In contrast, had the discriminations we required our subjects to complete been direction based, the presence of orientation information would likely have aided performance. Evidence from single-unit recordings in macaque V5/MT, highlight the presence of neurons selective for orientation and direction, with the peak orientation sensitivity typically (but not exclusively) perpendicular to the preferred direction (Maunsell & Van Essen, 1983; Albright, 1984). The results reported in Chapter 4, coupled with the selective disturbance to performance reported here demonstrate the specialized role played by V5/MT in the perception of motion, even when a second stimulus feature is present.

An interesting, but non-significant, pattern of results during orientation discrimination was that performance was best following TMS of V5/MT relative to all other conditions. Although this difference was small, relative to TMS of the CON, group averaged

discrimination performance was nonetheless, numerically greatest following TMS of V5/MT. A previous TMS study reported that TMS of V5/MT caused facilitation in performance of visual search tasks where motion was present, but irrelevant, or when attention was directed towards either form or colour (Walsh et al., 1998). The facilitation of performances following TMS of V5/MT was interpreted in a framework of mutual inhibition between different extrastriate cortical areas. That is, difference extrastriate visual areas compete for the limited processing resources available and that disruption of V5/MT had the effect of 'freeing-up' processing capabilities for regions of cortex processing stimulus features other than motion. Taken within this context, one interpretation of the effect of TMS of V5/MT during orientation discrimination of moving gratings, where motion was present, but irrelevant to the task, is that processing resources were 'freed-up' allowing more processing to be allocated to encoding orientation, presumably by LO1. Indeed, this pattern was not observed following TMS of V5/MT during static orientation discrimination reported in Chapter 4, where performance was greatest following TMS of the CON.

The data reported above add to the growing body of evidence from neuropsychological (Zihl et al., 1983), neuroimaging (Zeki et al., 1991; Orban et al., 1995) and neurostimulation studies (Beckers & Homberg, 1992; Walsh et al., 1998; McKeefry et al., 2008) that demonstrate the specialized role played by V5/MT in motion perception.

5.7.3: *Double Dissociation & Parallel Processing*

The planned contrast analysis revealed a double dissociation between the effects of TMS of LO1 and V5/MT during our visual tasks. The double dissociation is consistent with the data reported in Chapter 4 and provides further evidence for parallel processing between LO1 and V5/MT, although as mentioned previously, this double dissociation was only present following planned contrasts therefore should be interpreted with caution. The effects reported here for combined stimuli are much weaker than those reported in Chapter 4. The encoding of orientation information by LO1 appears to persist, despite the influence of motion. Likewise, the encoding of stimulus speed by V5/MT appears not to be altered by changes in orientation. Given the evidence for orientation sensitive responses in V5/MT one interpretation is that during motion discrimination attention increased the selectivity of V5/MT neurons tuned to detect speed over those tuned for orientation (Treue & Trujillo,

1999; Treue, 2001; Trujillo & Treue, 2004). As mentioned in Chapter 4, the functional independence between LO1 and V5/MT reported here may be underpinned by independent anatomical connections from antecedent (Beckers & Zeki, 1995) and in the case of V5/MT, even subcortical (Sincich et al., 2004) regions. The marginal facilitation in performances during motion discrimination following TMS of LO1 and orientation discrimination following TMS of V5/MT is a particularly intriguing pattern. Taken in the framework of mutual inhibition between different cortical areas suggested by Walsh et al., (1998), LO1 and V5/MT may compete for processing resources when orientation and motion signals are present simultaneously – an interesting avenue for future work could explore this potential mechanism for mutual inhibition more explicitly.

5.7.4.   The Role Played by LO2 in Visual Perception?

The current results, coupled with the data reported in Chapter 4, bring into focus the question of the role played by LO2 in visual computations. Recall that in Chapter 4 TMS of LO2 neither disrupted motion nor orientation discrimination relative to other conditions. The patterns of performances following TMS of LO2 in the current study are largely consistent with that reported in Chapter 4. TMS of LO2 neither disrupted performances on the combined motion nor orientation discrimination tasks. The lack of effect following TMS of LO2 is consistent with previous fMRI work, highlighted a lack of selectivity to orientation and motion in LO2 (Larsson & Heeger, 2006). Interestingly, LO2 has been shown to exhibit orientation-selective adaptation for motion-boundaries (Larsson et al., 2010), although the authors stress that this selectivity was ~50% of that exhibited by LO1. Speculation regarding the role played LO2 originated from the finding that BOLD signals following the presentation of everyday objects were larger in LO2 than any other retinotopically defined regions, including LO1 (Larsson & Heeger, 2006). A number of more recent reports also highlight the object-selective nature of responses in LO2 (Sayres & Grill-Spector, 2008; Amano et al., 2009). From this, it was originally suggested that a hierarchy existed between LO1 and LO2, with LO1 extracting boundary information and LO2 representing more complex shape information. The data reported in Chapter 4, coupled with the current data certainly suggest that orientation and boundary information is processed in LO1. Chapter 6 will explore whether LO2 is specialized for the processing of shape explicitly, by applying TMS to LO1

and LO2 whilst subjects perform shape discriminations of radial frequency patterns. We also include the static orientation discrimination task from Chapter 4, as a direct replication.

5.8:   Conclusion

Accurate orientation discrimination of moving stimuli is disrupted (to a degree) following TMS of LO1. Likewise, accurate discrimination of motion is significantly and selectively impaired following TMS of V5/MT, even when the stimuli contain orientation information. Following planned contrasts only, the data revealed specializations within LO1 and V5/MT that were consistent, albeit markedly weaker, than those reported in Chapter 4. Taken together, the data reported in this chapter provide a much weaker account for functional specialization and parallel processing than those data reported in Chapter 4. One alternative account of the data is that they provide support for a lack of cue-invariance in LO1. The effect of orientation was only present following planned contrasts and moreover following a non significant one-way orientation ANOVA. The current results extent those reported previously in terms of the sophisticated tuning of neurons present within these regions. The role played by LO2 in visual perception remains unclear.

Chapter 6

Specialized & Parallel Processing of Orientation & Shape in LO1 & LO2

6.1:   Overview

The overarching aim of this study was to investigate whether applying TMS to LO1 and LO2 could induce selective disturbances to performance on two visual tasks. Given the results reported in Chapter 4 a static orientation discrimination task was selected – a task demonstrated to be critically dependent on LO1. The second task was shape discrimination – a visual task that may well be crucially dependent on LO2. Whether or not LO1 and LO2 operate independently of one another is currently unknown and therefore, the predicted effects of TMS are considered with respect to both serial and parallel *map specific* processing frameworks.

6.2:   Introduction

The results reported in Chapters 4 and 5 revealed a number of important features regarding the visual computations performed by LO1 and LO2. First, LO1 was found to be critically involved in the perception of orientation of static gratings and to lesser extent moving gratings. In both cases, this functional specialization was not attributable to LO1's proximity to V1. Second, a single dissociation was present between the effects of TMS of LO1 and LO2 on orientation discrimination of static and drifting gratings. Although the difference during orientation discrimination of moving gratings was not significant it nonetheless approached significance (p = 0.075). Finally, TMS of LO2 was found not to disrupt either motion or orientation perception whether presented in isolation or combined. Taken together these findings suggest that LO2 may be specialized for the processing of different visual features. It has been suggested previously that LO2 may underpin the perception of shape and therefore, the current study aimed to test this explicitly. Whether or not LO1 and LO2 exhibit independent specializations for orientation and shape is currently unknown.

6.2.1:   Functional Specialization & Parallelism in the Human Brain

The current study aimed to reveal functional specializations for adjacent visual field maps LO1 and LO2. The design of this study was heavily influenced by the evidence for functional specialization and parallelism present in human visual cortex. The following sections summarise the evidence for functional specialization and parallelism taken from a number of investigative paradigms.

Human visual cortex has been shown to contain a number of spatially distinct regions that exhibit functional specializations for the encoding of specific visual attributes (Lueck et al., 1989; McKeefry & Zeki, 1997; Zihl et al., 1983; Zeki et al., 1991; Walsh et al., 1998; McKeefry et al., 2008; Amano et al., 2009) and even complex visual categories (Kanwisher et al., 1997; Grill-Spector et al., 1999; Epstein & Kanwisher, 1998; Malach et al., 1995; Kourtzi & Kanwisher, 2001; Grill-Spector et al., 2003; Taylor et al., 2007; Pitcher et al., 2009). Many of these specialized regions were originally identified through early neuropsychological work, and later extended through the use PET, fMRI and neurostimulation techniques, such as TMS.

An additional feature, common too many of the specialized areas mentioned above, is that of parallelism. Different spatial scales of parallelism have been identified within human cortex. First, at the largest spatial scale, parallel processing streams in dorsal and ventral cortex have been identified. These parallel processing streams, are suggested to encode visual features that underpin our ability to determine what a visual stimulus is (Ventral – What?) and where that stimulus may be (Dorsal – where?) (Goodale et al., 1991). Second, at smaller spatial scale, neuropsychological (Zihl et al., 1983; Goodale et al., 1991), neuroimaging (Malach et al., 1995; Kanwisher et al., 1997; Epstein & Kanwisher, 1998; Taylor et al., 2007) and neurostimulation (McKeefry et al., 2008; Pitcher et al., 2009) studies have identified specialized areas that encode specific visual features (colour and motion) as well as different visual categories (faces, places, bodies & objects) independently of the visual features and/or categories encoded by other nearby areas.   Third, at an even smaller spatial scale, visual field map clusters have been proposed as a general organisational principle of visual cortex (Wandell et al., 2005; Brewer & Barton, 2011). These clusters are suggested to form 'clover-leaf' configurations around a central foveal representation and

164

whilst the maps within a cluster are suggested to perform very similar computations these are thought to occur independently of the visual computations performed by adjacent visual clusters.

It was originally suggested that LO1 and LO2 may exhibit different functional properties from one another (explored below) and therefore, LO1 and LO2 offer a perfect opportunity to investigate whether functional specialization is present at the level of adjacent visual field maps in human cortex. Additionally, LO1 and LO2 offer the potential to reveal parallel processing between adjacent maps within a visual cluster (LO cluster) a feature currently unknown (Larsson & Heeger, 2006). Such a finding would show that in addition to the parallel processing present at the spatial scale of adjacent clusters (LO and V5/MT – see Chapters 4 & 5), there may also be parallel processing at the finer spatial scale of neighbouring maps. This would have an interesting implication about the way visual information is represented and processed *within* visual field map clusters.

6.2.2:   Segregation of Function between LO1 & LO2?

LO1 and LO2 have been shown previously to exhibit object-selective responses (Larsson & Heeger, 2006; Sayres & Grill-Spector, 2008; Amano et al., 2009), a feature consistent with data reported in Chapter 3. Despite the object-selectivity exhibited by both LO1 and LO2, a segregation of function between the two maps was proposed (Larsson & Heeger, 2006). First, fMRI adaptation revealed robust and significant orientation-selective responses in LO1, a feature that was not present in LO2 (Larsson et al., 2006). Second, the lack of orientation selective responses in LO2, coupled with its more marked selectivity to objects than LO1 (Larsson & Heeger, 2006; Sayres & Grill-Spector, 2008) led to the idea that LO2 undertakes more complex spatial analyses and perhaps processes shape information (Larsson & Heeger, 2006; Sayres & Grill-Spector, 2008; Amano et al., 2009). In these experiments however, neither the stimuli, nor the fMRI protocols employed were equivalent. The conclusion that LO1, but not LO2 exhibits orientation selectivity was based upon greater orientation selective fMRI adaptation in LO1; whereas, the suggestion that LO2 may process shape information was made on the basis that BOLD response magnitudes in LO2 were greater than those in LO1, following the presentation of greyscale 3D images of common objects. In addition these experiments, which exclusively employed fMRI, are

unable to determine the exact causal role that LO1 and LO2 play in visual processing. In order to address this and probe the possible segregation of function more explicitly, the current study employed TMS to ascertain whether neural activity in LO1 and LO2 causally underpins orientation and shape perception, respectively.

The current set of experiments aimed to investigate the segregation of function between LO1 and LO2 more explicitly, but crucially, aimed to do so by employing similar types of stimuli and tasks. To explore further the nature of processing between LO1 and LO2, there is a need to probe their respective selectivity to both orientation (for replication) and shape. In order to achieve this, and overcome the shortcomings mentioned above, there was a necessity to probe shape processing with stimuli and tasks that were equivalent (or close) to those employed previously in this thesis to probe orientation processing. The data reported in Chapter 4 demonstrated a dissociation between LO1 and LO2 and revealed a specialized role for LO1 in orientation processing. During orientation discrimination, only one visual feature changed (orientation). It was desirable therefore, to probe shape processing with the same level of stimulus control. That is, employ a stimulus set whereby shape processing could be assessed by changing only one visual feature. The stimuli selected to explore shape processing were radial frequency patterns (Wilkinson et al., 1998). Through the deformation of a circle via a sine wave these stimuli allow one to create different shapes. Modifying the contour of a circle with a sine wave creates smooth deviations from circularity, with the frequency of the sine wave defining the number of deformations and the amplitude of the sine wave defining the magnitude of each deformation. Importantly, the shapes of these radial frequency patterns can therefore, be modified via manipulation of the amplitude of the sine wave only. The selection of this stimulus was desirable as it provided equal measures of control across both orientation and shape tasks; altering only one variable modifies stimuli in both tasks.

6.3:   Theoretical Considerations

As in Chapters 4 and 5 an important factor to account for is that neurons in V1, which lies closer to LO1 than LO2, also exhibit orientation selectivity (Hubel & Wiesel, 1963; Hubel, Wiesel, & Stryker, 1978; Furmanski & Engel, 2000). Given the clear evidence for orientation selectivity in V1 it was crucial to ensure that any differential effects of TMS on orientation discrimination observed between LO1 and LO2 were not simply due to LO1s closer proximity to V1. Mindful of this potential proximity effect, coupled with a desire to be consistent with the experimental practices in Chapters 4 and 5, a control site (CON) was defined in each subject that lay medial to LO1 and therefore, closer to V1. The CON was defined by moving medial from LO1 by the distance separating the LO1-LO2 centroids. It is essential to note that the aim of selecting the control site was not to stimulate V1, which would likely disrupt performance in both tasks due to (1) disruption to the orientation selective neurons within V1 and (2) because V1 serves as the major feed-forward station for visual processing. Rather, the control site was selected only on the criteria that it is closer to V1 than LO1 is to V1. This allowed us to test whether the stimulation's proximity to V1 is the critical factor affecting orientation discrimination. If orientation discrimination is only disrupted following stimulation of LO1 and not the more medial control site (CON), then the effects of TMS spreading into V1 cannot explain the result. More generally, if the computations performed within LO1 and LO2 are causally involved in human perception of orientation and shape, only stimulation of these sites and not the CON will affect performance, relative to the no TMS baseline.

6.4:   Aims & Predictions

This study aimed to demonstrate that LO1 and LO2 exhibit functional specializations for orientation and shape processing, respectively. Whether these specializations operate within a strictly serial processing architecture or in parallel are currently unknown, although the data reported in Chapters 4, and to a lesser extent in Chapter 5, would suggest that parallel processing exists between LO1 and V5/MT, the area of cortex directly anterior of LO2. Considering the pattern of deficits induced by TMS of LO1 and LO2 across both tasks can disambiguate whether computations in LO1 and LO2 are performed in serial or parallel. Consideration of both alternatives however, results in very different predictions, depicted in

Figure 6.1. In a strictly serial processing architecture (left column Figure 6.1), one may assume that orientation information is first extracted in LO1 and then passed to LO2 to allow shape processing to occur. In this scenario, one would predict TMS of LO1 to disrupt orientation processing, but not TMS of LO2. For shape processing however, the pattern is different. If the computations in LO2 are reliant on those performed by LO1, TMS of both LO1 and LO2 should lead to disruptions in shape processing. In contrast, if LO1 and LO2 perform visual computations independently (right column Figure 6.1), TMS of LO1, but not LO2, should disrupt orientation processing and similarly, TMS of LO2, but not LO1, should disrupt shape processing – a double dissociation. It is important to note that the top panel of Figure 6.1 is meant to represent the serial and parallel alternatives and is not meant to convey anatomical connections between LO1, LO2 and antecedent visual areas, which are currently unknown.

The two alternatives mentioned above demonstrate the two components of the *map specific* framework outlined in Chapter 1. As mentioned in Chapter 1, in order to make *map specific* conclusions there is a need to consider the effects of TMS of LO1 and LO2 in the context of the effects of TMS CON and the no TMS baseline. If the effects of TMS are specific to LO1 and LO2 alone, then irrespective of whether these computations are performed in serial or parallel, there should be no statistical difference between the effect of TMS at the CON and the no TMS baseline for either task. Comparing the effect of TMS against a no TMS baseline provides a measurement for a general effect of TMS. In order to establish parallelism between LO1 and LO2, there would need to be, for orientation, an effect of TMS of LO1, but no statistical difference between the effects of TMS at the CON, LO2 and no TMS baseline. Likewise for shape, there would need to be an effect of TMS of LO2, but no statistical difference between the effects of TMS at the CON, LO1 and no TMS baseline.
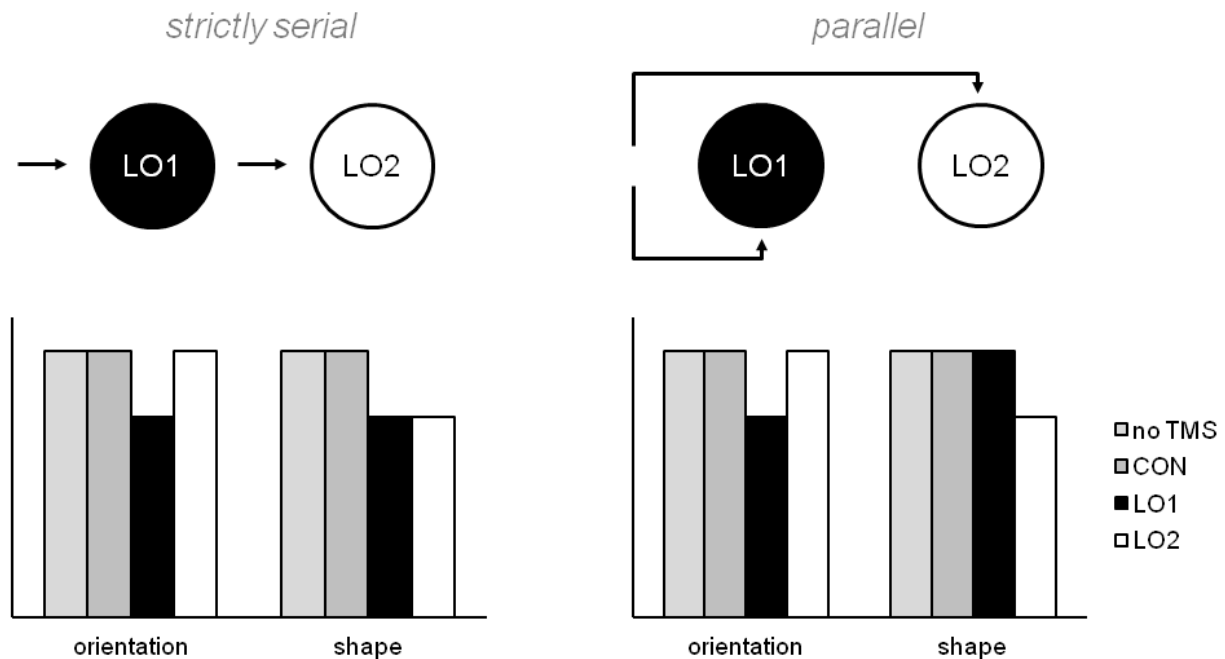
Figure 6.1: *Serial and parallel predictions for the effects of TMS on orientation and shape discrimination. In a serial processing architecture **(left)** TMS of LO1 alone disrupts orientation processing, but if LO2 is reliant on input from LO1, TMS of both LO1 and LO2 disrupts shape processing. In a parallel or independent processing architecture **(right)**, orientation processing is only disrupted following TMS of LO1 and shape processing is only disrupted following TMS of LO2 – a double dissociation. Note, these alternative predictions are restricted to effects of TMS that are 'map specific' and therefore, predict no effect of TMS at the control site (CON). If the effects of TMS are specific to LO1 and LO2, and not due to a general effect of TMS, there should be no effect at the CON for either task, expressed by no difference between CON and No TMS.*

6.5:   Methods

6.5.1:   Subjects

This study included 12 subjects (mean age = 28, range = 24, 5 male). Six of the subjects were tested in Chapter four. However, they are retested here to ensure the TMS data are not recycled. All subjects had normal or corrected to normal vision and gave informed consent in accordance with the Declaration of Helsinki. York Neuroimaging Centre (YNiC) Research Governance Committee approved the study.

6.5.2:   Visual Field Mapping

All subjects completed visual field mapping experiments using fMRI (Engel et al., 1994; Sereno et al., 1995; DeYoe et al., 1996). Data analysis, segmentation and delineation of visual areas were completed in accordance with previous work (Baseler et al., 2011) and the steps described in Chapter 3.

6.5.3:   Identification of Visual Field Maps LO1 & LO2

Definitions of LO1 and LO2 were made in at least one hemisphere in all subjects. Across subjects, LO1 and LO2 contained a complete hemifield map of the contralateral visual field and were located in the expanse of cortex in between V3d and V5/MT.

6.5.4:   Psychophysical Stimuli & Procedures

Stimuli for the behavioural/TMS experiments were generated using MATLAB (Mathworks, USA) and displayed on a Mitsubishi Diamond Pro 2070^{SB} display with a refresh rate of 60 Hz, controlled by a VISAGE graphics card (Cambridge Research Systems ^{TM}). Grating stimuli were luminance modulated sinusoidal gratings (50% contrast) presented in a circular aperture (diameter 4°) and had a spatial frequency of 2 cpd. Shape stimuli were radial frequency patterns (Wilkinson et al., 1998) (50% contrast) with a fixed radial frequency (3) All stimuli had a mean luminance of 31 cd.m^{-2} and were presented on a uniform grey background of the same luminance.

The visual tasks employed were orientation discrimination of sinusoidal gratings and shape discrimination of radial frequency patterns. Prior to TMS stimulation each subject completed orientation and shape discrimination experiments using the method of constant stimuli described in full in Chapter 2. The spatial and temporal organisation of the orientation and shape experiments was identical (see schematic Figure 6.2). The orientation discrimination experiment was identical to that employed in Chapter 4. For shape discrimination, a fixed amplitude was set as the reference shape. Test shapes were selected from seven pre-determined levels that spanned a range of amplitudes either side of the reference - creating a range of stimuli that were either spikier or smoother than the reference. Subjects were required to discriminate whether the test shape was spikier or smoother than the reference. The phases of the reference and test gratings were randomised within trials to prevent the orientation discrimination task being solved via local luminance cues. Similarly the phases (orientation) of the reference and test shapes were randomised within trials to prevent the shape discrimination task being solved via local orientation cues. Subjects completed a total of 350 trials (5 runs comprising 70 trials per run) for each task. Individual psychometric functions for orientation and shape discrimination were plotted from the average of five runs for each subject in order to determine the individual thresholds (75 % correct).

As mentioned in Chapter 4 and 5, in some subjects, the best fitting psychometric function may not pass through 50% correct identification when the reference and test stimuli were identical. This may result in an asymmetrical function, which in turn will lead to asymmetric thresholds relative to the reference. To account for this, the 75% correct thresholds were defined for orientations more vertical and horizontal than the reference and for shapes spikier and smoother than the reference. The range between these values was calculated, divided in half and added to the following equation: TMS stimuli = reference ± range/2. If for example, during shape discrimination the 75% correct spikier shape had an amplitude of 0.25 and the 75% correct smoother shape had an amplitude of 0.19, the range (0.06) would be halved (0.03) and then added to and taken away from the reference (0.2). This results in a spikier (0.23) and a smoother (0.17) shape, both of which are equidistant from the reference.
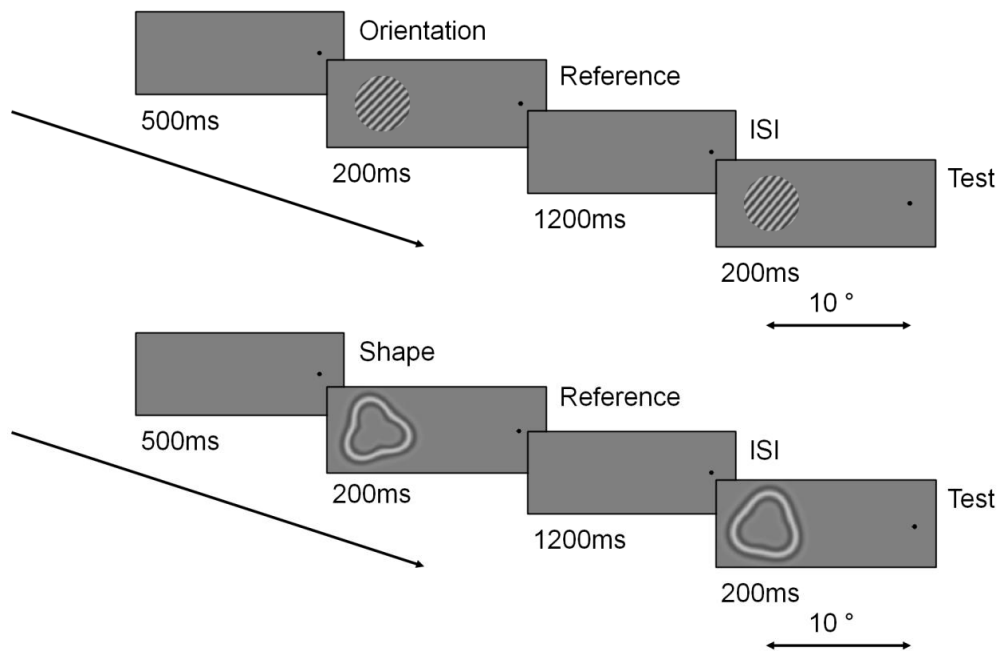
Figure 6.2: *Trial structure schematics for orientation **(Top)** and shape **(Bottom)** psychophysical tasks. During orientation discrimination the reference grating was fixed at 45°. During shape discrimination the reference shape had a fixed amplitude (0.2). Test stimuli for both tasks were randomly selected from a pre-determined list of seven orientations (orientation task) and amplitudes (shape task) that spanned a range of values either side of the reference stimuli*

6.5.5:　TMS Protocol

A train of 4 biphasic (equal relative amplitude) TMS pulses, separated by 50ms (20Hz) at 70% of the maximum stimulator output (2.6 Tesla) were applied to the subject's scalp using a figure-of-eight coil (50 mm external diameter of each ring) connected to a Magstim Rapid2 ™ stimulator (Magstim, Wales). Subjects were seated in a purpose built chair with chin rest and forehead support. The coil was secured mechanically and placed directly above each cortical target (CON, LO1, and LO2) with the handle orientated parallel with the floor. The position of the coil was monitored and tracked in real time allowing the displacement between the intended and actual site of TMS delivery to be recorded, along with two additional measurements; coil-target distance and coil-target orientation. Each subject underwent 8 counterbalanced sessions (2 tasks x [3 TMS sites + 1 no TMS]). During subsequent TMS sessions (and no TMS baseline) only the two stimuli defined using the method above were presented in a trial structure identical to that used to establish

thresholds. Each TMS session comprised 100 trials (50 per threshold stimulus). TMS pulses were delivered concurrently with the presentation of the test stimulus (Figure 6.3).

Figure 6.3: *Trial structure schematics for orientation **(top)** and shape **(bottom)** TMS tasks. During TMS, only the two threshold stimuli were presented as test stimuli. TMS pulses were delivered concurrently with the presentation of the threshold test stimuli represented by the red lightning bolts.*

6.5.6:   Data & Statistical Analysis

Before data analysis some trials (~6%) were removed on the basis of two criteria (1) trials for which coil displacement was >2.5 mm (~2% of trials) and (2) trials for which reaction time was greater than 2000 ms after the cessation of the presentation of the test stimulus (~4 % of trials). Statistical analyses of the results were performed using the SPSS (Version 18) software package (IBM). A series of two-way repeated-measures ANOVAs were employed to examine the effects of discrimination (% correct) and reaction times, along with two potentially confounding variables (coil-target distance and coil-target orientation). Subsequent one-way repeated-measures ANOVAs were calculated for each task considered separately. In the case of a significant main effect, pair-wise comparisons were calculated

and corrected for multiple comparisons (Bonferroni corrected). For each ANOVA, whether or not the ANOVA adhered to the assumption of sphericity was established initially using Mauchly's test. When the assumption of sphericity was violated, two approaches to correcting the degrees of freedom are typically employed to allow appropriate interpretation of the *F* value that resulted from the ANOVA. The Greenhouse-Geisser correction to the degrees of freedom is routinely used when the estimate of sphericity is less than 0.75, but when the estimate of sphericity exceeds this value, the more liberal Huynh-Feldt correction is applied. Departures from sphericity were only observed in the reaction time data. Even though, in these cases, sphericity never exceeded 0.75, both corrections are reported nevertheless, to ensure that any significant results that might indicate speed accuracy trade-offs are not masked by using a conservative correction.

6.6:   Results

6.6.1:   Identification of Visual Field Maps LO1 & LO2

LO1 and LO2 were identified in at least one hemisphere in all 12 subjects (8 right-hemisphere), using standard retinotopic mapping techniques, described in full in Chapter 3. Visual field maps from a representative subject (S10) are illustrated in Figure 6.4. LO1 and LO2 were defined as two adjacent hemifield representations of the contralateral visual field on the lateral surface of the brain extending anteriorly from V3d. In all subjects, LO1 displayed a gradual progression from the shared boundary with V3d at the lower vertical meridian towards the upper vertical meridian. LO2 was the mirror-reverse of LO1 and therefore, displayed a progression from the upper vertical meridian towards the lower vertical meridian. To create unbiased targets for TMS (in terms of visual field representation), the centroids or centre of mass coordinates of LO1 and LO2 were calculated in each subject and used for TMS targeting.
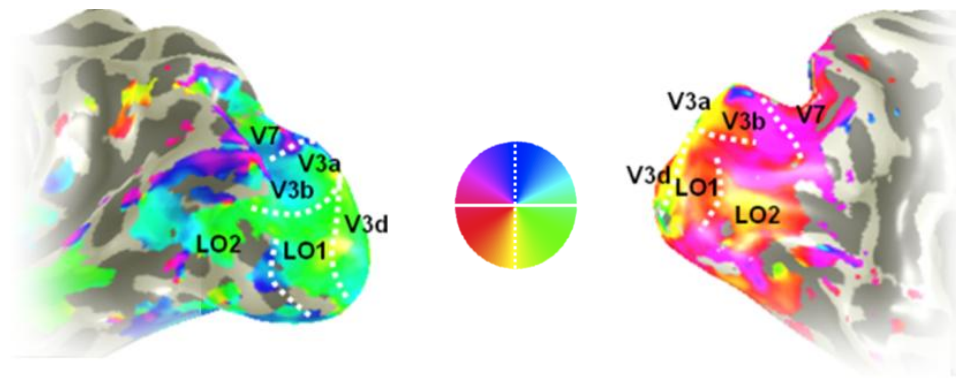
Figure 6.4: *Bilateral visual field maps in a representative subject. Surface reconstructions of the grey–white matter interface of the lateral surfaces of both the left and right hemispheres of S10 subjects are shown; gyri are light grey, sulci dark grey. Superimposed on these inflated surfaces, in false colour, are the response phases of the BOLD signal generated by fMRI retinotopic mapping procedures. The boundaries defining LO1 and LO2 occur at the upper (purple/blue) and lower (yellow/green) vertical meridians, as indicated on the colour wheel inset. White dashed and solid lines indicate the representations of the vertical and horizontal meridians, respectively. The meridians define the boundaries between neighbouring visual field maps.*

6.6.2:   The Control Site

The cortical targets of interest (LO1 and LO2) were on average separated by a relatively small distance (~11mm). Based on the results reported in Chapters 4 and 5 it was assumed that TMS would act sufficiently locally to elicit differential behavioral effects following stimulation of LO1 and LO2. In view of the previously identified dissociation, it was assumed that TMS had the spatial resolution to disrupt the processing in LO1 and LO2 independently. To test this assumption however, a control site (CON) was defined in each subject (Figure 6.5) by (1) calculating the distance between the centroids of LO1 and LO2 and (2) moving that distance toward the midline from the LO1 centroid. The control site was chosen to be closer to V1 than the other TMS targets and could therefore, be used to rule out the possibility that differential effects of TMS may arise from its action spreading into V1, when LO1 or LO2 were stimulated. The inclusion of a control site provides a means by which one can differentiate effects of TMS that are *specific* to LO1 and LO2 from effects that arise due to our targets proximity to V1. The effects of TMS at the CON can be used to assess any general effect of TMS.
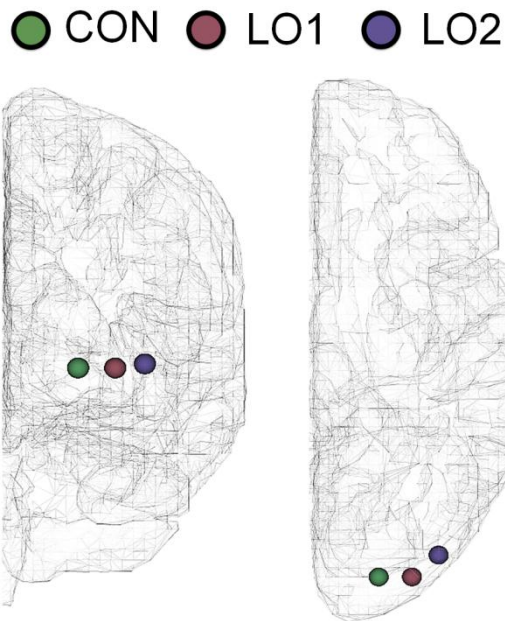
Figure 6.5: *TMS target locations in a representative subject transformed into MNI space. TMS targets (CON, LO1 and LO2) have been transformed into MNI space and overlaid on coronal **(left)** and axial **(right)** wire representations of the right hemisphere of the MNI brain. The centroids for LO1 (red; centre), LO2 (purple; most lateral) and the control site (CON, green; most medial) are shown. The CON site is anatomically closer to V1 than either LO1 or LO2 and therefore provides a*

6.6.3:   Orientation & Shape Psychophysics

Individual psychometric functions for both the orientation and shape discrimination tasks for all subjects (S1-S12) are plotted in Figure 6.6. As in Chapter 4, the axis of S6 has been rescaled relative to the other subjects. There is less individual variation in the shape task than in the orientation task. The range of values needed during shape psychophysics was more consistent across subjects than the range of values needed for during orientation psychophysics.
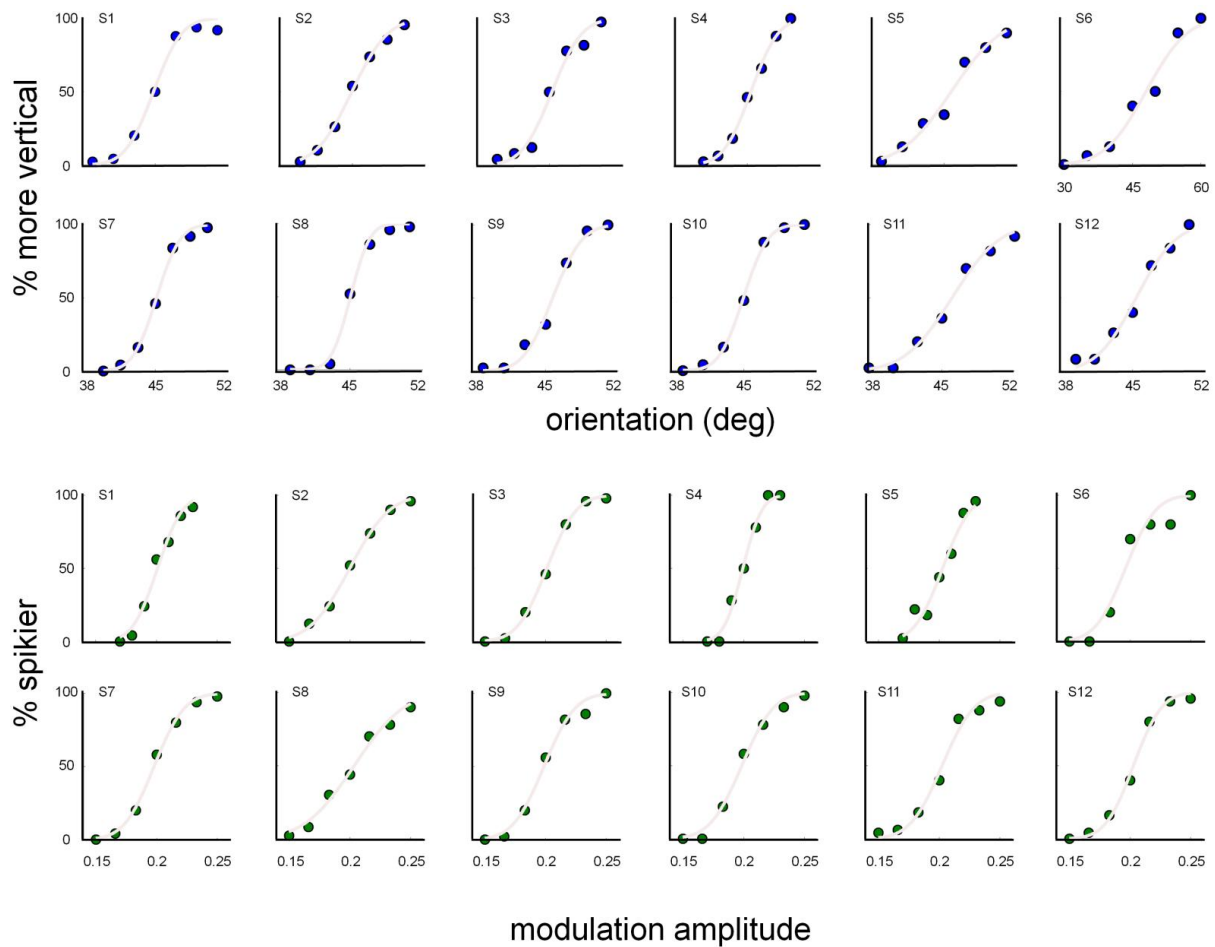
Figure 6.6: *Orientation and shape psychometric functions for subjects S1-S12. Individual subject psychometric functions for orientation **(top)** and shape **(bottom)** discrimination tasks are plotted. For orientation discrimination, the x axis of S6 is expanded relative to other subjects, a larger range of orientations were required for S6. The stimuli to be used in subsequent TMS (and no TMS) sessions were derived from these psychometric functions.*

Two stimuli were defined in each subject to be presented during orientation and shape TMS experiments. These stimuli (two orientations and two shapes) were equally different from the reference. Table 6.1 contains the 75% correct thresholds for orientation more vertical and more horizontal than the reference and for shapes spikier and smoother than the reference, for subjects S1-S12. Table 6.1 also includes the value added to and subtracted from the reference stimulus and finally the actual values presented to subjects during orientation and shape TMS experiments.

Table 6.1: *Threshold and TMS values derived from the orientation and shape psychometric functions for all subjects S1-12. For orientation **(top)**, table includes the 75% correct values for orientations more horizontal **(threshold H)** and more vertical **(threshold V)** than the reference, plus the value added too and taken away from the reference **(ref ±)** and the values used during TMS for the more horizontal **(TMS H)** and more vertical **(TMS V)** test stimuli. For shape **(bottom)** table includes the 75 % correct values for shapes smoother **(threshold SM)** and spikier **(threshold SP)** than the reference, plus the value added too and taken away from the reference **(ref ±)** and the values used during TMS for the smoother **(TMS SM)** and spikier **(TMS SP)** test stimuli.*

orientation (degrees)				
Subject	threshold H	threshold V	ref ±	TMS H	TMS V
S1	43.4400	46.3200	1.4400	43.5600	46.4400
S2	43.1250	46.8000	1.8375	43.1625	48.8375
S3	43.7250	46.7750	1.5250	43.4750	46.5250
S4	44.2800	46.2600	0.9900	44.0100	45.9900
S5	43.1400	48.2700	2.5650	42.4350	47.5650
S6	43.2000	52.8000	4.8000	40.2000	49.8000
S7	43.1550	49.4100	3.1275	41.8725	48.1275
S8	43.9000	46.3250	1.2125	43.7875	46.2125
S9	43.5600	46.6650	1.5525	43.4475	46.5525
S10	44.1900	47.1900	1.5000	43.5000	46.5000
S11	43.3875	46.5750	1.5938	43.4062	46.5938
S12	42.8650	48.0450	2.5900	42.4100	47.5900
shape (modulation amplitude)				
Subject	threshold SM	threshold SP	ref ±	TMS SM	TMS SP
S1	0.1900	0.2119	0.0110	0.1890	0.2110
S2	0.1825	0.2172	0.0175	0.1862	0.2174
S3	0.1880	0.2140	0.0130	0.1870	0.2130
S4	0.1910	0.2077	0.0083	0.1917	0.2083
S5	0.1905	0.2152	0.0123	0.1877	0.2123
S6	0.1830	0.2095	0.0133	0.1868	0.2132
S7	0.1847	0.2112	0.0133	0.1868	0.2132
S8	0.1817	0.2253	0.0218	0.1783	0.2218
S9	0.1850	0.2122	0.0136	0.1804	0.2136
S10	0.1845	0.2125	0.0140	0.1860	0.2140
S11	0.1885	0.2165	0.0140	0.1860	0.2140
S12	0.1905	0.2152	0.0124	0.1876	0.2124

6.6.4:   Effects of TMS on Orientation & Shape Discrimination

Group averaged performances (% correct) for all conditions and tasks are plotted in Figure 6.7. Inspection of Figure 6.7, reveals a number of important patterns of results. The pattern of deficits closely follows that predicated by *map specific* and *parallel* processing in LO1 and LO2 (right schematic inset in Figure 6.7). First, orientation discrimination is only disrupted following TMS of LO1 – directly replicating the effect reported in Chapter 4. Second, orientation discrimination performances are largely equivalent across all other conditions, and indicate no general effect of TMS. Interestingly, and unlike the data reported in Chapter 4, there is no inflation of performance during the no TMS baseline. For shape discrimination, performance is only altered following TMS of LO2. Again the performances are very similar across all other conditions and also support the lack of a general effect of TMS. The pattern of deficits induced by TMS follows closely that predicted by specialized and parallel processing of orientation and shape in LO1 and LO2.
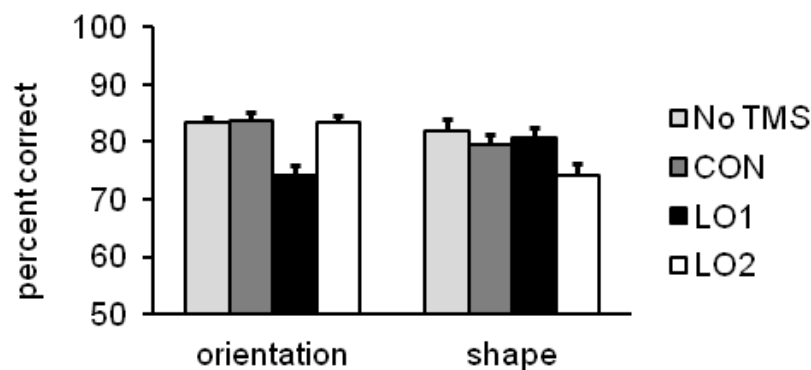
Figure 6.7: *Effects of TMS on orientation and shape discrimination. Mean discrimination performance (% correct) across all subjects for all conditions plotted by task. Inset into the figure are the schematics for serial **(left)** and parallel **(right)** processing. The pattern of deficits induced by TMS follows the predictions of map specific and parallel processing between LO1 and LO2. Orientation discrimination was disrupted following TMS of LO1 alone. Shape discrimination was only disrupted following TMS of LO2 – a double dissociation. Across both tasks, there was no effect of TMS at the CON (no difference between CON and No TMS), indicating that TMS effects were specific to LO1 and LO2, respectively. Error bars represent s.e.m.*

It was hypothesised that computations performed by LO1 and LO2 would play specialized and causal roles in orientation and shape discrimination, respectively. An interaction between Task (orientation *versus* shape) Site (LO1 *versus* LO2) and should therefore, be evident. In order to asses this a 2 x 4 repeated measures ANOVA with conditions Task (orientation, shape) and Site (No TMS, CON, LO1, LO2) was conducted. The analysis confirmed a highly significant Task by Site interaction ($F_{(3, 33)} = 15.154$, $p = 2.556$ x 10^{-6}). The effect of task was not significant ($F_{(1, 11)} = 1.391$, $p = 0.268$) suggesting that across subjects and conditions both tasks were equally difficult. The effect of site was significant ($F_{(3, 33)} = 5.572$, $p = 0.003$), presumably reflecting the overall drop in discrimination performance following TMS of LO1 and LO2, during the orientation and shape tasks, respectively. No pair-wise site comparisons were significant ($p = > 0.077$, Bonferroni corrected).

While it was essential to identify an initial Task by Site interaction, additional analyses are required to determine whether task dependant effects of TMS are specific to LO1 and LO2. For orientation discrimination, a one-way repeated measures ANOVA revealed a significant effect of site ($F_{(3, 33)} = 12.514$, $p = 1.260$ x 10^{-5}). Pair-wise comparisons (Bonferroni corrected) revealed that this was solely due to a decrease in performance when stimulating LO1 compared to all other conditions (LO1 *versus* No TMS, $p = 0.010$; LO1 *versus* CON, $p = 0.010$; LO1 *versus* LO2, $p = 0.008$). Importantly, no other pair-wise comparisons were significant ($p = 1.000$ in all cases). For shape discrimination, a one-way repeated measures ANOVA revealed a significant effect of site ($F_{(3, 33)} = 6.302$, $p = 0.002$). This effect was caused entirely by a decrease in performance when LO2 was stimulated compared to all other conditions (LO2 *versus* No TMS, $p = 0.023$; LO2 *versus* CON, $p = 0.019$; LO2 *versus* LO1, $p = 0.018$; Bonferroni corrected). Comparisons between all remaining conditions were not significant ($p = 1.000$, in all cases).

The nature of deficits induced by TMS closely follows the pattern predicted for *map specific* and *parallel* processing between LO1 and LO2. The result demonstrates that computations of orientation and shape are specific to LO1 and LO2, respectively. For either task, the effect of TMS of the control site was not significantly different to the no TMS baseline, arguing strongly against a general effect of TMS. The effects of TMS delivery to LO1 and LO2 exhibit both task and site specificity. The results also indicate a double

dissociation between these *map specific* computations, suggesting that orientation and shape are processed independently in LO1 and LO2, respectively. The pattern of deficits runs contrary to the prediction based upon a strictly serial processing architecture in this region of cortex.

6.6.5:   *Effect of TMS on Reaction Times*

Although discrimination performance was the primary measure used to asses the effects of TMS, reaction times were also recorded as a secondary measure. Reaction times are often the measure of choice in TMS experiments (Whitney, Kirk, O'Sullivan, Lambon Ralph, & Jefferies, 2011; 2012) and can provide valuable interpretive information. Group averaged reaction times for all conditions and tasks are plotted in Figure 6.8. Inspection of Figure 6.8, reveals a pattern of results that argues strongly against the presence of speed-accuracy trade-offs as an explanation for the disturbances to performance reported above. Indeed, within each task the slowest reaction times during TMS simulation occurred when poorest discrimination was recorded (LO1 for orientation discrimination and LO2 for shape discrimination). This is the opposite of a speed accuracy trade off.
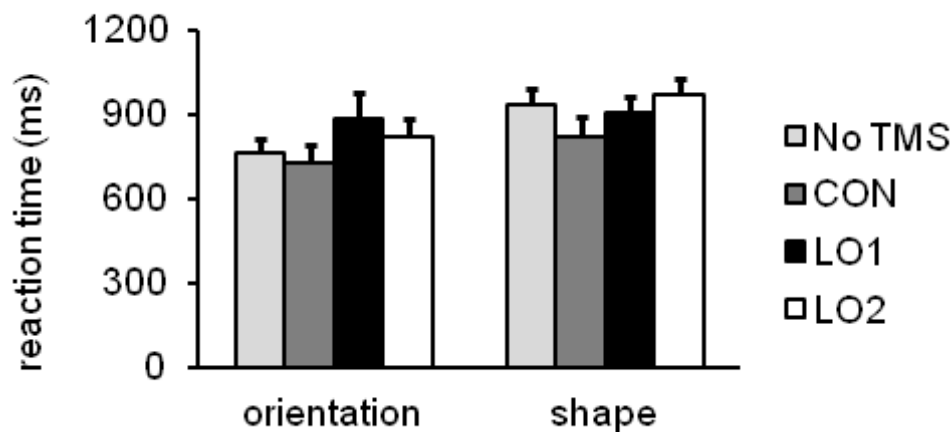
Figure 6.8: *Effects of TMS on reaction times during orientation and shape discrimination. The effects of TMS on reaction times are consistent with the main effect of TMS on discrimination. There is no evidence of a speed-accuracy trade off. Indeed, reaction times are slowest for those conditions in which performance is poorest (LO1-orietnation, LO2-shape). Error bars represent s.e.m.*

In order to assess formally the effect of TMS on reaction times a 2 x 4 repeated measures ANOVA with conditions Task (orientation and shape) and Site (no TMS, CON, LO1 and LO2) was conducted. The data for reaction times were the only measurements for which the assumption of sphericity was violated. As mentioned above, two approaches were adopted to correct the degrees of freedom when this violation occurred, in order to ensure that the more conservative Greenhouse-Geisser approach did not mask any significant effects. Mauchly's test of sphericity was not significant for either the main effect of Task or the interaction between Task and Site. Neither the main effect of Task, nor the interaction were significant; Task ($F_{(1, 11)}$ = 1.156, *p* = 0.305) and Task by Site interaction ($F_{(3, 33)}$ = 2.310, *p* = 0.094). Mauchly's test of sphericity was significant for the main effect of Site (Mauchly's $W_{(5)}$ = 0.250, *p* = 0.020, estimate of non-sphericity = 0.55). The effect of Site was not significant ($F_{(1.657, 18.232)}$ = 3.363, Greenhouse-Geisser corrected, *p* = 0.065: $F_{(1.915, 21.063)}$ = 3.363, *p* = 0.056, Huynh-Feldt corrected). However, given the trend in these data and a wish to be consistent with the approach used to analyse the discrimination data, one way ANOVAs were also applied to investigate the effect of Site for each task considered separately. For orientation discrimination, Mauchly's test of sphericity was significant for the main effect of Site (Mauchly's $W_{(5)}$ = 0.247, *p* = 0.019, estimate of non-sphericity = 0.664). There was no significant effect of Site ($F_{(1.991, 21.896)}$ = 2.574, Greenhouse-Geisser

corrected, p = 0.099: F $_{(2.429, 26.722)}$ = 2.574, p = 0.085, Huynh-Feldt corrected) and therefore, subsequent analyses were not conducted. For shape, Mauchly's test of sphericity was significant for the main effect of Site (Mauchly's W = 0.044, $_{(5)}$, p = 1.48x10^{-5}, estimate of non-sphericity = 0.403). There was no significant effect of Site (F $_{(1.209, 13.294)}$ = 3.975, Greenhouse-Geisser corrected, p = 0.061: F $_{(1.277, 14.045)}$ = 3.975, p = 0.058, Huynh-Feldt corrected). Despite the non-significant effect of site, the data nevertheless display a trend approaching significance. To explore further the nature of this effect, pair-wise comparisons (Bonferonni corrected) were undertaken. There were no significant pair-wise comparisons (No TMS *versus* CON, p = 0.462; No TMS *versus* LO1, p = 1.000; No TMS *versus* LO2, p = 0.880; CON *versus* LO1, p = 0.724; CON *versus* LO2, p = 0.261; LO1 *versus* LO2, p = 0.199).

It is clear that the parallel nature of processing observed in LO1 and LO2 cannot be due to speed-accuracy trade-offs. Analysis of the reaction time data indicate that the significant deficits in orientation and shape processing following TMS of LO1 and LO2, respectively, were not associated with significant decreases in reaction time – in fact they increased although not significantly. These tests demonstrate that the effect of TMS on reaction times cannot explain the main effect of TMS on orientation or shape discrimination.

6.6.6:   Potentially Confounding Variables

The current study made use of two measurements of the spatial relationship between the stimulating coil and the cortical targets. Although, the primary measure of the effects of TMS was discrimination performance (% correct) this measure could however, be affected by two potentially confounding variables, which relate to precision with which TMS was delivered; coil-target distance and coil-target orientation. These measurements are important as they inform as to whether operator error can explain the discrimination data. Of note, although the double dissociation provides compelling testimony to the conclusion that LO1 and LO2 are (1) specialized for orientation and shape, respectively and (2) perform these specialized roles in parallel, an alternative explanation may be that the observed effects of TMS were due to a single dissociation (as reported in Chapter 4) plus one (or more) confounding variables caused by the operator. Although unlikely, the effect of these potentially confounding variables nevertheless warrants consideration.

6.6.6.1:   Coil-Target Distance

The distance from the calibration point of the coil to the cortical target was recorded with each pulse train. This measurement allows one to determine whether the distance from the coil to the TMS targets varied across Task and Site in a way that might explain the discrimination results. Group averaged coil-target distances for all TMS sites and tasks are plotted in Figure 6.9. Inspection of Figure 6.9, illustrates that the coil-target distances were largely equivalent across both sites and tasks. These measurements are important as the location of the target within cortex cannot change as a function of task, and therefore the distance from the target to the stimulating coil should be equal across tasks. Differences in the coil-target distance must therefore, be caused by operator error, occurring through incorrect registration/coil-calibration procedures.
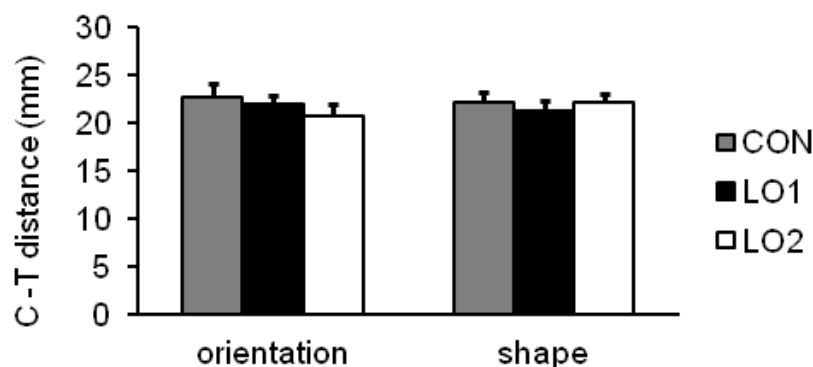
Figure 6.9: *Mean Euclidean distance between stimulating coil and cortical targets during orientation and shape discrimination. Group averaged coil-target distances (mm) across all TMS conditions grouped by task. The data indicate that the distance between the stimulating coil and cortical targets did not vary across tasks in a way that could explain the differential effects observed between LO1 and LO2 during orientation and shape discrimination, respectively. Error bars represent s.e.m.*

The effect of coil-target distance was analysed using a 2 x 3 repeated measures ANOVA with conditions Task (orientation and shape) and Site (CON, LO1, and LO2). There was neither a significant effect of Site ($F_{(2, 22)}$ = 0.538, *p* = 0.591), nor Task ($F_{(1, 11)}$ = 0.732, *p* = 0.411) nor Task by Site interaction ($F_{(2, 22)}$ = 0.762, *p* = 0.479). As with all variables, we also applied one-way ANOVA tests to examine the effect of site for each task separately. For

orientation, there was no significant effect of Site ($F_{(2, 22)}$ = 1.065, p = 0.362), for shape, there was no significant effect of Site ($F_{(2, 22)}$ = 0.332, p = 0.938), therefore further tests were not conducted. The results indicate that the effect of TMS on discrimination of orientation or shape cannot be explained by differences in the distance from the stimulating coil to the targets across tasks. Significant differences for one site across tasks would indicate errors in the calibration and/or registration procedures along with errors in coil-localisation. The inclusion of these data demonstrates that each TMS site was stimulated with equal precision across tasks.

6.6.6.2:   Coil-Target Orientation

Coil-target orientation provides a measure of the difference between the coil orientation and the vector joining the 'hotspot' of the coil and the TMS target (accurate targeting corresponds to 90° on this measure). Group averaged coil-target orientations for all TMS sites and tasks are plotted in Figure 6.10. Inspection of Figure 6.10, reveals that the angles of the stimulating coil are (1) very similar across all sites and tasks and (2) cluster around 90° for all sites, which is the optimum angle for stimulation.
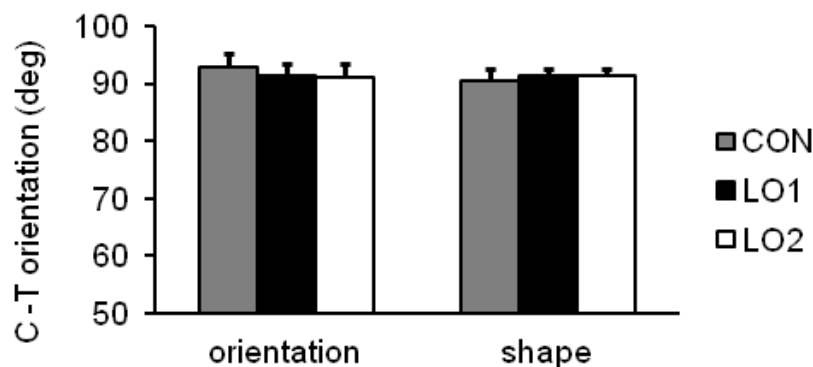
Figure 6.10: *Mean coil-target orientation during orientation and shape discrimination. Mean coil-target orientation (degrees) across all TMS conditions grouped by task. The data indicate that the orientation of the stimulating coil and cortical targets did not vary across tasks in a way that could explain the differential effects observed between LO1 and LO2 during orientation and shape discrimination, respectively. Error bars represent s.e.m.*

In order to determine whether variations in the orientation of the coil relative to the target might explain the discrimination results, the effect of coil orientation was assessed using a 2 x 3 repeated measures ANOVA with conditions Task (orientation and shape) and Site (CON, LO1, and LO2).   There was neither a significant effect of site ($F_{(2, 22)}$ = 0.236, *p* = 0.791), nor task ($F_{(1, 11)}$ = 0.305, *p* = 0.592) nor site by interaction ($F_{(2, 22)}$ = 0.150, *p* = 0.861). As with all variables, one-way ANOVA tests were also applied to examine the effect of site for each task separately. For orientation, there was no significant effect of site ($F_{(2, 22)}$ = 0.359, *p* = 0.702). For shape, there was no significant effect of site ($F_{(2, 22)}$ = 0.088, *p* = 0.916). Given the non-significant effects of site, further tests were not conducted. There is no evidence therefore, that the angular displacement of the coil varied in a way that could explain the selective disturbances to orientation and shape discrimination reported above. Again the data indicate that cortical targets were stimulated with equal precision.

6.6.7:   Individual Differences in Distance between LO1 & LO2

In the current study small distances relative to the estimated spread of TMS, separated our cortical targets of interest (LO1 and LO2). The actual separations of LO1 and LO2, along with their Talairach coordinates for each individual are given in Table 6.2. In all but one individual (S5), the separations of the TMS targets are greater than the mean separations of targets stimulated in another study (Pitcher et al., 2009) (7.8mm) in which clear dissociations in task performance were observed. However, that study used a 70mm coil, which is larger than the 50mm coil we employed to yield more focal stimulation. It is also worth mentioning that the distances reported in Pitcher et al., are those calculated from the transformation of TMS targets into MNI space, whereas those reported in Table 6.2 are the distances within each individual's native space. The transformation to MNI space may have reduced or indeed increased the actual distances between the peaks of activation. Nevertheless, the data indicate that the separations of each subjects TMS targets were sufficiently large to minimise the effects of TMS spread from one target into another.

Table. 6.2: *LO1 and LO2 centroids. Talairach coordinates of the centroids along with the actual distance between LO1-LO2 centroids are given for subjects S1-S12.*

| Subject | Hemisphere | Talairach coordinates | | | | | | LO1-LO2 distance (mm) |
| | | LO1 | | | LO2 | | | |
	Right/Left	x	y	z	x	y	z	
S1	Right	40	-82	3	48	-74	8	10.7700
S2	Right	36	-88	4	43	-81	5	9.0200
S3	Right	30	-86	4	40	-84	0	10.2900
S4	Right	24	-91	8	38	-88	4	13.7400
S5	Right	30	-84	8	36	-83	9	6.0600
S6	Right	33	-85	13	37	-72	11	11.8700
S7	Left	-26	-89	13	-37	-81	11	14.8930
S8	Right	29	-89	18	35	-86	15	11.2230
S9	Left	-29	-96	4	-35	-87	4	10.4800
S10	Left	-38	-87	4	-46	-76	3	10.8612
S11	Left	-22	-95	7	-31	-87	9	12.6800
S12	Right	28	-88	17	40	-83	19	14.7330
							Mean	SD
							11.38	2.481

6.6.8: *Cortical Orientation*

While LO1 and LO2 are adjacent visual field maps, it is possible that in an individual, the cortex comprising one visual field map may be systematically orientated differently from the other. Indeed, in their original report, Larsson and Heeger identified a high level of variability in the actual location and orientation of LO1 and LO2 relative to common gyral and sulcal patterns (Larsson & Heeger, 2006). The individual variation in anatomical location reported in Chapter 3 partially supports these findings. The difference in cortical orientation could in turn make TMS more effective when applied to one visual field map compared to the other. Importantly however, an effect specific to cortical orientation could only explain a main effect of site rather than a Task by Site interaction. Indeed, the cortical orientation of LO1 and LO2 within an individual cannot change across tasks, and therefore, cannot be used as an explanation for the double dissociation reported.

6.6.9:   TMS of the Control Site

The question of the control site and what role (if any) it plays in orientation and shape processing requires careful consideration. It is important to note that the location of the control site was defined not on the basis of retinotopic features (like LO1 and LO2), but rather on the basis of a geometric distance from LO1. That being said, analysis of the location of the control site relative to visual field maps revealed that the control site fell within the retinotopic boundaries defining V3d in all subjects. That is, the control site fell within the representations of the horizontal meridian at the V2d boundary and the lower vertical meridian boundary with LO1. In a strictly serial processing architecture, one may assume that for information to be processed in LO1, antecedent areas, such as V3d, must first process that information. This assumption however, is not based on known anatomical connections with and between LO1 and LO2 in the human brain. Indeed, in macaque anatomical connections at this level of the hierarchy suggest the existence of parallel, as well as serial processing pathways (Shipp & Zeki, 1985; Zeki & Shipp, 1988; Zeki, 1990). Nevertheless the close proximity of the TMS targets warranted the analysis of the potential effects of TMS at the control site.

The control site was specified primarily to account for a potential proximity effect of V1 arising when stimulating LO1 *versus* LO2 therefore, no '*a priori*' hypothesis was generated about the effect of TMS of the control site. Indeed, if a hypothesis were to be given it would have been heavily biased towards a strictly serial architecture. Whilst this study was under review, the question as to why TMS of the control site (V3d) did not lead to any measurable behavioural effects was raised. This question arose from the assumption that LO1 and therefore LO2, receives the majority of its input from V3d. An assumption heavily grounded in the framework of serial connectivity (Zeki, 1990; Zeki et al., 1991). We interpreted the lack of effect at the control site as confirmation of LO1 and LO2's specialized and parallel roles in orientation and shape processing. The lack of effect at the control site however, could have been interpreted as a finding regarding the functional properties of V3d itself. That is, the lack of effect when stimulating V3d could be interpreted as demonstrating that V3d does not exhibit specializations for either orientation or shape. This interpretation however is invalid. To comment upon the functional properties of V3d, one

would need to have targeted it on the basis of its retinotopic features and not on the basis of a distance from LO1. Indeed, based upon its retinotopic organisation, V3d would have been an unwise choice for a third cortical target of interest given that the visual field representation within V3d only extends to the contralateral lower quadrant, as reported previously (Larsson & Heeger, 2006; Wandell et al., 2007), and demonstrated in Chapter 3.

In order to assess formally the lack of effect at the control site it was necessary to demonstrate initially the visual field representations in LO1 and LO2 along with those in antecedent visual field maps V3d, V2d and V1. The retinotopic features of visual field maps V1, V2d, V3d, LO1 and LO2 were analysed to compare them with previous literature (Larsson & Heeger, 2006; Wandell et al., 2007; Amano et al., 2009; Wandell & Winawer, 2011) and to evaluate them with respect to the position and size of the visual stimuli presented in this study. To this end, 'visual field coverage' plots were computed for each cortical visual field maps, by assessing the phase (*delay*) of the BOLD responses of all subjects to the ring and wedge stimuli presented during fMRI experiments. Specifically, the average proportions of voxels in each visual field map that represented different 'patches' in the visual field were calculated. The patches were defined by dividing the visual field into 16 sectors of equal polar angle and then subsequently, dividing those sectors into eccentricity bands. In all plots, the crucial eccentricity band between 8 and 12 degrees, where the stimuli were presented was defined first. The other eccentricity bands were then defined to capture the proportion of voxels equal to that found in the stimulus eccentricity band. This helped account for cortical magnification of eccentricity, which varies across different visual field maps (Larsson & Heeger, 2006; Wandell et al., 2007). Taken together, these patches form a dartboard-like pattern. A grey-scale is used to show the proportion of a visual field map that represents a patch of visual field (Figure 6.11). For some participants (n = 4) the cortical visual field maps were identified in the left, rather than the right hemisphere. These data have been flipped to present a group average with respect to the right hemisphere (left visual field).
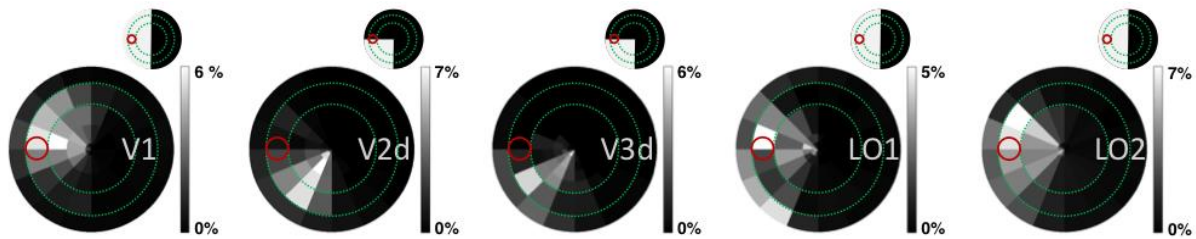
Figure 6.11: *The visual field representation found in early visual field maps V1, V2d and V3d, and visual field maps LO1 and LO2. In all diagrams, the circle in red on the horizontal meridian shows the stimulus location centred at 10° eccentricity and the green broken line defines the stimulus eccentricity band (8-12°). Scale bars measure the percentage of voxels in each patch. An average of the data is given for 12 subjects. No statistical threshold was applied to the data. Inset in each plot is a schematic of the visual field representations found in previous studies.*

In Figure 6.11, the visual field coverage within V1, V2d, V3d, LO1 and LO2 is plotted. Inset in each figure is a schematic representation of the visual field coverage from previous literature (Larsson & Heeger, 2006; Wandell et al., 2007; Amano et al., 2009; Wandell & Winawer, 2011). The plots of visual field coverage are entirely consistent with previous literature and show that along with V1, LO1 and LO2 have complete representations of the contralateral hemifield (Larsson & Heeger, 2006; Wandell et al., 2007; Amano et al., 2009; Wandell & Winawer, 2011), denoted by the largely symmetrical pattern of representation about the left horizontal meridian. In contrast, the coverage within cortical maps V2d and V3d is asymmetrical about the horizontal meridian and is largely restricted to the lower left quadrant. The representations within V2d and V3d are consistent with previous studies and demonstrate the lower quadrant representations within these dorsal visual field maps (Larsson & Heeger, 2006; Wandell et al., 2007; Amano et al., 2009; Wandell & Winawer, 2011). The corresponding upper quadrant representations are represeted within V2v and V3v on the ventral surface of the brain. The data demonstrate therefore, that the nearest full and contiguous representation of the visual stimulus in visual field maps antecedent to LO1 and LO2 lies within V1.

6.6.10:   The TMS Control Site in the Context of the Retinotopic Features of Visual Field Maps

The CON was located within V3d in all subjects and although this visual field map represents the contralateral lower quadrant only, there is still a chance that the action of TMS of the CON could be biased towards the representation of the horizontal meridian in V3d.   If this were the case, neural processing of part of the stimulus in V3d could be disrupted by TMS of the control site.   Whether the local action of TMS affected the stimulus representation in V3d, LO1 and LO2 was assessed by calculating visual field coverage plots for 10mm spheres centered on the three target sites, CON, LO1 and LO2 (Figure 6.12). Spheres of 10mm – marginally less than the mean separation of neighbouring TMS targets – were selected because they were very similar to the distances over which differential effects are being tested for.   Previous literature also indicates that differential effects can be observed between sites separated by this or even shorter distances (Cowey, 2005; Ellison & Cowey, 2009; Pitcher et al., 2009). It is also important to note that the distances from the coil to all three TMS targets were equivalent (see Figure 6.10) and therefore, modeling the effect of TMS over spheres of equal size is justified. The visual field coverage plots depicted in Figure 6.13 show that representations of the stimuli were only captured when LO1 and LO2 were targeted.   This indicates that if TMS acts locally one would not expect there to be an effect of stimulation of the control site on visual discriminations. The absence of any effect at the control site demonstrates that TMS acted sufficiently locally to examine the hypotheses regarding LO1 and LO2.   Moreover, the deficits induced by TMS of LO1 and LO2 cannot be attributed to non-focal spread of TMS into the representation of the stimulus in V1, or other antecedent visual field maps, V2 and V3
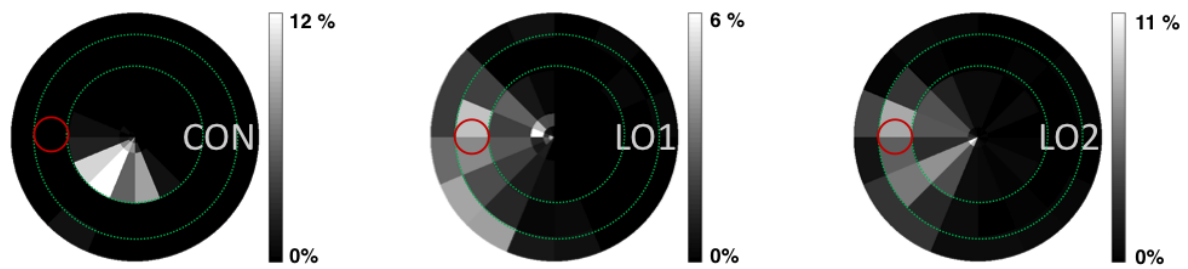
Figure 6.12: *Visual field coverage plots for 10mm spheres centred on the TMS target locations, CON, LO1 and LO2. The eccentricity bands are the same as those used in plots for V3d, LO1 and LO2 in the top row. It is noteworthy that a 10mm sphere centred on the control site captures visual field representations at more central eccentricities – a feature that results from using a geometric criterion to select this site, rather than the retinotopic criterion used to select LO1 and LO2.*

6.7:   Discussion

In this chapter TMS pulses were applied to adjacent visual field maps LO1 and LO2 in order to assess its effects on orientation and shape discrimination, respectively. A double dissociation was evident. TMS of LO1 led to a significant and selective disturbance during orientation discrimination, relative to all other conditions, whereas TMS of LO2 induced a significant and selective disturbance to normal shape processing, relative to all other conditions. These effects were found to be robust to the presence of speed-accuracy tradeoffs and differences in the spatial relationships between the stimulating coil and the cortical targets, caused by operator error.

6.7.1:   Functional Specialization in LO1 & LO2

It has been suggested that within cortex each discrete visual field map may perform unique sets of computations and therefore, contribute uniquely to visual perception (Zeki, 1990). The current results demonstrate that is indeed the case for adjacent visual field maps LO1 and LO2 (Larsson & Heeger, 2006). The striking feature of these specializations is that LO1 and LO2 are thought to be subdivisions of a larger object-selective region, LO. These results reveal a number of important features of extrastriate cortical function. Firstly, the results demonstrate that LO1 and LO2 play specialized roles in the processing of orientation and shape, two different relatively low-level visual features. The specific effect of TMS on orientation discrimination following TMS of LO1 not only extends recent neuroimaging

findings (Larsson & Heeger, 2006), but also, replicates directly the effect reported previously in Chapter 4 and finally, confirms LO1 as an area of extrastriate cortex that is causally involved in the perception of orientation.

The lack of an effect of TMS at the control site during orientation discrimination rules out LO1's proximity to V1 as a likely cause of this effect. Unlike the fMRI data reported previously (Larsson et al., 2006), the most parsimonious explanation for the pattern of deficits induced by TMS of LO1 is that computations within LO1 itself causally underpin orientation discrimination, not that LO1 selectively inherits its orientation selectivity from V1 (Larsson et al., 2006). These results, taken together with previous work (Larsson et al., 2006) indicate that LO1 is an area of the human brain that integrates visual information to extract orientation of boundaries, even when those boundaries are solely defined by luminance (first-order) changes. The effect observed at LO1 also suggests that while V1 contains neurons selectively tuned to the orientation (Hubel & Wiesel, 1963; Hubel et al., 1978) of gratings, such tuning alone may be necessary, but not sufficient for normal orientation processing. This interpretation is consistent with neuropsychological studies indicating deficient processing of orientation following damage to LO, despite intact V1 (Milner et al., 1991). In addition to a profound inability to recognise familiar objects, patient DF also exhibited an inability to correctly identify the orientation of slots. DF's damage appears to be relatively localised to the LO region (James, Culham, Humphrey, Milner, & Goodale, 2003) and likely encompasses LO1 and LO2. Indeed, a very recent study measured retinotopic maps in patient DF using standard retinotopic mapping procedures (Bridge, Thomas, Minini, Cavina-Pratesi, Milner & Parker, 2013). On flat representations of the occipital cortex of DF, the authors delineate early visual cortical regions (V1-V4). Importantly, they also outline the extent of DF's lesion on the flattened cortex. A large area of damaged cortex was identified anterior and lateral of V3d; a location commensurate with our definitions of LO1 and LO2. It is highly likely therefore, that DF's LO lesion encompasses the region of cortex, where if intact, LO1 and LO2 would likely be located (Bridge et al., 2013).

The pattern of deficits induced by TMS during shape discrimination reveals, for the first time, a causal link between computations within LO2 and the processing of shapes, defined by differences in curvature. It remains to be seen whether the perception of shape based on

visual features other than curvature are also causally dependent on computations within LO2. The current results nevertheless demonstrate that there is a hierarchy of increasingly sophisticated spatial computations performed within the retinotopic subdivisions of LO, a feature consistent with the suggestions put forward by others (Larsson & Heeger, 2006). Crucially however, these results indicate that the more sophisticated processing of shape in LO2 occurs in parallel with the more basic processing of orientation within LO1, a feature not previously suggested. Future work should seek to further classify the visual features that are selectively processed by LO2. Indeed, LO2's selectivity to shape stimuli likely extends beyond the simple modulations in curvature reported here. One likely candidate is concentric processing (circular shape). Dumoulin & Hess (2007) investigated the processing of circular shape in human visual cortex using fMRI. Subjects were presented with arrays of gabors that either formed circles or random flowfields. Highly significant activity related to the processing of circles over flowfields was present in ventral and dorsal cortex. Although the authors focused the majority of their discussion on the highly significant activity within the vicinity of area V4, an additional cluster of significant activity was present posterior of V5/MT, the area of cortex commensurate with the anatomical location of LO2. Recall that in ~50% of subjects tested, LO2 abutted V5/MT directly (Larsson and Heeger, 2006). It is likely therefore, that LO2 processes the shape of stimuli via a number of stimulus features.

6.7.2:   *Parallel Processing Between LO1 & LO2*

The double dissociation of orientation and shape processing demonstrates that LO1 and LO2 perform these specialized roles independently of one another. One interpretation of the data is that the lack of an effect of shape following TMS of LO1 indicates that computations performed by LO2 are not reliant on orientation computations performed within LO1, as would be predicted by a strictly serial processing architecture. An alternative is that despite a reduction in input to LO2, following TMS of LO1, LO2 can nonetheless perform its computations sufficiently well to not alter performance relative to baseline. In line with the initial interpretation, the existence of separable functional processing pathways mirrors those, which have been a persistent feature of many models of the primate visual system (Felleman & Mcclendon, 1991; VanEssen, Felleman, Deyoe, & Knierim, 1991). For example, lesion studies in non-human primates and later human

neuropsychological evidence highlighted the processing of different types of visual information within dorsal (Perenin & Vighetto, 1988) and ventral (Goodale et al., 1991) streams. The characterisation of visual cortex into dorsal *'where'* and ventral *'what'* streams (Mishkin et al., 1983) has had a large impact on models of human visual processing. Within these separate streams, but at a smaller spatial scale, a number of neuroimaging studies (Malach et al., 1995; Kanwisher et al., 1997; Epstein & Kanwisher, 1998; Kourtzi & Kanwisher, 2001) have identified discrete regions of visual cortex that exhibit selective responses to different visual stimuli whilst being in close proximity to one another. The independent nature of within these areas was later confirmed through neurostimulation studies demonstrating that these functionally selective regions of cortex process different types of visual information independently of one another (Pitcher et al., 2009). At an even smaller spatial scale, it has been proposed that visual field maps form clusters (Brewer et al., 2005; Brewer & Barton, 2011) around a common foveal representation and that different clusters perform independent visual analyses (Wandell et al., 2005). The current results go a step further by demonstrating parallel processing at the smaller spatial scale of neighboring visual field maps (within a cluster) in human visual cortex.

Importantly, in monkey the functional independence exhibited by neighboring visual field maps is underpinned by parallel anatomical connections from lower tier visual areas (Shipp & Zeki, 1985; Zeki & Shipp, 1988). Indeed, at the same level of the visual hierarchy in macaque cortex, V4d and V5/MT receive independent and parallel inputs from antecedent V2 (Shipp & Zeki, 1985). V4d and V5/MT in the macaque are commensurate in location to LO1 and LO2 in the human (Larsson & Heeger, 2006). It is plausible therefore, that the independent functional roles identified here also result from similar patterns of parallel connectivity with antecedent visual areas, a feature however, that is yet to be demonstrated empirically. While the interpretation of the results observed here relies upon there being parallel cortical connections, they do not however, rule out the presence of serial connections that are often highlighted as an important and influential feature of cortical organisation (Felleman & Van Essen, 1991).

6.7.3:   Implications for 'High-level' Visual Processing

Retinotopic mapping provides a means by which the visual cortex can be delineated into discrete maps of the visual field. A number of these visual field maps have recently been shown to subdivide larger functionally specialized areas and therefore, probing these visual field maps with TMS provides a means to study causal mechanisms in human visual processing at a spatial scale seldom achieved. Through the use of TMS, one can elucidate the functional properties of individual visual field maps echoing, to a degree, pioneering work in non-human primates (Zeki, 1978; Shipp & Zeki, 1985). The present results demonstrate that the retinotopic subdivisions of a larger category-selective area exhibit specializations for different relatively low-level visual features. One interpretation of these results is that these low-level specializations provide a potential mechanism to explain category selectivity. The parallel processing observed in LO1 and LO2 could be seen to create an organisational framework that offers a highly efficient mechanism for encoding complex visual forms across multiple visual field maps. That is, if individual visual field maps perform unique sets of computations, and moreover, performs those computations independently of one another, then replicated information, which is biologically expensive to compute (Kravitz et al., 2013), is reduced across those maps. The specialized and parallel nature of processing observed in LO1 and LO2, could extend to additional visual field maps within the LO cluster. Brewer and colleagues (Brewer & Barton, 2011) have proposed the existence of four additional maps in the LO cluster, with LO3-6 lying ventral to LO1 and LO2. The combined LO maps are suggested to form a cloverleaf configuration around a central foveal representation. All six LO maps are also suggested to have hemifield representations and show a high degree of overlap with the face-selective OFA (explored in Chapter 8 **General Discussion**). The presence of these additional LO maps offers the possibility that the unique and independent processing observed in LO1 and LO2 extends to the LO3-6 maps. If each map within this cluster performs unique computations and therefore, contributes uniquely to visual perception then perhaps the category-selectivity observed in these larger areas (LO-objects, OFA-faces) simply emerges from the unique and *map specific* computations of relatively low level spatial features performed by their respective retinotopically organised subdivisions. If each map contains a hemifield representation and performs unique computations then the visual system has a mechanism to decode multiple

unique low-level visual features efficiently at each point in the visual field (Kravitz et al., 2013). Indeed, selectivity for low-level visual features within higher-level visual areas has been shown previously (Andrews, Clarke, Pell & Hartley, 2010).

This framework is consistent with previous proposals that attempt to explain the emergence of category selectivity in terms of neural encoding of simple features (Op de Beeck, Haushofer, & Kanwisher, 2008). The previous model proposes that cortex contains a number of large overlapping maps, with each map having weak selectivity to particular visual features. The highly significant activation observed in response to complex objects is explained by the selectivity's within these large overlapping maps being multiplied together. In contrast to these features being computed in large overlapping maps however, the current results indicate that these features are computed independently in discrete regions that map the visual field. The specialized and parallel nature of processing observed in LO1 and LO2 is hard to accommodate with a model of large overlapping maps with weak selectivity (Downing, 2009). The results strongly suggest that the computations of orientation and shape are processed independently in LO1 and LO2. One way to conceptualise this is that the maps are in fact modules of selectivity, which are organised retinotopically. The results reported here can be viewed as consistent with the highly influential *recognition by components* model proposed by Biederman (Biederman, 1987). The low-level specializations present within LO1 and LO2 are similar in concept to the basic geons with which the recognition by components model suggest underpins the recognition of objects.

6.7.4:   Implications for Future Work

The results reported in this chapter reveal specializations for orientation and shape within LO1 and LO2, respectively. An important feature of this specialization is that the stimuli presented during TMS studies have been luminance modulated and therefore, achromatic. A logical extension of the work reported here is to investigate whether LO1 and LO2 causally underpin the perception of chromatic orientation and shape. The key conceptual advance here is whether or not LO1 and LO2 exhibit cue-invariant representations of orientation and shape. Evidence from the Inferior Temporal (IT) cortex of macaque, which is thought the homologue of human LOC, would suggest some form of

cue-invariance is present at this level of the visual hierarchy (Sary, Vogels & Orban, 1993). Accordingly, Chapter 7 will explore whether LO1 and LO2 contain cue invariant representations by assessing the effect of TMS of LO1 and LO2 on performance of chromatically defined orientation and shape discrimination.

6.8:   Conclusion

The results of the current study demonstrate that two different, relatively low-level visual attributes (orientation and shape) are analysed independently, in neighboring visual field maps LO1 and LO2. These results, combined with those reported in Chapters 4 and 5, confirm that LO1 is a cortical area specialized for orientation discrimination. This orientation selectivity is not solely inherited from antecedent visual areas. The results also indicate that LO2 is an area of cortex specialized for the perception of shape. Disturbances to shape discrimination were only evident following TMS of LO2. Additionally, the computations of shape performed by LO2 do not appear reliant on input from LO1, although an alternative account is that LO2 can function as normal, despite reduced input from LO1, in other words that the functions of these areas can operate independently of one another. The functional parallel processing observed between LO1 and LO2 may be underpinned by parallel anatomical connections. The double dissociation between LO1 and LO2 demonstrates that the retinotopic subdivisions of object-selective LO, have different and dissociable functional properties.

Chapter 7

Do LO1 & LO2 Contain Cue-Invariant Representations of Orientation & Shape?

7.1: Overview

The primary aim of this chapter was to investigate whether LO1 and LO2 contain cue-invariant representations of orientation and shape. We aimed to test this in a specific manner by applying TMS to LO1 and LO2 and measuring its effects on orientation and shape discrimination of chromatically defined stimuli. If LO1 and LO2 contain cue-invariant representations then TMS of LO1 should disrupt orientation processing and TMS of LO2 should disrupt shape processing. We also include the CON and no TMS conditions, in order to echo the experimental design employed in Chapter 6. If LO1 and LO2 contained specializations for chromatically defined orientation and shape, a secondary aim was to establish whether these specializations operated in serial or in parallel.

7.2: Introduction

The data reported in Chapters 4-6 revealed a number of important properties exhibited within subdivisions of lateral occipital cortex, in particular LO1 and LO2. First, the results of the motion discrimination studies reported Chapters 4 and 5 extend the body of evidence from neuropsychological (Zihl et al., 1983), neuroimaging (Zeki, 1990; Zeki et al., 1991) and neurostimulation (Beckers & Homberg, 1992; Walsh et al., 1998; McKeefry et al., 2008) studies demonstrating the causal role played by V5/MT in the perception of motion. Second, the orientation discrimination data reported in Chapters 4-6 revealed a causal role for LO1 in the processing of static, and to a lesser degree moving orientation. A consistent pattern of results in Chapters 4 and 5 were the lack of effect of TMS of LO2 on either motion or orientation discriminations. Third, the data reported in Chapter 6 revealed a specialized role for LO2 in the processing of shape information. Finally, the results from Chapters 4-6 demonstrate that: (1) TMS can be used effectively to reveal functional specializations between adjacent visual clusters - a double dissociation was evident between LO1 and V5/MT in the processing of orientation and motion, respectively and (2) TMS can be used to

elucidate the functional specializations between adjacent visual maps within a cluster. Crucially, the functional specializations revealed in Chapters 4-6 were observed for achromatic (luminance-modulated) stimuli only. This raises an intriguing question. Do the functional specializations observed previously in LO1 and LO2 extend to chromatically defined stimuli? The presence of these specializations would therefore, represent cue-invariant representations within these visual field maps. The following sections outline the evidence detailing chromatic processing in lateral occipital cortex (including LO1 and LO2) and the evidence in favour of cue-invariance.

7.2.1:   The Cortical Processing of Colour

Evidence from several neuroscience paradigms highlights the importance of ventral occipital areas in human cortical processing of colour (Wade, Augath, Logothetis & Wandell, 2008). First, damage to ventral occipital cortex can lead to cerebral achromatopsia, a perceptual deficit in colour processing (Meadows, 1974; Zeki, 1990).   Achromatopsic individuals report a monochromatic representation of the world (Heywood & Cowey, 1987). Patients with achromatopsia are also reported to have poor colour constancy, making systematic errors in colour naming when presented with colours under different illuminants (Kennard, Lawden, Morland & Ruddock, 1995; Clarke, Walsh, Schopping, Assal & Cowey, 1998), a finding initially reported following selective lesioning of macaque V4 (Walsh, Carden, Butler & Kulikowski, 1993). Second, a number of PET (Lueck et al., 1989; Zeki, et al 1990) and fMRI (Mckeefry & Zeki, 1997; Hadjikhani et al., 1998; Bartels & Zeki, 2000; Wade, Brewer, Rieger & wandell, 2002; Brewer et al., 2005) studies report consistent and powerful responses to chromatic stimuli in ventral occipital areas.

In non-human primates, the forth visual area (V4) is split into dorsal (V4d) and ventral (V4v) components, which have lower and upper quadrant representations of the visual field, respectively (Zeki, 1978). In contrast, the majority of evidence in human is in favour of a different model, whereby the forth visual area is a single complete hemifield map of the contralateral visual field on the ventral surface of the occipital lobe (Mckeefry & Zeki, 1997). The existence of a single human V4 sparked an intense debate between two competing groups of researchers. Originally Zeki and colleagues described the existence of a single complete hemifield map on the ventral surface of the brain that they labelled V4

(McKeefry & Zeki, 1997). V4 was found to be consistent with the location of lesions, which led to achromatopsia and responded significantly to chromatic over achromatic stimuli. In contrast, Hadjikhani and colleagues argued for the existence of an additional colour centre (V8) that neither, corresponded to V4 as proposed by Zeki and colleagues, or the 'putative' dorsal component of V4 (as in macaque cortex) (Hadjikhani et al., 1998). Since these publications, the vast majority of papers have reported a complete hemifield, chromatically sensitive map that corresponds well with the original definition of V4 (Wade et al., 2002, 2008; Brewer et al., 2005; Wandell et al., 2007; Goddard et al., 2008). Interestingly, a relatively recent publication shed some light on the possible reasons for the discrepancy across studies. Winawer and colleagues (Winawer, Horlguchi, Sayres, Amano & Wandell, 2010) observed that in 'most hemispheres' fMRI BOLD signals were contaminated by artefacts caused by the transverse sulcus, which lies within the vicinity of V4 and influences the visual field representations measured through fMRI within and around V4. By modelling the *'venus eclipse'* the authors were able to select subjects in whom the transverse sulcus was sufficiently displaced from the lateral edge of V4. In doing so the authors were able to reconstruct the visual field coverage without the artefact. In those subjects, the visual field coverage extended to the lower vertical meridian, making the measurements consistent with the model of a single hemifield map on the ventral surface originally reported by McKeefry & Zeki (1997).

Wade and colleagues (Wade et al., 2008) conducted an extensive analysis of the cortical colour responses in macaque and human cortex using fMRI. Consistent with electrophysiological recordings in macaque (Zeki, 1983), the responses in V4v and V4d to (L-M) cone chromatic contrast were found to be equal., suggesting that in macaque cortex, the two components fuse to create a single functional area, V4. In similar experiments (full field colour exchange) areas of human cortex exhibiting preferential responses to chromatic over achromatic stimuli were largely confined to ventral cortex. Indeed, the colour selectivity within V4, matched the location of V4 reported previously (McKeefry & Zeki, 1997). In recent years the debate surrounding the retinotopic organisation human of V4 resurfaced, with Hansen and colleagues proposing an alternative to the single hemifield V4 model (Hansen et al., 2007). The model suggests that V4 does not contain a complete hemifield representation, but rather, contains a representation that extends slightly beyond the upper

quadrant. Similarly they propose that a dorsal component of V4 (V4d) exists anterior of V3d and contains the lower quadrant counterpart to ventral V4 (V4v). This alternative model has important implications for the interpretation of the results of Larsson and Heeger, who proposed a model to divide lateral occipital cortex into two retinotopic regions (LO1 and LO2) that is dependent on V4 being a single hemifield map on the ventral surface (schematised in Chapter 3, *Figure 3.19*). If dorsal V4 (V4d) existed, it would need to be subtracted from the LO1 map, resulting in a map that contained just short of an upper quadrant representation only, with no ventral counterpart. Such an unexplained and fragmented visual field map would therefore, constitute an 'improbable area' (Zeki, 2003). Despite the alternative model, the majority of studies are in agreement with the retinotopic delineation of ventral visual cortex suggested by Zeki and colleagues and the retinotopic delineation of dorsal visual cortex proposed by Larsson and Heeger (2006).

7.2.2:   *Chromatic Processing in Lateral Occipital Cortex*

As mentioned above, evidence from neuropsychological and neuroimaging studies strongly suggest that chromatic signals are processed predominantly in ventral regions of human visual cortex. The role played by dorsal and lateral regions in colour processing has nevertheless, been a source of interest, and debate. The following section reviews the evidence, in favour of and against chromatic processing in lateral occipital cortex in general, but also, specifically in LO1 and LO2.

The evidence against a dorsal role for colour processing comes from a number of investigative paradigms. Neuropsychological evidence suggests that damage to lateral occipital cortex, although impairing visual object and shape recognition, leaves colour recognition and discrimination relatively preserved (Cavina-Pratesi, Kentridge, Heywood & Milner, 2010). Patient DF, was found to perform at chance levels (50% correct) on shape discrimination tasks, but above chance on both texture and colour discrimination tasks. Indeed, fMRI responses to chromatic visual stimuli in DF have been shown to be consistent with age-matched controls; generally localised to ventral regions of cortex (James et al., 2003; Bridge et al., 2013). Mullen and colleagues compared the selectivity of retinotopic cortex to L-M cone opponent and achromatic stimulation using fMRI. The authors report a large cluster of ventral cortex that exhibited a preferential response to the chromatic over

achromatic stimulation. Interestingly, the authors also report two clusters of dorsal and lateral cortex that exhibited a preferential response to achromatic over chromatic stimulation. These achromatically selective clusters were in the vicinity of V3A and V5/MT. The authors, labelled these clusters as dorsal occipital (DO) and lateral occipital (LO), respectively (Mullen, Dumoulin, McMahon, De Zubicaray & Hess, 2007). As mentioned in Chapter 4, LO1 and LO2 fall in between V3A and V5/MT on the lateral surface of the brain. The authors make no explicit mention of LO1 and LO2 and do not define them on the cortical surface reconstructions in the paper, making specific comments about LO1 and LO2 difficult. Wade and colleagues demonstrated that in human, regions of cortex exhibiting preferential responses to chromatic stimuli were confined to the ventral cortex, a pattern not found in macaques, where chromatic responses were found in both ventral and dorsal divisions of V4. Interestingly, the authors report that in single subject analyses (n = 7) no areas displaying significant activation to the colour exchange experiment were found on dorsal or lateral surfaces of the brain. Indeed, only through a more powerful surface-based group analysis did a small dorsal 'island' of colour selective cortex appear (Wade et al., 2008). The authors comment that although this dorsal island only just reached statistical significance, it nonetheless, is located in the approximate location of the 'putative' V4d proposed by others (Hansen et al., 2007).

To date, two studies have investigated chromatic processing in LO1 and LO2 directly. The first, used multivariate fMRI pattern analysis techniques to decode and subsequently reconstruct colours from BOLD responses in human visual cortex (Brouwer & Heeger, 2009). Subjects viewed concentric sinusoidal gratings in a circular aperture. Each sinusoid modulated from mid-grey to one of eight points in colour space. Stimulus colour could be correctly decoded at above chance levels from the activity within cortical areas V1, V2, V3 V4 and VO1, but not, LO1, LO2 or V5/MT. The correct colours were only accurately decoded (above chance) in 2/5 subjects in both LO1 and LO2, suggesting that LO1 and LO2 do not encode stimulus colour. The second, attempted to clarify the debate regarding the existence V4d alluded to above. The authors, used fMRI retinotopic mapping procedures to define multiple maps across both dorsal and ventral surfaces. The responsiveness of these maps to image colour were subsequently tested. The results not only confirm the full hemifield representation in V4, but also, show a robust preference for colour stimuli over luminance-

matched achromatic stimuli in V4, compared to little or no colour preference in the vicinity of putative V4d (LO1).

These fMRI based experiments are complimented by a TMS study, which aimed to elucidate the role played by LO (the area encompassing LO1 and LO2) in colour discrimination, amongst others (Ellison & Cowey, 2006). Three tasks (distance, shape and colour discrimination) were employed whilst TMS pulses were delivered to LO (plus other sites). Briefly, TMS of LO was found to selectively disrupt shape processing only, leaving distance and colour processing relatively unaffected. Consistent with the above findings, the data suggest that LO does not play a causal role in colour discrimination, but rather plays a causal role in shape discrimination. A caveat however, which the authors acknowledge, is that the colour task was a stand-alone task and not connected *per se* with the shape task. In order to assess the role played by LO (or LO1 and LO2), there is a need to make a shape task contingent on colour.

The results discussed above suggest that neither LO nor its retinotopic subdivisions (LO1 and LO2) exhibit preferential responses for chromatic over achromatic stimuli. A number of questions however, remain unanswered. Although LO1 and LO2 may not exhibit preferential fMRI responses to chromatic over achromatic stimulation, do they process the chromaticity of stimuli in some form? Do the specializations observed for achromatic orientation and shape reported in Chapter 6, extend to chromatic stimuli? That is, when the task is dependent on chromatic processing, do LO1 and LO2 play a causal role in chromatic orientation and shape processing?

In contrast to the reports above, Self and Zeki (2005) investigated the processing of colour and motion using fMRI. In their paradigm, subjects were shown shape stimuli composed of kinetic, coloured dots. The shapes were constructed by varying the amount of colour and motion coherence present in the arrays. In doing so, the authors created three different conditions under which shape detection could occur: (1) shapes defined purely by colour coherence; (2) shapes defined purely by motion coherence and (3) shapes defined by both colour and motion coherence. The results suggest that both colour and motion defined shapes activate regions within the LOC, with shapes defined by the integration of colour and motion signals activating a more ventral LOC region. The LOC contains therefore,

may contain cue-invariant representations, which are capable of representing the shape of objects independent of the cue used to define them. In addition, Clarys and colleagues (Claeys, Dupont, Cornette, Sunaert, Hecke, De Schutter & Orban, 2004) reported the involvement of both ventral and dorsal regions of cortex when active judgements regarding colour were required. The authors argues that ventral and dorsal regions cooperate in the processing of chromatic signals, when those signals require active judgements. Interestingly, Larsson and Heeger originally suggested that LO1 and LO2 were perfectly placed in the visual hierarchy to receive parallel projections from both ventral and dorsal streams, making a role in chromatic processing at least plausible.

7.2.3:   Chromatic Processing of Orientation & Shape

In both human and non-human primates, visual information is transferred from the retina to the cortex via two colour opponent channels and one luminance channel. It was originally suggested that the cortical pathways for colour and form adhered to the early segregation with the luminance channel specialized for form processing and the two chromatic channels specialized for colour perception (Livingstone & Hubel, 1988; Felleman & Van Essen, 1991). Evidence for single neurons jointly selective to both orientation and colour in areas V1-V4 of non-human primates (Leventhal, Thompson, Liu, Zhou & Ault, 1995; Johnson, Hawken & Shapely, 2001) however, argue against this strict segregation. In human, behavioural and neuroimaging studies have explored the coupling between colour and form. The tight coupling of orientation and colour has been demonstrated through such behavioural paradigms as the tilt-after effect and the tilt-illusion (Clifford, Sphehar, Solomon, Martin & Zaidi, 2003). Engel (2005) demonstrated the presence of oriented and unoriented colour selective neurons in V1 and other early retinotopic visual areas. Indeed, adaptation jointly selective for colour and orientation was observed in V1 and an area termed V3m, which comprised V3, V3A and V7. The extrastriate adaptation could have occurred either through local computation of both colour and orientation in these areas, or through feed-forward propagation from V1 (Engel, 2005). The joint representation of colour and orientation was later confirmed within early visual cortex (V1-V4) (McDonald, Mannion, Goddard & Clifford, 2010). Orientation and colour combinations can also be decoded accurately from BOLD responses in early visual areas (V1-V4) using MVPA analysis

techniques (Seymour, Clifford, Logothetis & Bartels, 2009; 2010). Whether LO1 is a cortical region also involved in the joint encoding of orientation and colour however, remains to be seen.

In addition to the evidence for a coupling of orientation and colour, a number of fMRI studies highlight the processing of shapes defined by colour within the LOC. Early fMRI work probing the response properties of the LOC demonstrated that shapes were more strongly represented within the LOC than random textures when defined by chromatic information alone (Grill-Spector et al., 1998; 1999; Kourtzi, Bulthoff, Erb & Grodd, 2000). Self and Zeki (2005) reported colour-defined shape selectivity within an area of the LOC consistent the original LOC definition (Malach et al., 1995). More recently, an area on the ventral aspect of the LOC was found to be commonly activated by stimuli that contained colour, shape and texture information (Cavina-Pratesi et al., 2010). This region, on the fusiform gyrus, was more active to the conjunction of visual features than to any single feature in isolation. Taken together, it appears that both chromatic orientation and shape are processed together in a number of extrastariate cortical regions. Whether or not LO1 and LO2 also processed these features jointly however, is currently unknown.

7.2.4:   Cue-Invariant Processing in Visual Cortex

Evidence from a number of investigative paradigms suggests the presence of cue-invariant representations within macaque and human visual cortices. In macaque, single-unit recordings highlight cue-invariant responses in V2, V3 and V4 with cells sensitive to the orientation, direction and colour of stimuli (Leventhal et al., 1995; Leventhal, Wang, Schmolesky & Zhou, 1998). Neurons in macaque inferotemporal cortex (IT) exhibit preferential responses to shapes than simple features and maintain this preference across multiple visual cues (Sary et al., 1993; Vogels & Orban, 1996; Tanaka, Uka, Yoshiyama, Kato & Fujita, 2001; Kriegeskorte, Mur, Ruff, Kiani, Bodurka, Esteky, Tanaka & Bandettini, 2008). In human, fMRI studies provided evidence for cue-invariance in the Kinetic Occipital area (KO) (Zeki, Perry & Bartels, 2003), as well as LOC, the 'putative' human homologue of macaque IT (Malach et al., 1995). The LOC responds more strongly to objects (Grill-spector et al., 1998; 1999; Kourtzi & Kanwisher, 2001) than uniform textures or random stimuli across a number of visual dimensions including luminance, texture, illusory contours,

motion and colour (Grill-Spector et al., 1998; 1999; Kastner, De Weerd & Ungerlieider, 2000; Kourtzi & Kanwisher, 2001). The LOC also represents shapes when integrated across multiple cues, such as motion and colour (Self & Zeki, 2005; Vinberg & Grill-Spector). The LOC therefore, may contain specialized regions with the potential to respond to their preferred visual feature irrespective of how that feature is defined.

Despite the scarceness of evidence in favour of pure colour processing in LO, LO1 or LO2, these visual field maps may nevertheless, contain neurons capable of representing orientation and shape across multiple cues, one of which may be colour. By making the orientation and shape tasks crucially dependent on the colour of the stimulus, we extend previous TMS work on chromatic processing in LO (Ellison & Cowey, 2006). The exact causal roles that LO1 and LO2 play in the processing of chromatic stimuli remains unclear, with conflicting results of chromatic processing in LO. The current experiment aims to test explicitly whether LO1 and LO2 exhibit specializations for the processing of chromatic orientation and shape defined by modulations in colour along the L-M axis; such specializations would provide compelling evidence for cue invariance.

7.3:   Theoretical Considerations

Consistent with the studies undertaken in Chapter 4 and 5, it was necessary to account for V1 proximity, due to the orientation (Hubel & Wiesel, 1963; Hubel, Wiesel, & Stryker, 1978; Furmanski & Engel, 2000), and colour (Leventhal et al., 1995; Clifford et al., 2003; Engel, 2005) selectivity of V1 neurons. Consistent with the methodology in previous chapters a control site (CON) was defined in each subject by moving medially from LO1 by the distance separating our LO1 and LO2 targets. The control site allows us to evaluate whether or not any differential effects observed between LO1 and LO2 are attributable to LO1's closer proximity to V1. We also include a no TMS baseline measurement in order to evaluate any general effect of TMS.

7.4:   Aims & Predictions

Establishing causal roles for LO1 and LO2 in chromatic orientation and shape processing would provide compelling evidence for cue-invariant processing within these visual field maps. Given the evidence for cue-invariant responses in macaque IT and human LOC, it was hypothesised that LO1 and LO2 would exhibit specializations for chromatically defined orientation and shape, respectively. If present, whether these specializations operate in serial or parallel however, is currently unknown, although the data reported in Chapter 6 would suggest the existence of parallel processing at this level of the visual hierarchy. Two alternate predictions of the effects of TMS are depicted in Figure 7.1. If LO1 and LO2 process chromatic orientation and shape information in serial, TMS of LO1 should disrupt orientation processing, but TMS of both LO1 and LO2 should disrupt shape processing (Left column Figure 7.1). If these processes operate independently of one another, then TMS of LO1 alone should disrupt orientation and TMS of LO2 alone should disrupt shape processing – a double dissociation (Right column Figure 7.1). As with previous chapters, the effects of TMS of LO1 and LO2 need to be considered within the context of TMS of the control site and the no TMS baseline.
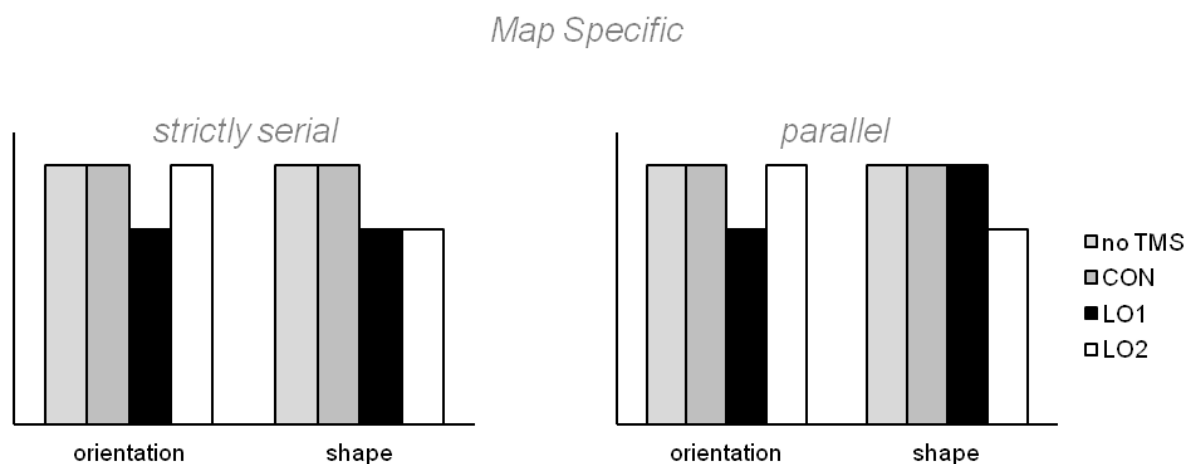
Figure 7.1: *Serial and parallel map specific predictions for the effects of TMS on chromatic orientation and shape discrimination. In a serial processing architecture **(left)** TMS of LO1 alone disrupts orientation processing, but if LO2 is reliant on input from LO1, TMS of both LO1 and LO2 disrupts shape processing. In a parallel or independent processing architecture **(right)**, orientation processing is only disrupted following TMS of LO1 and shape processing is only disrupted following TMS of LO2 – a double dissociation.*

7.5:   Methods

7.5.1:   Subjects

The current study included 12 subjects (mean age = 23, range = 17, 4 male). All subjects had normal or corrected to normal vision and gave informed consent in accordance with the Declaration of Helsinki. York Neuroimaging Centre (YNiC) Research Governance Committee approved the study.

7.5.2:   Visual Field Mapping

Prior to TMS stimulation, all subjects completed full fMRI visual field mapping experiments (~1 hour) using standard retinotopic mapping procedures. Data analysis, segmentation and delineation of retinotopic visual area boundaries were conducted in accordance with previous reports (Baseler et al., 2011) and the processing steps outlined in full in Chapter 3.

7.5.3:   Identification of Visual Field Maps LO1 & LO2

Retinotopic definitions of LO1 and LO2 were made in at least one hemisphere in all subjects tested. The representations within LO1 and LO2 were consistent not only with previous reports (Larsson & Heeger, 2006), but also, with previous definitions made throughout the thesis. LO1 began at the lower vertical meridian boundary with V3d and displayed a gradual progression towards the upper vertical meridian. LO2 began at the shared boundary with LO1 at the representation of the upper vertical meridian and displayed a gradual progression towards the lower vertical meridian.

7.5.4:   Establishing Isoluminance using Minimum Motion

Prior to completing psychophysical experiments, isoluminant thresholds were defined for each subject using the minimum motion paradigm (Anstis & Cavanagh, 1983; Cavanagh, Tyler & Favreau, 1984). Subjects viewed a coloured sinusoidal grating modulated along the L-M axis, presented in a circular aperture (diameter 4°) with a spatial frequency of 2 cpd. The grating was centred at 10° eccentricity along the horizontal meridian into the left visual field. The grating was presented at a fixed orientation (45°) and drifted left-right at a

209

constant speed (8°/sec). Subjects fixated a black dot (diameter 0.3°) at the centre of the screen and were required to modify the luminance of the red channel until the perceived movement of the grating slowed and/or stopped; this is the point at which the two colours are perceived as being of equal luminance (isoluminant). The value of the red channel was recorded, reset to its default value and repeated ten times for each subject. The mean value of the red channel for each subject was used in defining the luminance values presented during subsequent orientation and shape discrimination experiments. Saccades away from fixation could interfere with isolumianant values. Despite this eye tracking was not performed. (See Appendix for the exact RGB values used for each subject).

7.5.5:   Psychophysical Stimuli & Procedures

Stimuli for the psychophysical and TMS experiments were as described in the **Visual Stimuli** section in Chapter 2. Briefly, stimuli for the behavioural and TMS experiments were generated using MATLAB (Mathworks, USA) and displayed on a Mitsubishi Diamond Pro 2070^{SB} display with a refresh rate of 60 Hz, controlled by a VISAGE graphics card (Cambridge Research Systems^{TM}). Grating stimuli were coloured sinusoidal gratings modulated along the L-M axis, presented in a circular aperture (diameter 4°) with a spatial frequency of 2 cpd. Shape stimuli were coloured radial frequency patterns modified along the L-M axis, with a fixed radial frequency (3).

The visual tasks employed were orientation discrimination of isoluminant gratings and shape discrimination of isoluminant radial frequency patterns. The parameters for psychophysical and TMS experiments followed the protocol outlined in the **Psychophysical Protocol** section of Chapter 2. Prior to TMS stimulation each subject completed orientation and shape discrimination experiments using the method of constant stimuli described in full in Chapter 2. The spatial configuration of the stimuli and temporal trial structure for the orientation and shape experiments were identical (see schematic Figure 7.2). The phases of both the gratings and radial frequency patterns were randomised within trials. Individual psychometric functions for orientation and shape discrimination were plotted from the average for each subject (average of 350 trials – 50 presentations per stimulus level). Consistent with the practices in Chapters 4-6, we initially defined thresholds (75% correct) for orientations more vertical and horizontal than the reference and for shapes spikier and

smoother than the reference. The range between these values was calculated and halved. Stimuli for TMS were defined by the following equation: TMS stimuli = reference ± range/2.
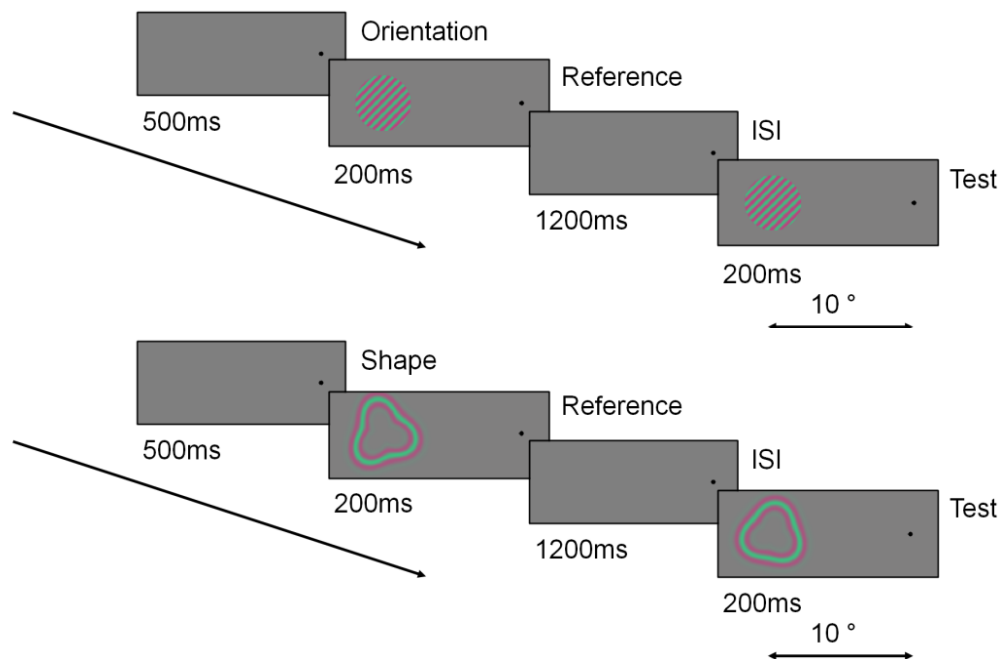
Figure 7.2: *Trial structure schematics for chromatic orientation **(top)** and shape **(bottom)** discrimination tasks. During chromatic orientation discrimination the reference orientation was fixed 45°. Test stimuli were randomly selected from a pre-determined list of seven stimuli that spanned a range of orientations more vertical and more horizontal than the reference. During chromatic shape discrimination the amplitude of the reference shape was fixed (0.2). Test stimuli were randomly selected from a pre-determined list of seven stimuli that spanned a range of shape spikier and smoother than the reference.*

7.5.6:   TMS Protocol

A train of 4 biphasic (equal relative amplitude) TMS pulses, separated by 50ms (20Hz) at 70% of the maximum stimulator output (2.6 Tesla) were applied to the subject's scalp using a figure-of-eight coil (50 mm external diameter of each ring) connected to a Magstim Rapid2 ™ stimulator (Magstim, Wales). Subjects were seated in a purpose built chair with chin rest and forehead support. The coil was secured mechanically and placed directly above each cortical target (CON, LO1, and LO2) with the handle orientated parallel with the floor. The position of the coil was monitored and tracked in real time allowing the displacement between the intended and actual site of TMS delivery to be recorded, along

with two additional measurements; coil-target distance and coil-target orientation. Each subject underwent 8 counterbalanced sessions (2 tasks x [3 TMS sites + 1 no TMS]). Each TMS session (orientation and shape) contained 100 trials (50 per threshold stimulus). TMS pulses were delivered concurrently with the presentation of the test stimulus, depicted in Figure 7.3.
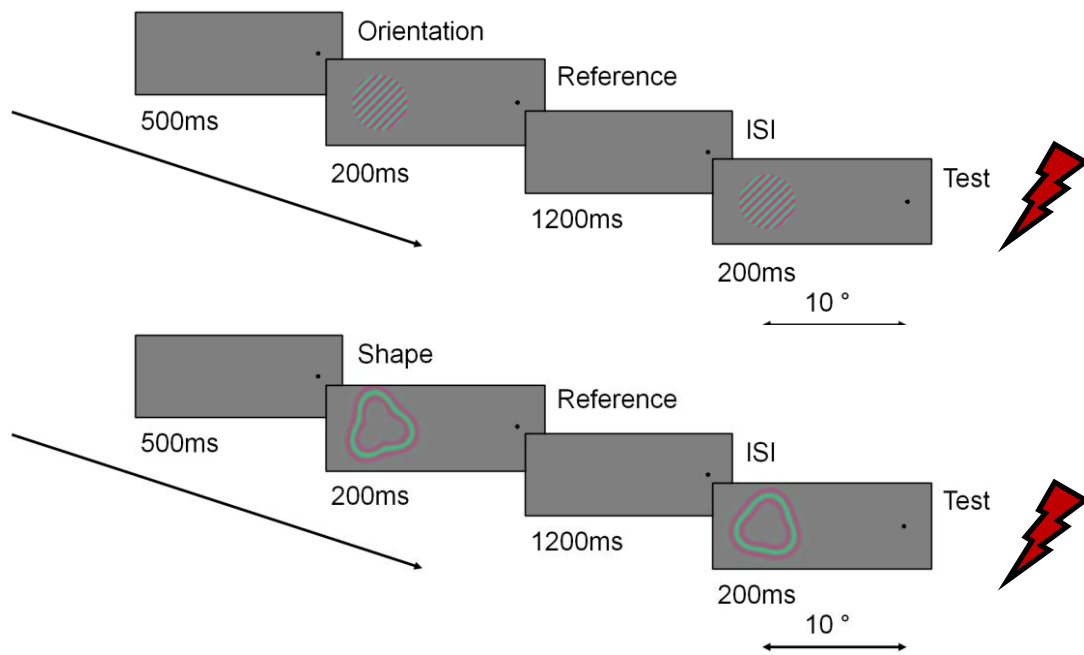
Figure 7.3: *Trial structure schematics for chromatic orientation **(top)** and shape **(bottom)** TMS tasks. During chromatic TMS sessions (and no TMS baseline) only the threshold stimuli were presented as test stimuli. TMS pulses were delivered concurrently with the presentation of the threshold test stimuli, depicted by the red lightning bolts.*

7.5.7:   Data & statistical Analysis

Before data analysis some trials (~4%) were removed on the basis of two criteria: trials for which coil displacement was large (>2.5 mm) and trials for which reaction time was greater than 2000 ms after the cessation of the presentation of the test stimulus. Statistics were calculated using the SPSS software package (IBM). A series of two-way repeated-measures ANOVAs were employed to examine the effects of discrimination (% correct) and reaction times (secondary measure), along with two potentially confounding variables (coil-target distance and coil-target orientation), which provide a measurement of operator error. In the case of a significant interaction, subsequent one-way repeated-measures

ANOVAs were calculated for each task considered separately. Given that our central hypotheses concern the processing within LO1 and LO2 specifically, in addition to the full ANOVAs, planned contrasts will be computed between LO1 and LO2, in order to assess with greater sensitivity whether any effects are observed. For each ANOVA, whether or not the ANOVA adhered to the assumption of sphericity was established initially using Mauchly's test.

7.6:   Results

7.6.1:   Visual Field Map Identification

LO1 and LO2 were clearly identifiable in at least one hemisphere in all subjects (See **visual field map** Gallery in Chapter 3 for full retinotopic breakdown of subjects S6, S7, S9, S11, S13-S20). The centroids of LO1 and LO2 were calculated to define TMS targets. Figure 7.4, illustrates visual field maps with respect to polar angle (including LO1 and LO2) on lateral views of both the left and right hemispheres of S12. In both hemispheres, LO1 extends anteriorly from the shared boundary with V3d, at the representation of the lower vertical meridian (yellow). LO1 displays a gradual progression from the lower vertical meridian towards the upper vertical meridian (purple/blue). LO2 is the mirror-reverse of LO1 and therefore, displays a gradual progression from the upper vertical meridian towards the lower vertical meridian.
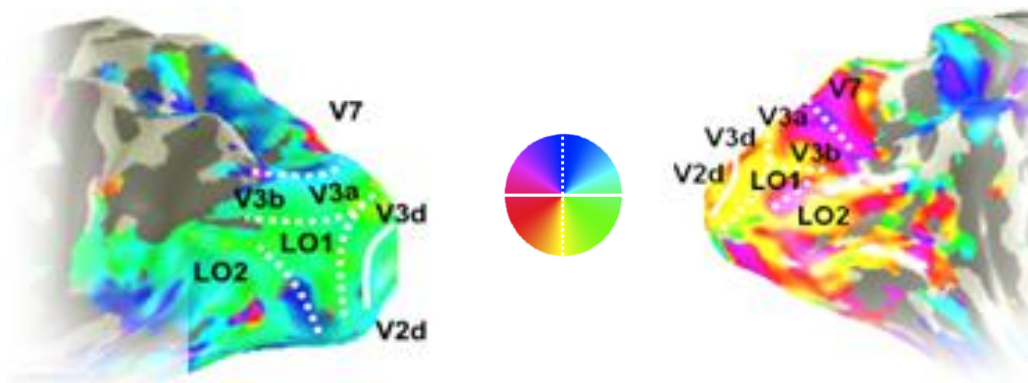
Figure 7.4: *Bilateral visual field maps in a representative subject. Lateral views depict visual field maps in the left and right hemispheres of a representative subject (S12). The BOLD responses to the rotating wedge stimulus are overlaid in false colour (see colour wheel, centre) onto surface reconstructions of the grey-white matter boundary of the left and right hemispheres. The vertical meridian representations are shown by the dashed white lines, with the horizontal meridian representations shown by the solid white lines. In both hemispheres the visual field representations in LO1 and LO2 are clearly identifiable. LO1 begins at the shared boundary with V3d at the representation of the lower vertical meridian. LO1 extends anterioraly from the lower vertical meridian toward the upper vertical meridian. LO2 is the mirror-reverse of LO1 and displays a gradual progression from the upper vertical meridian back toward the lower vertical meridian, LO1 and LO2 were identified in at least one hemisphere in each subject.*

7.6.2:   Chromatic Orientation & Shape Psychophysics

Chromatic orientation and shape psychometric functions for all subjects are plotted in Figure 7.5. Inspection of Figure 7.5 highlights the individual variation in orientation and shape discrimination performance and underscores the need to establish individual discrimination thresholds. For example, the range of orientations required for S6 is greater than the range of orientations required for S13, indicated by the much steeper slope for S13. As in previous chapters, the *x* axis of S6 has been rescaled relative to other subjects. Interestingly, it appears in some subjects that good orientation discrimination is not necessarily associated with good shape discrimination. For instance, S6 required the largest range of orientations yet has one of the steepest shape discrimination functions, indicating that S6 required a smaller range of values than other subjects during shape discrimination.
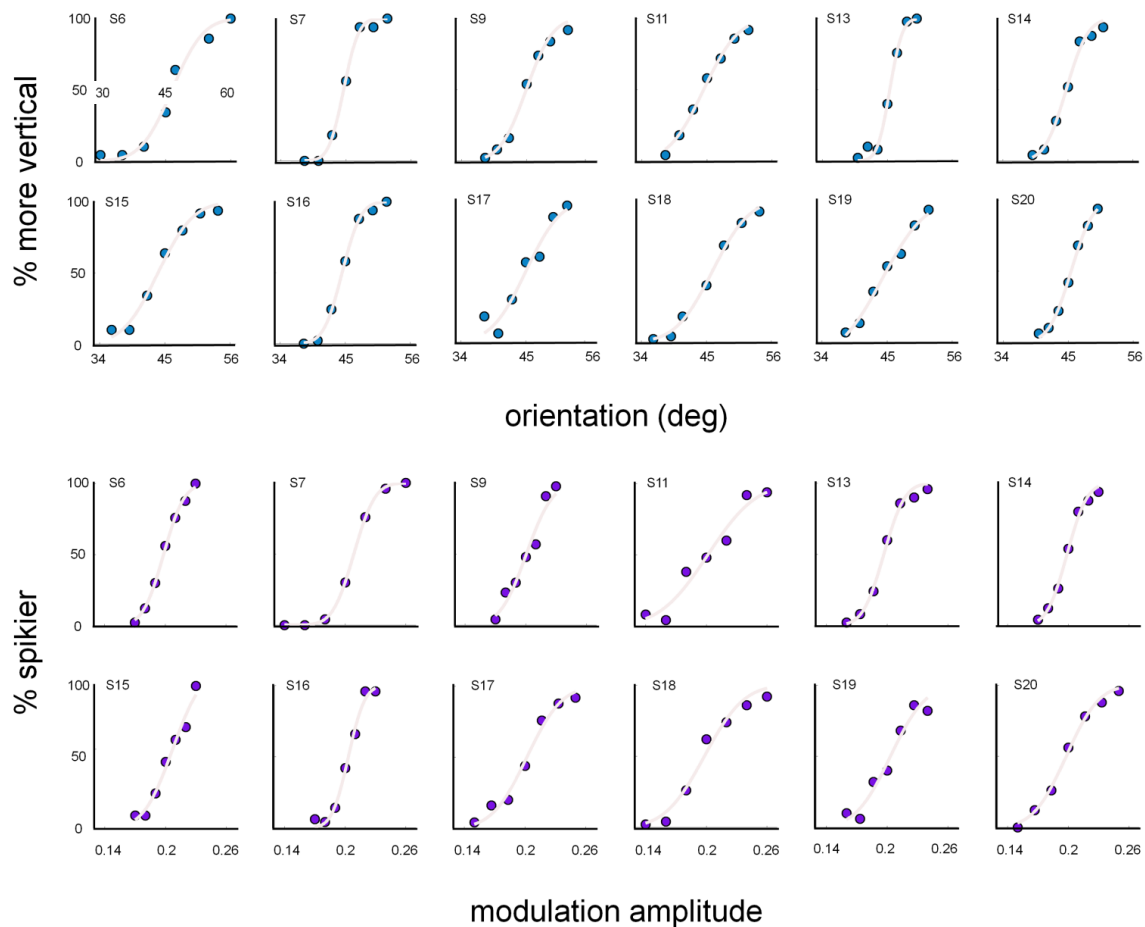
Figure 7.5: *Chromatic orientation and shape psychometric functions. Individual psychometric functions for the chromatic orientation **(top)** and shape **(bottom)** discrimination tasks. The threshold stimuli to be used in subsequent TMS sessions were derived from these psychometric functions. For orientation, the 75 % correct more vertical and horizontal orientations were calculated. The range between these values was divided in half and added to and subtracted from the reference orientation to create the two stimuli for TMS. For shape, the 75 % correct smoother and spikier shapes were calculated. The range between these values was divided in half and added and subtracted from the reference shape to create the stimuli for TMS.*

We defined, in each individual subject, two stimuli for each task to be presented during TMS sessions using the method described above. Table 7.1, contains the 75% correct thresholds for orientations more vertical and more horizontal than the reference and shapes spikier and smother than the reference. Table 7.1, also includes the value added to and subtracted from the reference stimulus and the actual values presented during TMS for all subjects.

Table 7.1: *Threshold and TMS values derived from the chromatic orientation and shape psychometric functions. For orientation (top), table includes the 75 % correct values for orientations more horizontal (threshold H) and more vertical (threshold V) than the reference, plus the value added too and taken away from the reference (ref ±) and the values used during TMS for the more horizontal (TMS H) and more vertical (TMS V) test stimuli. For shape (bottom) table includes the 75 % correct values for shapes smoother (threshold SM) and spikier (threshold SP) than the reference, plus the value added too and taken away from the reference (ref ±) and the values used during TMS for the smoother (TMS SM) and spikier (TMS SP) test stimuli.*

isoluminant orientation (degrees)				
Subject	threshold H	threshold V	ref ±	TMS H	TMS V
S6	43.2950	48.9050	2.8050	42.1950	47.8050
S7	43.2500	45.9450	1.4825	43.5175	46.4825
S9	43.3250	46.5750	1.1250	43.8750	46.1250
S11	42.7800	46.6800	1.9500	43.0500	46.9500
S13	42.5800	47.3450	2.3800	42.6200	47.3800
S14	41.3250	47.5900	3.1325	41.8675	48.1325
S15	40.6800	47.0250	3.1725	41.8275	48.1725
S16	42.8300	46.1900	1.6800	43.3200	46.6800
S17	41.9550	48.1850	3.1150	41.8850	48.1150
S18	42.7050	49.3650	3.3300	41.6700	48.3300
S19	40.2750	48.0450	3.8850	41.1150	48.8850
S20	43.5000	47.4750	1.9875	43.0125	46.9875
isoluminant shape (amplitude modulation)				
Subject	threshold SM	threshold SP	ref ±	TMS SM	TMS SP
S6	0.1876	0.2093	0.0109	0.1892	0.2109
S7	0.1976	0.2198	0.0111	0.1889	0.2111
S11	0.1870	0.2144	0.0138	0.1863	0.2138
S12	0.1763	0.2267	0.0252	0.1748	0.2252
S13	0.1858	0.2078	0.0110	0.1890	0.2110
S14	0.1883	0.2093	0.0105	0.1895	0.2105
S15	0.1918	0.2240	0.0153	0.1847	0.2153
S16	0.1946	0.2119	0.0087	0.1914	0.2087
S17	0.1837	0.2203	0.0183	0.1818	0.2183
S18	0.1772	0.2189	0.0209	0.1792	0.2209
S19	0.1850	0.2216	0.0183	0.1817	0.2183
S20	0.1807	0.2152	0.0173	0.1828	0.2173

7.6.3:   Effects of TMS on Chromatic Orientation & Shape Processing

Group average performance (% correct) for all conditions grouped by task is plotted in Figure 7.6. The results depicted in Figure 7.6, reveal a couple of interesting results. First, there is a clear effect of task. Performance on the shape task is worse relative to the orientation task for all conditions, indicating that on average subjects found the shape task more challenging. Second, there is no clear indication of an effect of condition for either task. For orientation discrimination, performances are very similar across conditions. Similarly, for shape discrimination, performances are largely equivalent across conditions. Indeed, performance is marginally increased following LO2 stimulation. The pattern of deficits induced by TMS across conditions does not follow either the serial or parallel predicted effects of TMS.
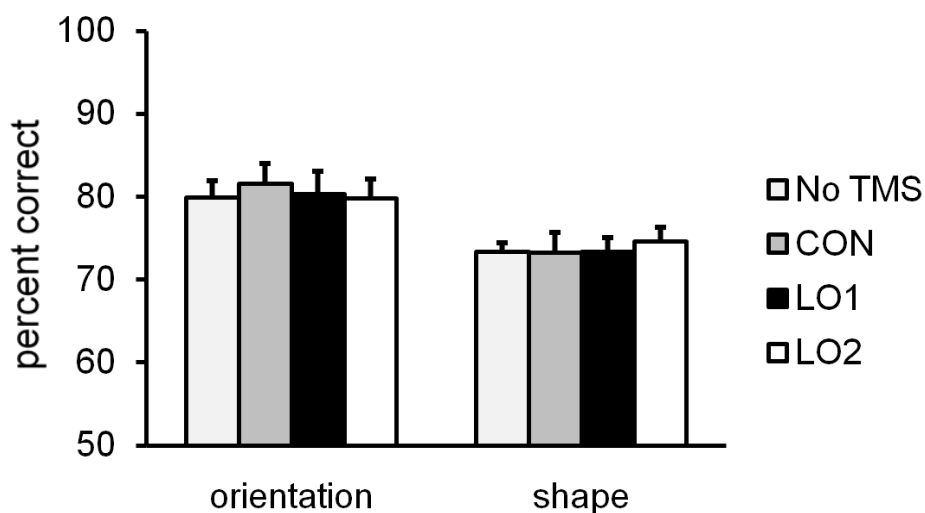
Figure 7.6: *Effects of TMS on chromatic orientation and shape discrimination. Group average performances are plotted for all conditions grouped by task. The pattern of deficits induced by TMS is not consistent with either the serial or parallel predictions. Performances are largely equivalent across conditions for both tasks. Specifically, TMS of LO1 did not lead to a selective disturbance to chromatic orientation discrimination, nor did TMS of LO2 lead to selective disturbance to chromatic shape discrimination. Error bars represent s.e.m.*

In order to assess formally the effect of TMS on performance a 2 x 4 repeated measures ANOVA was conducted with conditions Task (orientation & shape) and Site (no TMS, CON, LO1, & LO2). There was a significant effect of Task ($F_{(1, 11)}$ = 16.582, p = 0.002), indicating that across conditions performances were worse on the shape task than the orientation task. There was neither a significant effect of Site ($F_{(3, 33)}$ = 0.107, p = 0.955), nor Task x Site interaction ($F_{(3, 33)}$ = 0.547, p = 0.654). The lack of a significant Task x Site interaction suggests that neither LO1 nor LO2 underpinned the processing of chromatic orientation and shape. Due to the lack of a Task x Site interaction, further one-way ANOVAs on each site considered separately were not undertaken.

As previously mentioned the primary hypotheses pertained to the role of LO1 and LO2 in chromatic orientation and shape processing, with the inclusion of the CON and no TMS baseline serving as suitable foils for any effects observed. We are therefore justified in running planned contrasts to analyse the pattern of results across LO1 and LO2 alone. The interaction term between LO1 and LO2 was not significant ($F_{(1, 11)}$ = 0.608, p = 0.432). The data demonstrate that discrimination performance was not disrupted following TMS of LO1 and LO2 for either task. This pattern of results is inconsistent with the predicted effects of TMS and the achromatic data reported in Chapter 6.

7.6.4:   Effect of TMS on Reaction Times

In accordance with Chapter 4-6, discrimination performance was the primary measure of the effects of TMS. Nevertheless the effect of TMS on reaction times was also assessed. The analysis of reaction times is important. In the event that TMS effects on discrimination are subtle, the effect of TMS on reaction times can provide evidence for TMS induced interference. Group average reaction times across all conditions and tasks are plotted in Figure 7.7. Inspection of Figure 7.7, highlights a number of potentially important patterns of results. First, during orientation discrimination reaction times are notably slower during LO1 stimulation than any other condition. Indeed, reaction times across the other conditions are largely equivalent. Second, during shape discrimination reaction times are slower during stimulation of LO2 than any other conditions. Again, the reaction times during other conditions are more similar than between LO2 and any other condition.
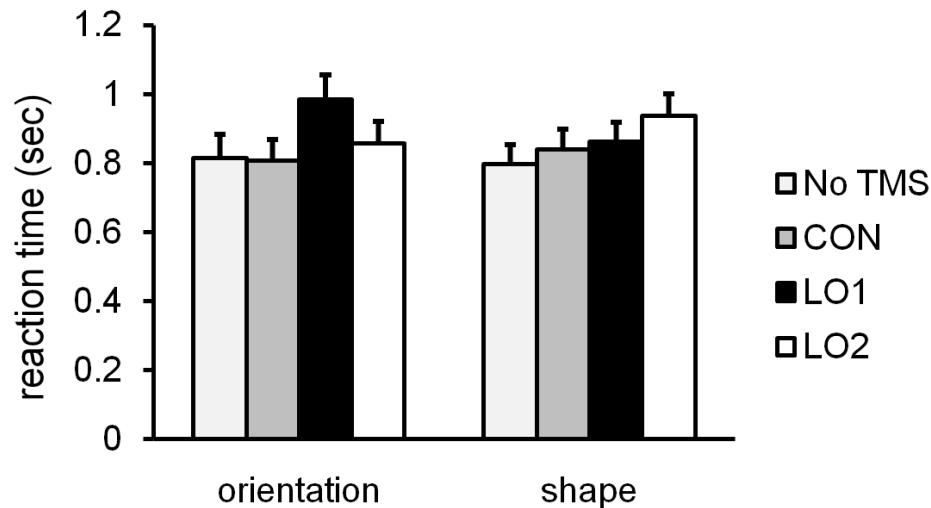
Figure 7.7: *Effects of TMS on reaction times during chromatic orientation and shape discrimination. Mean reaction time across sites and tasks. For chromatic orientation discrimination, reaction times during LO1 stimulation are considerably slower relative to all other conditions. Reaction times during all other conditions are largely similar. For chromatic shape discrimination, reaction times during LO2 stimulation were the slowest across all conditions. Again, reaction times across other conditions are largely equivalent. Error bars represent s.e.m.*

To assess the effect of TMS on reaction times, a 2 x 4 repeated measures ANOVA was conducted with conditions Task (orientation & Shape) and Site (no TMS, CON, LO1 & LO2). There was neither a significant effect of Task ($F_{(1, 11)}$ = 0.153, *p* = 0.704), nor Site ($F_{(3, 33)}$ = 2.671, *p* = 0.064). The Task x Site interaction however, was significant ($F_{(3, 33)}$ = 3.130, *p* = 0.039). Given the significant Task x Site interaction, one-way repeated measures ANOVAs were conducted on each task considered separately. For orientation, there was a significant effect of Site ($F_{(3, 33)}$ = 3.373, *p* = 0.030). Pairwise comparisons (Bonferroni corrected) revealed a single significant pairwise comparison (LO1 *versus* CON, *p* = 0.022), all other comparisons were not significant (*p* = > 0.186, in all cases). For shape, the effect of Site was not significant ($F_{(3, 33)}$ = 2.135, *p* = 0.155), there were no significant (Bonferroni corrected) pairwise comparisons (*p* = >0.411, in all cases). Given our primary hypotheses regarding LO1 and LO2, we are therefore justified in running planned contrasts to analyse the pattern of results across these targets sites alone. The interaction term between LO1 and LO2 was significant ($F_{(1, 11)}$ = 5.517, *p* = 0.039). Paired *t*-tests (two-tailed) revealed a significant difference in reaction times between LO1 and LO2 for orientation discrimination ($t_{(11)}$ = 2.474, *p* = 0.031), but not for shape discrimination ($t_{(1, 11)}$ = 1.363, *p* = 0.200).

219

7.6.5:   Analysis of Potentially Confounding Variables

Two additional measurements were recorded with each TMS pulse train in an attempt to account for two potentially confounding variables that relate to the spatial relationships between the stimulating coil and the targets within cortex; coil-target distance and coil-target orientation. These measurements are included as they provide a means by which to rule out differences in the precision of TMS, caused by operator error, as an alternative account of the data reported above.

7.6.5.1:   Coil -Target Distance

The mean Euclidean distance (mm) from the calibration point of the stimulating coil to the cortical targets is plotted in Figure 7.8, for all TMS sites and tasks. Inspection of Figure 7.8, reveals an interesting pattern of results. There is a slight indication that the coil-target distances vary across sites as a function of task - a result that can only be due to operator error. For example during orientation discrimination the coil-target distance was shortest during LO1 stimulation, whereas during shape discrimination the coil-target distance is longest during LO1 stimulation.
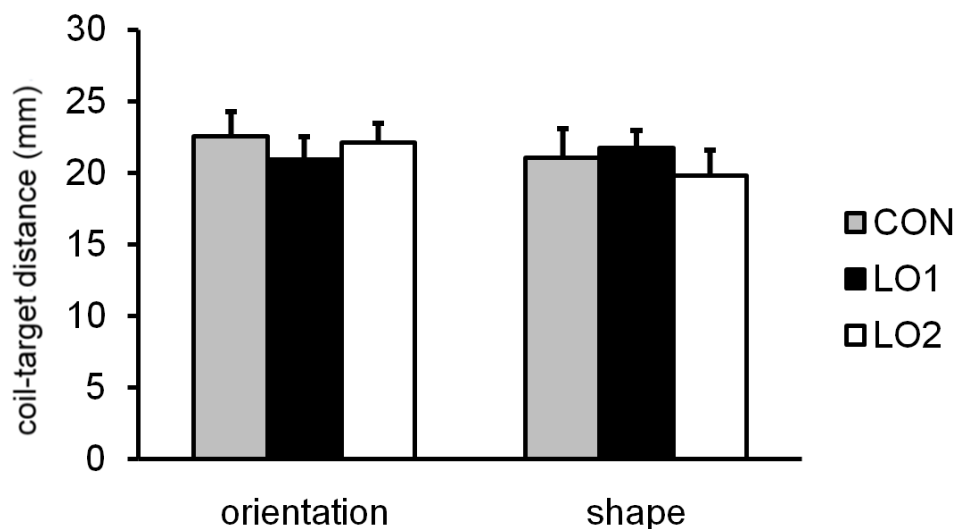
Figure 7.8: *Mean Euclidean distance between stimulating coil and cortical targets during chromatic orientation and shape discrimination. The results indicate that coil-target distance did not vary in a manner that explains the observed patterns of TMS on performance. Error bars represent the s.e.m.*

220

In order to assess whether differences in the coil-target distances could explain the effects of TMS on discrimination and reaction times a 2 x 3 repeated measures ANOVA was conducted with conditions Task (orientation & shape) and Site (CON, LO1 & LO2). There was neither a significant effect of Task ($F_{(1, 11)}$ = 2.607, p = 0.135), nor Site ($F_{(2, 22)}$ = 0.135, p = 0.757), nor Task x Site interaction ($F_{(2, 22)}$ = 2.391, p = 0.165). Given the lack of significant main effects and interaction, one-way ANOVAs for each task were not conducted. There is no evidence that the slight differences in coil-target distances account for the effects of TMS on discrimination or reaction times.

7.6.5.2:   Coil -Target Orientation

Coil orientation provides a measure of the difference between the coil orientation and the vector joining the calibration point of the coil and the TMS target. The group averaged coil-target orientations for all TMS sites and tasks are plotted in Figure 7.9. Inspection of Figure 7.9, reveals two interesting patterns of results. First, the mean coil-target orientations are largely equivalent across sites and tasks. Second, the mean coil-target orientations are further from the optimum orientation of 90° than reported in previous Chapters, where in general coil-target orientations clustered around 90°.
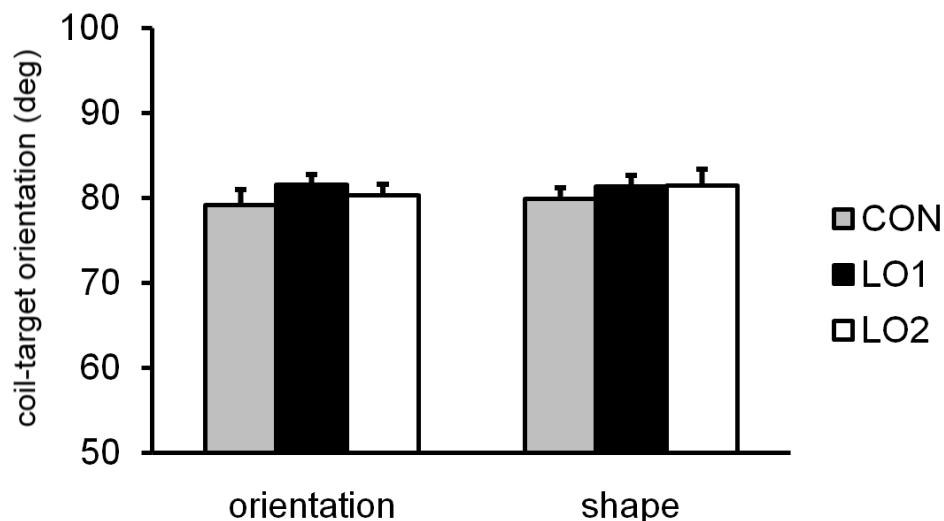
Figure 7.9: *Mean coil-target orientation during chromatic orientation and shape discrimination. The results indicate that each cortical target was stimulated at very similar orientations across both tasks. Interestingly, the orientations are less than optimum (90°) across all conditions. Error bars represent s.e.m.*

A 2 x 3 repeated measures ANOVA with conditions Task (orientation & shape) and Site (CON, LO1 & LO2) was conducted in order to assess the influence of coil-target orientation. There was neither a significant effect of Task ($F_{(1, 11)}$ = 1.706, p = 0.200), nor Site ($F_{(2, 22)}$ = 0.073, p = 0.359), nor Task x Site interaction ($F_{(2, 22)}$ = 0.219, p = 0.805). Given the lack of significant effects, one-way ANOVAs for each task were not conducted. Despite the non-optimum coil-target orientations across sites and tasks, there is no evidence that differences in coil-target orientation contributed to the effects of TMS on discrimination performance or reaction times.

7.7:   Discussion

In this study, TMS pulses were applied to LO1 and LO2 in order to assess whether they contain cue-invariant representations of orientation and shape. Specifically, TMS was applied to LO1 and LO2 to measure its effects on performance of two visual tasks; chromatic orientation and shape discrimination, respectively. The delivery of TMS produced several interesting patterns of results. First, TMS of LO1 and LO2 did not lead to selective disturbances to chromatic orientation and shape discrimination, respectively; a pattern of results inconsistent with either the serial or parallel predictions. This pattern is also in direct contrast to the results reported in Chapter 6. Additionally, neither chromatic orientation nor shape discrimination was effected by TMS of any site relative to the no TMS condition, ruling out a generalised effect of TMS. Second, the effect of TMS of LO1 and LO2 resulted in longer reaction times during orientation and shape discrimination respectively. These results need to be considered carefully however, as they may be associated with speed-accuracy tradeoffs. Taken together, the data provide limited evidence for cue-invariant representations within LO1 and LO2. These findings were immune to differences in the spatial relationships between the stimulating coils and the cortical targets.

7.7.1:   Lack of Chromatic Processing in Lateral Occipital Cortex

It is important to reflect that the data reported here are inconsistent with either the serial or parallel predictions for the effects of TMS. Moreover the data are in direct contrast with those reported in Chapter 6 for achromatic processing of orientation and shape, despite both studies comprising the same methodology and stimuli. It appears that the speciailisations for orientation and shape exhibited by LO1 and LO2 are highly dependent on the manner with which these stimuli are defined – this is the opposite of cue-invariance.

Taken at a first glance, the discrimination data reported in the current study can be seen to be consistent with a number of studies from several different paradigms. To begin, recall that in human, the majority of evidence for chromatic processing highlights the importance of ventral occipital regions. Achromatopsia, a deficit in colour vision is most commonly associated with lesions to ventral occipital cortex (Meadows, 1974; Zeki, 1990; Heywood & Cowey; Kennard et al., 1995; Clarke et al., 1998). The results of studies using neuroimaging techniques including PET (Lueck et al., 1989; Zeki et al., 1990 and fMRI (Mckeefry & Zeki, 1997; Bartels & Zeki, 2000; Brewer et al., 2005; Wade et al., 2008) are largely consistent with the neuropsychological evidence suggesting that ventral occipital regions and V4 in particular play a critical role in the cortical processing of chromatic signals.

Evidence from several paradigms has investigated the role of lateral occipital cortex (including LO1 and LO2) in the processing of chromatic information. First, neuropsychological evidence highlights that damage to LO although impairing visual object and shape recognition, leaves colour processing and colour discrimination relatively unaltered (Cavina-Pratesi et al., 2010). Indeed, patient DF, performed at chance levels on shape discrimination tasks, but was significantly above chance on tasks that required colour or texture discriminations to be made. Moreover, these spared texture and colour processing abilities were contrasted with a second Patient (MS), who presented with bilateral ventral occipital lesions and was severely impaired at both colour and texture discriminations, but was relatively unimpaired during shape discrimination (Cavina-Pratesi et al., 2010). Very recently, it has been reported that fMRI responses to chromatic stimuli in patient DF are largely consistent with aged-matched controls (Bridge et al., 2013). The above chance colour discrimination observed in DF, despite extensive LO lesions, could be

interpreted as evidence against a role for LO in chromatic processing. Taken within this context the lack of a disruptive effect of TMS following stimulation of LO1 and LO2 could be seen as consistent with the evidence from DF.

Second, several fMRI experiments highlight a lack of chromatic processing in LO. Wade and colleagues conducted an extensive study comparing the chromatic sensitivity in macaque and human using fMRI. In human, chromatically preferring regions of cortex were largely confined to ventral occipital regions, a pattern not found in macaques. Intriguingly, there were no significant chromatically preferring voxels in dorsal and lateral regions of cortex during single subject analyses (n = 7). Moreover, only following a more powerful surface-based group analysis did a small dorsal island of colour selectivity appear. A general lack of chromatic processing in LO, is further refined by two studies that investigated chromatic processing within individual visual field maps, including LO1 and LO2. Brouwer & Heeger (2009) employed a number of MVPA fMRI analysis techniques to decode and reconstruct colours from the pattern of BOLD responses measured across visual cortex. Stimulus colour was only correctly classified (above chance) in 2/5 subjects across both LO1 and LO2, compared to significantly above chance classification in V1, V2, V3, V4 & VO1. The inability to accurately decode stimulus colour from signals in LO1 and LO2 suggests that chromatic signals are not present within these visual field maps and offers a potential explanation for the lack of a disruptive effect of TMS on discrimination performance reported here. A further study demonstrated a clear preference for chromatic stimuli in ventral occipital regions, with little or no chromatic preferences in LO1 or LO2. Indeed, group averaged colour responses in LO1 and LO2 were lower in magnitude than all other visual areas tested, except V3A (Goddard et al., 2011). The fact that TMS to LO1 and LO2 did not lead to disturbances in chromatic orientation and shape processing could be interpreted as consistent with the lack of chromatic processing in general measured within these regions of cortex.

Third, the accuracy data reported here are consistent with a previous study that investigated the role played by LO in colour discrimination (plus other tasks) (Ellison & Cowey, 2006). During colour discrimination, subjects were presented with three coloured squares (each subtending 1° x 1°) with one square positioned 5° to the left of the vertical meridian (along the horizontal meridian) and two further squares positioned 4° either side

of the horizontal meridian (one above, one below). Subjects were required to select which of the two vertically displaced squares matched the colour of the central square. TMS of LO during colour discrimination did not disrupt discrimination performance. Importantly, the shape discrimination task employed in the current study was contingent on the colour of the stimulus, a feature that was absent from the previous TMS experiment, in which the colour task was a stand-alone chromatic discrimination task. Nevertheless the data reported here are consistent with the results of Ellison & Cowey (2006), but extend them by showing that TMS of LO1 and LO2 did not lead to significant disturbances in orientation and shape processing despite both tasks being contingent on colour.

One interpretation of the current TMS data, which is consistent with the evidence reported above, is that LO1 and LO2 are specialized for achromatic over chromatic orientation and shape (Mullen et al., 2007). Mullen and colleagues investigated the selectivity of visual cortex to   L-M cone-opponent and achromatic stimulation using fMRI. Early visual areas V1-V4, exhibited robust responses to colour, although a clear preference for colour was only apparent in a region of ventral occipital cortex anterior of V4. Additionally, two regions on the dorsal and lateral surfaces exhibited robust and preferential responses to achromatic over chromatic stimulation. The locations of these areas were suggested to show considerable overlap with V3A and V5/MT, two cortical areas known to play causal roles in the perception of visual motion (Zihl et al., 1983; Zeki, 1990; Walsh et al., 1998; McKeefry et al., 2008). The authors suggest that these two regions form part of a functional network of dorsal and lateral areas that have receive strong magnocellular inputs. Of note, these locations were based on transforming the peak voxel in each area into Talairach space. As previously mentioned, LO1 and LO2 are located in close proximity to V3A (posterioraly) and V5/MT (anteriorly) and therefore, the achromatic selectivity exhibited by these regions may extend into LO1 and LO2. The data reported in Chapters 4-6 certainly suggest that LO1, LO2 and V5/MT play causal roles in processing of achromatic visual features and thus, provides evidence for strong magnocellular input to these regions. Importantly however, the equivalent achromatic measurements were not taken for all 12 subjects, making conclusions regarding the achromatic *versus* chromatic selectivity, and by extension magnocellular *versus* parvocellular inputs within LO1 and LO2 problematic. An

important goal for future research would be to compare directly the effects of TMS during both achromatic and chromatic visual tasks.

LO1 and LO2 appear therefore, not to be causally involved in the processing of chromatic orientation and shape. Visual areas antecedent in the visual hierarchy of LO1 and LO2 have been shown previously to be involved in the joint encoding of colour and orientation (Clifford et al., 2003; Engel, 2005; Seymour et al., 2009; 2010; McDonald et al., 2010). Indeed, combined colour and orientation selectivity has been reported in areas V1-V4. The encoding of colour and orientation may be resolved prior to signals reaching LO1. In addition, regions of the LOC have been shown to encode shapes defined by chromatic signals (Grill-Spector et al., 1998; 1999, Self & Zeki, 2005; Cavina-Pratesi et al., 2010). The selective processing for colour defined shapes however, was localised to ventral regions of the LOC, whereas our LO2 targets are located on the lateral and dorsal aspect of the LOC. The processing of chromatic shape may therefore, take place in regions of cortex anterior and ventral of LO2.

Limited, rather than absent selectivity may offer an alternative account for these data. That is, despite the lack of an effect on percent correct, if more sensitive measurements of behavior, such as adaptation or changes in the slope/shape of psychometric functions were employed, the effects of TMS of LO1 and LO2 on chromatic processing may emerge.

7.7.2: *Possible Mechanisms Underpinning the Effects of TMS on Reaction Times*

An intriguing result was that TMS of LO1 and LO2 induced a pattern of reaction times that were longest during orientation and shape discrimination, respectively. These data require careful consideration. The longer reaction times may be associated with increased performances during these conditions. Indeed for orientation discrimination, performance was higher following TMS of LO1 relative to TMS of LO2. Likewise for shape discrimination, performance was improved following TMS of LO2 relative to TMS of LO1. The increased reaction times may under-pin the better performances in these conditions, rather than indicating a role for LO1 and LO2 in chromatic processing. One interpretation of the reaction

time data relates to the temporal processing of chromatic information. Evidence from behavioural, neuroimaging and neurostimulation studies indicate that chromatic signals are processed more slowly than achromatic signals, with Parvocellular cells responding more slowly than their Magnocellular counterparts (Livnigstone & Hubel, 1988; Burr, Fiorentini & Morrone, 1998). Regan and He (1995) measured the electrical and magnetic time-courses for chromatic and luminance processing and found the processing of chromatic singles to be delayed with respect to the processing of luminance signals by approximately 100-160ms. The delay in chromatic processing has also been reported from MEG recordings in V1 (Fylan, Holliday, Singh, Anderson & Harding, 1997). Beaudot & Mullen (2001) investigated the temporal mechanisms of chromatic and luminance processing during a contour-integration task, which required the linking of orientations across space. A delay in reaction times was evident between the achromatic and chromatic contour integration tasks, with achromatic contour integration being detected more quickly. Finally, TMS of both occipital cortex and temporal-parietal-occipital junction (TPO) was reported to maximally disrupt performance on a colour-defined-form task when TMS pulses were delivered on average 120 and 127ms post stimulus onset, respectively (Anand, Olson & Hotson, 1998). Taken in the context of these findings it is possible that, given the adopted TMS protocol, TMS pulses were delivered to LO1 and LO2 prior to the arrival of chromatic signals, thereby rendering the disruptive effects of TMS mute. Recall that TMS pulses were always delivered with the onset of the test stimuli. It is possible therefore, that the chromatic signals were processed in LO1 and LO2 post TMS stimulation, offering a potential mechanism for the lack of effect of TMS on discrimination.

Given the evidence reported above, a likely candidate for the preliminary processing of chromatic information is V4. Indeed, chromatic, orientation and shape (curvature) sensitive responses have been reported in both macaque (McAdams & Maunsell, 1999; 2000) and human (Zeki et al., 1991; Fang, Murray, Kersten & He, 2005; Engel, 2005; Wilkinson, James, Wilson, Gati, Menon & Goodale, 2000) ventral occipital regions, including V4. Advancements on the current work could potentially elucidate the interactions between these regions. First, varying the delivery of TMS pulses relative to the onset of the visual stimuli could potentially inform as to the temporal window within which chromatic signals are present within LO1 and LO2. Second, a relatively recent study suggests that TMS

stimulation of V4 may be possible (Banissy, Walsh & Muggleton, 2012), providing an opportunity to study the timing of chromatic processing within this region.

The temporal encoding of chromatic signals offers a potential mechanism for the lack of effect following TMS of LO1 and LO2, although a more parsimonious explanation may reflect the lack of cue-invariance within these visual field maps, discussed below.

7.7.3:   Cue-Invariance in LOC, but not LO1 or LO2

Despite the lack of evidence for chromatic processing in LO (including LO1 and LO2), several pieces of evidence suggest the presence of cue-invariant representations within macaque and human visual cortices. In macaque, cue-invariant responses have been reported within early visual areas (V-V4) (Leventhal et al., 1995; 1998) and also higher level areas, such as IT, the 'putative' macaque homologue of human LOC (Vogels & Orban, 1996; Tanaka et al., 2001; Kriegeskorte et al., 2008). In human, cue-invariant responses have been reported in KO (Zeki et al., 2003) as well as the LOC (Malach et al., 2005), both of which are reported to encompass LO1 and LO2 (Larsson & Heeger, 2006). Indeed the LOC has been reported to represent the global shape of stimuli across multiple cues including luminance, texture, illusory contours, motion and colour (Grill-Spector et al., 1998; Grill-Spector et al., 1999; Kastner et al., 2000; Kourtzi & Kanwisher, 2001; Vinberg & Grill-Spector, 2008). The discrimination data reported here is inconsistent with the reports of cue-invariance in the LOC. The cue-invariance observed previously in the LOC may occur in anterior and ventral regions further progressed along the visual hierarchy than LO1 and LO2. The spatial extent of the LOC typically extends beyond the retinotopic boarders of LO1 and LO2 (Sayres & Grill-Spector, 2008), activating more anterior and ventral regions of visual cortex. Indeed, although macaque IT is thought of as the homologue of human LOC, the locus of this homology is likely to be anterior of LO1 and LO2.

Self and Zeki (2005) reported observing shape selectivity within LOC whether defined by motion, colour or their integration. Subjects viewed stimuli that varied in the amount of colour and motion coherence present. Initially, the authors report an area of LOC that was equally responsive to shapes defined by either 100% motion or 100% colour coherence, relative to stimuli that contained 100% coherence, but with no visible shape. The peak shape selective voxel was found to be consistent with previous definitions of the LOC

(Malach et al., 1995; Grill-Spector et al., 1998; 1999; Kourtzi & Kanwisher, 2001). An additional region of LOC was found to be selectively responsive to shapes defined by the integration of motion and colour coherence over shapes defined by a single feature in isolation. A further adaptation experiment revealed that the adaptation observed within this area to shapes defined by alterations in motion and colour coherence was equal to that observed for shapes defined by either cue in isolation, suggesting that this region of LOC indeed contained cue-invariant representations. Sections of the LOC therefore, may contain specialized regions with the potential to respond to their preferred visual feature irrespective of how that feature is defined. The cue-invariant region of LOC reported by Self & Zeki (2005) however, was found to be ventral of previous definitions of the LOC, and therefore is unlikely to overlap with our definitions of LO1 and LO2. Indeed comparisons of the Talairach coordinates for our mean LO1 and LO2 centroids and the shape selective voxels reported by Self & Zeki (2005), depicted in Figure 7.10, support this view.
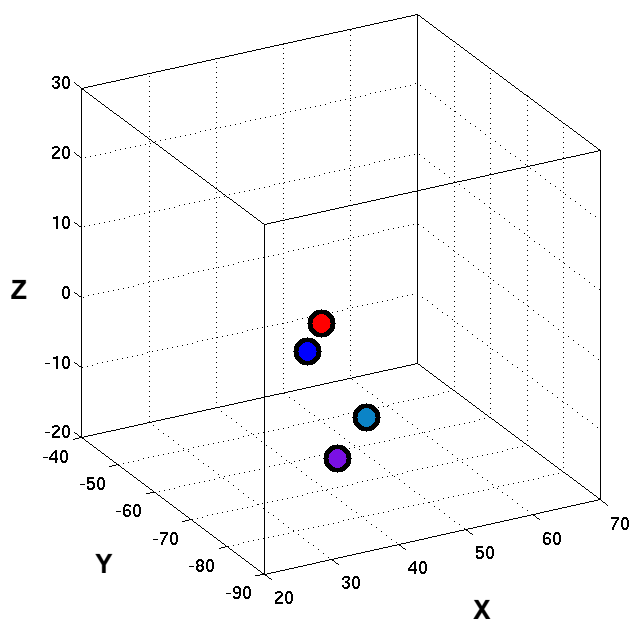
Figure 7.10: *Comparison of the mean LO1 and LO2 centroids and the peak shape selective voxels from Self & Zeki (2005). The centroids of LO1 **(red)** and LO2 **(blue)** in Talairach space are shown. The peak shape selective voxel elicited by the presentation of either 100% motion or 100% colour coherence shapes over non shape 100% coherence arrays **(light blue)** can be seen to be ventral of LO1 and LO2. The peak shape selective voxel to the integration of motion and colour coherence **(purple)** can also be seen to be ventral of LO1 and LO2.*

From Figure 7.10, it is clear that: (1) the motion and colour shape selective LOC voxel falls ventral of our LO1 and LO2 definitions. Indeed relatively large Euclidean distances, (relative to the separation of LO1 and LO2) separate these coordinates (LO1 – peak LOC = ~27mm; LO2 – peak LOC = ~18mm) and (2) the cue-invariant region of the LOC lies further ventral than our LO1 and LO2 centroids. Again relatively large Euclidean distances, separate

these coordinates (LO1 – peak cue-invariant LOC = ~34mm; LO2 – peak cue-invariant LOC = ~26mm). Taken within the context of these findings, the inability to disrupt chromatic orientation and shape processing in LO1 and LO2 may reflect that more ventral and anterior regions of LOC contain cue-invariant representations and not LO1 and LO2. Interestingly, the anatomical location of the cue-invariant patch of LOC reported by Self and Zeki (2005), ventral to LO1 and LO2 is consistent with very recent reports of additional visual field maps within LO (Brewer & Barton, 2011). The response properties of these additional maps (LO3-6), reported to be ventral of LO1 and LO2, may become increasingly complex in a hierarchical fashion, beginning with luminance defined edge and curvature detection in LO1 and LO2 and continuing towards cue-invariant representations in latter regions (LO3-6). The retinotopic representations suggested to be common to these maps (LO1-6 are suggested to contain full hemifields, respectively) offers a plausible mechanism for efficient communication of information between these maps, which may facilitate cue-invariance (Kravitz et al., 2013).

The location of our LO1 and LO2 targets relative to previously identified cue-invariant regions, coupled with the lack of effect of TMS on percent correct performance for chromatic processing suggests a lack of cue-invariance in LO1 and LO2. The data reported here are in contrast with the highly selective effects reported for achromatic orientation and shape and suggest a lack of cue-invariant representations within LO1 and LO2.

7.8:   Conclusion

The results of the current study are mixed. TMS of LO1 and LO2 during chromatic orientation and shape discrimination did not induce the selective disturbances predicted by either the serial or parallel predictions. Moreover the data run against those reported in Chapter 6 for achromatically defined stimuli. The increase in reaction times is potentially misleading and could be susceptible to the presence of speed accuracy tradeoffs. Taken as a whole, the discrimination results reported here, coupled with those reported in Chapters 4-6 suggest specialized roles for LO1 and LO2 in the processing of achromatic orientation and shape, making the presence of cue-invariant representations within LO1 and LO2 unlikely.

Chapter 8

General Discussion

8.1:   Overview

Human visual cortex contains regions that exhibit functional specializations for the processing of different visual features (Lueck et al., 1989; Zeki, 1990; Zeki et al., 1991) and object categories (Malach et al., 1995; Kanwisher et al., 1997; Epstien & Kanwisher, 1998; Pitcher et al., 2009). Why and, possibly more importantly, how these functional specializations emerge, remains poorly understood. One organisational feature of human visual cortex that has only relatively recently emerged, is the presence of multiple retinotopic subdivisions within larger functionally selective regions of cortex (Larsson & Heeger, 2006; Wandell et al., 2007; Arcaro et al., 2009; Amano et al., 2009). These visual field maps may in turn perform unique visual computations (Zeki, 1990) of low-level visual properties, which when combined (Op de Beeck & Kanwisher, 2008), allow complex visual forms to be encoded efficiently (Kravitz et al., 2013). A crucial step therefore, is to establish what role (if any) these individual visual field maps play in visual perception. This thesis has focused on using TMS to elucidate the functional specializations present within several retinotopic subdivisions of lateral occipital cortex. Through the combination of fMRI visual field mapping and TMS, functional specializations for the processing of orientation, motion and shape have been demonstrated. The following sections outline the principle findings from the thesis and the implications they have for our understanding of the cortical organisation of visual function.

8.2:   Retinotopic Features of Lateral Occipital Cortex

In order to complete the current body of work, reliable identification of LO1 and LO2 in individual subjects was necessary. This presented a substantial challenge. Previous reports documented high levels of individual variation in anatomical location and reliability of LO1 and LO2 (Larsson & Heeger, 2006; Sayres & Grill-Spector, 2008). Indeed, LO1 and LO2 were originally identified in just over 50% of hemispheres tested (Larsson & Heeger, 2006). Throughout the entirety of the thesis, LO1 and LO2 continued to be reliably identifiable, with successful delineation of these maps in ~90% of tested hemispheres. The reasons behind this higher identification rate are difficult to determine definitively, but may reflect the retinotopic protocols

231

adopted. For example, in their original paper, Larsson and Heeger employed a 45° wedge stimulus with an angular extent of 6°. A recent study reported that neurons within LO (the region of cortex encompassing LO1 and LO2) have large receptive fields (Dumoulin & Wandell, 2008) with sensitivities that extend beyond the areas stimulated by Larsson and Heeger, which has led some researchers to suggest that Larsson and Heeger systematically underestimated the size of LO1 and LO2 (Dumoulin & Wandell, 2008). The retinotopic mapping experiments conducted throughout the thesis employed a 90° wedge with an angular extent of 15°. The increase in size of the visual stimuli employed during retinotopic mapping likely underpins the higher identification rates.

The visual field representations observed in LO1 and LO2 were consistently demonstrated at both the single subject and group levels in Chapter 3. Furthermore, the retinotopic organisations we observed within LO1 and LO2 are largely consistent with the delineation of lateral occipital cortex suggested by others (Larsson & Heeger, 2006), dividing the expanse of cortex between V3d and V5/MT into two adjacent hemifield maps. The retinotopic organisation of LO1 and LO2 described in this thesis runs contrary to an alternative model suggested by Hansen and colleagues (Hansen et al, 2007). This model makes two assumptions. The first is that V4 contains an upper quadrant representation only, rather than the hemifield representation often reported (McKeefry & Zeki, 1997). Second, LO1 is suggested to contain a lower quadrant representation, which when combined with V4, completes the hemifield map. The visual field coverage we measured in these two areas argues against the split V4 model. In essence, whereas in macaque cortex the combination of V4v and V4d constitutes a full hemifield map, in human, both V4 and LO1 contain full hemifield representations and therefore, it is improbable that they constitute the ventral and dorsal components of a single visual area (Zeki, 2003). Instead the data support the delineation of dorsal cortex by Larsson & Heeger (2006) and the delineation of ventral cortex suggested by Zeki and colleagues (McKeefry & Zeki, 1997). The representations in LO1 and LO2 relative to the position of our visual stimuli are important. If LO1 were a lower quadrant map, as Hansen as colleagues suggest, then the action of TMS of LO1 could only have disrupted half of the stimulus representations.

The use of fMRI visual field mapping was essential to the work described in this thesis, without which reliable and precise identification of LO1 and LO2 would not have been possible. Although LO1 and LO2 show some adherence to common gyral and sulcal patterns (demonstrated by retinotopic structure following surface-based averaging), these maps also show individual

variations in location and orientation (Larsson & Heeger, 2006), making individual identification through fMRI essential. Indeed, the results from Sack et al., (2009) demonstrate the advantages of fMRI-guided TMS over other identification techniques, including structural MRI, group averaged Talairach/MNI coordinates and the EEG 10-20 method. Combining fMRI visual field mapping with TMS provides the opportunity to investigate the properties of individual visual field maps and probe the visual system at not only a causal level, but also a finer spatial scale than that made possible by many standard fMRI paradigms.

8.3: Functional Specializations & Parallel Processing Revealed within Subdivisions of Lateral Occipital Cortex

The results reported in this thesis make several novel contributions to our understanding of the functional specializations present within human lateral occipital cortex. The uniform three-stage approach of: (1) identification of cortical targets through a combination of anatomical (V5/MT) and functional (LO1 and LO2) MRI procedures; (2) establishing individual discrimination thresholds for a variety of visual tasks using method of constant stimuli and (3) independent stimulation of cortical targets with TMS, whilst subjects perform visual discriminations at threshold, proved capable of teasing apart the functional specializations exhibited by our cortical regions of interest, despite their close anatomical proximity to one another. Through the use of TMS, the current body of work builds on previous fMRI research regarding LO1 and LO2, and the neuroimaging and neurostimulation studies of V5/MT, by demonstrating specialized roles for LO1, LO2 and V5/MT in the perception of low-level visual attributes of orientation, shape and motion, respectively.

First, the results of the motion discrimination experiments reported in Chapters 4 and 5, add to the large body of work from neuropsychological (Zihl et al., 1983), neuroimaging (Zeki, 1990, Zeki et al., 1991) and neurostimulation (Beckers & Homberg, 1992; Walsh et al., 1998; McKeefry et al., 2008) studies demonstrating the specialized role played by V5/MT in the perception of motion. Second, the effects of TMS during orientation discrimination, reported in Chapters 4-7, demonstrate that LO1 represents an extrastriate cortical area specialized for the processing of static orientation. The orientation specialization exhibited by LO1 was demonstrable across three independent TMS studies, providing evidence for the reliability of this effect. Third, the data reported Chapter 6 revealed, for the first time, a causal link between neural activity

within LO2 and the accurate processing of shape, based on changes in curvature. The computations of curvature performed by LO2 are more complex than those of orientation performed by LO1. Larsson and Heeger (2006) suggested that a hierarchy of increasingly sophisticated computations existed within lateral occipital cortex. The shape processing observed in LO2 could be interpreted as consistent with this hierarchical processing.

The specializations exhibited by our cortical targets were shown to operate largely independently of one another. Indeed, parallel processing was evident across two different spatial scales. First, specializations were evident for LO1 and V5/MT, which can be considered as two adjacent visual clusters – LO1 can be conceptualised as part of the LO cluster; whereas V5/MT has long been considered a separate motion specific cluster. Second, at a smaller spatial scale, specializations were observed for LO1 and LO2, which constitute adjacent visual field maps within an object-selective cluster. The data are consistent with previous reports of parallelism in human cortex, but extend them in terms of the spatial scale at which this parallelism is expressed. In order of spatial scale, previous demonstrations of parallelism include the delineation of visual cortex into dorsal and ventral processing streams (Perenin & Vighetto, 1988; Goodale et al., 1991), the identification of independent and close proximity category-selective areas (Malach et al., 1995; Kanwisher et al., 1997; Epstien & Kanwisher, 1998; Taylor et al., 2007; Pitcher et al., 2009) and the emergence of visual field map clusters

The results reported in Chapters 4-5 are consistent with the idea that adjacent visual clusters perform independent computations (Wandell et al., 2005). The double dissociation observed between LO1 and V5/MT, demonstrates that orientation and motion are computed independently in separate (close proximity) clusters. The double dissociation also extends the evidence in favour of parallel processing at the level of V5/MT. The parallel processing evident at the level of V5/MT is likely underpinned by parallel anatomical routes from antecedent and even subcortical (Sincich et al., 2004) areas. The results reported in Chapter 6 go one step further by demonstrating parallel processing at the level of adjacent field maps within a cluster. The results indicate that LO1 plays a causal role in orientation, but not shape processing and LO2 plays a causal role in shape, but not orientation processing. The pattern of results suggests a hierarchy of increasingly sophisticated computations performed by the retinotopic subdivisions of LO. This finding is consistent with previous proposals (Larsson & Heeger, 2006), but differs in that this hierarchy of cortical processing operates largely in parallel, rather than as part of a serial

processing architecture. The more sophisticated shape processing in LO2 is not reliant on the more basic orientation processing in LO1. If computations in LO2 were reliant on those performed by LO1, as they must in a serial framework, TMS of LO1 would have disrupted shape processing. This pattern was not found. Although the data cannot rule out the existence of serial connections, the data provide compelling evidence for parallel processing pathways at this level of the visual hierarchy. Intriguingly, parallel connections from antecedent areas have been found at a commensurate stage in the visual hierarchy of the macaque (Shipp & Zeki, 1989). The demonstration of dissociable functional properties between LO1 and LO2 echoes that found in macaque cortex for visual field maps V4v and V5/MT (Zeki, 1990). Despite the current lack of clear evidence for such pathways in human, it is plausible, at least, to suggest that such pathways may persist and moreover, that these pathways provide a plausible explanation for the parallel processing observed between LO1 and LO2.

8.4:   Lack of Cue-Invariance in LO1 & LO2

An important feature of the specialized and parallel processing reported in Chapters 4-6 is that the visual stimuli used were all luminance-modulated and therefore, achromatic. Chapter 7 aimed to directly assess whether the specializations for achromatic orientation and shape observed within LO1 and LO2 extended to isoluminant chromatic stimuli. Demonstrating such specializations would provide compelling evidence for cue-invariant representations within LO1 and LO2. Indeed, cue-invariant responses have been reported previously within the IT of macaque monkeys (Vogels & Orban, 1996; Tanaka et al., 2001; Kriegeskorte et al., 2008), an area commonly believed to be the macaque homologue of human LOC (Malach et al., 1995). In human, fMRI studies have highlighted the presence of cue-invariant responses within the LOC (Malach et al., 1995; Grill-Spector et al., 1998; 1999; Self & Zeki, 2005; Vinberg & Grill-Spector, 2008).

The pattern of results reported in Chapter 7 ran contrary to not only those predicted, but also those reported in Chapters 4-6. TMS of LO1 and LO2 did not lead to selective disturbances to chromatic orientation and shape discrimination, and although reaction time data hint at effects, those data may be susceptible to speed-accuracy tradeoffs. Overall, the results from the experiments in chapter 7 point to a lack of cue-invariant representations within LO1 and LO2. The LOC, the region of cortex encompassing LO1 and LO2, may well contain regions which exhibit cue-invariant capabilities (Self & Zeki, 2005; Vinberg & Grill-Spector, 2008), however the data reported

here suggest strongly that these representations are not present at the level of LO1 and LO2. A further example regarding the lack of cue-invariance can be seen when comparing the size of the effect following TMS of LO1 during static *versus* moving orientation discrimination. Recall that in Chapter 4, TMS of LO1 induced a significant and selective disturbance to orientation processing relative to all other conditions. This selectivity was statistically robust despite the relatively small sample size (n = 6). In Chapter 5, the effect of TMS of LO1 was found to be markedly weaker, indeed there was no significant effect of site for the orientation task, and it was only following planned contrasts that a significant effect was observed. If LO1's specialization for orientation were cue-invariant, one would predict TMS induced disturbances to orientation processing irrespective of how such orientations were defined. Taken together, the data reported in this thesis argue against the existence of cue-invariant representations within LO1 and LO2, indeed they are heavily in favour of achromatic cue-dependent specializations.

8.5:   Implications for 'high-level' Visual Processing

The findings from this thesis have a number of important implications in terms of the mechanisms by which humans process complex visual forms. A central hypothesis proposes the existence of multiple retinotopically organised divisions within larger category-selective areas. Such an organisation creates a computational framework capable of rapidly and efficiently decoding complex visual forms. This framework not only reduces replicated information between maps, which is biologically expensive to compute (Kravitz et al, 2013), but also, due to the adherence to retinotopic organisation, creates a common mechanism for communication across visual field maps with different specializations (Kravitz et al, 2013). Consider a scenario whereby a cluster within visual cortex contains four visual field maps, each one of which displays a full hemifield representation. If each map within this cluster computes at least one unique feature, then the system has the ability to encode up to four unique visual features, independently, at each point in visual space.

This framework is consistent with previous models that have attempted to explain the emergence of category selectivity on the basis of processing of low-level visual attributes (Op de Beeck & Kanwisher, 2008). Kanwisher and colleagues proposed the existence of large overlapping maps in visual cortex, with each map exhibiting weak selectivity for particular visual features. When encountered with complex stimuli, these overlapping maps were suggested to multiply

their respective selectivities together, allowing the object to be encoded efficiently (Op de Beeck & Kanwisher, 2008).

The data reported in this thesis are consistent with the premise put forward by Kanwisher and colleagues however, instead of these visual features being computed weakly across large, mainly overlapping maps, the data reported here suggests these visual attributes are computed locally in discrete visual field maps that exhibit high levels of functional specialization. Indeed, the level of specialization observed in LO1, LO2 and V5/MT is hard to accommodate within a model of large overlapping maps with weak selectivities.

The pattern of responses across LO1 and LO2 suggests the possibility that the object selectivity observed in LO, simply emerges as a property of the unique and parallel map specific computations that are performed by LO1 and LO2. This interpretation has important implications for the emergence of category-selectivity in several other regions of visual cortex. Very recently, four additional retinotopic maps were reported to exist in lateral occipital cortex (Brewer & Barton, 2011). These additional maps (LO3-6) are suggested to lie ventral to LO1 and LO2 and show considerable anatomical overlap with the location of the OFA (Brewer & Barton, 2011). The presence of these additional LO maps suggest that the pattern of unique and parallel processing identified within LO1 and LO2 extends to LO3-6. If each map in the LO cluster performs unique computations and therefore, contributes uniquely to visual perception then perhaps the category selectivity observed in these larger areas (LO-objects, OFA-faces) emerges from the unique computations performed by their respective retinotopic subdivisions.

A schematic representation of this framework is depicted in Figure 8.1. The left plot of Figure 8.1, depicts the LO cluster, divided into its six putative retinotopic subdivisions. Overlaid onto these maps are larger areas corresponding to the object-selective LO and face-selective OFA. LO comprises LO1 and LO2, with the spatial extent of the OFA encompassing LO3-6. The right of Figure 8.1, depicts hypothetical patterns of activity across the six LO maps to the presentation of two objects and two faces. The patterns of responses across these maps vary as a function of the stimuli they are encoding. Viewed within a framework whereby each map encodes unique visual features, the encoding of objects can thus be accomplished by the pattern of greater activity within LO1 and LO2 relative to the LO3-6 maps. In contrast, the encoding of faces results in a different pattern of results across the maps, with signals in LO3-6 being greater in general than

those in LO1 and LO2. Taken together, these schematics predict that the ability to encode objects and faces emerges from the pattern of unique specializations for low-level visual attributes present within the retinotopic subdivisions of these larger category-selective areas.
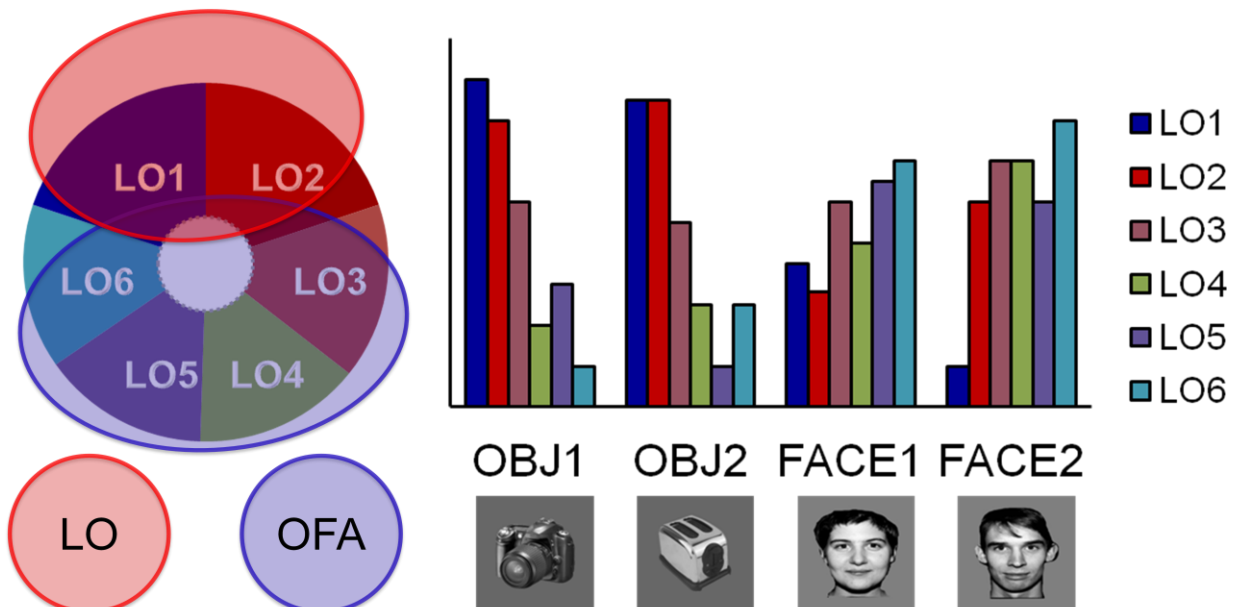
Figure 8.1: *Schematic representation of retinotopically driven object and face selectivity.* ***Left:*** *A schematic of the six retinotopic subdivisions (LO3-6) within the LO cluster. Object-selective LO* ***(green oval)*** *and face-selective OFA* ***(red oval)*** *can be seen to encompass these maps.* ***Right:*** *Hypothetical patterns of activity across the six LO maps to two objects and two faces. The category of object could be derived from the pattern of activity across these maps, rather than reflecting a large region responding heterogeneously. Each map may encode a unique visual feature, which when combined allows category-selectivity to emerge.*

8.6:   Future Directions

Until very recently, the retinotopic organisation ventral of LO1 and LO2 remained largely uncharacterised. Indeed inspection of Figure 8.2 (taken from Wandell et al., 2007) illustrates a cluster of 'non-retinotopic' cortex ventral of LO1 and LO2 on the lateral surface of the brain (black arrow). Intriguingly, this area of cortex is surrounded by retinotopic maps posteriorly (V3d, V2d, V1), anteriorly (V5/MT), dorsally (LO1, LO2, V3A, V3B, IPS-0-4) and ventrally (V2v, V3v, V4, VO1, VO2).
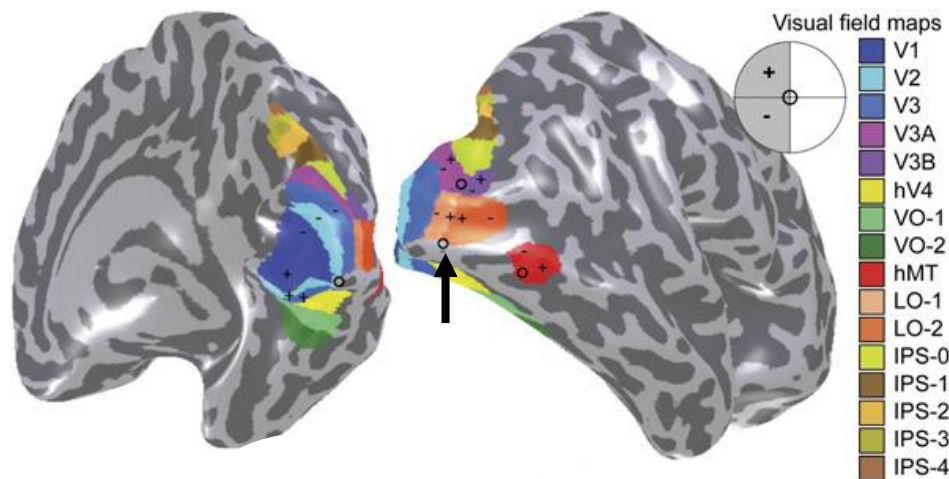
Figure 8.2: *Known visual field maps in human cortex in 2007. Visual field maps are shown on medial **(left)** and lateral **(right)** views of the right hemisphere of a single subject. Multiple representations of the visual field are evident (see key far right). Intriguingly, there is a region of uncharacterised (retinotopically) cortex ventral of LO1 and LO2 (tip of black arrow). This region of cortex is in close proximity with functional definitions of the OFA. Since 2007, more visual field maps have been identified, with two maps in the V5/MT complex (TO1 & TO2), and two maps within the PPA (PHC1 & PHC2) Adapted from Wandell et al (2007).*

The anatomical location of LO3-6 is in very close proximity to functional definitions of the OFA. This proximity suggests that like LO, the OFA may also contain multiple retinotopically organised subdivisions. Inspection of the retinotopic data acquired throughout the thesis revealed evidence for LO3-6 in a subset of individuals (n = 5, see appendix for delineation of LO3-6 in each individual). Within those individuals, the visual field representations were largely consistent with previous proposals (Brewer & Barton, 2011). Figure 8.3 illustrates the retinotopic organisation of the LO1-6 maps in a single subject. The LO3-6 maps were found to fall ventral of LO1 and LO2. Moving ventrally and rotating clockwise from the anterior boundary of LO2 four more hemifield representations are evident. The proposal suggests that LO3 begins at the anterior boundary of LO2 and shows a gradual progression from the lower vertical meridian to the upper vertical meridian. LO4 is the mirror-reverse of LO3, with the visual field representations within LO5 and LO6 following the same mirror-reverse configuration. Additionally, a subset of those subjects exhibiting evidence for LO3-6, also participated in experiments investigating higher-level visual representations, such as faces, places and objects. The right plot in Figure 8.3 depicts the correspondence between visual field maps LO3-6 and functional definitions of the OFA in a single subject. Intriguingly, functional definitions of the OFA (Faces > scrambled faces) show a high anatomical correspondence with the location of LO3-6. These data, albeit in preliminary form,

suggest as others have, that the OFA may be retinotopically organised. If so, the unique and parallel pattern of processing observed in LO1 and LO2 may extent to these additional maps. Characterising the reliability with which LO3-6 can be identified, coupled with a formal assessment of their overlap with the OFA are crucial stages for future work.
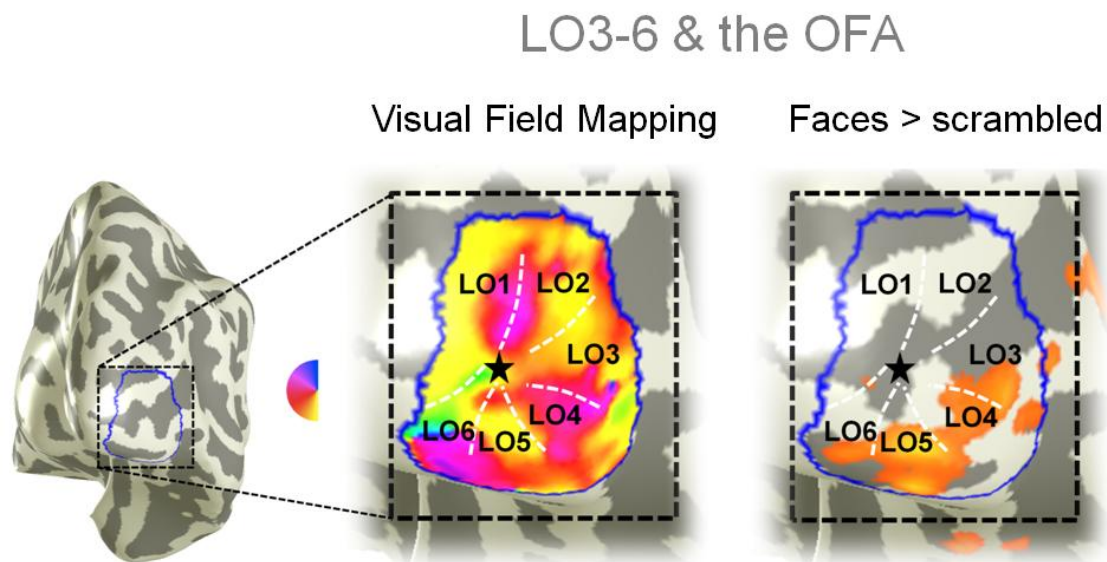
Figure 8.3: *Visual field maps LO1-6 and the OFA. A partially-inflated surface reconstruction of the right hemisphere of a single subject is shown (**left**). The hemisphere is viewed from behind. The black dashed box focuses on the posterior and lateral surface of the occipital lobe and encompasses the lateral occipital cortex (**blue outline**). The organisation of visual field maps within the LO are shown (**middle**). Data have been restricted to the LO cluster for clarity. LO1 and LO2 can be seen at the most dorsal point of the LO cluster. Moving ventrally from the anterior boundary of LO2, at the representation of the lower vertical meridian (yellow) an additional four visual field reversals can seen running clockwise. LO3 is the mirror-reverse of LO2 and this pattern continues through to LO6. The star indicates the representation of the fovea. The responses to images of faces > scrambled faces is shown (**right**). The anatomical location of this face-selective cluster is consistent with functional definitions of the occipital face area (OFA). The visual field boundaries (dashed white lines) delineating LO1-6 are overlaid onto the same anatomy. The OFA shows a high level of overlap with the visual field maps LO3-6.*

8.7: Conclusions

Through the relatively novel approach of retinotopic fMRI-guided TMS, this thesis has elucidated the functional specializations present within several retinotopic subdivisions of human lateral occipital cortex. Across a number of visual tasks LO1, LO2 and V5/MT were found to exhibit specializations for orientation, shape and speed, respectively. Our cortical targets of interest exhibited these specializations largely independently from one another, providing evidence for parallel processing at the spatial scales of adjacent clusters within human visual cortex and at the relatively unachieved spatial scale of adjacent visual field maps within a cluster.

Taken together, the data reported in this thesis suggest that the category-selectivity exhibited by many regions of cortex, may simply emerge from patterns of unique and low-level visual computations performed by individual visual field maps that subdivide such regions. Mutual retinotopic information and parallel processing not only reduces replicated information across maps, which is biologically expensive to compute, but also, provides a common mechanism for communication between maps with different specializations.

Appendices

A.1:   Motion-Selective Responses in Visual Cortex

In order to assess the reliability of our anatomical definitions of V5/MT, we analysed, in a subset of subjects (n = 4), the correspondence with functional definitions of V5/MT. These subjects participated in an fMRI motion localiser. There were two conditions: Static and motion. A central black fixation dot (diameter 0.3°) remained throughout the experiment. Subjects viewed two sinusoidal gratings (diameter 4°), presented in a circular aperture. Stimuli were centred at 10° eccentricity along the horizontal meridian into both the left and right visual fields. A standard block design was used (12sec on/12sec off). Static and motion blocks were alternated. Grating stimuli were orientated at 45°. During motion blocks, grating stimuli drifted at 8°/sec, the direction of drift (left-right/right-left) alternated every 3sec. Each block was repeated 10 times.

Structural and Functional MRI Protocols: Multi-average, whole-head T1-weighted anatomical volumes were acquired for each subject (TR = 7.8ms, TE = 3ms, TI = 450ms, FOV = 290 x 290 x 176, matrix = 256 x 256 x 176, flipangle = 20°, 1.13 x 1.13 x 1.0mm^3). **Functional data 8 channel:** Gradient recalled echo pulse sequences were used to measure T2* BOLD data (TR = 2000ms, TE = 30ms, FOV = 192cm, 64 x 64 matrix, 26 contiguous slices with 3mm slice thickness).

fMRI data analysis: Data analysis was performed in Matlab using the mrVISTA fMRI analysis package, part of the Vista toolbox (www.white.stanford.edu/software/). Functional volumes were motion corrected using FSL's MCFLIRT. Images were also corrected for spatial inhomogeneity. The EPI volumes were initially aligned to individual high-resolution anatomical volumes manually and subsequently refined with automated procedures. This procedure allowed the parameters derived from the analysis of the functional data to be visualised on the inflated cortical surfaces. Data were analysed using a general linear model (GLM) to determine regions of cortex differentially active during the motion compared to static blocks. Statistical maps were thresholded statistical at p = < 0.001, uncorrected. The mean time series across conditions within the V5/MT ROI was calculated for each subject along with the mean percentage signal change.

A.2: Object-Selective Responses in Visual Cortex

In order to assess the object-selective responses in LO1 and LO2 an fMRI LOC localiser was conducted on a subset of subjects (n = 6). There were three conditions: faces, objects and scrambled versions of the same stimuli. Images were all greyscale. Images from each condition were presented in a blocked design with ten images in each block. Each image was presented for 700ms, followed by 200ms fixation. Blocks were separated by a 9sec fixation screen. Each condition was repeated four times in a counterbalanced fashion. Subjects were required, whilst maintaining central fixation, to detect the presence of a red-dot that was superimposed onto some of the images.

Structural and Functional MRI Protocols: All imaging experiments were performed using a GE 3-tesla HD Excite MRI scanner at York Neuroimaging Centre at the University of York. An 8-channel phase array head coil was used in conjunction with a birdcage, radio-frequency coil tuned to 127.4 MHz. A gradient-echo echoplanar imaging (EPI) sequence was used to collect data from 38 contiguous axial slices [time of repetition (TR) = 3, time of echo = 25 ms, field of view = 28 × 28 cm, matrix size = 128 × 128, slice thickness = 4 mm]. These were coregistered onto a T1-weighted anatomical image (1 × 1 × 1 mm) from each participant. To improve registrations, an additional T1-weighted image was taken in the same plane as the EPI slices.

fMRI data analysis: Statistical analyses of the fMRI data were performed using FEAT (www.fmrib.ox.ac.uk/fsl). The initial 9sec of data from each scan were discarded to minimise the effects of magnetic saturation. Motion correction was followed by spatial smoothing (Gaussian, FWHM 6 mm) and temporal high-pass filtering (cutoff, 0.01 Hz). Initially, object and face-selective regions of cortex were defined separately in each individual subject by computing the following contrasts (1) objects > scrambled objects and (2) faces > scrambled faces. Statistical images were thresholded at $P < 0.001$ (uncorrected). In each individual subject, LO1 and LO2 ROIs were transformed from the grey-matter surface reconstructions back into each subject's native anatomical space. The mean percentage signal change within LO1 and LO2 across blocks was calculated in each subject and averaged together. High-level analyses were also performed using FEAT. The individual

subject analyses were averaged together and registered to the MNI average brain. Statistical images were cluster threholded at Z = 2.3.

A.3: Overlap between LO3-6 & the OFA

In order to assess the correspondence between our retinotopic definitions of LO3-6 and the functional definitions of the OFA, we analysed in a subset of subjects (n = 5), the regions of cortex maximally responsive to faces. The structural and functional parameters, along with the stimuli employed for these experiments, were identical to the procedures outlined in Appendix 2. fMRI data analysis was conducted in mrVista, allowing the results derived from the retinotopic and face localiser experiments to be overlaid onto the same anatomical grey-matter surface reconstructions. Functional volumes were motion corrected using FSL's MCFLIRT. Images were also corrected for spatial inhomogeneity. The EPI volumes were initially aligned to individual high-resolution anatomical volumes manually and subsequently refined with automated procedures. This procedure allowed the parameters derived from the analysis of the functional data to be visualised on the inflated cortical surfaces. Data were analysed using a general linear model (GLM) to determine regions of cortex differentially active during the face compared to scrambled face blocks. Statistical maps were thresholded statistical at p = < 0.001, uncorrected.

Figure A.1, depicts a schematic representation of the spatial layout of LO1-6. LO1 and LO2 are located at the most dorsal section, and run left-right. LO3-6 are located by rotaing about the centre of the cluster in a clockwise manner.
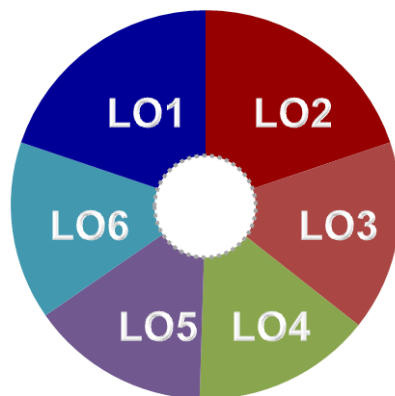
Figure A.1: *Schematic representation of the spatial layout of visual field maps LO1-6. LO1 and LO2 are located at the most superior portion of the LO cluster. Moving ventrally and clock-wise, four additional visual field maps are suggested to exist. LO3-6, along with LO1 and LO2 also contain full hemifield representations of the contralateral visual field. These visual field maps are suggested to form around a central representation of the fovea, depicted by the white circle in the centre. To date the existence of these maps have not been reported in peer-reviewed format.*

The spatial overlap between our retinotopic definitions of LO3-6 and functional definitions of the OFA are plotted in Figure A.2, in each subject. In each case, a surface reconstruction of the right hemisphere is shown from behind. A black dashed box focuses on the posterior and lateral region of the occipital lobe, with the LO cluster outlined in blue. This section is enlarged to the right. Initially, we delineate visual field maps LO1-6 based on representations of the visual field. In each case, the visual field representations within these areas are found to contain (largely) complete hemifield representations of the contralateral visual field. Additionally, we project the results of the face-localiser onto the same anatomical surface reconstructions, including the boundaries between each visual area. In all cases, regions of cortex differentially responsive to face stimuli can be seen to overlap with one or more of the LO3-6 maps. These data, suggest that perhaps like LO, the OFA contains multiple maps of the visual field, which may perform unique and specialized sets of visual computations.
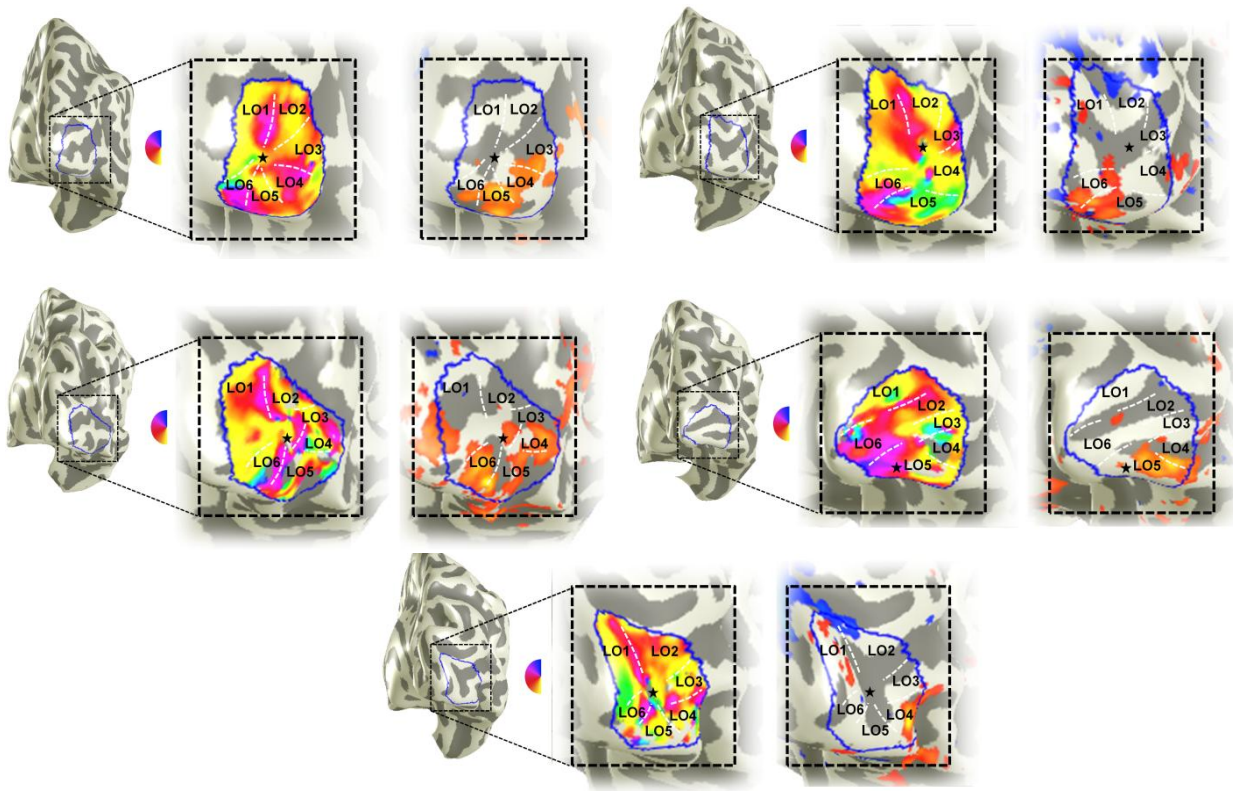
Figure A.2: *Overlap between retinotopic definitions of LO3-6 and functional definitions of OFA. To the left of each plot is a partially-inflated surface reconstruction of the grey-white matter boundary of the right hemisphere. Hemispheres are viewed from behind. The black dashed box focuses on the posterior and lateral aspect of the occipital lobe. The blue outline within the black box highlights the LO complex, and is enlarged to the right. The middle column in each plot depicts the visual field representations within the LO cluster. LO1 and LO2 are clearly delineable in all cases. Moving ventrally from the anterior boundary of LO2, four more reversals in the visual field representation can be seen. These reversals rotate about LO1 and LO2 in a clock-wise fashion. The stars in each plot represent the location of foveal representations derived from eccentricity scans in the same subjects.*

A.4: Minimum Motion & Isoluminant Values

Prior to the collection of psychophysical data, isoluminant thresholds were defined for each subject using the minimum motion paradigm (Anstis & Cavanaugh, 1983; Cavanagh, Tyler & Favreau, 1984). During the isoluminant threshold experiment, subjects viewed a sinusoidal grating presented in a circular aperture (diameter 4°) with a spatial frequency of 2cpd (Figure A.3). The grating stimulus drifted from left-right at a constant speed (8°/sec). The colours of the grating were modulated sinusoidally along the L-M axis. Subjects were required to fixate centrally and modify the luminance of the red channel, until the grating was perceived to exhibit minimum/slowest motion. The value of the red channel was recorded and reset to its default value. This procedure was repeated 10 times for each subject and the mean value of the red channel was calculated and used as a measurement of the isoluminant value.

Figure A.3: *Stimuli used to establish isoluminance using the minumim motion paradigm. Subjects viewed a sinusoidal grating modulated along the L-M axis centred at 10°eccentricity along the horizontal meridian into the left visual field. The grating drifted from left-right at a constant speed (8°/sec) and was at a fixed orientation (45°). Subjects could modify the luminance of the red channel until the grating appeard to slow down/stop. The value of the red channel was then stored and reset. This procedure was repeated ten times per subject.*

Initially a baseline luminance value was defined (baselum = 0.5). Additionally, red and green contour values were also defined (CONR = 0.2; CONG = 0.05) At the onset, the red and green values from which the stimuli ranged were defined as follows;

RedRGB = [(baselum + CONR, baselum – CONG, baselum)], in RBG values = [0.7, 0.45, 0.5]

GreenRGB = [(baselum - CONR, baselum + CONG, baselum)], in RBG values = [0.3, 0.55, 0.5]

Subjects could either increase or decrease the value of the red contour (CONR) in increments of 0.01, by pressing one of two buttons on the keyboard. Subjects adjusted the value of CONR until they perceived the grating stimulus to slow down/stop. The value of CONR was then stored and reset to its default value (0.2). Subjects performed ten repetitions and the mean CONR value was used as the isoluminant threshold value for the red contour. Subsequent stimuli were then specified in terms of the CONG (0.05) and each subjects CONR value. For example, if a CONR value of 0.25 was defined then subsequent stimuli would be defined in terms of RedRGB = [0.75, 0.45, 0.5] and GreenRGB = [0.25, 0.55, 0.5]. The actual red and green values (RGB) presented during TMS are given for each subject in Table A.3.

Table A.1: *Isoluminant values derived from the minimum motion experiment. The values of the red and green channels are given in RGB. The stimuli presented in Chapter 7 were defined by using these values for each subject.*

	Isoluminant values using minimum motion	
Subject	Red Channel (RGB)	Green Channel (RGB)
S6	0.2370	0.0500
S7	0.2290	0.0500
S9	0.2520	0.0500
S11	0.2610	0.0500
S13	0.2940	0.0500
S14	0.1960	0.0500
S15	0.2120	0.0500
S16	0.2970	0.0500
S17	0.2320	0.0500
S18	0.2370	0.0500
S19	0.2320	0.0500
S20	0.2230	0.0500
Average	0.2418	0.0500

References

Adelson, E. H., & Movshon, J. A. (1980). Phenomenal coherence of moving gratings. *Journal of the Optical Society of America, 70*(12), 1605-1605.

Albright, T. D. (1984). Direction and orientation selectivity of neurons in visual area mt of the macaque. *Journal of Neurophysiology, 52*(6), 1106-1130.

Albright, T. D., Desimone, R., & Gross, C. G. (1984). Columnar organization of directionally selective cells in visual area mt of the macaque. *Journal of Neurophysiology, 51*(1), 16-31.

Allen, E. A., Pasley, B. N., Duong, T., & Freeman, R. D. (2007). Transcranial magnetic stimulation elicits coupled neural and hemodynamic consequences. *Science, 317*(5846), 1918-1921.

Amano, K., Wandell, B. A., & Dumoulin, S. O. (2009). Visual field maps, population receptive field sizes, and visual field coverage in the human MT plus complex. *Journal of Neurophysiology, 102*(5), 2704-2718.

Anand, S., Olson, J. D., & Hotson, J. R. (1998). Tracing the timing of human analysis of motion and chromatic signals from occipital to temporo-parieto-occipital cortex: A transcranial magnetic stimulation study. *Vision Research, 38*(17), 2619-2627.

Andrews, T. J. (2005). Visual cortex: How are faces and objects represented? *Current Biology, 15*(12), 451-453.

Andrews, T. J., Clarke, A., Pell, P., & Hartley, T. (2010). Selectivity for low-level features of objects in the human ventral stream. *Neuroimage, 49*(1), 703-711.

Andrews, T. J., Davies-Thompson, J., Kingstone, A., & Young, A. W. (2010). Internal and external features of the face are represented holistically in face-selective regions of visual cortex. *Journal of Neuroscience, 30*(9), 3544-3552.

Andrews, T. J., & Ewbank, M. P. (2004). Distinct representations for facial identity and changeable aspects of faces in the human temporal lobe. *Neuroimage, 23*(3), 905-913.

Andrews, T. J., Halpern, S. D., & Purves, D. (1997). Correlated size variations in human visual cortex, lateral geniculate nucleus, and optic tract. *Journal of Neuroscience, 17*(8), 2859-2868.

Anstis, S., & Cavanagh, P. (1983). A minimum motion technique for judging equiluminance. *Colour Vision.* 165-166.

Arcaro, M. J., McMains, S. A., Singer, B. D., & Kastner, S. (2009). Retinotopic organization of human ventral visual cortex. *Journal of Neuroscience, 29*(34), 10638-10652.

Arcaro, M. J., Pinsk, M. A., Li, X., & Kastner, S. (2011). Visuotopic organization of macaque posterior parietal cortex: A functional magnetic resonance imaging study. *Journal of Neuroscience, 31*(6), 2064-2078.

Bandenttini, P. A., Jesmanowicz, A., Wong, E. C., & Hyde, J S. (1993). Processing stratergies for time-course data sets in functinal MRI of the human brain. *Magn Reson Med, 30*(2), 161-173.

Banissy, M. J., Walsh, V., & Muggleton, N. G. (2012). A disruption of colour priming following continuous theta burst transcranial magnetic stimulation. *Cortex, 48*(10), 1359-1361.

Bartels, A., & Zeki, S. (2000). The architecture of the colour centre in the human visual brain: New results and a review. *European Journal of Neuroscience, 12*(1), 172-190.

Baseler, H. A., Gouws, A., Haak, K. V., Racey, C., Crossland, M. D., Tufail, A., & Morland, A. B. (2011). Large-scale remapping of visual cortex is absent in adult humans with macular degeneration. *Nature Neuroscience, 14*(5), 649-U148.

Beaudot, W. H., & Mullen, K. T. (2001). Processing time of contour integration: The role of colour, contrast, and curvature. *Perception, 30*(7), 833-853.

Beckers, G., & Homberg, V. (1992). Cerebral visual-motion blindness - transitory akinetopsia induced by transcranial magnetic stimulation of human area V5. *Proceedings of the Royal Society B-Biological Sciences, 249*(1325), 173-178.

Beckers, G., & Zeki, S. (1995). The consequences of inactivating areas V1 and V5 on visual-motion perception. *Brain, 118*, 49-60.

Bell, J., Badcock, D. R., Wilson, H., & Wilkinson, F. (2007). Detection of shape in radial frequency contours: Independence of local and global form information. *Vision Research, 47*(11), 1518-1522.

Biederman, I. (1987). Recognition-by-components: A theory of human image understanding. *Psychol Rev, 94*(2), 115-147.

Blakemor.C, & Campbell, F. W. (1969). On existence of neurones in human visual system selectively sensitive to orientation and size of retinal images. *Journal of Physiology-London, 203*(1), 237-&.

Brewer, A. A., Liu, J., Wade, A. R., & Wandell, B. A. (2005). Visual field maps and stimulus selectivity in human ventral occipital cortex. *Nature Neuroscience, 8*(8), 1102-1109.

Brewer, A.A., & Barton, B. (2011). 'Clover leaf' clusters in human visual cortex. *Peception (ECVP 2011,Toulouse, France), 40*, 48.

Bridge, H., Thomas, O. M., Minini, L., Cavina-Pratesi, C., Milner, A. D., & Parker, A. J. (2013). Structural and functional changes across the visual cortex of a patient with visual form agnosia. *Journal of Neuroscience, 33*(31), 12779-12791.

Broca, P. (1861). Remarques sure le siege de la faculte du language articule: suivies d'uneobservation d'aphemie. *Bull. Soc. Anat. Paris*, **6**, 330–357.

Brouwer, G. J., & Heeger, D. J. (2009). Decoding and reconstructing color from responses in human visual cortex. *Journal of Neuroscience, 29*(44), 13992-14003.

Burr, D. C., & Wijesundra, S. A. (1991). Orientation discrimination depends on spatial-frequency. *Vision Research, 31*(7-8), 1449-1452.

Burr, D. C., Fiorentini, A., & Morrone, C. (1998). Reaction time to motion onset of luminance and chromatic gratings is determined by perceived speed. *Vision Research, 38*(23), 3681-3690.

Campbell, F. W., & Kulikowski, J. J. (1966). Orientational selectivity of the human visual system. *Journal of Physiology, 187*, 437–445.

Cavanagh, P., Tyler, C. W., & Favreau, O.E. (1984). Perceived velocity of moving chromatic gratings. *J Opt Soc Am A, 1*(8), 893-899.

Cavina-Pratesi, C., Kentridge, R. W., Heywood, C. A., & Milner, A. D. (2010b). Separate processing of texture and form in the ventral stream: Evidence from fMRI and visual agnosia. *Cerebral Cortex, 20*(2), 433-446.

Charcot, J. (1883). Reprinted in " Leons sur les Maladies du Systeme Nerveux ". *Paris, 3*, 178.

Cichy, R. M., Chen, Y., & Haynes, J. D. (2011). Encoding the identity and location of objects in human LOC. *Neuroimage, 54*(3), 2297-2307.

Cichy, R. M., Sterzer, P., Heinzle, J., Elliott, L. T., Ramirez, F., & Haynes, J. D. (2012). Probing principles of large-scale object representation: Category preference and location encoding. *Human Brain Mapping*.

Claeys, K. G., Dupont, P., Cornette, L., Sunaert, S., Van Hecke, P., De Schutter, E., & Orban, G. A. (2004). Color discrimination involves ventral and dorsal stream visual area. *Cerebral Cortex, 14*(7), 803-822.

References

Clarke, S., Walsh, V., Schoppig, A., Assal, G., & Cowey, A. (1998). Colour constancy impairments in patients with lesions of the prestriate cortex. *Exp Brain Res, 123*(1-2), 154-158.

Clifford, C. W., Spehar, B., Solomon, S. G., Martin, P. R., & Zaidi, Q. (2003). Interactions between color and luminance in the perception of orientation. *Journal of Vision, 3*(2), 106-115.

Cowey, A. (2005). The ferrier lecture 2004 - what can transcranial magnetic stimulation tell us about how the brain works? *Philosophical Transactions of the Royal Society B-Biological Sciences, 360*(1458), 1185-1205.

Cowey, A., & Walsh, V. (2000). Magnetically induced phosphenes in sighted, blind and blindsighted observers. *Neuroreport, 11*(14), 3269-3273.

Damasio, A. R., Damasio, H., & Vanhoesen, G. W. (1982). Prosopagnosia - anatomic basis and behavioral mechanisms. *Neurology, 32*(4), 331-341.

DeYoe, E. A., Carman, G. J., Bandettini, P., Glickman, S., Wieser, J., Cox, R., & Neitz, J. (1996). Mapping striate and extrastriate visual areas in human cerebral cortex. *Proceedings of the National Academy of Sciences of the United States of America, 93*(6), 2382-2386.

Dilks, D. D., Julian, J. B., Paunov, A. M., & Kanwisher, N. (2013). The occipital place area is causally and selectively involved in scene perception. *Journal of Neuroscience, 33*(4), 1331.

Dougherty, R. F., Koch, V. M., Brewer, A. A., Fischer, B., Modersitzki, J., & Wandell, B. A. (2003). Visual field representations and locations of visual areas V1/2/3 in human visual cortex. *Journal of Vision, 3*(10), 586-598.

Downing, P. E. (2009). Visual Neuroscience: A Hat-Trick for Modularity. *Current Biology, 19*(4), 160-162.

Drucker, D. M., & Aguirre, G. K. (2009). Different spatial scales of shape similarity representation in lateral and ventral LOC. *Cerebral Cortex, 19*(10), 2269-2280.

Dumoulin, S. O., Bittar, R. G., Kabani, N. J., Baker, C. L., Le Goualher, G., Pike, G. B., & Evans, A. C. (2000). A new anatomical landmark for reliable identification of human area V5/MT: A quantitative analysis of sulcal patterning. *Cerebral Cortex, 10*(5), 454-463.

Dumoulin, S. O., & Hess, R. F. (2007). Cortical specialization for concentric shape processing. *Vision research, 47*(12), 1608-1613.

Dumoulin, S. O., & Wandell, B. A. (2008). Population receptive field estimates in human visual cortex. *Neuroimage, 39*(2), 647-660.

Duncan, R. O., & Boynton, G. M. (2003). Cortical magnification within human primary visual cortex correlates with acuity thresholds. *Neuron, 38*(4), 659-671.

Dupont, P., de Bruyn, B., Vandenberghe, R., Rosier, A., Michiels, J., Marchal G., Mortelemans, L., & Orban, G. A. (1997). The kinetic occipital region in human visual cortex. *Cereb Cortex 7*, 283–292

Edelman, S., & Intrator, N. 2000. (Coarse coding of shape fragments) + (retinotopy) approximately = representation of structure. *Spatial Vision, 13*, 255—264.

Ellison, A., & Cowey, A. (2006). Tms can reveal contrasting functions of the dorsal and ventral visual processing streams. *Exp Brain Res, 175*(4), 618-625.

Ellison, A., & Cowey, A. (2009). Differential and co-involvement of areas of the temporal and parietal streams in visual tasks. *Neuropsychologia, 47*(6), 1609-1614.

Engel, S. A., Glover, G. H., & Wandell, B. A. (1997). Retinotopic organization in human visual cortex and the spatial precision of functional MRI. *Cerebral Cortex, 7*(2), 181-192.

Engel, S. A. (2005). Adaptation of oriented and unoriented color-selective neurons in human visual areas. *Neuron, 45*(4), 613-623.

Engel, S. A., Rumelhart, D. E., Wandell, B. A., Lee, A. T., Glover, G. H., Chichilnisky, E. J., & Shadlen, M. N. (1994). fMRI of human visual cortex. *Nature, 369*(6481), 525.

Engel, S., Zhang, X., & Wandell, B. (1997). Colour tuning in human visual cortex measured with functional magnetic resonance imaging. *Nature, 388*(6637), 68-71.

Epstein, R., & Kanwisher, N. (1998). A cortical representation of the local visual environment. *Nature, 392*(6676), 598-601.

Ewbank, M. P., & Andrews, T. J. (2008). Differential sensitivity for viewpoint between familiar and unfamiliar faces in human visual cortex. *Neuroimage, 40*(4), 1857-1870.

Fang, F., Murray, S. O., Kersten, D., & He, S. (2005). Orientation-tuned fmri adaptation in human visual cortex. *Journal of Neurophysiology, 94*(6), 4188-4195.

Felleman, D. J., & Mcclendon, E. (1991). Cortical connections of posterior inferotemporal cortex of macaque monkeys. *Investigative Ophthalmology & Visual Science, 32*(4), 1036-1036.

Felleman, D. J., & Van Essen, D. C. (1991). Distributed hierarchical processing in the primate cerebral cortex. *Cerebral Cortex, 1*(1), 1-47.

Fischl, B., Sereno, M. I., & Dale, A. M. (1999). Cortical surface-based analysis. II: Inflation, flattening and a surface-based coordinate system. *Neuroimage, 9*(2), 195-507.

Furmanski, C. S., & Engel, S. A. (2000). An oblique effect in human primary visual cortex. *Nature Neuroscience, 3*(6), 535-536.

Fylan, F., Holliday, I. E., Singh, K. D., Anderson, S. J., & Harding, G. F. (1997). Magnetoencephalographic investigation of human cortical area V1 using color stimuli. *Neuroimage, 6*(1), 47-57.

Gardner, J. L., Merriam, E. P., Movshon, J. A., & Heeger, D. J. (2008). Maps of visual space in human occipital cortex are retinotopic, not spatiotopic. *Journal of Neuroscience, 28*(15), 3988-3999.

Gegenfurtner, K. R. (2003). Cortical mechanisms of colour vision. *Nature Reviews Neuroscience, 4*(7), 563-572.

Goddard, E., Mannion, D. J., McDonald, J. S., Solomon, S. G., & Clifford, C. W. G. (2011). Color responsiveness argues against a dorsal component of human V4. *Journal of Vision, 11*(4).

Golomb, J. D., & Kanwisher, N. (2012). Higher level visual cortex represents retinotopic, not spatiotopic, object location. *Cerebral Cortex, 22*(12), 2794-2810.

Golomb, J. D., & Kanwisher, N. (2012). Retinotopic memory is more precise than spatiotopic memory. *Proceedings of the National Academy of Sciences of the United States of America, 109*(5), 1796-1801.

Goodale, M. A., Milner, A. D., Jakobson, L. S., & Carey, D. P. (1991). A neurological dissociation between perceiving objects and grasping them. *Nature, 349*(6305), 154-156.

Gouws, A., Woods, W., Millman, R., Morland, A., & Green, G. (2009). Dataviewer3d: An open-source, cross-platform multi-modal neuroimaging data visualization tool. *Front Neuroinform, 3*, 9.

Grill-Spector, K. (2003). The neural basis of object perception. *Current Opinion in Neurobiology, 13*(2), 159-166.

Grill-Spector, K., Edelman, S., Kushnir, T., Itzchak, Y., & Malach, R. (1999). Differential processing of objects under various viewing conditions in the human lateral occipital complex. *Investigative Ophthalmology & Visual Science, 40*(4), S399-S399.

Grill-Spector, K., Kourtzi, Z., & Kanwisher, N. (2001). The lateral occipital complex and its role in object recognition. *Vision Research, 41*(10-11), 1409-1422.

Grill-Spector, K., Kushnir, T., Edelman, S., Avidan, G., Itzchak, Y., & Malach, R. (1999). Differential processing of objects under various viewing conditions in the human lateral occipital complex. *Neuron, 24*(1), 187-203.

Grill-Spector, K., Kushnir, T., Edelman, S., Itzchak, Y., & Malach, R. (1998). Cue-invariant activation in object-related areas of the human occipital lobe. *Neuron, 21*(1), 191-202.

Grill-Spector, K., Kushnir, T., Edelman, S., Itzchak, Y., & Malach, R. (1998). Differential processing of objects under various viewing conditions in the human lateral occipital complex. *Neuroscience Letters*, S17-S17.

Grill-Spector, K., Kushnir, T., Hendler, T., Edelman, S., Harvey, P. R., Itzchak, Y., & Malach, R. (1997). Convergence of visual cues in the human lateral occipital complex (LO). *Neuroscience Letters*, S22-S22.

Hallett, M. (2002). Advances in stroke rehabilitation. *Neurological Rehabilitation, Proceedings*, 201-206.

Hallett, M. (2007). Transcranial magnetic stimulation: A primer. *Neuron, 55*(2), 187-199.

Hansen, K. A., Kay, K. N., & Gallant, J. L. (2007). Topographic organization in and near human visual area v4. *Journal of Neuroscience, 27*(44), 11896-11911.

Harris, J. A., Clifford, C. W. G., & Miniussi, C. (2008). The functional effect of transcranial magnetic stimulation: Signal suppression or neural noise generation? *Journal of Cognitive Neuroscience, 20*(4), 734-740.

Hasson, U., Harel, M., Levy, I., & Malach, R. (2003). Large-scale mirror-symmetry organization of human occipito-temporal object areas. *Neuron, 37*(6), 1027-1041.

Haxby, J. V., Hoffman, E. A., & Gobbini, M. I. (2000). The distributed human neural system for face perception. *Trends in Cognitive Sciences, 4*(6), 223-233.

Hess, R. H., Baker, C. L., & Zihl, J. (1989). The motion-blind patient - low-level spatial and temporal filters. *Journal of Neuroscience, 9*(5), 1628-1640.

Heywood, C. A., & Cowey, A. (1987). On the role of cortical area V4 in the discrimination of hue and pattern in macaque monkeys. *Journal of Neuroscience, 7*(9), 2601-2617.

Heywood, C. A., Wilson, B., & Cowey, A. (1987). A case study of cortical colour "blindness" with relatively intact achromatic discrimination. *J Neurol Neurosurg Psychiatry, 50*(1), 22-29.

Huang, Y. Z., Edwards, M. J., Rounis, E., Bhatia, K. P., & Rothwell, J. C. (2005). Theta burst stimulation of the human motor cortex. *Neuron, 45*(2), 201-206.

References

Hubel, D. H., & Wiesel, T. N. (1965). Receptive fields and functional architecture in two nonstriate visual areas (18 and 19) of the cat. *Journal of Neurophysiology, 28*, 229-289.

Hubel, D. H., Wiesel, T. N., & Stryker, M. P. (1978). Anatomical demonstration of orientation columns in macaque monkey. *Journal of Comparative Neurology, 177*(3), 361-379.

Huk, A. C., Dougherty, R. F., & Heeger, D. J. (2002). Retinotopy and functional subdivision of human areas MT and MST. *Journal of Neuroscience, 22*(16), 7195-7205.

James, T. W., Culham, J., Humphrey, G. K., Milner, A. D., & Goodale, M. A. (2003). Ventral occipital lesions impair object recognition but not object-directed grasping: An fMRI study. *Brain, 126*, 2463-2475.

Kammer, T. (1999). Phosphenes and transient scotomas induced by magnetic stimulation of the occipital lobe: Their topographic relationship. *Neuropsychologia, 37*(2), 191-198.

Kanwisher, N., McDermott, J., & Chun, M. M. (1997). The fusiform face area: A module in human extrastriate cortex specialized for face perception. *Journal of Neuroscience, 17*(11), 4302-4311.

Kastner, S., DeSimone, K., Konen, C. S., Szczepanski, S. M., Weiner, K. S., & Schneider, K. A. (2007). Topographic maps in human frontal cortex revealed in memory-guided saccade and spatial working-memory tasks. *Journal of Neurophysiology, 97*(5), 3494-3507.

Kastner, S., De Weerd, P., & Ungerleider, L. G. (2000). Texture segregation in the human visual cortex: A functional mri study. *Journal of Neurophysiology, 83*(4), 2453-2457.

Kennard, C., Lawden, M., Morland, A. B., & Ruddock, K. H. (1995). Colour identification and colour constancy are impaired in a patient with incomplete achromatopsia associated with prestriate cortical lesions. *Philosophical Transactions of the Royal Society B-Biological Sciences, 260*(1358), 169-175.

Kolster, H., Peeters, R., & Orban, G. A. (2010). The retinotopic organization of the human middle temporal area MT/V5 and its cortical neighbors. *Journal of Neuroscience, 30*(29), 9801-9820.

Kourtzi, Z., & Kanwisher, N. (2001). Representation of perceived object shape by the human lateral occipital complex. *Science, 293*(5534), 1506-1509.

Kravitz, D. J., Kriegeskorte, N., & Baker, C. I. (2010). High-level visual object representations are constrained by position. *Cerebral Cortex, 20*(12), 2916-2925.

Kravitz, D. J., Saleem, K. S., Baker, C. I., Ungerleider, L. G., & Mishkin, M. (2013). The ventral visual pathway: An expanded neural framework for the processing of object quality. *Trends in Cognitive Sciences, 17*(1), 26-49.

Kriegeskorte, N., Mur, M., Ruff, D. A., Kiani, R., Bodurka, J., Esteky, H., & Bandettini, P. A. (2008). Matching categorical object representations in inferior temporal cortex of man and monkey. *Neuron, 60*(6), 1126-1141.

Larsson, J., & Heeger, D. J. (2006). Two retinotopic visual areas in human lateral occipital cortex. *Journal of Neuroscience, 26*(51), 13128-13142.

Larsson, J., Heeger, D. J., & Landy, M. S. (2010). Orientation selectivity of motion-boundary responses in human visual cortex. *Journal of Neurophysiology, 104*(6), 2940-2950.

Larsson, J., Landy, M. S., & Heeger, D. J. (2006). Orientation-selective adaptation to first- and second-order patterns in human visual cortex. *Journal of Neurophysiology, 96*(2), 963-963.

Lavidor, M., & Walsh, V. (2004). Opinion - the nature of foveal representation. *Nature Reviews Neuroscience, 5*(9), 729-735.

Leventhal, A. G., Thompson, K. G., Liu, D., Zhou, Y., & Ault, S. J. (1995). Concomitant sensitivity to orientation, direction, and color of cells in layers 2, 3, and 4 of monkey striate cortex. *Journal of Neuroscience, 15*(3 Pt 1), 1808-1818.

Leventhal, A. G., Wang, Y., Schmolesky, M. T., & Zhou, Y. (1998). Neural correlates of boundary perception. *Vis Neurosci, 15*(6), 1107-1118.

Levy, I., Hasson, U., Avidan, G., Hendler, T., & Malach, R. (2001). Center-periphery organization of human object areas. *Nature Neuroscience, 4*(5), 533-539.

Li, B. W., Peterson, M. R., & Freeman, R. D. (2003). Oblique effect: A neural basis in the visual cortex. *Journal of Neurophysiology, 90*(1), 204-217.

Liu, J., & Newsome, W. T. (2003). Functional organization of speed tuned neurons in visual area MT. *Journal of Neurophysiology , 89*, 246 –256.

Liu, J., & Newsome, W. T. (2005). Correlation between speed perception and neural activity in the middle temporal visual area. *Journal of Neuroscience, 25,* 711–722.

Livingstone, M., & Hubel, D. (1988). Segregation of form, color, movement, and depth - anatomy, physiology, and perception. *Science, 240*(4853), 740-749.

Logothetis, N. K. (2008). What we can do and what we cannot do with fMRI *Nature, 453*(7197), 869-878.

Logothetis, N. K., & Wandell, B. A. (2004). Interpreting the bold signal. *Annu Rev Physiol, 66*, 735-769.

Lueck, C. J., Zeki, S., Friston, K. J., Deiber, M. P., Cope, P., Cunningham, V. J., & Frackowiak, R. S. (1989). The colour centre in the cerebral cortex of man. *Nature, 340*(6232), 386-389.

Malach, R., Reppas, J. B., Benson, R. R., Kwong, K. K., Jiang, H., Kennedy, W. A., & Tootell, R. B. (1995). Object-related activity revealed by functional magnetic resonance imaging in human occipital cortex. *Proceedings of the National Academy of Sciences of the United States of America, 92*(18), 8135-8139.

Martinez-Trujillo, J. C., & Treue, S. (2004). Feature-based attention increases the selectivity of population responses in primate visual cortex. *Current Biology, 14*(9), 744-751.

Marcar, V. L., Xiao, D. K., Raiguel, S. E., Maes ,H. &, Orban, G. A. (1995). Processing of kinetically defined boundaries in the cortical motion area MT of the macaque monkey. *Journal of Neurophysiology, 74*, 1258 –1270.

Maunsell, J. H. R., & Newsome, W. T. (1987). Visual processing in monkey extrastriate cortex. *Annual Review of Neuroscience, 10*, 363-401.

Maunsell, J. H. R., & Vanessen, D. C. (1983). Functional-properties of neurons in middle temporal visual area of the macaque monkey .1. Selectivity for stimulus direction, speed, and orientation. *Journal of Neurophysiology, 49*(5), 1127-1147.

Maunsell, J. H., Ghose, G. M., Assad, J. A., McAdams, C. J., Boudreau, C. E., & Noerager, B. D. (1999). Visual response latencies of magnocellular and parvocellular LGN neurons in macaque monkeys. *Vis Neurosci, 16*(1), 1-14.

McAdams, C. J., & Maunsell, J. H. (1999). Effects of attention on orientation-tuning functions of single neurons in macaque cortical area V4. *Journal of Neuroscience, 19*(1), 431-441.

McDonald, J. S., Mannion, D. J., Goddard, E., & Clifford, C. W. (2010). Orientation-selective chromatic mechanisms in human visual cortex. *Journal of Vision, 10*(12), 34.

McKeefry, D. J., Burton, M. P., Vakrou, C., Barrett, B. T., & Morland, A. B. (2008). Induced deficits in speed perception by transcranial magnetic stimulation of human cortical areas V5/MT+ and V3a. *Journal of Neuroscience, 28*(27), 6848-6857.

McKeefry, D. J., Gouws, A., Burton, M. P., & Morland, A. B. (2009). The noninvasive dissection of the human visual cortex: Using fMRI and TMS to study the organization of the visual brain. *Neuroscientist, 15*(5), 489-506.

McKeefry, D. J., & Zeki, S. (1997). The position and topography of the human colour centre as revealed by functional magnetic resonance imaging. *Brain, 120 (Pt 12)*, 2229-2242.

Meadows, J. C. (1974a). Anatomical basis of prosopagnosia. *Journal of Neurology Neurosurgery and Psychiatry, 37*(5), 489-501.

Meadows, J. C. (1974b). Disturbed perception of colors associated with localized cerebral lesions. *Brain, 97*, 615-632.

Miniussi, C., Ruzzoli, M., & Walsh, V. (2010). The mechanism of transcranial magnetic stimulation in cognition. *Cortex, 46*(1), 128-130.

Mishkin, M., Ungerleider, L. G., & Macko, K. A. (1983). Object vision and spatial vision - 2 cortical pathways. *Trends in Neurosciences, 6*(10), 414-417.

Mullen, K. T., Dumoulin, S. O., McMahon, K. L., de Zubicaray, G. I., & Hess, R. F. (2007). Selectivity of human retinotopic visual cortex to s-cone-opponent, L-M-cone-opponent and achromatic stimulation. *European Journal of Neuroscience, 25*(2), 491-502.

Mysore, S. G., Vogels, R., Raiguel, S. E., & Orban, G. A. (2006). Processing of kinetic boundaries in macaque V4. *Journal of Neurophysiology, 95*(3), 1864-1880.

Newsome, W. T., & Pare, E. B. (1988). A selective impairment of motion perception following lesions of the middle temporal visual area (MT). *Journal of Neuroscience, 8*, 2201–2211.

Op de Beeck, H. P., Haushofer, J., & Kanwisher, N. G. (2008). Interpreting fMRI data: Maps, modules and dimensions. *Nature Reviews Neuroscience, 9*(2), 123-135.

Orban, G. A., Dupont, P., De Bruyn, B., Vogels, R., Vandenberghe., & Mortelmans, I. (1995). A motion area in human visual cortex. *Proceedings of the National Academy of Sciences of the United States of America, 92*(4), 993-997.

Orban, G. A., Fize, D., Peuskens, H., Denys, K., Nelissen, K., Sunaert, S., & Vanduffel, W. (2003). Similarities and differences in motion processing between the human and macaque brain: Evidence from fMRI. *Neuropsychologia, 41*(13), 1757-1768.

Orban, G. A., Van Essen, D., &Vanduffel, W. (2004). Comparative mapping in higher visual areas in monkeys and humans. *Trends Cogn Sci, 8*(7), 315-324.

Pascual-Leone, A., Walsh, V., & Rothwell, J. (2000). Transcranial magnetic stimulation in cognitive neuroscience - virtual lesion, chronometry, and functional connectivity. *Current Opinion in Neurobiology, 10*(2), 232-237.

Perenin, M. T., & Vighetto, A. (1988). Optic ataxia - a specific disruption in visuomotor mechanisms .1. Different aspects of the deficit in reaching for objects. *Brain, 111*, 643-674.

Pitcher, D., Charles, L., Devlin, J. T., Walsh, V., & Duchaine, B. (2009). Triple dissociation of faces, bodies, and objects in extrastriate cortex. *Current Biology, 19*(4), 319-324.

Pitcher, D., Walsh, V., & Duchaine, B. (2011). The role of the occipital face area in the cortical face perception network. *Experimental Brain Research, 209*(4), 481-493.

Price, C. J., & Friston, K. J. (2002). Functional imaging studies of neuropsychological patients: Applications and limitations. *Neurocase, 8*(5), 345-354.

Priebe, N. J., Cassanello, C. R., & Lisberger, S. G. (2003). The neural representation of speed in macaque area MT/V5. *Journal of Neuroscience, 23*(13), 5650-5661.

Regan, D., & He, P. (1995). Magnetic and electrical responses of the human brain to texture-defined form and to textons. *Journal of Neurophysiology, 74*(3), 1167-1178.

Rodman, H. R., Gross, C. G., & Albright, T. D. (1989). Afferent basis of visual response properties in area MT of the macaque: I. effects of striate cortex removal. *Journal of Neuroscience, 9*, 2033–2050

Rodman, H. R., & Albright, T. D. (1987). Coding of visual stimulus velocity in area MT of the macaque. *Vision Research, 27*(12), 2035-2048.

Rushton, W. A. H. (1972). Pigments and signals in color-vision. *Journal of Physiology-London, 220*(3).

Ruzzoli, M., Marzi, C. A., & Miniussi, C. (2010). The neural mechanisms of the effects of transcranial magnetic stimulation on perception. *Journal of Neurophysiology, 103*(6), 2982-2989.

Sack, A. T., Kadosh, R. C., Schuhmann, T., Moerel, M., Walsh, V., & Goebel, R. (2009). Optimizing functional accuracy of TMS in cognitive studies: A comparison of methods. *Journal of Cognitive Neuroscience, 21*(2), 207-221.

Sary, G., Vogels, R., Kovacs, G., & Orban, G. A. (1995). Responses of monkey inferior temporal neurons to luminance-defined, motion-defined, and texture-defined gratings. *Journal of Neurophysiology, 73*(4), 1341-1354.

Sary, G., Vogels, R., & Orban, G. A. (1993). Cue-invariant shape selectivity of macaque inferior temporal neurons. *Science, 260*(5110), 995-997.

Sayres, R., & Grill-Spector, K. (2008). Relating retinotopic and object-selective responses in human lateral occipital cortex. *Journal of Neurophysiology, 100*(1), 249-267.

Self, M. W., & Zeki, S. (2005). The integration of colour and motion by the human visual brain. *Cerebral Cortex, 15*(8), 1270-1279.

Sereno, M. I., Dale, A. M., Reppas, J. B., Kwong, K. K., Belliveau, J. W., Brady, T. J., & Tootell, R. B. H. (1995). Borders of multiple visual areas in humans revealed by functional magnetic-resonance-imaging. *Science, 268*(5212), 889-893.

Seymour, K., Clifford, C. W., Logothetis, N. K., & Bartels, A. (2009). The coding of color, motion, and their conjunction in the human visual cortex. *Current Biology, 19*(3), 177-183.

Seymour, K., Clifford, C. W., Logothetis, N. K., & Bartels, A. (2010). Coding and binding of color and form in visual cortex. *Cerebral Cortex, 20*(8), 1946-1954.

Shipp, S., & Zeki, S. (1985). Segregation of pathways leading from area V2 to areas V4 and V5 of macaque monkey visual-cortex. *Nature, 315*(6017), 322-325.

Silvanto, J., Muggleton, N. G., Cowey, A., & Walsh, V. (2007). Neural adaptation reveals state-dependent effects of transcranial magnetic stimulation. *European Journal of Neuroscience, 25*(6), 1874-1881.

Silvanto, J., & Pascual-Leone, A. (2012). Why the assessment of causality in brain-behavior relations requires brain stimulation. *Journal of Cognitive Neuroscience, 24*(4), 775-777.

Silvanto, J., Schwarzkopf, D. S., Gilaie-Dotan, S., & Rees, G. (2010). Differing causal roles for lateral occipital cortex and occipital face area in invariant shape recognition. *European Journal of Neuroscience, 32*(1), 165-171.

Silver, M. A., & Kastner, S. (2009). Topographic maps in human frontal and parietal cortex. *Trends in Cognitive Sciences, 13*(11), 488-495.

Sincich, L. C., Park, K. F., Wohlgemuth, M. J., & Horton, J. C. (2004). Bypassing V1: A direct geniculate input to area MT. *Nature Neuroscience, 7*(10), 1123-1128.

Singh, K. D., Smith, A. T., & Greenlee, M. W. (2000). Spatiotemporal frequency and direction sensitivities of human visual areas measures using fMRI. *Neuroimage, 12*(5), 550-564.

Smith, A. T., Greenlee, M. W., Singh, K. D., Kraemer, F. M., & Hennig, J. (1998). The processing of first- and second-order motion in human visual cortex assessed by functional magnetic resonance imaging (fMRI). *Journal of Neuroscience, 18*(10), 3816-3830.

Solomon, S. G., & Lennie, P. (2007). The machinery of colour vision. *Nature Reviews Neuroscience, 8*(4), 276-286.

Stensaas, S. S., Eddingto.Dk, & Dobelle, W. H. (1974). Topography and variability of primary visual-cortex in man. *Journal of Neurosurgery, 40*(6), 747-755.

Tanaka, H., Uka, T., Yoshiyama, K., Kato, M., & Fujita, I. (2001). Processing of shape defined by disparity in monkey inferior temporal cortex. *Journal of Neurophysiology, 85*(2), 735-744.

Taylor, M. M. (1963). Visual discrimination and orientation. *J Opt Soc Am, 53,* 763–765.

Taylor, J. C., & Downing, P. E. (2011). Division of labor between lateral and ventral extrastriate representations of faces, bodies, and objects. *J Cogn Neurosci, 23*(12), 4122-4137.

Taylor, J. C., Wiggett, A. J., & Downing, P. E. (2007). Functional mri analysis of body and body part representations in the extrastriate and fusiform body areas. *Journal of Neurophysiology, 98*(3), 1626-

Thompson, P., Stone, L. S., & Stone, R. (1992). Contrast-dependence of speed perception - effects of temporal presentation. *Investigative Ophthalmology & Visual Science, 33*(4), 973-973.

Tootell, R. B. H., & Hadjikhani, N. (2001). Where is 'dorsal V4' in human visual cortex? Retinotopic, topographic and functional evidence. *Cerebral Cortex, 11*(4), 298-311.

Tootell, R. B. H., Reppas, J. B., Dale, A. M., Sereno, M., Malach, R., Kwong, K. K., & Rosen, B. R. (1995). Visual-motion, retinotopy, eye-movements and a search for color in human cortex. *Investigative Ophthalmology & Visual Science, 36*(4), S612-S612.

Tootell, R. B. H., Tsao, D., & Vanduffel, W. (2003). Neuroimaging weighs in: Humans meet macaques in "primate" visual cortex. *Journal of Neuroscience, 23*(10), 3981-3989.

Treue, S. (2001). Neural correlates of attention in primate visual cortex. *Trends Neurosci, 24*(5), 295-300.

Treue, S., & Martinez Trujillo, J. C. (1999). Feature-based attention influences motion processing gain in macaque visual cortex. *Nature, 399*(6736), 575-579.

Tyler, C. W., Baseler, H. A., Kontsevich, L. L., Likova, L. T., Wade, A. R., & Wandell, B. A. (2005). Predominantly extra-retinotopic cortical response to pattern symmetry. *Neuroimage, 24*(2), 306-314.

Vanessen, D. C., Felleman, D. J., Deyoe, E. A., & Knierim, J. J. (1991). Probing the primate visual-cortex - pathways and perspectives. *From Pigments to Perception, 203*, 227-237.

Verrey (1888). Hemiachromatopsie droite absolue. *Arxhives d'Ophtalmologie, Paris, 8, 289-300.*

Vinberg, J., & Grill-Spector, K. (2008). Representation of shapes, edges, and surfaces across multiple cues in the human visual cortex. *Journal of Neurophysiology, 99*(3), 1380-1393.

Vogels, R., & Orban, G. A. (1996). Coding of stimulus invariances by inferior temporal neurons. *Prog Brain Res, 112*, 195-211.

Wade, A., Augath, M., Logothetis, N., & Wandell, B. (2008). fMRI measurements of color in macaque and human. *Journal of Vision, 8*(10).

Wade, A. R., Brewer, A. A., Rieger, J. W., & Wandell, B. A. (2002). Functional measurements of human ventral occipital cortex: Retinotopy and colour. *Philosophical Transactions of the Royal Society B-Biological Sciences, 357*(1424), 963-973.

Walsh, V., & Cowey, A. (1998). Magnetic stimulation studies of visual cognition. *Trends in Cognitive Sciences, 2*(3), 103-110.

Walsh, V., & Cowey, A. (2000). Transcranial magnetic stimulation and cognitive neuroscience. *Nature Reviews Neuroscience, 1*(1), 73-79.

Walsh, V., Ellison, A., Battelli, L., & Cowey, A. (1998). Task-specific impairments and enhancements induced by magnetic stimulation of human visual area V5. *Proceedongs of the Royal Society B-Biological Sciences, 265*(1395), 537-543.

Walsh, V., Carden, D., Butler, S. R., & Kulikowski, J. J. (1993). The effects of v4 lesions on the visual abilities of macaques: Hue discrimination and colour constancy. *Behav Brain Res, 53*(1-2), 51-62.

Walsh, V., & Rushworth, M. (1999). A primer of magnetic stimulation as a tool for neuropsychology. *Neuropsychologia, 37*(2), 125-135.

Wandell, B. A., Brewer, A. A., & Dougherty, R. F. (2005). Visual field map clusters in human cortex. *Philosophical Transactions of the Royal Society B-Biological Sciences, 360*(1456), 693-707.

Wandell, B. A., Dumoulin, S. O., & Brewer, A. A. (2007). Visual field maps in human cortex. *Neuron, 56*(2), 366-383.

Wandell, B. A., & Wade, A. R. (2003). Functional imaging of the visual pathways. *Neurol Clin, 21*(2), 417-443, vi.

Wandell, B. A., & Winawer, J. (2011). Imaging retinotopic maps in the human brain. *Vision Research, 51*(7), 718-737.

Webster, M. A., Devalois, K. K., & Switkes, E. (1990). Orientation and spatial-frequency discrimination for luminance and chromatic gratings. *Journal of the Optical Society of America a-Optics Image Science and Vision, 7*(6), 1034-1049.

Weiner, K. S., & Grill-Spector, K. (2010). Sparsely-distributed organization of face and limb activations in human ventral temporal cortex. *Neuroimage, 52*(4), 1559-1573.

Weiner, K. S., & Grill-Spector, K. (2012). The improbable simplicity of the fusiform face area. *Trends in Cognitive Sciences, 16*(5), 251-254.

Westheimer, G. (1975). Visual-acuity and hyper-acuity. *Investigative Ophthalmology, 14*(8), 570-572.

Wilkinson, F., James, T. W., Wilson, H. R., Gati, J. S., Menon, R. S., & Goodale, M. A. (2000). An fMRI study of the selective activation of human extrastriate form vision areas by radial and concentric gratings. *Current Biology, 10*(22), 1455-1458.

Wilkinson, F., Wilson, H. R., & Habak, C. (1998). Detection and recognition of radial frequency patterns. *Vision Research, 38*(22), 3555-3568.

Wilson, H. R., Loffler, G., & Wilkinson, F. (2002). Synthetic faces, face cubes, and the geometry of face space. *Vision Research, 42*(27), 2909-2923.

Wilson, H. R., & Wilkinson, F. (2002). Symmetry perception: A novel approach for biological shapes. *Vision Research, 42*(5), 589-597.

Winawer, J., Horiguchi, H., Sayres, R. A., Amano, K., & Wandell, B. A. (2010). Mapping hV4 and ventral occipital cortex: The venous eclipse. *Journal of Vision, 10*(5), 1.

Zeki, S. (1990). Parallelism and functional specialization in human visual cortex. *Cold Spring Harb Symp Quant Biol, 55*, 651-661.

Zeki, S. (2003). Improbable areas in the visual brain. *Trends Neuroscience, 26*(1), 23-26.

Zeki, S. M. (1978). Functional specialisation in the visual cortex of the rhesus monkey. *Nature, 274*(5670), 423-428.

Zeki, S., McKeefry, D. J., Bartels, A., & Frackowiak, R. S. J. (1998). Has a new color area been discovered? *Nature Neuroscience, 1*(5), 335-335.

Zeki, S., & Shipp, S. (1988). The functional logic of cortical connections. *Nature, 335*(6188), 311-317.

Zeki, S., Watson, J. D., Lueck, C. J., Friston, K. J., Kennard, C., & Frackowiak, R. S. (1991). A direct demonstration of functional specialization in human visual cortex. *Journal of Neuroscience, 11*(3), 641-649.

Zeki, S., Perry, R. J., & Bartels, A. (2003). The processing of kinetic contours in the brain. *Cerebral Cortex, 13*(2), 189-202.

Zihl, J., Voncramon, D., & Mai, N. (1983). Selective disturbance of movement vision after bilateral brain-damage. *Brain, 106*, 313-340.